Myelin plasticity in mouse resilience and susceptibility to psychosocial stress – implications for anxiety disorders

Mikaela A. Laine

SleepWell Research Program
Research Programs Unit
Faculty of Medicine
University of Helsinki
Finland

and

Department of Psychology and Logopedics
Faculty of Medicine
University of Helsinki
Finland

and

Molecular and Integrative Biosciences Research Programme
Faculty of Biological and Environmental Sciences
University of Helsinki
Finland

and

Doctoral Programme Brain & Mind
University of Helsinki
Finland

Doctoral Thesis

to be presented for public examination with the permission of the Faculty of Biological and Environmental Sciences of the University of Helsinki, in Biomedicum, Lecture Hall 3, Haartmaninkatu 8, on the 15th of January, 2021 at 13 o'clock.

Supervisor	Professor Iiris Hovatta, PhD *SleepWell Research Program* *Department of Psychology and Logopedics* *Faculty of Medicine* *University of Helsinki* *Helsinki, Finland*
Thesis committee	Professor Pentti Tienari, MD PhD *Department of Neurosciences* *Faculty of Medicine* *University of Helsinki* *Helsinki, Finland* *Neurocenter* *Helsinki University Hospital* *Helsinki, Finland* Professor Eero Castrén, MD PhD *Neuroscience Center* *Helsinki Institute of Life Sciences (HiLIFE)* *University of Helsinki* *Helsinki, Finland*
Pre-examiners	Professor Laura Airas, MD PhD *Department of Clinical Neurosciences* *Turku University Hospital and University of Turku* *Turku, Finland* Adjunct Professor Jukka Jolkkonen, PhD *Institute of Clinical Medicine / Neurology* *University of Eastern Finland* *Kuopio, Finland*
Opponent	Professor Jaanus Harro, MD PhD *Institute of Psychology* *Faculty of Social Sciences* *University of Tartu* *Tartu, Estonia*

The Faculty of Biological and Environmental Sciences uses the Urkund system (plagiarism recognition) to examine all doctoral dissertations.

ISBN (print): 978-951-51-6843-6
ISBN (online): 978-951-51-6844-3
ISSN (print): 2342-3161
ISSN (online): 2342-317X
Printing by Unigrafia Oy, Helsinki, Finland, December 2020

Preface

Every dissertation about the science of stress needs at least one remark about stress being a part of the PhD process, so here it is. Stress is a healthy and necessary aspect of life, signalling to us a challenge that needs to be met by stretching above and beyond what we thought we were capable of. You hold in your hands a product of such a protracted response, and the irony of it also being the topic of this thesis has not escaped the author.

With that matter out of the way, I want to thank you for your interest in this piece of work. Given the high prevalence of stress-related psychiatric disorders, each person present at the public defence of this thesis or reading it afterwards is likely to know at least one affected person. In fact I'm sure you do. This work is dedicated to those who, despite working up the courage to seek help with the ever-looming demons of anxiety or depression, did not receive it. Perhaps you were not taken seriously, or perhaps you were but did not get relief. These experiments do not provide a solution by themselves, but hopefully they will be a drop in the ocean of a solution to come. I promise; we are working on it.

Abstract

Psychiatric disorders are very common, with anxiety disorders being the most prevalent (16 % lifetime prevalence). While moderately heritable, their incidence is also strongly influenced by environmental risk factors, chiefly psychosocial stress. However, our knowledge of how, in neurobiological terms, these disorders arise is lacking, slowing down the development of efficient treatments.

The aim of this thesis was firstly to identify which brain regions are recruited by chronic psychosocial stress, by using mice as model organisms. To model psychosocial stress we used chronic social defeat stress (CSDS), which involves short confrontations between intruder and resident-aggressor male mice, repeated daily for 10 consecutive days. A week after stress exposure C57BL/6NCrl (B6) mice had a higher number of cells expressing ΔFOSB, a marker of repeated neural activation, in several stress-related brain regions. These included the bed nucleus of the stria terminalis (BNST) and ventral hippocampus (vHPC). We also found significant correlations in the numbers of $\Delta FOSB^{+}$ cells between medial prefrontal cortex (mPFC) subregions (infralimbic and prelimbic cortices) and the vHPC of stress-exposed but not non-stressed control mice.

Our second aim was to discover, by using unbiased RNA-sequencing (RNA-seq) of stress-related brain regions (the mPFC and vHPC), biological pathways perturbed by CSDS. Additionally, we used mice from two inbred strains, representing different levels of baseline anxiety-like behaviour: B6 (low-anxiety) and DBA/2NCrl (D2, high-anxiety). This enabled us to explore how genetic background modulates the response to stress. While some mice exposed to CSDS show social avoidance (called stress-susceptibility), others are behaviourally similar to non-stressed control mice. This phenomenon, known as resilience, is also observed in humans. We found that B6 and D2 mice showed vastly different behavioural responses to CSDS. B6 mice displayed a predominantly resilient phenotype (66.1 % of CSDS-exposed mice across several cohorts), while the majority (85.0 %) of D2 mice were susceptible. Pathway analysis of RNA-seq data suggested that differentially expressed genes (DEGs) were enriched in genes related to oligodendrocytes (OLGs), the myelin-producing cells of the CNS. For example, genes encoding myelin components were downregulated in the mPFC and vHPC of B6 susceptible mice compared to controls. Myelin is a lipid-rich ensheathment around axons, and it enables both fast nerve conduction and adjustment thereof via myelin plasticity. We followed up the gene expression findings with a structural analysis of myelinated axons using transmission electron microscopy (TEM). We found that in the vHPC, B6 susceptible mice had thinner myelin sheaths than controls. In the mPFC, B6 resilient mice had thicker myelin than controls,

restricted to axons with small diameters. By contrast, D2 resilient mice had thinner myelin in this region than susceptible mice, indicating potential bidirectional dynamics of myelin plasticity in resilience.

Lastly, we performed RNA-seq of enriched OLGs and myelin from the mPFC. The aim of this experiment was to identify pathways affected by CSDS specifically in these cells and in myelin. Additionally, we used this dataset to identify genes (24.8 % of all genes and 18.8 % of expressed micro-RNAs [miRNAs]) which were enriched in the myelin fraction compared to OLGs in non-stressed control mice. This suggests selective transport of certain mRNAs and microRNAs into the myelin sheath, potentially for local regulation. When comparing CSDS-exposed mice and controls, we found lower expression of myelin-related genes in B6 susceptible, D2 susceptible and D2 resilient mice compared to same-strain controls. In the B6 strain this was found in the myelin fraction, while in the D2 strain these genes were differentially expressed only in OLGs. Ingenuity Pathway Analysis (IPA) predicted TCF7L2, a transcription factor, to be an upstream regulator of these DEGs.

In summary, we showed involvement of a broad but selective network of brain regions in CSDS. Genetic background had a large influence on the response to stress, highlighting a source of individual variation with implications for understanding human stress-resilience and -susceptibility. This moderation by genetic background was also seen at the level of gene expression in the brain. Finally, our findings suggest that myelin plasticity is an important part of the chronic response to stress. Future work will identify by which mechanisms stress influences myelin, and how this could be best harnessed for improving therapeutic strategies.

Tiivistelmä

Mielenterveyden häiriöistä erityisesti ahdistuneisuushäiriöt ovat erittäin yleisiä (16 % elämänaikainen esiintyvyys). Ahdistuneisuushäiriöt ovat kohtalaisen periytyviä, mutta myös ympäristötekijät vaikuttavat niiden puhkeamiseen. Erityisesti psykososiaalinen stressi lisää ahdistuneisuushäiriön riskiä. Ymmärrämme näiden häiriöiden neurobiologisista taustoista vielä hyvin vähän, mikä on hidastanut tehokkaiden hoitomenetelmien kehitystä.

Tämän väitöskirjan ensimmäinen tavoite oli tunnistaa, mitkä aivoalueet krooninen psykososiaalinen stressi aktivoi, käyttäen hiirtä malliorganismina. Mallintaaksemme psykososiaalista stressiä käytimme kroonista sosiaalista alistamista (eng. *chronic social defeat stress*, CSDS). CSDS:ssä uroshiiri asetetaan sitä vanhemman alistavasti käyttäytyvän uroshiiren kotihäkkiin lyhyeksi ajaksi. Nämä alistavat kohtaamiset toistetaan päivittäin 10 päivän ajan. Tutkimme aivoalueiden aktivaatiota värjäämällä aivonäytteitä vasta-aineella, jonka kohde oli solun toistuvasta aktivaatiosta indusoituva ΔFOSB proteiini. Viikko stressin jälkeen C57BL/6NCrl (B6) kannan hiirillä oli enemmän ΔFOSB-positiivisia soluja usealla aivoalueella, kuten *bed nucleus of the stria terminaliksessa* (BNST) sekä ventraalisessa aivotursossa (eng. *ventral hippocampus*, vHPC), kuin stressille altistamattomilla verrokkihiirillä. Lisäksi ΔFOSB-positiivisten solujen lukumäärät korreloivat useiden eri aivoalueiden välillä, muun muassa etuaivokuoren (eng. *medial prefrontal cortex*, mPFC) ala-alueiden (infralimbinen sekä prelimbinen aivokuori) ja vHPC:n välillä.

Toinen tavoitteemme oli selvittää genominlaajuisen RNA-sekvensoinnin avulla, mihin biologisiin toimintoihin CSDS mPFC ja vHPC aivoalueilla vaikuttaa. Tämän lisäksi selvitimme, miten perinnölliset tekijät muokkaavat näitä vaikutuksia käyttämällä hiiriä kahdesta eri kannasta. Valitsimme sellaiset hiirikannat, jotka eroavat ahdistuneisuustyyppisen käyttäytymisen suhteen: B6 (vähäistä ahdistustyyppistä käyttäytymistä) sekä DBA/2NCrl (D2; korkeaa ahdistustyyppistä käyttäytymistä). CSDS:n jälkeen osa hiiristä on stressialttiita (eng. *susceptible*), mikä tarkoittaa niiden välttelevän sosiaalista kanssakäymistä verrattuna stressille altistamattomiin verrokkihiiriin. Osa stressille altistetuista hiiristä on resilienttejä, eli ne käyttäytyvät sosiaalisessa tilanteessa samoin kuin verrokkihiiret. Resilienssi on myös ihmisillä havaittava piirre. Osoitimme, että B6 ja D2 hiirten käyttäytyminen erosi huomattavasti CSDS:n jälkeen. B6 hiiret olivat pääasiallisesti resilienttejä (66.1 % CSDS:lle altistetuista), kun taas suurin osa (85.0 %) D2 hiiristä oli stressialttiita. Käytimme bioinformatiivista polkuanalyysiä selvittääksemme, ovatko resilienttien, stressialttiiden ja verrokkihiirten välillä eritasoilla ilmentyneet geenit rikastuneet joidenkin tiettyjen biologisten toimintojen osalta. Oligodendrosyyttien (OLG) toimintaan liittyvät geenit olivat näissä vertailuissa

rikastuneet. Oligodendrosyytit tuottavat myeliiniä eristeeksi hermosyiden ympärille, mikä nopeuttaa aktiopotentiaalien kulkua. Myeliini muovautuu myös aikuisiällä, ja pienetkin muutoksen myeliinissä voivat säätää hermosolujen välistä viestintää. Havaitsimme esimerkiksi, että myeliiniin kuuluvia proteiineja tuottavat geenit ilmentyivät alhaisemmalla tasolla sekä mPFC:ssä että vHPC:ssä B6 kannan stressialttiilla hiirillä verrokkeihin nähden. Tutkimme näiden tulosten perusteella myeliiniä transmissioelektronimikroskopialla (TEM). Osoitimme, että B6 stressialttiilla hiirillä oli vHPC:ssä ohuemmat myeliinitupet kuin verrokeilla. B6 resilienteillä hiirillä puolestaan oli verrokkeihin nähden paksummat myeliinitupet mPFC:n ohuissa hermosyissä. D2 kannan resilienteillä hiirillä oli samalla aivoalueella ohuemmat myeliinitupet kuin stressialttiilla hiirillä. Nämä löydökset viittaavat siihen, että molemman suuntainen muovautuminen myeliinissä voi liittyä stressivasteeseen.

Viimeisessä osatyössä eristimme stressille altistettujen hiirten mPFC:stä OLG:t ja myeliinin. Tavoitteemme oli selvittää, mitkä geenit erityisesti OLG:issä reagoivat stressiin, sekä miten OLG:t ja myeliini eroavat toisistaan geenien ilmentymisen osalta. Tunnistimme useita geenejä (24.8 % ilmentyvistä lähetti-RNA:ista ja 18.8 % mikroRNA:ista [miRNA]), jotka olivat merkitsevästi rikastuneet myeliinissä verrattuna OLG:ihin verrokkihiirissä. Tämä voi johtua valikoivasta lähetti- sekä miRNA:iden kuljetuksesta tumasta myeliiniin paikallista säätelyä varten. Verratessamme CSDS:n kokeneita ja verrokkihiiriä totesimme myeliiniin liittyvien geenien ilmentyvän alemmalla tasolla B6 stressialttiissa, D2 stressialttiissa sekä D2 resilienteissä hiirissä samojen kantojen verrokkeihin nähden. B6 kannassa tämä ero näkyi myeliinissä, mutta D2 kannassa erot näkyivät ainoastaan OLG:issä. Ingenuity Pathway Analysis (IPA) ohjelman avulla selvitimme, että näiden eritavoin ilmentyvien geenien mahdollinen säätelijä on TCF7L2, OLG:ssä tunnetusti ilmentyvä säätelyproteiini.

Osoitimme laajan mutta erikoistuneen aivoalueiden verkoston aktivoituvan CSDS altistuksessa. Hiirten geneettinen tausta vaikutti merkitsevästi stressinjälkeiseen käyttäytymiseen, mikä voi liittyä myös ihmisyksilöiden välisiin eroihin resilienssissä ja stressialttiudessa. Geneettisen taustan vaikutus näkyi myös aivoissa geenien ilmentymisessä. Löydöksemme viittaavat myeliiniplastisuuteen tärkeänä stressivasteeseen kuuluvana tekijänä. Jatkotutkimuksia tarvitaan tunnistamaan, minkä mekanismien kautta stressi vaikuttaa myeliiniin, ja miten tätä tietoa voisi hyödyntää ahdistuneisuushäiriöiden hoidon kehityksessä.

Abbreviations

ANOVA	analysis of variance
APEX2	ascorbate peroxidase 2
B6	C57BL/6NCrl
BDNF	brain-derived neurotrophic factor
BLA	basolateral nucleus of the amygdala
BNST	bed nucleus of the stria terminalis
CC	corpus callosum
CC1	adenomatous polyposis coli clone CC1
CD1	Clr:CD1
CEA	central nucleus of the amygdala
ChIP	Chromatin immunoprecipitation
CNP	2',3'-Cyclic Nucleotide 3' Phosphodiesterase
CRH/CRF	corticotropin releasing hormone/factor
CSDS	chronic social defeat stress
CUS/CVS	chronic unpredictable/variable stress
D2	DBA/2NCrl
DEG	differentially expressed gene
DSM	Diagnostic and Statistical Manual
DTI	diffusion tensor imaging
ELS	early life stress
EPM	elevated plus maze
FA	fractional anisotropy
FLARE	Fast Light- and Activity-Regulated Expression
fMRI	functional magnetic resonance imaging
FOSB	FBJ murine osteosarcoma viral oncogene homolog B
GABA	γ-aminobutyric acid
GAD	generalized anxiety disorder
GAS	general adaptation syndrome
GC	glucocorticoid
GEE	generalized estimating equations
GO	Gene Ontology
GR	glucocorticoid receptor
GSEA	Gene Set Enrichment Analysis
GSK3β	glycogen synthase kinase 3 β
GWAS	genome-wide association study
HDAC1/2	histone deacetylase 1/2
HPA	hypothalamic-pituitary-adrenal
HPC	hippocampus
ICD	International Classification of Diseases
IHC	immunohistochemistry
IL	infralimbic cortex
IPA	Ingenuity Pathway Analysis
IZ	interaction zone in the SA test
KO	knock-out
LD	light-dark box
LTP/LTD	long-term potentiation(depression
MACS	magnetic-activated cell sorting
MAOI	monoamine oxidase inhibitor
MBP	myelin basic protein
MDD	major depressive disorder
MEMRI	manganese-enhanced magnetic resonance imaging
miRNA	micro-RNA
mPFC	medial prefrontal cortex
MS	multiple sclerosis
MSN	medium spiny neuron
MTR	magnetization transfer ratio
MYRF	myelin regulatory factor
NAc	nucleus accumbens
NMDA	N-methyl-D-aspartate
NT	no-target trial of the SA test
OCD	obsessive-compulsive disorder
OFT	open field test
OLG	oligodendrocyte
OLIG2	oligodendrocyte transcription factor 2
OPC	oligodendrocyte progenitor cells
PAG	periaqueductal grey
PBS	phosphate-buffered saline
PDGFRA	platelet-derived growth factor receptor α
PFA	paraformaldehyde
PFC	prefrontal cortex
PLP1	proteolipid protein 1
PrL	prelimbic cortex
PTSD	post-traumatic stress disorder
RNA-seq	RNA-sequencing
SA test	social avoidance test
SAD	social anxiety disorder
SI ratio	social interaction ratio
SOX10	SRY-box transcription factor 10
SpeRe	spectral reflectometry
SSRI	selective serotonin re-uptake inhibitor
TCF7L2	transcription factor 7-like 2
TEM	transmission electron microscopy
TF	transcription factor
UF	uncinate fasciculus
vHPC	ventral hippocampus

Table of Contents

List of publications

This thesis is based on two peer-reviewed publications (Study I and Study II) and one manuscript in preparation (Study III), with some additional unpublished data. Studies I and II are reprinted under the Creative Commons Attribution 4.0 International (CC BY 4.0) license.

Study I **Laine, M.A**., Sokolowska, E., Dudek, M., Callan, S. A., Hyytiä, P., Hovatta, I. (2017). Brain activation induced by chronic psychosocial stress in mice. *Scientific Reports,* 7, 15061, doi:10.1038/s41598-017-15422-5

Study II **Laine, M.A**.*, Trontti, K.*, Misiewicz, Z.*, Sokolowska, E.*, Kulesskaya, N., Heikkinen, A., Saarnio, S., Balcells, I., Ameslon, P., Greco, D., Mattila, P., Ellonen, P., Paulin, L., Auvinen, P., Jokitalo, E., & Hovatta, I. (2018). Genetic control of myelin plasticity after chronic psychosocial stress. *eNeuro,* 4(5), doi:10.1523/eneuro.0166-18.2018

* = These authors contributed equally to this work

Study III **Laine, M.A.,** Trontti, K., Gigliotta, A., Saarnio, S., Paranko, B., Kulesskaya, N., & Hovatta, I. (2020). Differential gene expression response of oligodendrocytes and myelin to chronic psychosocial stress in C57BL/6NCrl and DBA/2NCrl mice. *Manuscript in preparation.*

This author's contribution to the included studies:

Study I: Conducted immunohistochemical staining and imaging, analysed immunohistochemical data; produced Figures 1, 3 and 4 and Table 1, and wrote the manuscript together with M.D., P.H. and I.H.

Study II: Contributed to data collection (behavioural experiments) and analysis for, and produced, Figure 1. Established the protocol, supervised the student performing the immunohistochemical staining, analysed the data for and produced Figure 3. Produced Figure 4 based on data collected by other authors. Planned and conducted dissections and sample preparations of transmission electron microscopy, performed image acquisition and data analysis for two brain regions (medial prefrontal cortex and ventral hippocampus), produced Figure 5, and extended data Figures 5-1, 5-2 and 5-3. Wrote the manuscript parts detailing the aforementioned experiments. Other parts of this publication were previously used in the doctoral thesis of Zuzanna Misiewicz, PhD.

Study III: Planned, conducted and analysed mouse behavioural data. Established the protocol for and conducted magnetic-associated cell sorting. Performed bioinformatic pathway analysis (Ingenuity Pathway Analysis). Wrote the manuscript together with K.T., A.G. and I.H.

1. Introduction

While navigating a world with more or less perilous threats waiting for us at many corners, a well-functioning capacity to feel anxious is an advantage. If we can anticipate a problem, we have a good chance of dealing with it successfully. However, as with many functions, the anxiety system can dysfunction, giving rise to anxiety disorders. Suffering from an anxiety disorder involves disproportionate worry about and vigilance towards threats, sometimes even intense feelings of fear where none are warranted. As a collective term in the Diagnostic and Statistical Manual (DSM-5) and International Classification of Diseases (ICD-11) these disorders are the most common psychiatric ailment, with 16 % of people experiencing one or several of them during their lifetime [1]. Specific, curative treatments for patients with anxiety disorders are not yet available, although symptoms can be managed with pharmaco- and psychotherapeutic options. The reasons for this are complex, but an important hurdle in this quest is that we know surprisingly little about what the key pathology in anxiety disorders, and many other CNS disorders, is. Big questions in the field include why some people develop an anxiety disorder while others do not, and which aspects of neurobiology are involved in either vulnerability to or protection from them.

What we do know is that genetic factors matter; these disorders are heritable at least to a moderate degree (30-40 %, [3]), with much of the genetic risk shared with other psychiatric disorders such as major depressive disorder [4, 5]. Specific causal variants have not been found, and for such a common disorder it is unlikely that a high-penetrance causative allele would exist. Rather, the field today agrees that the genetic risk is composed of several small-effect variants, which likely interact and affect various biological pathways. Another reason why describing the genetics of anxiety disorders is a complex endeavour is that environmental factors also play a significant role. The best known environmental risk factor is the exposure to chronic psychosocial stress, particularly in early life [6]. However, it remains largely unknown how or why such a relationship between stress and psychiatric disorders exists. What does stress do to the brain, and why does stress do different things to different brains?

Researching these matters in the human brain is limited in many ways. For example, we do not have access to brain tissue at selected time points, nor precise knowledge of when and what types of risk factors an individual experiences. Because addressing these questions is necessary for improving our understanding of disordered anxiety, many researchers select alternative model systems in which the required features are evolutionarily conserved to a sufficient

degree. Mice (*Mus musculus*) share a considerable number of genes with us [7] due to conservation from our shared ancestry, along with a highly similar stress response system (such as the hypothalamic-pituitary-adrenal axis, [8]) and the capacity to display anxiety-like behaviours on specifically designed tests [9]. The commercial availability of inbred strains of mice, with innate variability in anxiety-like behaviour, also enables to the study of influences by genetic background. This makes mice a suitable model system for the study of the neurobiology of anxiety and stress. Species-specific features, such as the extended evolution of the human cortex and the capacity to verbally express subjective anxiety, limit the ability to generalise from animal models to human populations. However, with these limitations in mind we can still meaningfully enhance understanding of the mechanisms of disordered anxiety.

Such studies have over the years pointed to the importance of brain plasticity in the development of and recovery from psychiatric disorders [10]. Until quite recently, the concept of plasticity was rarely extended beyond that occurring in neurons, specifically at synapses. However, experience-related alterations in another part of the nervous system has been proposed to operate alongside this, including myelin plasticity [11]. Myelin provides insulation and sites of optimal ion channel placement for axons, enabling fast action potential propagation. Optimally timed action potentials are at the core of brain function, which involves networks of neurons in near and far regions communicating in a synchronous manner [12]. Indeed, synchronous inputs are even critical for synaptic plasticity [13]. The discovery of experience-related myelin plasticity broadened our conceptualisation of adaptive brain plasticity, but also raised the possibility of maladaptations. Anxiety disorders and other psychiatric disorders are today seen as occurring from maladaptive processing across networks, rather than within single brain regions. Mechanisms affecting such network-level processes, such as myelin plasticity, are thus attractive candidates in the search for neurobiological underpinnings of anxiety disorders.

In this thesis we first mapped which brain regions within the network are engaged by chronic psychosocial stress in mice. To then explore more deeply what happens in some of these regions, we performed RNA-sequencing of tissue collected from stress-exposed and control mice from two different genetic background. We identified myelin-related genes as differentially expressed following stress. Finally, we used structural (transmission electron microscopy) and genomic (RNA-sequencing of enriched OLGs and myelin) approaches to study how myelin is involved in stress-resilience and -susceptibility, with implications for understanding of anxiety disorders and other stress-related psychopathology.

2. Literature review

2.1 Anxiety & Stress

2.1.1. Anxiety and anxiety disorders

In order to avoid danger, our ancestors adapted the capacity to anticipate threats and respond in preventive ways before the threats manifested. In psychological terms we call this anxiety, which refers to a broad range of both subjective and objective experiences with the goal of self-preservation. The word *anxiety* has its roots in the Greek word *angh* referring to a state of physical or philosophical constriction. The Finnish word for anxiety (*ahdistus,* the root word *ahdas* translates to "restricted/tight space") also captures the feeling of anxiety. The connotations of *anxiety* are often negative, as the subjective feelings that arise with it are generally unpleasant. We feel worried, hypervigilant and agitated, and may start ruminating over the possible threat, such as an upcoming course deadline or interpersonal conflict. When experiencing anxiety we are influenced by much of the same physiological response as we are when facing stressful situations in broader terms (discussed in detail below). Colloquially the term *fear* is sometimes used interchangeably with anxiety, but strictly speaking these two feelings are distinct, albeit often intertwined [14]. Fear refers to a threat response directed at an imminent, certain threat, while anxiety is directed at ambiguous or merely potential threats. Although these responses provide an animal with an adaptive edge, such as avoiding novel environments not because there definitely is a predator, but because there might be, anxiety comes at a cost. This cost is the loss of opportunities to, for example, gain resources or new mates. Thus, the anxiety system needs to be active in a balanced way, keeping us safe from harm while allowing us to take appropriate risks to survive and advance.

Like most of our bodily systems, the anxiety system can become disordered. This refers to a state where an individual's drive to avoid risk comes at a significant and disproportionate cost to well-being, both as resources lost and as subjective suffering. Clinically speaking, *anxiety disorders* is an umbrella term for a heterogeneous group of syndromes with both shared and distinct symptoms. In the Diagnostic and Statistical Manual (DSM-5, [15]) and International Classification of Diseases (ICD-11, [16]) this includes generalized anxiety disorder (GAD), social anxiety disorder (SAD, also called social phobia), panic disorder, specific phobias, agoraphobia, separation anxiety disorder and selective mutism. The common feature of these disorders is that the patient experiences prolonged and disproportionate anxiety, which may be targeted toward certain kinds of stimuli or without a specific target and impairs functioning.

The symptoms should also not be attributable to other somatic or psychiatric diagnostic categories. Due to her or his anxiety the person is unable to partake fully or at all in many of life's joys, such as social activities or spending time in public spaces. As a whole these disorders have the highest lifetime prevalence rate across all psychiatric disorders globally (16 %), with women 1.7 times as likely as men to be affected [1, 17-19]. They are highly comorbid with both psychiatric and somatic illnesses, such as major depressive disorder (MDD; 46 % of cases also meet criteria for an anxiety disorder during their lifetime, [20]) and cardiovascular disorders [18], which may in part be due to shared underlying genetic risk factors [21, 22].

In older revisions of the diagnostic manuals, obsessive-compulsive disorder (OCD) and post-traumatic stress disorder (PTSD) were also included under the anxiety disorders term. While they share some features with today's anxiety disorders, they have been separated into their own respective classes in the new revision [15]. For example, while PTSD is intimately connected to stress, the symptoms that cause distress to the patient stem from a very specific traumatic exposure [23], as opposed to the more diffuse or general worries of a patient with GAD.

Given that anxiety is a necessary part of life, how can we distinguish this from a disordered state that requires treatment? Grupe & Nitschke [24] conceptualized disordered anxiety as a biased anticipation of future events to be threatening rather than safe. Disorders would thus arise from disturbances in the anticipation system. For example, a person may be hypervigilant to perceive signals of possible threats, hyperreactive to these signals, inflate their estimation of how threatening a stimulus really is, or not be able to learn that a neutral stimulus is in fact not dangerous. These features may promote an individual to choose avoidance strategies where none are required, because avoidance is incorrectly thought to have prevented a negative outcome. Finally, Grupe and Nitschke suggest that disordered anxiety may also stem from deficient top-down control over behaviour and cognition when faced with potential threats. This provides a framework within which to understand how an adaptive response can, in some individuals, become maladaptive.

Clinically, the distinction between adaptive and pathological anxiety remains a point of debate. Some, like Wakefield and colleagues [25], have argued that the diagnostic criteria for anxiety disorders often capture a part of the anxiety spectrum which may be inconvenient according to social norms but not a medical disorder requiring intervention. They acknowledge that

disordered forms of anxiety do exist, but suggest that we need to consider carefully the criteria at which they are considered disorders. To use SAD as an example, it may not be disproportionate to even feel uncomfortably anxious in the face of social situations where one may be scrutinized. Treating such a state would thus not in every case be productive. This also brings us to the distinction to be made between *state* and *trait* anxiety. The former refers to a momentary condition elicited by an anxiogenic stimulus, while the latter refers to the tendency of an individual to have high state anxiety, possibly arising from the mechanisms proposed by Grupe and Nitschke. An anxiety disorder could thus be understood as an extreme form of trait anxiety. Considerable care is required on behalf of diagnosing clinicians and of researchers using animal models to study features of anxiety disorders. The aim of treating anxiety disorders is not to remove the adaptive capacity for state anxiety when the situation warrants it, so an understanding of the full range of anxiety-like features is necessary.

The diagnostic categories, and particularly their use in a research setting, have also been criticised on the basis that they assign symptoms from quite different neurobiological modalities under one nosological term. This implies that all different symptoms afflicting the patient would stem from a single common disturbance, and treating this disturbance should ameliorate all symptoms. Recent efforts, such as the NIMH's Research Domain Criteria (RDoC, [26]), have been made to re-frame our thinking about anxiety and other psychiatric disorders into multiple functional, continuous domains. In this framework, each disorder is characterised by disturbances in several different systems, and these disturbances are not exclusive to a particular diagnosis. On the other hand, the heritability of different anxiety disorders has been eloquently described as "not respecting DSM boundaries"[27], which suggest that the biological basis for different syndromes is at least in part shared. Specificity is required in both clinical and research contexts to ensure that nothing gets lost in translation in order to move our understanding of these conditions forward.

2.1.2. Current treatment of anxiety disorders

When a person seeks treatment for their anxiety symptoms (which have typically started at least months if not years prior, [28]), the first line of treatment in Finland is pharmacotherapy, or a combination of pharmacotherapy and psychotherapy if available [29]. Anxiolysis can be achieved by several compounds. The earliest ones were pharmacologically non-specific with high risk of undesirable side effects. These include benzodiazepines, which became the first line of treatment at their discovery in the 1950s [30]. While acutely anxiolytic, these

compounds are also generally sedative as they act on several subtypes of γ-aminobutyric acid (GABA) receptors, and addiction, non-adherence, tolerance are also major concerns [31, 32]. The search for better options for treatment quickly became relevant, and remains an active field today.

Around the same time as benzodiazepines became available, the monoamine oxidase inhibitor (MAOI) class of drugs was observed to have beneficial effects on low mood in tuberculosis patients [33]. More specific promoters of the monoaminergic system, such as selective serotonin re-uptake inhibitors (SSRIs) became the standard for treating MDD. Later evidence also emerged suggesting their efficacy in treating at least some of the anxiety disorders, and currently they are often prescribed for certain anxiety disorders [34]. The issues with SSRIs and the similarly implicated selective norepinephrine re-uptake inhibitors (SNRIs), MAOIs and tricyclic antidepressants are today also well known. They have limited effectiveness in achieving remission (approximately 30 %, [35]), even when they do work the therapeutic action comes with significant delay, and many patients experience side effects, including worsening of anxiety symptoms [35, 36]. A highly efficacious treatment should arguably target the core dysfunction(s), reversing or otherwise improving them rather than merely alleviating symptoms, and this is naturally the goal of ongoing preclinical and clinical research. While the field is looking for new ways of targeting treatment, the old ways are not forgotten. Many are also working on understanding the non-serotonergic effects of SSRIs on, for example, neural plasticity [37], which could help optimise treatment protocols to benefit more patients.

Concurrent with or independently of pharmacological treatment, many patients with an anxiety disorder are also treated with psychotherapy. Among the plethora of different types of psychotherapy, cognitive-behavioural therapy is suggested to be the most efficacious approach [38]. Evaluating the effectiveness of psychosocial interventions is challenging because the response criteria are not as standardised as those used for evaluating pharmacological approaches [39]. Approximately half of treated patients across several trials showed signs of improvement. A substantial portion of patients thus respond only partially or not at all, similarly to pharmacological strategies. Although the hope surrounding neurobiological research of anxiety disorders is often phrased as providing new pharmacological treatment targets, such work is equally necessary for driving non-pharmacological treatments forward. An understanding of pathobiological dynamics, the influence of environmental exposures, and individual differences can also be integrated to develop better-informed psychotherapies.

No compounds with novel mechanisms of action have been approved for the treatment of anxiety disorders in over 10 years at the time of writing, although clinical trials are on-going for compounds targeting nearly all known neurotransmission and neuropeptide systems [2, 32]. For example, the partial N-methyl-D-aspartate (NMDA) receptor agonist D-cycloserine has shown promising results in both preclinical animal studies and studies using human patients. Through its action on the glutamatergic system it is thought to facilitate the extinction of previously acquired fear memories, which are prevalent in e.g. SAD as well as PTSD [40]. In long-term follow-up studies the effect was not found, suggesting benefits may be short-lived [41]. Efforts are also made to produce more personalised treatments, underscoring the complex heterogeneity underlying anxiety disorders. Corticotropin releasing hormone (CRH, also called corticotropin releasing factor [CRF]) antagonists did not show efficacy in the early clinical trials, but if targeted to patients carrying specific genetic variants affecting the CRH system one may see more encouraging results [42]. However, while knowledge about the pathobiological mechanisms underlying anxiety is lacking, pinpointing an optimal drug or treatment target will be extremely difficult. As preclinical and clinical work proceeds to uncover these mechanisms, hope renews for us one day achieving this goal.

2.1.3. Aetiology of anxiety disorders

Until very recently, the genetics of anxiety disorders were a black box; genetic factors have long been known to contribute, but specific variants and how they contributed to disorder development were not known [27]. Twin studies have demonstrated that they are moderately heritable (approximately 40 % of variability attributable to genetic factors, [3, 22]). For complex and common disorders like anxiety disorders it was never likely that one would find singular causative variants. Rather, the genetic risk is composed of several variants collectively increasing risk in small increments [43]. To detect such variants to be associated with disorder cases compared to healthy controls, a genome-wide association study (GWAS) needs to have a large sample size. Within the last two years, such sample sizes have finally been achieved.

Meier et al. 2019 [44] report a genome-wide significant association with variants in the gene *PDE4B* in a combined patient group with anxiety or stress-related disorders (n ~ 13 000). The homologous mouse gene *Pde4b* was differentially expressed in the medial prefrontal cortex (mPFC) and ventral hippocampus (vHPC) in mice which, after exposure to chronic stress, displayed social avoidance. This lends support to variants within this gene possibly being aetiologically relevant, and future work will be needed to probe this further. Purves et al. 2019

[5] utilized the large UK Biobank sample to define over 19 000 and 25 000 participants as currently experiencing anxiety symptoms or having a current or past anxiety disorder diagnosis, respectively. This report also produced significant associations, but not in the same genomic loci as Meier et al. Some of their hits, such as one in the intron of *NTRK2*, raised enthusiasm. *NTRK2* encodes a receptor for brain-derived neurotrophic factor (BDNF), a critical stimulator of synaptic plasticity, which is perturbed by stressful life experiences [45]. The functional relevance of the variant found in this receptor remains unknown.

One of the major questions within the field has been how much of the genetic risk toward different diagnostic entities within the anxiety disorders umbrella is shared. A large twin study by Tambs et al. [22] suggests that the majority of the genetic risk comes from factors common across these disorders, with only a small portion predicting risk towards one diagnosis but not others. A meta-analysis [46] also found a significant hit associating with many DSM classes of anxiety disorders, this time in a non-coding region. Meier and colleagues additionally analysed correlation between the overall "genetic signature" of their patient group and found significant association also with other traits, including other psychiatric disorders. High correlations between anxiety disorders and MDD have also been reported by others [4, 5, 44]. This suggests that a substantial portion of the biology underlying these disorders is shared. While this may give hope of eventually finding a mutual actionable treatment target, it is worthwhile to note that within-diagnosis heterogeneity in symptoms may still represent distinct biological mechanisms. The study of both discrete and shared genetic factors is thus valuable.

Given the conceptual relationship between disordered and adaptive anxiety, many have chosen to explore anxiety as a dimensional variable. Such an analysis was carried out in nearly 200 000 participants of the Million Veterans Program [47], which revealed 6 significant loci. Of note, the majority of the participants in this study were male, so potential sex-specific effects could not be assessed. Keeping in mind the higher female prevalence, sex differences remain an important avenue of study, although rarely addressed. Nagel et al. [48] quantified trait neuroticism, a personality parameter associated with risk of developing an anxiety disorder, in nearly 500 000 people. With over 100 independent variants, mostly in non-coding regions, and nearly 600 implicated genes derived through computational modelling, this represents the largest study of an anxiety-related trait to date. Among the associated variants was one within the encoding corticotropin-releasing hormone receptor 1 (*CRHR1*), an important player in the hypothalamic-pituitary-adrenal (HPA) axis (see below). Whether and how these variants

contribute to the transition from non-pathological neuroticism to an anxiety disorder will require further study.

Genetic factors also interact with other factors to add to anxiety disorder risk. The aforementioned large GWAS studied have unfortunately not included analyses of other phenotypic data, such as exposure to known environmental risk factors, in order to assess potential gene-environment interactions. These risk factors, such as chronic psychosocial stress, have been shown to increase risk particularly in those with high genetic risk [49, 50]. This is the most well-characterized environmental risk factor for anxiety disorders, and for a host of other psychiatric disorders [51]. For example, adolescents who experienced sexual abuse in their childhood have 3.9 – 4.8 times higher risk of developing an anxiety disorder [52]. As stress-exposure is also a common occurrence in human life, understanding how it contributes to disorder aetiology is a major field of research and the focus of the next section of this thesis. Studies focusing on stress interacting with specific variants in candidate genes (genes which are of interest because of prior hypotheses regarding pathophysiology) have been performed but with very limited sample size. For example, Nestor et al. [53] report an interactive increase in risk for a range of psychiatric symptoms, including anxiety, in students reporting childhood trauma who also carry the short allele of the *5-HTTLPR* gene. A significant challenge in this and other similar studies relates to measurement timing. Retrospective reports of trauma may be biased by current affective state; a person currently suffering from anxiety may be more likely to recall early traumatic experiences than those without anxiety. Longitudinal follow-up studies shield against this, but require large sample sizes to capture affected persons and are extremely lengthy to conduct [51]. The study of how environmental and genetic factors may interact in anxiety disorder aetiology is still in relative infancy, but hopes are high for future break-throughs.

There is hope that the study of psychiatric genetics will eventually provide benefits for patients in various ways. A lesson in how this can be achieved can be learned from another common and heterogeneous disease state: cardiovascular disease [43]. Despite its complexity, accumulating data on both genetic and environmental risk factors has enabled the generation of personalized prediction tools which inform treatment selection, and the development of treatments based on novel biological mechanisms discovered via genetics (e.g. *PCSK9*). There is no logical hindrance as to why, with sufficient data, these paths could not be followed by psychiatric genetics at some point in time.

2.2. Stress as a risk factor for anxiety disorders

2.2.1. What is stress?

Since the primordial pool, organisms have needed to contend with various threats to their existence. When, for example, a predator approaches, many species employ what we today call the stress response. It is also often referred to as the fight/flight(/freeze) response, as the goal is to adjust available resources to deal with the acute threat to survival; either confronting it, fleeing from it, or in some cases minimize the chance of being spotted and waiting for the threat to pass. Anxiety is conceptually related to stress as they both pertain to dealing with threats. In this context, stress refers to a general response to any challenge that requires an individual to respond, while anxiety is a response specifically to a non-imminent and/or potential threat. By contrast, fear describes the response to an imminent, certain threat [14]. Experimentally stress, fear and anxiety are notoriously difficult to separate, and many of their neurobiological and endocrine features are shared.

The term *fight or flight response* dates back to Walter Cannon's notion of organisms needing an emergency response system to deal with external threats to internal balance [54]. Despite being limited in terms of available methods to determine the molecular components of this response, Cannon reasoned that it should exist to guide metabolic processes towards either fleeing from the approaching threat, or aggressive confrontation of it. Hans Selye [55] posited that the same system becomes activated even when faced with quite different stimuli, such as cold temperatures and imminent predators, prompting his theory of a general adaptation syndrome (GAS). Cannon's emergency response is essentially the first stage of Selye's GAS, also called the alarm reaction. Capturing the transient nature of the response, Selye suggested that the alarm reaction is followed by a resistance phase, where the body attempts to terminate the response, which succeeds if the cause of the alarm reaction is no longer present or threatening. Interestingly, Selye also pointed out that the GAS seems to be relevant for a host of somatic illnesses, such as hypertension and inflammatory conditions. To explain this relationship, he suggested that the third phase of GAS is exhaustion, caused by depletion of resources necessary for resistance. In situations with consistent and relentless stress triggers, a person would be vulnerable to exhaustion, and thus to a host of health problems. This matter is discussed below in more detail.

2.2.2. Physiology and neurobiology of stress and anxiety

Physiologically, the alarm reaction portion of the stress response consists of activity of two parallel systems; the HPA axis and the sympathetic adrenomedullary (SAM) system. Both involve the coordinated systemic release of hormones (glucocorticoids [GCs] and adrenaline/epinephrine, respectively) which enable optimal allocation of resources, such as glucose and blood flow, to systems which are necessary for immediate survival [56]. Many of these hormones, such as GCs, are also stimulated by non-threatening stimuli, such as physical exercise, the ingestion of food, and simply variation in circadian time. These endocrine events have self-regulatory capacity, and are initiated and coordinated by the brain. Decades of work in both animals and humans has corroborated evidence that stress and anxiety (at least as a state) involve largely overlapping neural circuits, and these will thus be discussed in parallel.

In order for the stress and anxiety responses to be initiated, several interlinked circuits of the brain are involved (Figure 1, [2, 57]). These circuits are not organized in a linear manner, where one region receives input from another, processes it and moves it forward to the next target region. Rather, the processing is layered and composed of several bidirectionally connected loops, allowing feedback regulation and updating new information. This ensures that an appropriate early, potentially life-saving response is generated as fast as possible, but the response is adjusted by the involvement higher cognitive functions.

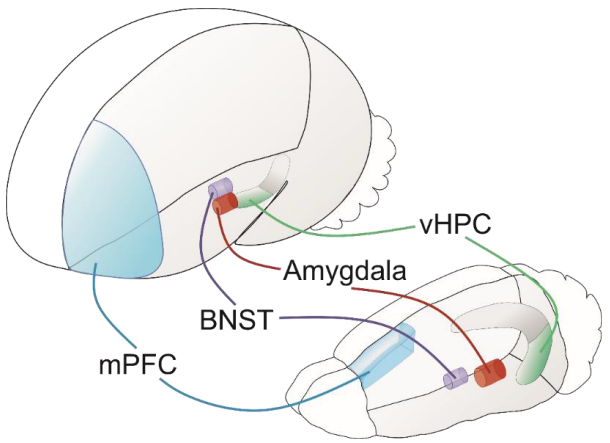

Figure 1. Illustration of critical nodes of the brain's stress and anxiety network. The same regions are depicted in the human (top) and mouse (bottom) brains. mPFC = medial prefrontal cortex, BNST = bed nucleus of the stria terminalis, vHPC = ventral hippocampus.

Firstly, most obviously in the case of external threats, sensory systems need to convey a perception of the stimulus. At this level most stimuli are arguably processed as neutral in valence, although exceptions exist in terms of innately threatening stimuli [58]. For both innate and non-innate stimulus processing to proceed towards the stress response, the stimulus must be interpreted as potentially threatening. The amygdala, specifically the basolateral nucleus (BLA), is critical for assigning a stimulus as threatening, as well as learning about novel threatening stimuli [59, 60]. Chronic stress in animals has been shown to increase dendritic branching in this region, in addition to an adjacent structure called the bed nucleus of the stria terminalis (BNST, historically also called the extended amygdala, [61, 62]). While also involved in threat assessment, the BNST's role has been suggested to apply more to uncertain threats, such as those eliciting anxiety, rather than immediate ones [63, 64]. The central nucleus of the amygdala (CEA) receives input from the BLA and can in turn stimulate the hypothalamus to activate the HPA axis and the periaqueductal grey (PAG) to elicit behavioural responses, such as freezing in rodents [57, 65]. The BNST is similarly connected with regions mediating the outward stress response [64]. Within these regions lie several distinct neuronal populations, some of which when active promote anxiogenic responses to new situations while others suppress them [66]. Dissecting the roles of these regions and their internal and projecting connections has revealed a lot about the complexity of initiating the stress response

For a proportional response to occur, a well-working brain also evaluates the level of the threat to modulate the intensity and duration of the stress response. This includes processing memories of similar past stimuli, what responses they elicited, and with how much success. Memories of the stimulus are also formed or updated to inform response selections on potential re-encounters in the future. This regulation of the stress response is critically mediated by the prefrontal cortex (PFC), a region also associated more generally with executive control [67]. Hernan and Cullinan [68] review evidence suggesting that innate/non-learned stressors, such as hypoxia, produce HPA-activation with little input from the PFC, while the response to stressors involving learning or integration of signals from multiple sources depends on PFC involvement. Joseph LeDoux has also argued that cortical processing is fundamental for the subjective experiences of states like anxiety and fear, operating to a degree separately from the limbic structures controlling physiological states [14]. Owing to this being one of the last regions of the brain in mammals to reach maturity, it is argued to be particularly sensitive to

insults such as chronic exposure to stress [69]. Subregions of the PFC, such as the prelimbic cortex (PrL) in rodents and ventromedial PFC in humans, are intricately connected with the amygdala, providing top-down modulation of its activity and facilitating the learning of threatening and safety stimuli [57]. This level of processing enables online regulation of the stress response as it is carried out.

Some minutes after the stress response has been initiated the self-regulatory negative feedback loop of GCs guides the system to return to a homeostatic state, ready to deal with the next incoming crisis. The hippocampus (HPC) contains a high density of GC receptors (GRs), and early lesion studies demonstrated its role as an inhibitor of HPA activation [70]. Unlike the amygdala and BNST, where chronic stress produces more complex dendritic morphology, in the rodent HPC chronic stress causes atrophy and simplification of neurons and their dendrites [62]. Reduced hippocampal volume is also seen in humans with extensive stress-related psychopathology, such as MDD [71]. In addition to its established role in memory and cognition, which are also altered by stress exposure [72], this complex structure also involves circuits which interact heavily with the mPFC and the amygdala to moderate anxiety-like responses to situations with novel, uncertain stimuli. Lesioning the ventral, but not the dorsal, HPC reduces the expression of anxiety-like behaviour [73]. Specific kinds of oscillatory activity becomes increasingly synchronised between the ventral HPC (vHPC) and mPFC in mice while performing an anxiogenic task [74]. Exogenously induced activation of the vHPC-mPFC connection, achieved by viral targeting of specific artificial receptors and delivery of a specific activating ligand, also increases anxiety-like behaviour in mice [75].

These circuits orchestrate the selection of appropriate responses, including behavioural (ceasing irrelevant behaviours, re-directing attention), emotional (feeling uneasy, anxious or frightened), and physiological (HPA-axis activity) responses. Many of the critical nodes of the circuit have been demonstrated to be functionally altered in patients with anxiety disorders. One frequent finding is that compared to healthy controls, participants with an anxiety disorder show exaggerated amygdala reactivity when presented with threatening stimuli during functional magnetic resonance imaging (fMRI). Similarly to genetic risk factors, this finding applies across diagnostic categories, representing a general feature of disordered anxiety [76]. This hyperreactivity relates at least in part to lower activation of PFC subregions during a threat perception task in people who score higher on measures of anxiety than those who score lower [77]. Interestingly, high anxiety relates to increased functional connectivity when viewing

angry or fearful faces between some regions (right amygdala and dorsomedial PFC) but decreased connectivity between others (left amygdala – anterior cingulate cortex). In this and many similar studies it is difficult to separate the influence of state and trait anxiety on outcome measure. Imaging studies of clinical populations, which have high trait anxiety, typically have small sample sizes of heterogeneous patients and often lack coverage of the whole disorder process from a presymptomatic stage through treatment responses. Hence it is difficult to entangle if imaging features represent pre-existing vulnerabilities, the disorder process itself, or adaptations to treatment.

In terms of cortisol, the major endocrine output of HPA activation, links to anxiety disorders are inconsistent. Some report an increase in daytime cortisol [78, 79], while others report a decrease [80]. In the latter, the decrease is only observed in anxiety disorder patients with a history of childhood maltreatment; patients with no known maltreatment history show a trend for increased cortisol. A more recent study reports no differences in constant levels (as measured from hair) or responsivity to a stressful task in generalized anxiety disorder compared to non-anxious controls [81]. These data suggest that disordered anxiety does not involve alterations in all nodes of the stress system, but associates with disturbances in certain brain regions. How these disturbances develop, and the role chronic stress plays in this development, are an area of active enquiry.

2.2.3. Chronic stress and implications for health

The described stress response is best suited for dealing with acute and transient stressors. As opposed to a homeostatic system, which aims to maintain a specific adaptive state, the stress response system is allostatic [82]. Allostasis refers to an adaptive change in the system intended to respond to a change in the demands placed on the organism to survive, such as encountering a threat. An allostatic system is responsive and dynamic, but ultimately it aims to return the system to a state where homeostasis can once again be achieved and maintained. When an organism is continuously exposed to stress-inducing stimuli, the system is not able to return to a homeostatic state, as noted by Selye when he described the state of exhaustion. Instead, as Bruce McEwen proposed, the organism starts to incur damage from an allostatic load [83]. On repeated encounters with the same stressor, provided it was successfully dealt with and hence deemed non-threatening, it is advantageous for the organism to habituate. Habituation refers to a gradual diminishment of the response to repeatedly encountered stimuli, and it acts as a resource conservation mechanism, saving the strong responses to either unfamiliar or known

severe threats. Habituation of HPA activation has been consistently observed across species and triggering stimuli [84]. Thus, allostatic load can be caused by a failure to habituate to continuous stressors or to appropriately downregulate the allostatic response [83, 85].

As noted before, exposure to stress poses a major risk factors for anxiety disorders as well as other harmful outcomes in terms of psychiatric health and brain development. This is particularly true of stress experienced in early life, possibly because of ongoing development during sensitive periods which close later in life [6, 86]. For example, myelination of cortical regions is largely incomplete during adolescence and early adulthood [87, 88], a period of significant potentially stressful life experiences as well as the most common period of onset for mood and anxiety disorders [89]. Subjective recall of early life trauma is a superior predictor of adult internalizing psychopathology (such as mood and anxiety disorders) than objective records of traumatic events, suggesting that how an individual experienced the event is critical for downstream consequences [90]. Biases in recollection of earlier trauma, caused by current symptoms, may also account for this relationship. Brody et al. [91] reported that physiological indicators of allostatic load (high resting blood pressure and morning cortisol) in an adolescent sample were related to previously reported adversities, but these indicators were high even in those without current depressive symptoms. This suggests that the mechanisms by which chronic stress affects certain physiological measures may not be the same as the mechanisms responsible for the association with psychiatric disorders. These findings raise important questions about how stress could have such long-term detrimental effects on mental health; while the relationship is well-established, the mechanisms underlying it have remained elusive.

We now know that Selye's resistance phase on the molecular level involves a negative feedback loop of GC signalling. The binding of GCs to GRs at the hypothalamus and HPC initiates a signalling cascade that inhibits the release of further GCs [70]. Chronic stress curiously associates with a reduced density of GRs at the HPC [92]. This in turn arguably lowers the capacity for negative feedback, leading to perpetually elevated levels of GCs [93] and reduced ability to downregulate the stress response [94] seen in for example MDD. In addition to the immediate fight/flight response, GCs produce various effects on our cells via GRs which, when activated, alter gene transcription. Adaptations at the level of GRs and their actions may in part mediate the effects of chronic stress on health, and while statistically this mediation has been reported it remains unknown whether there is a true causal chain particularly when it comes to psychiatric health [95].

Chronic stress also affects fine structural features of the brain, but whether these effects are due to GCs or other factors remains unknown. For example, as mentioned above, neurons in the HPC and PFC of rats have fewer dendritic branches after chronic stress compared to non-stressed rats, while dendritic arborisation was increased by chronic stress in the amygdala and BNST [61, 62, 96]. Given that these regions are critical nodes of the stress and anxiety networks, such structural changes may be relevant for disordered stress responses and anxiety. Indeed, both traditional and novel treatments for MDD, such as fluoxetine and ketamine respectively, act on synapses in at least the HPC as part of their antidepressant effect [97-99]. However, the varied patterns on synaptic effects of stress seen between different brain regions may explain why these mechanisms have yet to be fully harnessed as efficacious treatment targets. To this end, we need to expand our understanding of how these effects arise in different brain regions as a function of stress exposure.

2.2.4. Behavioural neuroscience in the study of anxiety and stress

Due to the aforementioned high evolutionary conservation of threat detection and survival systems, stress and anxiety can be studied in multiple different organisms, each with unique advantages and disadvantages. Human subjects can be recruited to study the effects of experimentally simulated stress or anxiety disorder status on parameters like GC responses, subjective feelings of stress or anxiety, and brain-wide metabolic and electrical activity. However, in humans we cannot access brain tissue for the study of how particular cells respond to stress or other molecular-level endeavours. We also lack the ability to control the nature and timing of naturalistic stressors as well as the genetic make-up of the study sample, which adds considerable variability to output measures. To complement human research, we thus turn to animal models where these limitations can be addressed at least to an extent.

For an animal model to be useful, one must carefully consider how its features match its purpose, all while considering ethical constraints and animal well-being. When it comes to psychiatric phenotypes, it is widely agreed that non-human models cannot fully recapitulate every feature of the disorder [100]. Rather, an animal model is used to capture some specific feature or dimension involved in the disorder, thus building on the knowledge base. When selecting an appropriate model system for a desired feature it is critical to consider the validity of the model. Broadly speaking, validity refers to the accuracy with which a test or model targets what it is intended to target. A good animal model system would need to share key features (construct validity), appear similar on observation (face validity), and respond to the

same manipulations, such as pharmacology (predictive validity) [101]. A challenge for animal models of complex psychological phenomena is that validity can only be determined against current knowledge about the target construct, such as disordered anxiety. However, our knowledge about these phenomena are also limited until expanded upon by work from both the clinical and preclinical sides [9].

Two additional aspects of validity are external and internal validity. The former refers to the generalizability of knowledge gained from the model, such as the ability to apply findings from a non-human animal species to human patients. The more similar the study sample thus is to humans, the higher its external validity. However, human populations are highly heterogeneous. A heterogeneous research sample poses many challenges such as added variability, which in turn necessitates the use of larger numbers of animals. It also risks lowering internal validity, i.e. the consistency of the model. This is at odds with prevailing initiatives to reduce the numbers of animals used, such as the 3Rs [102]. To improve internal validity, one strategy is to make use of a highly homogenous study sample. Inbred mouse strains, commercially available in over a hundred varieties, have become a standard tool in behavioural neuroscience. Mice belonging to the same strain are genetically isogenic, thus considerably reducing variability and improving the consistency, but potentially reducing generalizability of the data across other strains and even species. Selecting a model system is thus a balancing act between achieving a high internal validity without losing external validity.

Another advantage of inbred mouse strains as models is that each strain has unique features. Employing several different strains in the same study provides a way to model how genetic background moderates the effect of an independent variable, such as a genetic mutation, on an outcome variable like anxiety-like behaviour. Sittig et al. [103] demonstrated this beautifully by producing a heterozygous knock-out of TCF7L2 in 30 different inbred strain crosses. In the A/J strain the effects of this haploinsufficiency included higher startle response to a sudden sound. By contrast, in the DBA/2J strain the effect was reduced startle response compared to wildtype littermate control mice. Research involving several strains has also demonstrated notable differences between even naïve mice from different strains. For example, mice from the C57BL/6J strain show low tendency for anxiety-like behaviour across several tests (see below), while DBA/2J mice behave in a manner consistent with a high-anxiety state [104]. Thus, considerate use of multiple inbred mouse strains with carefully selected features can

provide several improvements both in terms of internal and external validity compared to using just one strain.

2.2.5. Animal models of anxiety-like behaviour and chronic stress

For the study of anxiety, one common approach is to measure the degree to which an animal in a specific environment expresses relevant behavioural, metabolic, sympathetic or endocrine responses. Self-report of subjective sensations like worry or rumination cannot be collected, but the aforementioned factors are critical also in human anxiety and can thus be used as valid indicators of animal anxiety-like phenomena [9]. Tests of anxiety-like behaviour in rodents place the animal in a novel context with a conflict; approach a potentially dangerous part of the environment (e.g. an open, brightly lit area) or remain in a dark confined part (Figure 2). These tests are useful for detecting anxiolytic properties (at least of GABAergic compounds; they may not be optimal for detecting novel compounds) and for examining the effects of a genetic modification on anxiety-like behaviour [32]. As evidence for their external validity, in a naturalistic study of human behaviour Walz et al. [105] showed that patients with an anxiety disorder were more likely to avoid walking across an open market place than healthy controls. When conducting these tests it is critical to note that they are susceptible to various confounding factors, such as alterations in locomotor, sensory or motivation systems caused by pharmacological compounds or genetic modifications of interest, as well as stress [106, 107]. Most tests are also sensitive to habituation; repeated exposure to an environment or stimulus affects how the animals behave on subsequent trials. Particularly in the elevated plus maze (EPM) rodents typically show low motivation to explore the open arms on consequent trials, unless a considerable delay is introduced, at which point the readout cannot be reliably interpreted to reflect anxiety [108, 109]. Other tests relying less on motivational or locomotor factors, such as operant conflict conditioning (also known as the Vogel Conflict Test, [110]), novelty-suppressed feeding [111] and hyponeophagia [112], are becoming increasingly utilised in test batteries to provide more diverse data on anxiety-like behaviour in experimental animals.

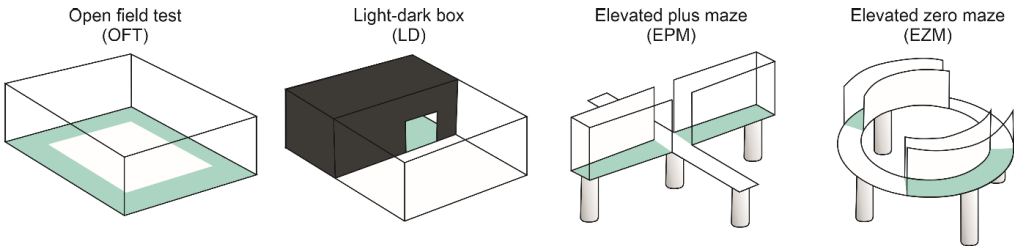

Figure 2. Illustrations of common approach-avoidance tests of anxiety-like behaviours for rodents. The safe/enclosed area is shaded in green. The open areas of the apparatuses is considered anxiogenic, and the more time the animal spends in these areas the less anxiety-like behaviour they are considered to display. From left to right, open field test (OFT [113]), light-dark box (LD [114]), elevated plus maze (EPM [115]) and elevated zero maze (EZM [116]).

As also noted before, anxiety is, to a point, a normal and necessary feature. Based in this many have called to question to what extent a difference between two experimental groups on tests measuring anxiety-like behaviour can be said to have relevance for disordered anxiety. Ethologically speaking, a lack of anxiety-driven avoidance of novel open spaces would be life-threatening for a rodent, so removing this response with pharmacological means is not a desirable end point. However, high trait anxiety does pose a risk for later disordered anxiety [117]. Current conceptualisations of anxiety disorders (and most other psychiatric disorders) also highlight their dimensional nature [118]. Thus an understanding of basic mechanisms across the whole spectrum should, unless significant nonlinearity can be shown, advance our understanding of the dysfunctional state as well.

With this said, a model with high construct validity should also capture anxiety which meets some degree of maladaptivity, similarly to our requirement for a human being diagnosed with an anxiety disorder. Inducing such a condition can be done by exposure to chronic stressors. Such procedures include early (maternal separation [119], altered maternal care [120]) and later (acute or chronic restraint stress [121, 122], chronic unpredictable/variable stress [CUS/CVS, [123, 124]], chronic social defeat stress [CSDS, [125]]) life stress. CSDS involves confrontations between resident aggressor mice and younger less dominant intruder mice, which makes it primarily a psychosocial stressor as opposed to the physical and environmental stressors used in models like CUS (for example wet cage bedding and altered light cycles). Following a confrontation, the intruder mice are housed in an adjacent compartment of the aggressor's cage, with continuous sensory contact but without physical contact. The confrontation and housing arrangement is repeated for typically 10 days, each day with a novel

aggressor to minimize habituation, creating a chronic source of predominantly psychosocial stress.

Rodents exposed to CSDS often develop both acute and chronic signs of increased anxiety-like behaviour, but also despair-like behaviour (an endophenotype of MDD) and social avoidance [126]. Firstly, this is interesting because the same environmental risk factor also predisposes humans to a broad range of psychiatric symptoms. Anxiety disorders and MDD are highly comorbid [20, 127], suggesting possible common underlying pathophysiology, so a stress model that recapitulates the comorbidity has good construct validity. Secondly, much like humans vary in their response to stress, so do rodents. Many people experience significant traumatic events but do not develop later psychiatric symptoms, a phenomenon known as resilience. Similarly, many mice exposed to CSDS demonstrate resilience; their behaviour resembles that of non-stressed controls. Resilience is an active process rather than a lack of effect by stress [128]. These features make CSDS a suitable system for studying the complex consequences of stress on the mammalian brain and body.

In addition to affecting the behaviour of rodents long-term, CSDS also has neurobiological effects. Induction of activity-related protein FBJ murine osteosarcoma viral oncogene homolog B (FOSB), and particularly its truncated highly stable isoform (ΔFOSB) has been shown 24 hours after the end of CSDS in brain regions including the mPFC, BNST and PAG [129]. Several groups have reported effects on neuronal plasticity, such as long-term potentiation and –depression of synapses (LTP & LTD, [130, 131]). Specifically, in hippocampi of stress-exposed rodents *ex vivo* electrical stimulation is not able to produce hallmarks of LTP as it would in non-stressed animals [132]. BDNF, a critical factor for promoting plasticity, is reduced by CSDS exposure in the PFC [133] but increased in the nucleus accumbens (NAc), a reward-related brain region [45]. Such dynamic regionally varying effects on plasticity are thought to underlie many of the behavioural maladaptations, as intervening with them directly or by using antidepressant compounds have been shown to rescue the maladaptive responses [45, 133]. Long-term bidirectional plasticity in stress is a major avenue of research today, but different effects observed in different brain regions have rendered it a difficult direct treatment target. This highlights the need for simultaneous molecular and network level studies of stress and its consequences; only with a complete understanding of the process will we be able to find the critical nodes to target.

2.3. Myelin plasticity

2.3.1. What is myelin?

As noted above, neural plasticity mechanisms have become increasingly the focus of research efforts when it comes to stress-related psychopathology [10]. However, the notion of plasticity to many neuroscientists still primarily refers the plasticity of neurons and their synapses (e.g. LTP or LTD), while plastic properties are also found in terms of adult neurogenesis [134] and angiogenesis [135]. The neurobiological features in anxiety and depression are largely considered to be circuit-level rather than single neuronal populations within selected regions [136, 137], and thus a circuit-level form of long-term bidirectional plasticity could reasonably be expected to play a critical role. Through the next chapters I hope to convince you that myelin plasticity represents such a mechanism, and that this is a novel frontier from which to tackle the challenges we have faced in understanding these disorders.

Myelin is to most synonymous with a lipid insulator of axons, enabling fast conduction of action potentials. Myelin is produced by specialised cells (oligodendrocytes [OLGs] in the brain and spinal cord, and Schwann cells on peripheral nerves) as enormous extensions and re-organizations of their cellular membranes (Figure 3). The largely cholesterol-based membrane is wrapped around nearby axons in several layers (called lamellae), and specialised proteins compact the membrane tightly and form channels necessary for transporting components from the cell body to the inner layers of the growing sheath.

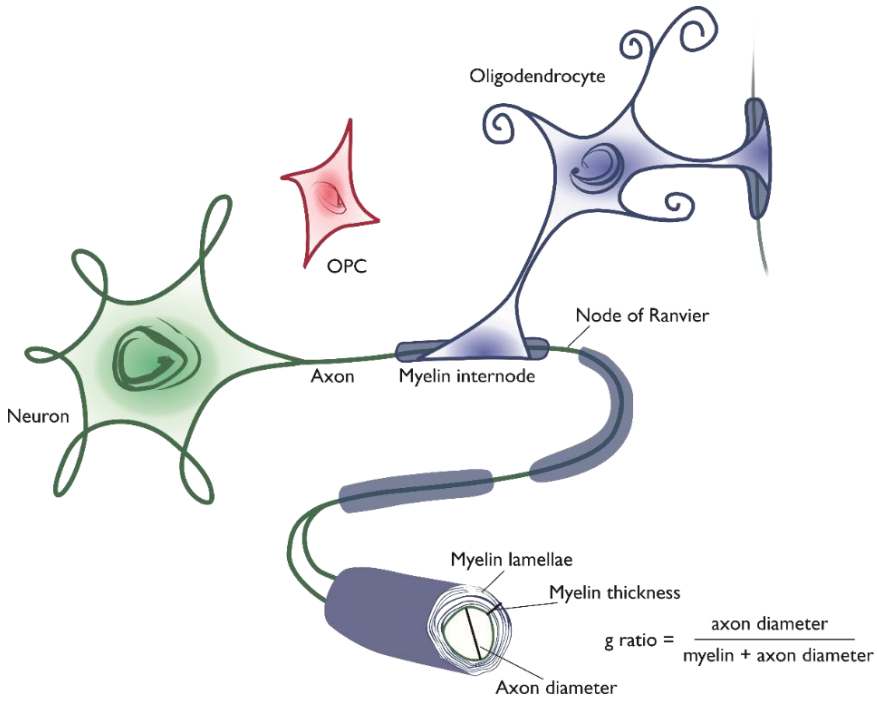

Figure 3. Illustration of the relationships between neurons, OPCs and OLGs. OPCs during development and even in adult brains can differentiate into OLGs, which ensheath axons with multi-layered (lamellae) myelin sheaths. Key parameters include myelin thickness, axon diameter, and their relative ratio expressed as the g ratio.

Unlike the insulators applied in engineering settings, which tend to be complete, a critical property of myelin is that it is interspersed with gaps called nodes of Ranvier. These gaps enable localised ion flow between the axon and the extracellular space, triggered by the arrival of a depolarizing action potential. The result is an even faster mode of signalling called saltatory conduction. In addition to being fast, most brain processes require tight temporal control of the signals involved. For example, for the auditory cortex to provide sensible processing of localised incoming auditory signals, action potentials originating at vastly different parts must arrive simultaneously at their projection targets [138, 139]. Adjusting the speed as well as intra-circuit timing can be achieved by adjusting myelin along the tracts.

The mammalian brain follows a developmentally orchestrated programme of myelination close to and after birth, resulting in largely predictable patterns of high myelin content in axon-rich areas (also known as white matter) and sparse myelination in other regions such as the cortex where cell bodies dominate (grey matter). A computationally optimal g ratio (ratio of the diameter of the axon to the diameter of the whole fibre, including myelin, see Figure 3) for fast conduction has been determined to be 0.6, but most axons in both grey and white matter have

considerably larger (indicating relatively thinner myelin sheaths) and more variable g ratios [140]. Given that speed is ultimately not as important as synchrony, it is imperative that the developmental programme leaves some room for variation.

2.3.2. Developmental myelination

Myelination is a highly conserved feature of cephalised organisms. Much of what we know today both about developmental myelination comes from studies opting for non-mammalian models. For in vivo imaging, the preferred organism for many is the zebrafish (*Danio rerio*), particularly at the early postnatal larval stage. Zebrafish larvae are practically transparent, and combined with their efficient production and ease of genetic modification they lend themselves exceptionally well to developmental biology. We have learned from these organisms that during early development, similarly to synapse dynamics, there is an overproduction of myelin [141]. This is followed by later retraction of some sheaths and stabilisation of others, a process which involves Ca^{2+} signalling in the OLGs [142], at least in part initiated by activity of the neuron which signals via the wrapped axon [143]. Of note, neuronal activity is not a requirement for myelination initiation, as evidenced by the OLGs' tendency to wrap even inorganic nanofibers [144]. Vesicular glutamate release promotes initial myelination on at least some types of axons, although how these events may relate to the Ca^{2+} signals is to date not known [145]. Many proteins which have traditionally been considered synaptic, such as post synaptic density protein 95 (PSD95), also localise in clusters along the myelin sheath, making contact with the axon membrane. Although the exact signals exchanged between the neuron and myelin through these domains are not yet known, disrupting them also disrupts myelin formation in zebrafish [146]. A complex, bidirectional interaction between neurons and OLGs thus impact how specific axons get myelinated de novo.

In order for the OLG to be able to produce myelin, a network of transcription factors (TFs) are employed to both determine lineage progression and coordinate the production of myelin components. Two critical TFs expressed throughout the lineage, from proliferating oligodendrocyte progenitor cells (OPCs) to the postmitotic mature OLGs, are oligodendrocyte transcription factor (OLIG2) and SRY-box transcription factor 10 (SOX10). They regulate the expression of both stage-specific and non-stage-specific genes. Whether a cell remains as a proliferating OPC or differentiates into an OLG depends largely on other TFs. These include SOX6 and HES5 maintaining the OPC state, which are silenced upon initiation of differentiation [147]. During this switch, a TF called transcription factor 7-like 2 (TCF7L2)

plays an important role. In the OPC state it is expressed at a low level and interacts with the Wnt/β-catenin pathway. Via currently unknown mechanisms, differentiation initiation causes TCF7L2 to instead interact with Kaiso, which also alters its DNA binding sites. Finally, when myelination is initiated, TCF7L2 interacts with SOX10 [148]. For proper transcription of myelin component genes (see below), SOX10 in maturing OLGs promotes the transcription of myelin regulatory factor (MYRF), a quite recently discovered TF with several unknown functions. The N-terminal of MYRF is cleaved at the endoplasmic reticulum by an additional unknown mechanism, and the trimerised N-terminal translocates to the nucleus and binds to DNA [149-151]. To maintain the expression of myelin components throughout the long life span of the OLG, TFs like MYRF and SOX10 remain active at high levels, and many have postulated they may also have a role in myelin plasticity, although this function is as of yet unproven [147].

The myelin sheath consists of specialised proteins and lipids. Myelin basic protein (MBP) is a highly abundant CNS myelin protein, and it is critical for compaction of the lamellae [152]. Mice lacking this protein have a very severe and early phenotype involving motor deficits, nearly absent myelin, and early lethality [153]. Other structural proteins include proteolipid protein 1 (PLP1) and 2',3'-cyclic nucleotide 3' phosphodiesterase (CNP), the latter of which is known to oppose the actions of MBP in order to maintain channels passing through the sheath. These channels allow the shuttling of components, such as proteins, nutrients and lipids, from the OLG cytoplasm through the myelin layers into the growth zone located adjacent to the axonal surface called the inner tongue [154]. At least in vitro, neuronal activity promotes myelin formation via inducing the translation of mRNAs localised at the distal processes of the OLG [155]. The lipid composition on the myelin sheath relies on locally synthesised cholesterol, glycosphingolipids and phosphoinositides. Each lipid type appears to have specific functions, including interaction with local proteins and insulation [156]. The molecular complexity of myelin is what enables its specialised function, but it also provides several avenues for adaptations or malfunctions to occur. Whether and how the same components are important for early developmental and adult myelin continues to be an active area of research.

2.3.3. Adult myelin plasticity

Curiously, while other aspects of brain development such as the number of neurons reaches a plateau rather early in life, myelin is still highly malleable in early adulthood and retains this capacity at least until the 4th decade of life [87, 157]. For a structure whose purpose would be

merely to provide a pre-programmed amount of insulation to enable neuronal function, this type of protracted development seems out of place.

In terms of adjusting action potential speed, even subtle alterations in myelin parameters, such as thickness and length, can have functionally relevant consequences, with relatively low metabolic cost to the cells [158, 159]. While zebrafish have illuminated the basic mechanisms of myelin dynamics [160], it has taken rodents to start grasping how these dynamics may be relevant for behaving, adult animals. The lack of transparency of their organs introduces technical challenges when moving from zebrafish to rodents, so other clever manipulations have been used to address the dynamic nature myelin plasticity.

While de novo myelination during development proceeds in a reasonably straight-forward way, adult myelin plasticity is by nature bidirectional and complex. Several parameters of the established myelin sheaths and their parent OLGs are subject to modification (Figure 4). Sheaths can lengthen or retract, they can become thicker or thinner, more or less numerous, or disappear altogether. These changes likely occur interactively, with similar events eliciting changes in several parameters rather than just one [161]. It is possible that these alterations are orchestrated by different kinds of molecular events and a collaboration between the OLG and other cell types, but our understanding of what these events are remains in its infancy [162, 163].

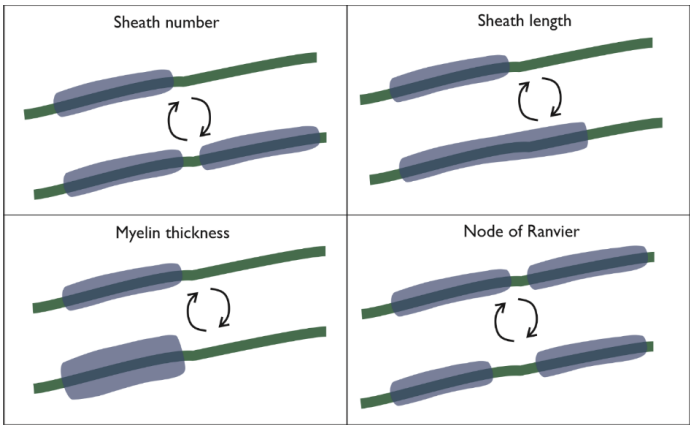

Figure 4. Types of myelin plasticity. Illustrations of the different parameters of myelin sheaths (number, length or thickness) and the nodes of Ranvier which may be bidirectionally altered by experience.

Recent advances in longitudinal imaging have demonstrated that pre-existing myelin sheaths can be remodelled (extended or retracted) in adult mice [164, 165]. Experiences such as learning a motor task induce a burst in remodelling events. Bacmeister et al. [164] showed that this type of learning causes retraction of a portion of myelin sheaths in the motor cortex of 2-3 month old mice along with generation of new OLGs. Hughes et al. [165] used environmental enrichment in older adult mice to demonstrate a similar increase in oligodendrogenesis, but no evidence of remodelling of existing sheets was observed, possibly due to age- or brain region-related features. Neuronal activity, even of the artificially induced kind, also promotes myelin formation and oligodendrogenesis [166, 167]. Optogenetically promoted activity-related adult myelin generation is dependent on BDNF signalling on OPCs, but the role of this signalling pathway in OLGs remains unknown [168]. Using elegant labelling techniques, it has been established that the myelin-promoting effect of pharmacogenetically driven neuronal activity is specific to the axons being activated, leaving adjacent axons with unaltered activity also without myelin alterations [167]. The aforementioned studies also demonstrated that the changes in myelin parameters associated with performance improvement. McKenzie et al. [169] further demonstrated the necessity of oligodendrogenesis on motor learning by knocking out the *Myrf* gene from OPCs selectively at learning. The capacity for myelin plasticity is also necessary for the stabilisation of fear memories, showing a potential downside to an otherwise-adaptive process in that fear generalisation is relevant for several anxiety disorders [170]. Plastic, bidirectional alterations in myelin properties can thus occur even in adult animals, with relevance for learning and adapting to one's surroundings.

While neuronal activity has been consistently pinned as a causal factor, this is more of a description than an explanation. A mechanistic explanation would need to encompass the factors that transmit the activity signal from the axon to the myelin, and in adult mammals this mechanism is yet to be recognized. Unlike OPCs, mature OLGs and their myelin sheaths do not express de facto synapses, but they do express glutamatergic α-amino-3-hydroxy-5-methyl-4-isoxazolepropionic acid (AMPA) and NMDA receptors. When activated by release of glutamate along the active axon, Ca^{2+} waves in the myelin sheath are triggered [171]. However, this event has not yet been associated with dynamic changes in myelin parameters like sheath thickness or internode length. Genetic tools have also been used to identify some relevant signalling pathways, but their relationship to upstream neuronal activity is not known. For example, conditionally activating extracellular signal-regulated kinase (ERK1/2) signalling pathway in existing mature OLGs caused them to increase the thickness of their myelin sheaths

[172]. Overall we still lack many of the pieces needed to understand how myelin plasticity occurs, and how it can malfunction.

Another major question in the field is what effect each of these parameter changes has on the neuronal circuit. Computational modelling has been used to estimate how incremental changes could be expected to affect axonal conduction velocity [158] and self-organised synchrony [159]. Altering activity of retinal neurons (via either visual deprivation or exogenous interference with local glutamatergic signals) also alters myelin internode length and conduction velocity along the optic tract [173]. However, *in vivo* confirmation of such effects in other circuits is extremely difficult because of technical limitations to observe myelin at a sufficient resolution while simultaneously recording activity, and the heterogeneity of myelination even along single axons which is poorly captured by simulations [174]. Kato et al. [175] used a transgenic mouse overexpressing the *Plp1* gene with mild but global defects in myelin, and showed concurrent deficits in motor learning and abnormally large variation in spike timing at thalamocortical projection targets. Optogenetic stimulation of these axons was able to improve both motor performance and firing synchrony, but concurrent improvements in myelination were not shown. Development of *in vivo* methods allowing measurement of both myelin and conduction parameters from the same axons are necessary to truly understand the contribution of activity-related adaptations in myelin on axon and circuit function.

2.3.4. Evidence of myelin plasticity in humans

Due to practical limitations, acquiring evidence of myelin plasticity in humans has been challenging. The earliest evidence of such structural and experience-dependent plasticity came from neuroimaging studies. Repeated diffusion tensor imaging (DTI) sessions interspersed with training in a new motor skill, such as piano-playing or juggling, showed changes in relevant sensorimotor tracts which were indicative of adaptive changes in myelin [176, 177]. Similarly, cognitive reasoning training associated with decreased mean diffusivity (generally associated with improved white matter tract integrity) in a performance-related manner [178]. These indicators rely on the diffusive permissiveness of the tissue to water molecules, the vibrations of which are sensed by their magnetic resonance. In white matter tracts, consisting primarily of myelinated and unmyelinated axons rather than cell bodies, the degree and amount of myelination is one parameter which affects the diffusivity readouts. Intact white matter is highly restrictive in some directions (across axon/myelin membranes) but not others (along the axons lengthwise), while diffusion in demyelinated or otherwise harmed white matter is less

directionally restricted. For example, in demyelinating diseases such as multiple sclerosis (MS), a key finding in patients is lower fractional anisotropy (FA, [179]), which indexes how directionally specific the restriction of the movement of water molecules is within an imaged voxel. The findings of Sholtz and Bengtsson and their colleagues [176, 177] suggest that learning-related experience increased FA, possibly indicative of thicker or more frequently myelinated axons post-training compared to pre-training. The resolution of DTI is far outside the nanometer scale at which many myelin plasticity events take place, and thus the explanatory power of these findings remains limited. In rodents a considerable correlation between experience-related changes DTI parameters and myelin gene expression has been demonstrated, lending some validity to deductions made from imaging data [180]. However, changes in imaging parameters can also occur via other mechanisms, such as changes in axon diameter or the extracellular environment, and as such the recommendation is to merely consider these readouts as proxies of myelin, rather than direct evidence of it [181].

Currently the only option for studying myelin at the cellular resolution in humans is to use *post mortem* donations, and indeed the growing data banks of brain tissue have been employed for the study of myelin and OLGs. Samples tend to be small and heterogeneous, and unlike imaging study designs, system dynamics cannot be gauged as the only time point available is *post mortem*. Nevertheless, recent publications have compared tissues from groups with myelin abnormalities, such as MS to healthy control groups. Despite extensive myelin degradation seen in these patients, there is also evidence of remyelination, i.e. the generation of new myelin sheaths in lesion sites [182, 183]. Throughout the course of the disease this process is not sufficient to rescue the pathological phenotype, but it is suggested to delay it and retain some level of functioning [184]. However, here it is not possible to draw direct parallels between the pathology-associated changes and those also occurring in adaptive myelin plasticity. Indeed, animal work suggests that remyelination after cuprizone-induced injury and myelin plasticity occur via at least somewhat non-overlapping mechanisms [164]. In terms of myelin plasticity, *post mortem* analyses may reach a suitable resolution, but lack the ability to gauge its dynamic nature.

In an elegant study, Yeung and colleagues [185] managed to combine the cellular resolution of *post mortem* research with an element of timing, capturing the lifetime dynamics of oligodendrocytes and myelin. They used the known high incidence of carbon isotope 14 occurring around the time of frequent nuclear detonation testing as a marking pulse, as the

isotope would be integrated into us carbon-based life-forms. The isotope would decay both as a result of the passage of time but also the biological turnover rates, and thus it could be used as a marker of (at least relative) age of specific biological components. The authors deduced that while there seems to be very little turnover of the oligodendrocytes in the adult corpus callosum (CC), the myelin sheath is renewing much more dynamically. This capacity of protein-level turnover indirectly suggests the capacity for plasticity; if parts of a system can be replaced, they can presumably also be altered. Later work using animal models has also shown that different components of the myelin proteome turn over at different rates [186, 187]. While impossible to replicate in an empirical setting, this work managed to combine molecular-level analysis with available human *post mortem* techniques, showing that in a non-clinical sample myelin is subject to alterations even in adulthood.

2.3.5. Myelin and its plasticity in stress and psychopathology

Myelin plasticity has in recent years been repeatedly associated with chronic consequences of stress exposure, including both molecular animal studies and human neuroimaging with parameters sensitive to variations in myelin [188]. Among the earliest demonstrations that stress could influence myelin thickness and relevant gene expression even in adult animals was a study of social isolation. Both juvenile and adult mice showed thinner myelin sheaths and lower expression of myelin-related genes in the mPFC after prolonged isolation from peers [189-191]. The behavioural consequences of stress could be reversed with a compound that promotes OLG differentiation, with consistent recovery of myelin thickness [192]. To date there have been numerous studies utilizing different stress models, associating changes in myelin or its components with maladaptive consequences of stress. Findings from such studies are summarised in Table 1. Generally, the data suggest that stress associates with lower myelin gene expression, protein abundance or gene expression, in brain regions including the PFC and HPC.

Table 1. Summary of studies linking myelin and chronic stress in rodent models. HPC = hippocampus, (m)PFC = (medial) prefrontal cortex, OLGs = oligodendrocytes, (ic)KO = (inducible-conditional) knock-out, OPCs = oligodendrocyte progenitor cells, wt = wild type, NAc = nucleus accumbens, CVS = chronic variable stress, CSDS = chronic social defeat stress, CUS = chronic unpredictable stress

Publication	Species (strain/stock), sex	Stress/anxiety model, age	OLG/myelin manipulation	Finding
Alttoa et al. 2010 [193]	Rat (Wistar), male	Low/high exploratory phenotype, adult	None	Lower *Mbp* in the HPC and PFC of low-exploring rats compared to high-exploring.
Teissier et al. 2019 [194]	Mouse (Balb/c), male	Maternal separation (2 weeks, pups)	None	Higher expression of myelin-related genes and more OLGs as pups, fewer OPCs as adults.
Chen et al. 2020 [195]	Mouse, *Cnp-Cre*$^{+/-}$ on a 129SV background, sex unknown	Social isolation (5 weeks, juvenile)	*Olig2* cKO in OLGs	Socially isolated cKO mice had lower social interaction and higher anxiety-like behaviour compared to isolated wt mice.
Swire et al. 2019 [196]	Mouse (C57BL/6), male	Social isolation (2 weeks, juvenile)	*Ednrb* cKO in OPCs.	Vascular endothelin signals to OLGs reduced after social isolation, promoting this rescued hypomyelination and social interaction deficits.
Liu et al. 2012 [189]	Mouse (C57BL/6), male (some experiments findings replicated in females)	Social isolation (2 or 8 weeks, adults)	None	Thinner myelin in PFC (2 and 8 weeks isolation), and lower expression of e.g. *Mbp* (only in those isolated for 8 weeks). No differences in OLG density.
Makinodan et al. 2012 [191]	Mouse, PLP-EGFP line on a B6/CBA background, male	Social isolation (2 or 4 weeks, juveniles)	*ErBb3* icKO in OLGs.	Higher g ratios and lower expression of e.g. *Mbp* in the PFC of socially isolated wt mice. icKO in group-housed mice replicates effects of social isolation (reduced social interest, myelin defects).
Liu et al. 2016 [192]	Mouse (C57BL/6), male	Social isolation (10 weeks, adults)	Clemastine for 2 weeks (promotes oligodendro-genesis)	Smaller MBP^{+} area and higher g ratios in socially isolated vehicle-treated mice in the PFC. Clemastine rescued myelin defects and social behaviour.
Liu et al. 2018 [190]	Mouse (C57BL/6), male	CVS (1-4 weeks), adults	None	Lower expression of e.g. *Mbp* in the PFC after 4 weeks of CVS, and in the NAc already after 1 week of CVS.
Zhang et al. 2016 [197]	Mouse (Balb/c)	CSDS (12 1 min defeat sessions across 15 days), adolescents	None	Smaller MBP^{+} area in the mPFC of stress-exposed mice compared to controls.

Edgar et al. 2011 [198]	Mouse, *Cnp1*$^{+/-}$ on C57BL/6 background, males and females combined	CVS (4 weeks, adults)	*Cnp1* KO	Lower composite score of emotionality (depressive and anxiety-like behaviours) in KO mice, both in non-stressed and stressed conditions.
Lehmann et al. 2017 [199]	Mouse (C57BL/6), male	CSDS (14 days with 5 min daily defeat), age unknown	None	Smaller MBP^{+} area in the mPFC of stress-exposed mice compared to controls.
Bonnefil et al. 2019 [200]	Mouse (C57BL/6), male	CSDS (10 days with max. 5 min daily defeat), adults	Focal lysolecithin demyelination	Thinner myelin, fewer OLGs and more OPCs in mice susceptible to CSDS in the mPFC compared to controls, MBP^{+} area unaltered. Demyelination at mPFC reduced social preference.
Cathomas et al. 2019 [201]	Mouse, *Cnp1*$^{+/-}$ on C57BL/6 background, male	CSDS (14 days of 1-10 min daily defeat), adults	*Cnp1* KO	Lower myelin gene expression in the PFC and amygdala, abundance of myelin proteins and the number of OLGs unaltered by CSDS.
Luo et al. 2019 [202]	Rat (Sprague-Dawley), male	CUS, age unknown	None	Lower abundance of 17 and 21 kDa isoforms of MBP and OLIG2 in the HPC, partially restored by physical exercise.

Transcriptome-wide investigations, without pre-existing myelin-related hypotheses, of the effects of CSDS on the mouse brain have also flagged myelin-related genes. Pena et al. [203] compared RNA-sequencing (RNA-seq) findings from male CSDS-exposed mice to female mice exposed to another form of stress (sub-threshold variable stress), with or without additional exposure to early life stress (ELS). Analysing the enrichment of genes specific for certain cell types, they report that OLG genes were enriched among the genes affected by ELS in males and a double-hit of early and adult stress in females in the PFC. An additional analysis of biological pathways (Gene Ontology [GO]) suggested an enrichment of myelination-related genes in the male PFC after ELS. Ingenuity Pathway Analysis (IPA) was used to search for potential upstream regulators of differentially expressed genes (DEGs), and the top predicted regulator in this group was TCF7L2, a regulator of OLG maturation. In the female PFC, TCF7L2 was the top predicted regulator in the double-hit group. While this analysis did not separate resilient and susceptible mice, another publication from the same research group has implicated myelin-related genes (GO term "Nerve ensheathment") in the PFC in successful response of CSDS-susceptible mice to the antidepressant effects of ketamine [204]. Together

these findings implicate broad biological pathway-level involvement of OLGs and myelin in the mouse stress response, with relevance for eventual recovery.

Evidence for the role of myelin in stress and psychopathology in humans has also emerged. Aston et al. [205] used a microarray to survey gene expression in the temporal lobes on *post mortem* samples from patients with MDD and psychiatrically healthy controls, revealing a cluster of myelin-related genes to be expressed at a lower level in the patients. Nagy et al. [206] report RNA-seq of single cells gathered from the mPFC of male suicide victims with concurrent MDD and psychiatrically healthy control males. By comparing the numbers of DEGs across identified brain cell types they conclude that the largest number DEGs are seen in immature OPCs. To get clues about the potential biological meaning of this finding, Nagy et al. analysed enrichment of known biological pathways and found classes related to synaptic plasticity to be implicated among the DEGs in OPCs. Considering the emerging findings about synaptic genes potentially having novel functions in myelin discussed above, this finding may implicate similar pathways in MDD-related myelin pathology. Lutz et al. [207] also performed both transcriptomic and electron microscopic profiling of PFC tissue of suicide victims with MDD, with or without a family-reported history of childhood maltreatment and severe stress. The patients with a maltreatment history had lower expression of myelin-related genes and higher g ratios, indicative of lower relative myelin thickness. These findings implicate myelin both on the gene expression and structural level to psychiatric disease and stress, but leave open many questions still. There are currently no reports of similar analyses from patients with an anxiety disorder. It is also possible that the differences seen *post mortem* were pre-existing vulnerabilities, part of the disease aetiology, a chronic adaptation to disease, or a response to failed or successful treatment, with next to no possibility to untangle these scenarios.

In vivo assessment of myelin in humans by neuroimaging, as noted above, lacks the resolution and specificity of molecular-level work. Additionally, much of the work on white matter structure in stress and psychopathology is done retrospectively, at a stage when the patients have had at worst years of symptoms as well as treatments, making it again difficult to parse what the role that differences in myelin-related features may be. In a group of healthy participants reporting some degree of early life stress, Poletti et al. [208] found lower FA in the cingulate cortex compared to participants with low to no history of childhood stress. This effect was seen in the cingulate gyrus, a white matter region in the PFC, and was more pronounced in males than females. In a male-only sample, early childhood and adolescent stress associated with higher magnetization transfer ratio (MTR) in distinct parts of the CC when imaged in

early adulthood [209]. MTR is sensitive to the proportion water in a semisolid medium, such as compacted myelin, versus water in an aqueous medium, such as the intra-axonal space, but like FA it cannot be used to specifically quantify myelin. McCarthy-Jones et al. [210] report lower FA in several white matter tracts including the CC and uncinate fasciculus (UF) in participants reporting a history if childhood adverse events. The UF connects limbic structures like the amygdala with the PFC, and lower structural integrity is hypothesised to reflect compromised top-down control of amygdalar reactivity by the PFC. Of note, as the participants in both of these studies were adults currently reporting no psychiatric symptoms, it is possible that the observed white matter differences relate to resilience to stress rather than stress exposure. In another study, participants rated as high in harm avoidance, an anxiety-related trait and risk factor for anxiety disorders, showed lower FA and higher radial diffusivity along several white matter tracts connecting limbic and cortical regions [211]. As participants were screened based on any lifetime history of psychiatric symptoms, the authors interpret the result as a marker of vulnerability to anxiety disorders. However, as the participants were also past the peak anxiety disorder incidence age, it remains possible that the participants with high harm avoidance harboured some protective/resilience factors, which may or may not include the white matter differences compared to the low harm avoidance group. Thus, in addition to technical limitations, when studying humans we have limited ability to determine which features of two groups of people truly associate with an observed difference between them.

DTI studies of patients with one or more anxiety disorder diagnoses are to date sparse, and typically conducted with very small sample sizes rendering them underpowered [212, 213]. Despite these shortcomings, a consistent finding across diagnoses (at least GAD and SAD) is reduced FA along the UF. This finding is not anxiety-specific a similar findings have been reported for MDD [214] and PTSD [215]. Prospective studies managing to catch patients in the years prior to symptom emergence as well as after would be needed to separate structural vulnerability factors from disorder progression-related myelin plasticity. The present evidence nonetheless implicates myelination of relevant tracts in anxiety; future work will hopefully advance from here.

3. Aims

The overarching aim of this work was to determine the effect of environmental and genetic risk factors of anxiety disorders on brain structure and function. To investigate the effects of stress we employed a mouse model of chronic psychosocial stress (the chronic social defeat stress paradigm; Studies I-III). To study how genetic factors moderate these effects, we used mice from two inbred strains (C57BL/6NCrl and DBA/2NCrl; Studies II-III).

The specific aims of this thesis were:

1. To investigate which regions in the mouse brain are repeatedly engaged by CSDS by two complementary methods; manganese-enhanced magnetic resonance imaging (MEMRI) and immunohistochemical staining of a chronically inducible marker protein (ΔFOSB).

2. To determine major biological pathways differentiating between stress-resilient, -susceptible and control mice from two different genetic backgrounds using unbiased RNA-seq. Moreover, to follow up the discovered pathways by structural of functional analyses.

3. To identify molecular mechanisms underlying CSDS-related myelin plasticity via RNA-seq of cortical oligodendrocyte- and myelin-enriched samples from resilient, susceptible and control mice. Furthermore, to assess the influence of genetic background on this gene expression response by using mice from two inbred strains.

4. Methods

4.1. Animal procedures

4.1.1. Ethics statement (Studies I-III)

Animal procedures were approved by the authorization board of the Regional State Administration Agency for Southern Finland (ESAVI/2766/04.10.07/2014 and ESAVI/3119/04.10.07/2017). All experiments were carried out in accordance with directive 2010/63/EU of the European Parliament and of the Council, and the Finnish Act on the Protection of Animals Used for Science or Educational Purposes (497/2013).

4.1.2. Animal husbandry (Studies I-III)

All animals were ordered from a commercial breeder (Table 2). On arrival, mice were housed in groups of 3-5 (B6 and D2) in open Makrolon III cages, or singly (CD1) in individually ventilated cages. Single housing was used when necessary to prevent conspecific aggression. All cages included bedding material, nesting material, and wooden sticks for enrichment (Tapvei Oy), and cages were changed once per week (except during CSDS). The animal facility was temperature (22 ± 2 °C) and humidity (50 ± 15 %) controlled, with a 12-hour light cycle (lights on: 6:00, lights off: 18:00). With the exception of active behavioural experiments, animals had *ad libitum* access to food and water.

Table 2. Details about mice used for experiments.

Mouse strain/stock	Sex	Age (on arrival)	Provider
C57BL/6NCrl (B6)	Male	5 weeks	Charles River, Sulzfeld, Germany
DBA/2NCrl (D2)	Male	5 weeks	Charles River, Sulzfeld, Germany
Clr:CD1 (CD1)	Male	13 weeks	Charles River, Sulzfeld, Germany or Envigo, Horst, The Netherlands

A summary of conducted experiments and included animals can be found in Table 3.

Table 3. Summary of experiments. Summary of the number animals included, in total, in each of the Studies in this thesis and the unpublished data, separately for the B6 and D2 strains and for mice in the control condition (non-stressed) and stress-exposed condition (exposure to CSDS). B6 = C57BL/6NCrl, D2 = DBA/2NCrl, CSDS = chronic social defeat stress, MEMRI = manganese-enhanced magnetic resonance imaging, IHC = immunohistochemistry, RNA-seq = RNA-sequencing, MACS = magnetic-activated cell sorting

Study	Methods (all)	Number of animals			
		B6		D2	
		Control	Stress-exposed	Control	Stress-exposed
I	CSDS, MEMRI, IHC	11	10	-	-
II	CSDS, Behavioural tests, RNA-seq, qRT-PCR, IHC	72	102	39	42
III	CSDS, MACS, RNA-seq	6	13	6	18
Unpublished data	CSDS, IHC	8	15	10	15

4.1.3. Chronic social defeat stress (CSDS, Studies I-III)

Following a 7-day acclimatization period we screened the CD1 aggressor mice for appropriate levels of aggressive behaviour. We did this by assessing their latency to attack a novel intruder B6 or D2 mouse in the home cage on three consecutive days. Appropriate aggressors attacked no sooner than 10 seconds on more than one test day, or later than 90 seconds on more than one test day. Both aggressor screening and CSDS took place at the end of the light phase. Twenty-four hours before CSDS each screened aggressor mouse was placed alone into a cage to be used for CSDS to facilitate home cage behaviour.

To allocate B6 and D2 mice to CSDS or control conditions we balanced them for body weight before the start of the first defeat session. Each group cage contributed at least one mouse to each of the conditions to ensure a random distribution. Each defeat session consisted of an intruder (B6 or D2) mouse being placed into the home cage compartment of a CD1 mouse (Figure 5 A). During the ensuing maximum 10-minute interaction the CD1 mice behaved dominantly towards the intruder. To prevent and minimize physical injury to the intruder a trained experimenter monitored each interaction closely. Persistent attacks were prevented by separating the mice from each other. If any degree of wounding occurred, the interaction was

stopped, and the wound was treated with an antiseptic (Dermacool Vet, Biofarm, Karkkila, Finland).

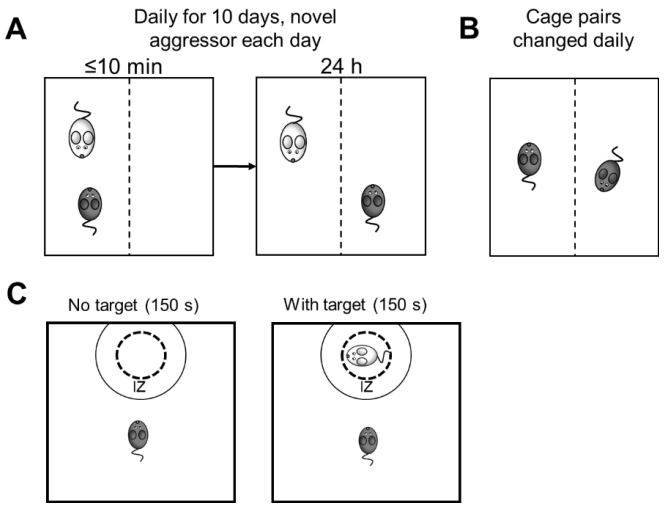

Figure 5. Chronic social defeat stress (CSDS). A) Illustration of the CSDS procedure. **B)** Illustration of the housing of control mice. **C)** Illustrations of the two trials of the SA test. CSDS = chronic social defeat stress, SA = social avoidance test, IZ = interaction zone.

Once the defeat session was over, the intruder mice were moved to a separate compartment of the CD1 cage they were just in. This compartment was separated from the CD1 mouse by a perforated plexiglass divider, allowing only sensory contact. Both compartments had the same bedding, nesting and enrichment materials as the previous home cages. The cages were maintained in Scantainers (Scanbur, Karlslunde, Denmark) in the same room as the defeat sessions took place in, minimizing sensory exposure to other cages undergoing CSDS. After 24 hours of this paired housing, each B6 and D2 mouse was removed and taken to a new cage with a novel CD1 aggressor, and the physical interaction + paired housing procedure was repeated. These 24 hour cycles were repeated for a total of 10 consecutive days.

Mice allocated to the control condition were housed in similar paired cages, but always paired with another control mouse (Figure 5 B). House pairs were exchanged daily, and no control mouse stayed in the same home cage for more than three consecutive days. This equalised the experience of moving to a novel home cage and handling incurred by the CSDS mice, without the aggressive physical encounter. The control cages were kept in the same room as the CSDS cages, but in a separate Scantainer which was not opened while defeat was ongoing to minimize sensory exposure.

Mice were weighed on the first day of defeat (for group allocation) and on every even numbered defeat day to monitor health and well-being.

Twelve hours after the last physical encounter phase, all mice were separated into single cages containing the same enrichment items as above. The same evening, at the beginning of the dark phase (17:00 – 20:00), we performed the social avoidance (SA) test (Figure 5 C). This allows phenotyping the CSDS-exposed mice as resilient or susceptible. The test room was dimly lit (15 lux) during the entire test, and the mice were brought into the test room 30 minutes prior to the start to acclimatise. The test consisted of two trials (no-target [NT] and target), always in the same order. In the first (NT) trial, the mouse was placed in the centre of an open arena (42 x 42 cm) with dark plexiglass walls and a perforated plexiglass cylinder next to one of the walls. Surrounding the plexiglass cylinder was a virtually drawn interaction zone (IZ). To quantify how much time the mouse spent interacting the cylinder, the number of seconds spent in the IZ was recorded from a video tracking using EthoVision XT software (versions 10 and 13, Noldus, Wageningen, the Netherlands). Total distance travelled and the amount of time spent in the corners opposite to the IZ were also calculated. After 2.5 minutes the test was stopped, the mouse returned to the home cage, and the arenas cleaned from any feces and urine. The cylinder was then replaced with a new cylinder containing an unfamiliar CD1 male mouse for the second trial (target). The CSDS-exposed or control mouse was returned to the arena for another 2.5 minutes, during which the same parameters are measured. After each target trial the arena was cleaned with 70 % EtOH and water to remove odours.

Social avoidance was operationalized as the social interaction (SI) ratio. This was calculated by dividing the amount of time the mouse spent in the IZ during the target trial by the amount of time spent there during the NT trial, multiplied by 100. A score of 100 thus means equal interaction with the empty cylinder as with the cylinder containing a social target. The SI ratio was calculated for both control and CSDS-exposed mice. During several cohorts of experiments performed in the lab, it was noted that control mice from different inbred strains differed in their social behaviour. Resilience in the context of CSDS refers to a stress-exposed mouse being behaviourally similar to non-stressed controls. Thus, in order to phenotype the CSDS-exposed mice from different strains as resilient or susceptible, it would not be optimal to use the same cut-off point for determining susceptibility for different strains. Instead we determined strain-specific cut-off values for the SI ratio. To do this we first determined and removed outliers of the control mice included in experiments up to the most recent cohort at the time (3 interquartile ranges above or below the median), separated by strain, and normalized

the values using a log transformation. The mean control SI ratio and standard deviation for each strain was then calculated. The cut-off value (SI ratio below which CSDS-exposed mice are considered susceptible) was set as the mean – 1 standard deviation. For B6 mice this cut-off value without log transformation was 76.49, while for D2 mice it was 105.99. Consequent CSDS cohorts were always compared to these established values.

Following the SA test all mice were returned to single cages and housed individually until dissection.

4.1.4. Manganese-enhanced magnetic resonance imaging (Study I)

In Study I, manganese-enhanced magnetic resonance imaging (MEMRI) was used as a way of assessing chronic neural activity. Both CSDS and MEMRI for this experiment were performed by co-authors, and the procedures are described in detail in the publication (Study I). Briefly, mice were surgically implanted with a $MnCl_2$-dispensing subcutaneous minipump prior to CSDS. One week after the SA test mice were anaesthetised and scanned with a 4.7 T scanner (Bruker, PharmaScan 47/16 US, Ettlingen, Germany). Mn^{2+} ions are rapidly taken in through voltage-gated Ca^{2+} channels, and accumulate in activated cells due to slow efflux kinetics [216-218]. This chronic activation is then detected as an increase in T1-weighted signal intensity.

4.2. Tissue dissection and RNA-sequencing (Study II)

Six-eight days after the SA test, at the beginning of the light phase, all mice were dissected. This time point was selected to reveal preferentially chronic effects of stress, rather than those occurring acutely but subsiding soon after stress cessation. Euthanasia was completed by cervical dislocation and the brain promptly removed onto a cold Petri dish. Tissue of interest (mPFC and vHPC bilaterally) was dissected by a trained experimenter and immediately snap-frozen in liquid N_2. The BNST was also dissected, and the data collected from the RNA-sequencing of this structure are presented in full in Study II and the PhD dissertation of a co-author (Dr Zuzanna Misiewicz). Although relevant for anxiety and threat processing, the amygdala was not dissected for this study due to limitations in the ability to separate the distinct subregions. Dissections were split onto three mornings to minimize circadian effects on gene expression while maintaining fast enough processing speed (max 7 minutes between cervical dislocation and snap-freezing of the tissue sample).

Procedures for RNA-seq [RNA extraction, ribosomal RNA depletion, library preparation, sequencing, read alignment, differential gene expression analysis, and gene set enrichment analysis (GSEA)] are described in detail in Study II, as performed by other co-authors. The

gene expression data set is available on Gene Expression Omnibus (accession number: GSE109315).

4.3. Magnetic-activated cell sorting (MACS, Study III)

Mice were anaesthetized 6-8 days after CSDS with a lethal dose of pentobarbital and transcardially perfused with 4 °C sterile saline to remove blood cells from the brain (0.9 % NaCl) and the mPFC dissected on ice. We dissociated the cells by incubating tissue pieces in papain (LK003150, Worthington Biochemical Corporation) in 37 °C under constant agitation for 45-90 min, in accordance with the manufacturer's instructions. The reaction was stopped by the addition of DNase and the suspension triturated to fully separate the cells. The resulting cell suspension was washed with 4 °C Dulbecco's PBS (14287080, ThermoFisher Scientific) by centrifugation. Next, we separated cells and myelin into distinct phases using a Debris Removal Solution (130-109-398, Miltenyi Biotec). The debris phase (containing myelin) was separated from the cell phase (containing OLGs), and each incubated for 15 minutes in 4 °C with anti-myelin (130-104-257, Miltenyi Biotec) or anti-O4 (130-094-543, Miltenyi Biotec) magnetic microbeads respectively. These beads label the target structures with a small magnetic particle. We then used the octoMACS (Miltenyi Biotec) set-up to positively select for the labelled myelin and OLGs separately. The collected material was immediately lysed by vortexing in RLT lysis buffer (RNeasy Plus Micro kit, Qiagen) and stored in -20 °C until RNA extraction. RNA-seq procedures are explained in detail in Study III.

To gain insight into which biological pathways were affected by CSDS in OLGs and myelin, we used Ingenuity Pathway Analysis (IPA v. 01-12, July 2019 release; Qiagen, Hilden, Germany, [219]). Focus was placed on predicted upstream regulators, as these molecules are positioned to mediate the effects of CSDS on gene expression and the behavioural response. Only interactions reported in the IPA data base for "Nervous System" tissue were included. Input differentially expressed genes (DEGs) were filtered by average expression level to restrict the analyses to robustly expressed genes (limma-normalized counts > 0). A nominal significance threshold $p < 0.05$ and effect size threshold logFC > |0.25| were used as criteria for including genes in the analysis.

4.4. Immunohistochemistry (Studies I-II, and unpublished data)

Brain samples were prepared 6-8 days after the SA test by transcardial perfusion with a fixative. Briefly, mice were anaesthetised with a lethal dose of pentobarbital (Mebunat Vet, Orion Pharma, Espoo, Finland). Blood was removed by perfusion with phosphate-buffered saline

(PBS) warmed to 37 °C, followed by perfusion with 4 % paraformaldehyde (PFA) at 37 °C for approximately 10 minutes. Specific treatments are listed in Table 4. All brains were sectioned in the coronal orientation, and a mouse brain atlas [220] was used to determine anatomical ROIs.

Table 4. Protocols used for immunohistochemical labelling in Studies I-III. NGS = normal goat serum, BSA = bovine serum albumin, NDS = normal donkey serum, TBS-T = Tris-buffered saline with Tween-20, PBS-T = phosphate buffered saline with Tween-20, OPC = oligodendrocyte progenitor cell, OLG = oligodendrocyte, DAB = 3,3′-diaminobenzidine, CC = corpus callosum

Method	Study I	Study II	Unpublished OLG-OPC quantification
Postfixation	2-24 h	24 h	2-4 h
Additional sample preparation	Cryoprotection for 24 h, freezing in 2-methyl butane, storage at -80 °C	None	None
Sectioning (thickness)	Cryostat (40 µm)	Vibratome (20 µm)	Vibratome (40 µm)
Long-term storage	-20 °C free-floating in ethylene glycol cryoprotectant	-20 °C free-floating in ethylene glycol cryoprotectant	-20 °C free-floating in ethylene glycol cryoprotectant
Blocking endogenous peroxidase activity	Yes (0.05 % H_2O_2)	No	No
Antigen retrieval	No	0.01 M citrate buffer	No
Blocking nonspecific antigens	10 % NGS in 0.5 % TBS-T	2.5 % BSA + 7.5 % NGS in 0.5 % PBS-T	5 % NDS in 0.5 % TBS-T
Primary antibody	Rabbit anti-FOSB (sc-7203, Santa Cruz Biotechnology), overnight at RT	Mouse anti-CNPase (#MAB326R, Merck), overnight at 4 °C	Goat anti-PDGFRA (af1062, R&D Systems), mouse anti-CC1 (OP80, Merck), and rabbit anti-OLIG2 (AB9610, Merck)
Target	ΔFOSB (marker of repeated activation)	Myelin sheaths and OLG cell bodies	OPCs ($PDGFRA^+/OLIG2^+$) and OLGs ($CC1^+/OLIG2^+$)
Secondary antibody	Biotinylated goat anti-rabbit (ABC detection kit [PK-6101], Vector laboratories), 2 h at RT	Goat anti-mouse AlexaFluor 488 (#A-11029, ThermoFisher Scientific), 2 h at RT	Donkey anti-goat AlexaFluor 647 (705-605-147), anti-mouse AlexaFluor 488 (715-545-150), and anti-rabbit AlexaFluor 594 (711-585-152), all from Jackson Immunoresearch
Visualization method	DAB (Vector Laboratories)	Fluorescence	Fluorescence

Image acquisition	Pannoramic FLASH II digital scanner (3DHistech)	AxioImager Apotome.2 system (Zeiss)	AxioImager Apotome.2 system (Zeiss)
Imaging parameters	20x magnification scans of whole sections	4x magnification	10x magnification
Quantification	Semi-automatic (automatic deconvolution, manual thresholding, automatic cell body quantification)	Manual (CC thickness (mean of two points on either side of the midline at Bregma 0.22 – -0.10)	Custom semi-automated macro (manual thresholding, automated masking of $OLIG2^+$ cell bodies and detection of lineage-specific marker)

All staining, imaging and quantification steps were done blind to the condition of each animal, and staining batches were balanced across conditions. ΔFOSB cells were counted from a total of 18 brain regions, each as the average from 3-6 sections per animal. The quality of semi-automatic quantification of cell numbers was checked for each image. For CC measurements, 2-6 sections were acquired per animal and their average taken as a data point. OLG and OPC quantification accuracy of the semi-automated pipeline was controlled by comparing cell identity annotations to manual annotations of a randomly selected subset of images, by an investigator blind to the phenotype of the animal and the pipeline's annotations (Pearson's correlation coefficients (r) for number of OLGs, OPCs, or undefinable cells/field of view = 0.858 – 0.949). The mean number of sections used per animal following exclusion of images of insufficient quality for quantifying the staining reliably was 6 (range: 3 – 14).

4.5. Transmission electron microscopy (Study II)

We anaesthetized the mice 6–8 days after CSDS with a lethal dose of pentobarbital (Mebunat Vet). Transcardial perfusion was done with PBS followed by fixation with 100 ml of 37 °C 2 % glutaraldehyde (GA) + 2 % PFA in 0.1 M sodium cacodylate (NaCac) buffer (all components from Sigma Aldrich). The brains were removed and postfixed in the same fixative for 2–4 h and maintained in 0.1 M NaCac buffer for 2–24 h, both at 4 °C. We cut 200 µm sagittal sections using a Leica VT-1200S vibratome (Leica Biosystems) in 0.1 M phosphate buffer. Samples (mPFC and vHPC) were manually excised using anatomical landmarks from both hemispheres.

We additionally postfixed the samples in 1 % osmium tetroxide and 1.5 % $K_4[Fe(CN)_6]$ in 0.1 M NaCac buffer for 2 h at 4 °C. Uranyl acetate was applied for *en bloc* staining for 1 h at 4 °C, followed by dehydration with EtOH and acetone, and embedding into hard Epon. 60–70 nm sections were cut with an ultramicrotome and placed on copper grids. Some samples were additionally stained with lead citrate for increased contrast, but this step was omitted for most samples as the *en bloc* staining was deemed sufficient. We acquired images containing myelinated axons from grey matter using a Jem-1400 transmission electron microscope (Jeol) at 5000× magnification. All sample numbers were blinded for the imaging and image analysis steps. To capture the heterogeneity of axons present in the samples we acquired 93–104 myelinated axons per animal from mPFC (mostly grey matter) and 54-62 myelinated axons per animal from the vHPC (both grey and white matter).

Image analysis was performed manually using ImageJ. We measured myelin thickness, axon diameter, and g ratio using ImageJ. Myelin thickness was measured by manually drawing vectors at three fully compacted positions and their average length was calculated (Figure 6). To determine axon diameter we measured the area of the axon (inside the compacted myelin sheath) and calculated the diameter of the corresponding geometric circle. We calculated the g ratio by dividing the diameter of the axon with the diameter of the whole fibre, calculated from the area of the whole fibre (circumference of the compacted myelin sheath). Comparisons of resilient, susceptible and control mice were performed for all measured axons collectively, as well as divided into size groups based on axon diameter (small, medium and large, based on diameter distribution within the brain region). Projections of different neuronal types may have different typical axon diameters [221], and differences occurring selectively in one size group may thus be of interest.

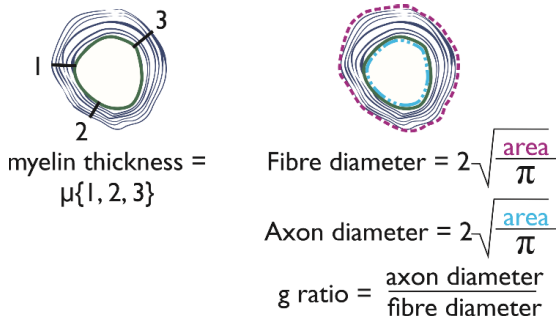

Figure 6. Illustration of quantification of myelin thickness, axon diameter and g ratio from TEM images. Short dashed magenta outline indicates whole fibre circumference, and the blue variable dashed outline indicates the axon circumference.

4.6. Statistical analysis (Studies I-III)

Data analysis was conducted with inferential statistical tests appropriate for the specific data structure (for example normality of the distribution, assessed with the Shapiro-Wilk test). *Ad hoc* determination of sample size through power analysis for CSDS experiments is challenging in practice. The number of resilient and susceptible animals cannot be predetermined as they are defined based on outcome of the SA test. Thus sample sizes were based on estimates derived from prior literature. Criteria for excluding animals or data points as outliers were pre-determined as 3 standard deviations above or below the mean for normally distributed data, and 1.5 interquartile ranges from the median for non-normally distributed data.

Specific tests used to analyse mouse behavioural data are outlined in section 5.1, as the tests applied differed between outcome measures. To adjust significance levels for multiple comparisons we used a test-wise Bonferroni correction within each strain.

The DEG analyses of RNA-seq data, including correction for false discovery rate, are detailed in Studies II and III.

Data on $FOSB^+$ cells was compared only between control and stress-exposed mice, using either independent *t*-tests (when both groups were normally distributed) or the Mann-Whitney U-test (when one or both groups were non-normally distributed). Correlation of $FOSB^+$ cell quantities between different regions (separately for control and stress-exposed groups) was determined by calculating Pearson's *r* coefficients for each brain region paired with each of the other brain regions. Because of the large number of brain regions included, Bonferroni correction was deemed to be overly conservative. To correct for false discovery across multiple tests we used the Benjamini-Hochberg method [222].

The other immunohistochemical (corpus callosum [CC] thickness measurement, OPC and OLG cell quantification) experiments were analysed by one-way analysis of variance (ANOVA) with test-wise Bonferroni corrections. Each data point represents the average dependent variable value for one animal, calculated as the average of all images acquired from that animal.

Group differences in TEM data were assessed using generalized estimating equations (GEEs) because the assumption of independence of ANOVAs were violated by axons imaged from the same animal. Averaging the axons of each animal would have produced groups too small to be reliably analysed by ANOVA (n = 3-6). Using each axon as a data point avoided this issue, and allowed us to capture the variance within an animal. GEE allows control for such within-subject

dependencies. This has been applied in other fields for analysing data with non-independent features [223, 224]. To compare groups (control, resilient and susceptible mice within a strain) we computed *p* values with Fisher's LSD, and statistical significance was assessed against the Bonferroni corrected α-level within-strain as above.

5. Results

5.1. B6 and D2 mice show different rates of susceptibility and resilience to CSDS (Studies I-III)

In Studies I-III we exposed mice to chronic social defeat stress (CSDS) to study the effects of stress on the brain and behaviour. Additionally, in Studies II and III we used mice from two different inbred strains, representing high (D2) or low (B6) levels of innate anxiety-like behaviour [104]. In Study I we only used B6 mice. Stress-exposed and control mice were subjected to the social avoidance (SA) test 24 hours after the last CSDS encounter. Throughout CSDS exposure and control housing in Studies II and III we also tracked the weights of the animals. In Study III we also recorded the duration of the physical interaction phase of each defeat session to test whether resilient and susceptible mice were differentiated by their CSDS ex perience.The results of behavioural measures are presented in Table 5 according to availability. In Study I, the SI ratios between control and stress-exposed mice did not differ (independent *t* test, $p = 0.12$). One outlier in the CSDS-exposed group was removed (> 3 * IQR above sample median). In Studies II and III, susceptible mice from both strains had significantly lower SI ratios than controls ($p_{adj} = 6.33 * 10^{-7} – 0.0043$) as tested by one-way ANOVAs. Resilient mice generally did not differ from controls, except for the B6 resilient mice in Study II which had significantly higher SI ratios than controls ($p_{adj} = 0.023$). Across Studies II and III, we found that 66.1 % of B6 mice were resilient, while only 15.0 % of D2 mice were resilient to CSDS.

Table 5. Summary of behavioural features after CSDS-exposures across Studies I-III. Numbers represent mean ±standard deviation. Group means which significantly differ from the same-strain control group are marked with an asterisk (*). Significant differences between two trials within the same group are denoted by ⁑. NT = no target trial of the SA test, T = target trial of the SA test, n/a = not applicable or available.

		B6			D2		
		Control	Stress-exposed		Control	Stress-exposed	
Measure	Study		Resilient	Susceptible		Resilient	Susceptible
Number of mice	I	9	10		n/a	n/a	n/a
	II	72	70	32	39	2	40
	III	6	6	7	6	7	11
SI ratio	I	224.06 ±84.07	386.28 ±286.08		n/a	n/a	n/a
	II	174.03 ±103.83	**266.99 ±321.16***	**34.10 ±26.26***	241.42 ±226.40	232.88 ±29.66	**12.46 ±14.22***
	III	342.43 ±220.88	272.00 ±240.98	**41.98 ±22.40***	322.02 ±81.81	150.26 ±77.6	**22.77 ±22.55***
Time spent in the IZ, NT → T (s)	II	**37.00 ±12.99 → 58.64 ±25.76⁑**	**31.87 ±16.61 → 63.44 ±31.69⁑**	**40.12 ±27.35 → 15.63 ±17.77⁑**	**33.77 ±15.53 → 62.92 ±25.33⁑**	11.26 ±7.84 → 25.06 ±14.91	**35.98 ±18.47 → 4.19 ±5.17⁑**
	III	20.02 ±14.12 → 50.31 ±25.64	**23.98 ±14.84 → 72.23 ±31.73⁑**	**59.06 ±36.03 → 23.58 ±19.32⁑**	**25.17 ±8.12 → 76.80 ±14.54⁑**	10.59 ±9.77 → 39.39 ±41.97	27.30 ±23.03 → 5.01 ±6.22
Time spent in corners, NT → T (s)	II	26.48 ±12.03 → 23.87 ±20.67	31.45 ±21.88 → 25.22 ±26.72	**34.97 ±27.59 → 63.35 ±42.44⁑**	29.70 ±13.84 → 22.51 ±17.60	60.60 ±22.57 → 83.70 ±12.76	**26.02 ±17.80 → 52.19 ±38.02⁑**
	III	36.39 ±24.48 → 31.10 ±27.64	54.68 ±39.87 → 14.53 ±18.96	22.51 ±18.11 → 44.96 ±37.41	41.70 ±8.98 → 15.36 ±10.49	43.72 ±27.59 → 37.79 ±36.66	40.30 ±25.46 → 62.40 ±44.72
Distance travelled (NT, cm)	II	1124.06 ±243.23	**944.58 ±290.14***	**788.59 ±241.39***	1047.07 ±276.42	662.24 ±41.16	**766.69 ±204.75***
	III	806.51 ±318.78	712.16 ±253.63	695.83 ±297.28	960.88 ±135.16	**597.26 ±279.35***	**641.77 ±124.91***
Δ Body weight (g)	II	1.48 ±0.83	**0.98 ±1.01***	**0.63 ±0.95***	0.16 0.75	-0.06 ±0.35	**-0.87 ±1.28***
	III	1.48 ±1.73	1.92 ±1.95	1.50 ±1.91	0.32 ±0.49	0.18 ±0.55	-0.11 ±1.19
Defeat duration (s)	III	n/a	426.9 ±38.0	473.5 ±35.9	n/a	254.9 ±84.2	209.1 ±71.1

In Studies II and III we also had access to data on the amount of time spent in the interaction zone (IZ) during the first trial without a social target (no-target, NT) and the second trial with the restrained CD1 as a social target (target, T). Within resilient, susceptible and control groups, we compared the NT and T trials using a two-way ANOVA. *Post hoc* comparisons revealed that in Study II, within all except for the D2 resilient mice (likely due to very low *N*), there were significant differences in time spent in the IZ between trials (p_{adj} = 4.20 * 10^{-17} – 6.08 * 10^{-6}). Resilient and control mice from both strains spent more time in the IZ when there was a social target present than when there was not. By contrast, susceptible mice from both strains spent significantly less time interacting with the CD1 mouse than with the empty cylinder. In Study III we found a similar pattern, with significant differences in B6 resilient, B6 susceptible and D2 control comparisons (p_{adj} = 0.0012 – 0.029). As another angle on avoidance behaviour, we compared the amount of time the mice spent in the corners furthest away from the IZ between the two trials. In Study II, susceptible mice of both strains spent significantly more time in the corners when the social target was present than when it was not (p_{adj} = 1.72 * 10^{-6} – 3.42 * 10^{-6}). In Study III the pattern of means was similar to Study II but no comparison reached significance after adjustment. As a measure of locomotor behaviour, we compared the distance the mice travelled during the NT trial of the SA test. The mean distances travelled by resilient and susceptible mice from both strains were lower than the distance travelled by controls. In Study II this was significant for the B6 resilient, B6 susceptible and D2 susceptible (p_{adj} = 2.89 * 10^{-9} – 0.0002), while in Study III the difference was significant for D2 susceptible and resilient mice (p_{adj} = 0.036 – 0.047) compared to controls.

As a measure of broad metabolic consequences of CSDS we recorded the animals' weight throughout the experiment (Studies II and III). We compared the weight at the start (first day of defeat) and at the end of CSDS (day after the SA test). Using a two-way ANOVA we found that in both studies all B6 mouse groups gained weight between the two time points (p_{adj} = 1.35 * 10^{-9} – 0.026). None of the D2 groups gained weight, and D2 susceptible mice in Study III lost weight (p_{adj} = 0.041). However, the amount of weight gained (Δ body weight) in B6 resilient and B6 susceptible was significantly lower compared to controls (p_{adj} = 1.17 * 10^{-8} – 0.0023) in Study II.

For Study III, we also compared the phenotypes and strains on duration of the physical interaction phase of CSDS averaged across each of the 10 encounters using a two-way ANOVA. While there were no differences between resilient and susceptible animals within

either strain (p_{adj} = 0.29 – 0.39), there was a main effect of strain ($F_{(1, 27)} = 87.59$, $p = 5.76 * 10^{-10}$), with D2 mice having significantly shorter defeat durations than B6 mice.

5.2. CSDS associates with a specific pattern of neural activity across brain regions (Study I)

In Study I our objective was to determine which of several stress-related brain regions were chronically recruited during 10-day CSDS in B6 mice. We used an immunohistochemical marker which accumulates during repeated neural (and possibly glial [225, 226]) activity called ΔFOSB. Although the antibody used to detect this protein has a binding site on the parent isoform (FOSB), this isoform degrades relatively quickly while the Δ isoform accumulates in the cell, thus remaining detectable several days after activation [227, 228].

We compared the numbers of $\Delta FOSB^+$ cells in several regions pre-selected for analysis based on prior literature on stress neurobiology. A full list on the included regions can be seen in Study I, Figure 3 and Table 1. Significant increases in $\Delta FOSB^+$ cell numbers were seen in the BNST and vHPC, among others. Although we found a trend for higher numbers of active cells in the IL and PrL subregions of the mPFC, the difference between CSDS-exposed and control mice here did not reach significance. These regions also showed significantly ($p_{adj} < 0.01$) increased MRI signal intensity, reflecting accumulation of Mn^{2+}. In addition to relevant grey matter, containing largely cell bodies, increased MEMRI signal was also observed in white matter regions such as the forceps minor in the frontal cortex. For full activation maps refer to Study I Figure 2.

In addition to a region-by-region activation, we explored the correlation structure of activation between different regions. As illustrated in Figure 7 for mPFC subregions, the BNST and vHPC, the correlation structures differed broadly between control and stress-exposed mice. The radar plot indicates the strength of the correlation (Pearson's *r*) between the title region and each of the regions on the periphery of the radar. In control mice there were markedly few significant correlations, and some regions (e.g. BNST – lateral hypothalamus [LH] and infralimbic cortex [IL] – basomedial amygdala [BMA]) even show a trend for a negative correlation (r = -0.87 and -0.45, respectively). By contrast, in the stress-exposed mice several significant positive correlations emerge. For example, activation in the vHPC is significantly correlated with the IL (r = 0.79) and PrL (r = 0.84), and the PrL with the BNST (r = 0.79), in stress-exposed mice, while their correlations are not significant in controls.

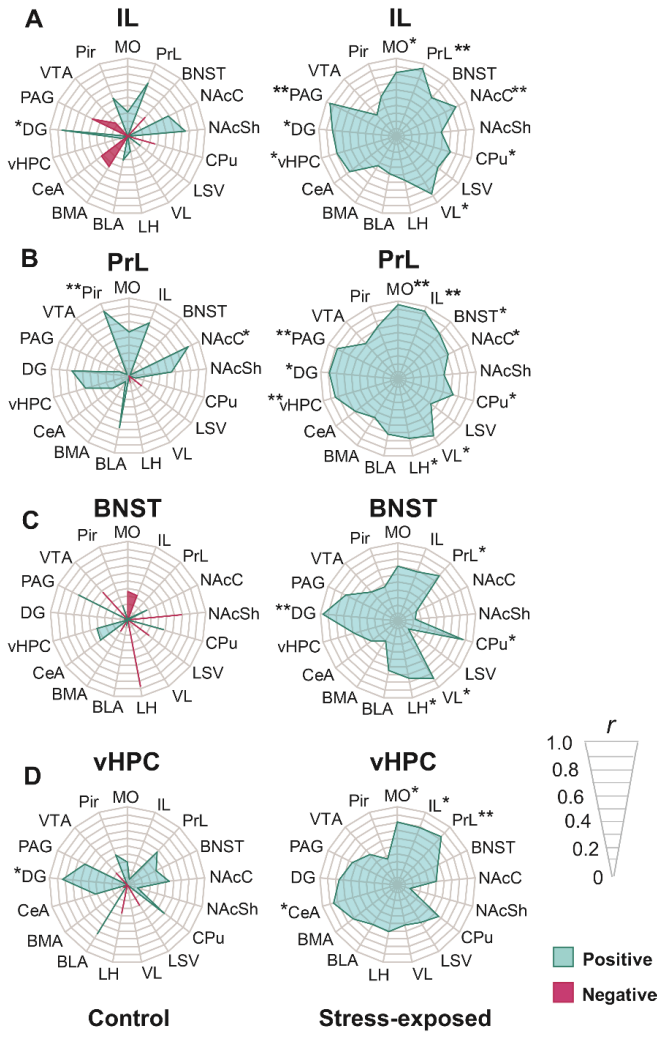

Figure 7. Correlation of activation between stress-related brain regions after CSDS. A-D) Radar plots depicting the correlation (Pearson's *r*) of the IL **(A)**, PrL **(B)**, BNST **(C)**, and vHPC **(D)** and each of the other brain regions included in the ΔFOSB quantification study. Correlations were computed separately for control (left-hand panels) and stress-exposed (right-hand panels) B6 mice. Correlated region pairs with significant nominal *p* values are marked with asterisks (* = $p < 0.05$, ** = $p < 0.01$). Legends on the bottom right denote the magnitude of *r*, and the direction of the correlation (positive or negative). MO = medial orbital cortex, IL = infralimbic cortex, PrL = prelimbic cortex, BNST = bed nucleus of stria terminalis (anterodorsal), NAcC = nucleus accumbens (core), NAcSh = nucleus accumbens (shell), CPu = caudate putamen, LSV = lateral septum (ventral), VL = thalamus (ventrolateral), LH= lateral hypothalamus, BLA = basolateral amygdala, BMA = basomedial amygdala, CeA = central amygdala, vHPC = ventral hippocampus (ventral portions of CA1 & CA3), DG = dentate gyrus (ventral portion), PAG = periaqueductal grey (dorsolateral), VTA = ventral tegmental area, Pir = piriform cortex.

5.3. Myelin-related genes are differentially expressed after CSDS, with expression patterns varying by genetic background and brain region

To investigate how chronic stress alters brain gene expression we performed RNA-seq of tissue dissected from the mPFC and vHPC of CSDS-exposed and non-stressed control mice. Additionally, we analysed differences between stress-resilient and -susceptible mice, defined by their behaviour during the SA test. Susceptible mice displayed a lower SI ratio than same-strain control mice, while resilient mice behaved similarly to the controls despite their stress exposure (see Table 5). Finally, we included mice from two different inbred strains (B6 and D2) to assess the impact of genetic background on the transcriptomic response.

The gene expression patterns were collectively analysed by other co-authors of Study II using GSEA, which searches for enrichment of genes belonging to known common biological functions among the differentially expressed genes (DEGs). This analysis revealed enrichment of oligodendrocyte (OLG) genes in several comparisons in both the vHPC (Table 6) and mPFC (Table 7, see also Study II, Figure 2 E). Due to low number of animals available, analyses of D2 resilient animals were not possible in this study.

In the vHPC we found significant downregulation of several myelin component genes, such as *Mbp*, *Mobp*, *Plp1*, *Cnp* and *Opalin*. These were downregulated in B6 susceptible, B6 resilient and D2 susceptible mice compared to respective controls (see Study II, Figure 2 D). TEM analysis revealed that B6 susceptible mice had thinner myelin sheaths than controls, consistent with the gene expression findings.

Table 6. Summary of myelin-related gene expression and electron microscopy findings for the vHPC. The mean difference for the named comparison is given for myelin thickness, axon diameter and g ratio. Unless otherwise specified, the mean difference is reported for all axon diameters combined. Significant differences ($p_{adj} < 0.05$) are marked with an asterisk (*). n/a = not available, Res = resilient, Sus = susceptible, Con = control, vHPC = ventral hippocampus, B6 = C57BL/6NCrl, D2 = DBA/2NCrl.

vHPC	B6			D2		
	Res vs Con	Sus vs Con	Res vs Sus	Res vs Con	Sus vs Con	Res vs Sus
Expression of myelin-related genes (bulk tissue RNA-seq)	Down	Down	n/a	n/a	Down	n/a
Myelin thickness (µm)	-0.001	-0.0085*	0.0074	-0.0014	0.0019	-0.0033
Axon diameter (µm)	-0.0048	-0.024	0.020	0.00064	0.018	-0.017
g ratio	-0.0014	0.013	-0.015	0.0049	0.0014	0.0036

Gene expression was also analysed in the BNST by a co-author. This revealed upregulation of myelin-related genes in B6 susceptible mice, consistent with thicker myelin sheaths observed with TEM.

In the mPFC we also found downregulation of myelin component genes in the B6 susceptible mice compared to controls, but not in the other comparisons. By TEM we did not see differences in myelin thickness between B6 susceptible mice compared to other groups. However, B6 resilient mice had thicker myelin on small-calibre axons than controls (see Study II, Figure 5 G), while D2 resilient mice had thinner myelin compared to D2 susceptible mice (see Study II, Figure 5 H).

While bulk tissue RNA-seq can, via pathway analysis, give clues about specific biological functions, it is possible that stress does not impact the same functions across all cell types. To understand how a particular cell type, such as OLGs, respond to stress, a cleaner starting material is required. To study how gene expression specifically in OLGs was influenced by CSDS, we performed magnetic-activated cell sorting (MACS) to enrich OLGs from mPFC tissue from resilient, susceptible and control B6 and D2 mice. Interestingly, the myelin fraction has been previously shown to differ in transcript content and protein abundance [229, 230] from bulk tissue, suggesting possible local regulation. Thus, we assessed whether CSDS induced differential transcriptomic responses in the OLG and myelin fractions by separately sorting these with MACS.

No DEGs survived correction for multiple comparisons by the Benjamini-Hochberg method. For exploratory analyses we considered a threshold for nominal significance ($p < 0.05$, log2 fold change > |0.25|) as a criterion for differential expression. We found that the myelin component genes (including *Mbp, Mobp, Plp1, Opalin, Cnp, Cldn11* and *Ermn*) were downregulated in the B6 susceptible mice compared to both resilient and control mice, but only in the myelin fraction. The *Mog* gene was additionally upregulated in the myelin fraction of B6 resilient compared to control mice. By contrast, both D2 susceptible and resilient mice exhibited downregulation of *Mbp* and *Mobp* in the OLG fraction (see Study III, Figure 4 B).

Table 7. Summary of myelin-related gene expression and electron microscopy findings for the mPFC. The mean difference for the named comparison is given for myelin thickness, axon diameter and g ratio. Unless otherwise specified, the mean difference is reported for the analysis of all axon diameters combined. Significant differences ($p_{adj} < 0.05$) are marked with an asterisk (*). Δ = Mean difference and significance reported only for small diameter axons (mean difference for the comparison including all axons = 0.00069, n.s.). - = No difference in gene expression pattern, n/a = not available, Res = resilient, Sus = susceptible, Con = control, vHPC = ventral hippocampus, B6 = C57BL/6NCrl, D2 = DBA/2NCrl, OLGs = oligodendrocytes.

mPFC	B6			D2		
	Res vs Con	Sus vs Con	Res vs Sus	Res vs Con	Sus vs Con	Res vs Sus
Expression of myelin-related genes (bulk)	-	Down	n/a	-	-	n/a
Expression of myelin-related genes (OLGs)	-	-	-	Down	Down	-
Expression of myelin-related genes (myelin)	Up	Down	Down	-	-	-
Myelin thickness (µm)	0.0069*Δ	0.0010	-0.00035	-0.0084	-0.0011	-0.0073*
Axon diameter (µm)	-0.012	0.007	-0.020	-0.0081	-0.022*	0.014
g ratio	-0.0079	-0.0044	-0.0035	0.015	-0.0063	0.022*

One plausible explanation for the observation of lower myelin gene expression and thickness in specific groups is a global myelin atrophy, such as that seen in neurodegenerative disorders like MS. To address this possibility on the structural level, we measured the thickness of the CC in CSDS-exposed and control animals. The CC is a white matter tract which connects multiple regions across hemispheres. Measured at a position close to the Bregma point, we found no differences in CC thickness between groups within either strain (see Study II, Figure 4).

Considering gene expression findings, differences in expression levels could reflect differences in cell numbers. While OLGs are postmitotic, they can undergo cell death or population expansion via differentiating OPCs. We performed an IHC staining study to quantify the numbers of OPCs and differentiated OLGs in three brain regions (mPFC, vHPC and BNST). OPCs and OLGs were defined by expression of cell-type specific proteins platelet-derived

growth factor receptor α (PDGFRA) and adenomatous polyposis coli clone CC1 (CC1) respectively. However, these markers are expressed at low levels also in a few other cell types (endothelial cells [231] and astrocytes [232], respectively), so to restrict the analysis to the OLG lineage we co-stained these markers with OLIG2, an OLG-specific transcription factor. We did not find any group differences in either strain within any of the assessed brain regions ($p_{adj} \geq 0.28$, Figure 8).

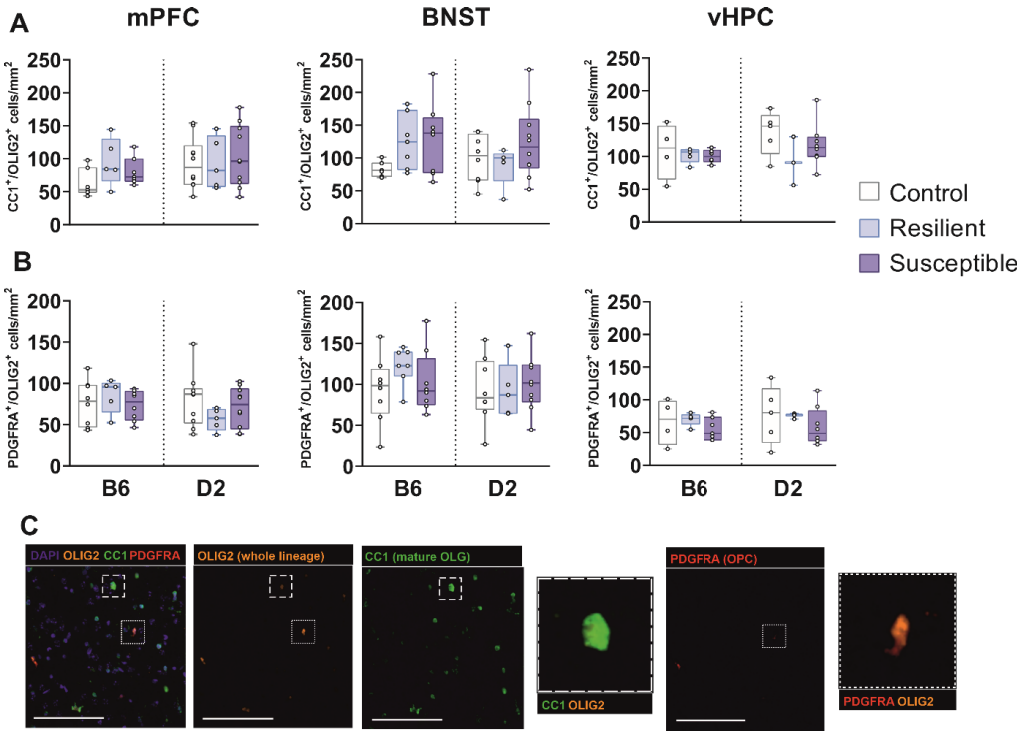

Figure 8. The density of OLGs and OPCs does not differ between resilient, susceptible and control mice in three brain regions. A-B) Box plots of OLGs **(A)** and OPCs **(B)** in three brain regions (mPFC, BNST and vHPC). Each data point represents one animal's average number of cells across 3–14 images. Max *N* of animals for B6 = 21 (8 control, 7 resilient, 8 susceptible) and D2 = 25 (10 control, 5 resilient, 10 susceptible), animals with < 3 images of a specific region were excluded from analyses of that region. **C)** Representative image demonstrating the triple-staining, showing a $CC1^+/OLIG2^+$ cell (OLG, large dashed outline) and a $PDGFRA^+/OLIG2^+$ (OPC, small dashed outline).

5.4. OLGs and myelin show enrichment of different genes

Past work has suggested that some mRNAs are transported from the OLG soma to myelin sheath for local translation [233, 234], and that the transcriptome and proteome of isolated myelin differs from that of bulk brain tissue [229, 230]. However, as membrane extensions of OLGs, a direct comparison of mRNAs found in the OLGs and myelin of the same individuals is needed to assess the extent of transport. We compared gene expression levels of MACS-enriched OLGs and myelin from non-stressed control animals (B6 and D2 strains). A higher number of genes met the criteria for reliable detection in OLGs than myelin (1 count per million in at least 6 samples; 17 112 genes in OLGs and 15 648 genes in myelin). Comparing mice from the two strains we found that few genes were differentially expressed (372 genes in OLGs of B6 vs D2, and 115 in myelin of B6 vs D2), so the comparison of OLG and myelin fractions is presented as the average of the strains (see Study III, Figure 2). Of genes expressed in both fractions, 24.8 % were expressed at a significantly ($p_{adj} < 0.05$) higher level in OLGs than myelin. By contrast, 20.2 % were expressed at a higher level in myelin than OLGs. Using miRNA-sequencing we also identified miRNAs enriched in OLGs (14.3 %) and in myelin (18.8 %).

5.5. MACS-enriched RNA-seq suggests potential functional regulators of myelin component gene expression and myelin sheath properties

Next, we investigated whether any molecules served as predicted regulators of the stress-related gene expression patterns in OLGs and myelin. We applied IPA on differential gene expression data. Across all 12 comparisons including both OLG and myelin fractions, we discovered that TCF7L2 was predicted to be a significant upstream regulator in four comparisons (Z-score range -2.67 – -5.49). These included the myelin fraction of B6 susceptible mice compared to both control and resilient mice, and the OLG fraction of both D2 resilient and susceptible mice compared to controls. In all of these, based on the direction of differential expression of predicted targets, TCF7L2 was predicted to be inhibited. Among the predicted target genes differentially expressed in the predicted direction (Figure 9) were several myelin component genes. Each of these genes was downregulated in the named comparison.

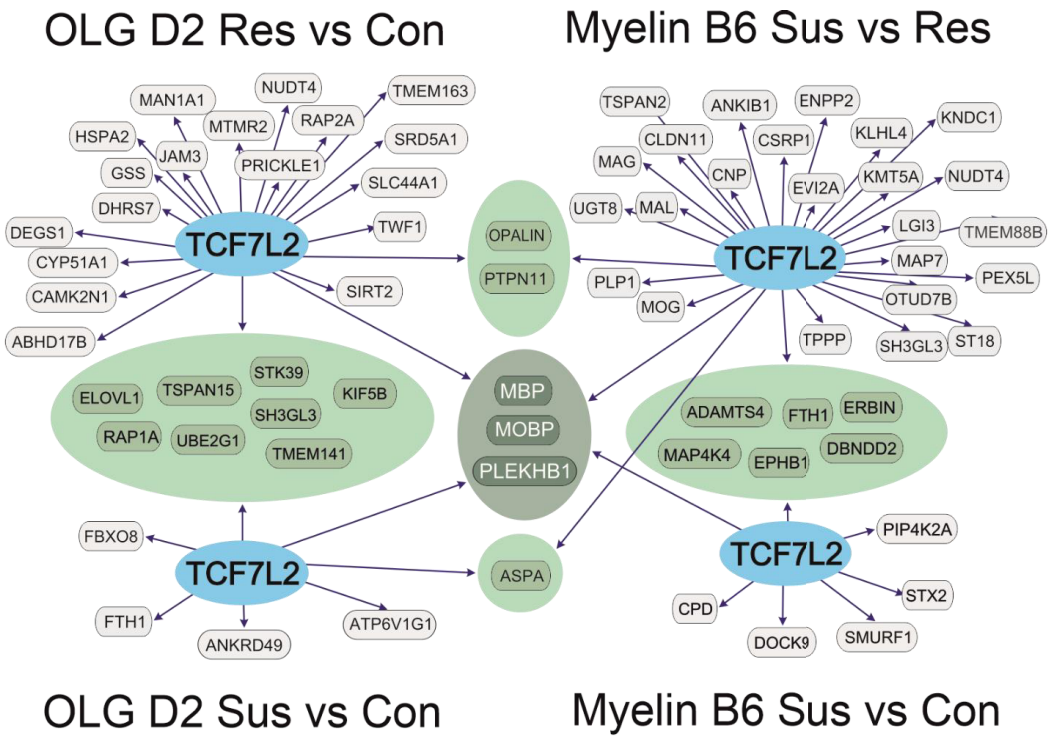

Figure 9. Illustration of Ingenuity Pathway Analysis (IPA) predicted targets of TCF7L2. Network plot showing genes DE in each contrast in which TCF7L2 was predicted to be a significant upstream regulator. In each of these, TCF7L2 was predicted to be inhibited, and each predicted target gene was downregulated. Only genes DE in the direction consistent with the one predicted by IPA are presented. Genes DE in several comparisons are grouped and indicated by arrows. Res = resilient, Sus = susceptible, Con = control, vHPC = ventral hippocampus, B6 = C57BL/6NCrl, D2 = DBA/2NCrl, OLG = oligodendrocyte.

6. Discussion

6.1. General conclusions

In this thesis we first identified brain regions repeatedly activated during chronic psychosocial stress (CSDS) in mice (Aim 1). B6 stress-exposed mice showed higher numbers of $\Delta FOSB^+$ cells in several regions, including the BNST and vHPC. To explore possible functional connections between activated regions, we analysed the correlations between $\Delta FOSB^+$ cell counts between regions. We found significant correlations between mPFC subregions (IL and PrL) and the vHPC of stress-exposed, but not non-stressed mice. This suggests functional connectivity between these regions may be enhanced during and after stress.

In the next experiment, we performed RNA-seq of mPFC and vHPC tissue from mice exposed to CSDS and phenotyped as resilient or susceptible, comparing to non-stressed control mice. To address the role of genetic background we used two inbred mouse strains, B6 and D2. We found that B6 and D2 mice differed in the proportions in which they were resilient or susceptible to CSDS, with B6 mice being mostly resilient and D2 mice mostly susceptible. GSEA suggested that OLG-related genes were downregulated in the vHPC (B6 resilient, B6 susceptible and D2 susceptible compared to controls) and mPFC (B6 susceptible vs control), addressing the second Aim of this thesis. CC thickness was not altered by stress, suggesting that stress does not cause global demyelination. Electron microscopy revealed myelin thickness differences. In the vHPC B6 susceptible mice had thinner myelin than controls. In the mPFC, B6 resilient mice had thicker myelin sheaths than controls in small calibre axons. Interestingly, resilient mice from the D2 strain had thinner myelin in this region compared to controls. These findings suggest myelin plasticity as a potential major component of the prolonged stress response. As the numbers of OPCs and OLGs were unchanged, we hypothesized that the gene expression differences are more likely to stem from functional differences occurring within the cells rather than effects of stress on their survival or differentiation.

To follow up on these findings we enriched oligodendrocytes and myelin from the mPFC of resilient, susceptible and control B6 and D2 mice. First, we compared the OLG and myelin fractions from non-stressed control mice. We found several genes enriched specifically in one fraction over the other, with limited influence by genetic background, suggesting transport signals are relatively resistant towards influence by genetic background. Furthermore, we replicated the bulk tissue RNA-seq finding of lower expression levels of myelin-related genes in the mPFC in myelin of B6 susceptible compared to resilient and control mice. We also found

downregulation of these genes in the OLG fractions of D2 susceptible and resilient mice compared to controls. Bioinformatic analysis predicted that these DEG result may be downstream of inhibition of TCF7L2, a transcription factor (TF) with a known role in OLG biology. This represents a potential molecular mechanism of stress-related myelin gene expression differences, as per Aim 3. We propose a pathway of stress affecting OLG gene expression via acting on TCF7L2, with genetic background-dependent deviations from this path underlying resilience.

6.2. Stress-related activation of brain region and putative networks

In Study I, we demonstrated that CSDS exposure in B6 mice associated with higher levels of markers of chronic activation (ΔFOSB and MEMRI) in several brain regions known to be relevant for stress and psychopathology [2, 57, 76, 235]. Other studies utilizing rodent models of stress and quantifying $\Delta FOSB^{+}$ cells have reported higher numbers in stressed than control mice in several of the same regions (e.g. the BNST and dentate gyrus, [236]). However, there are also some differences, such as the NAc, PAG and the BLA showing higher activation after stress in other publications [227, 237-240] but not in our experiment. A possible explanation for this discrepancy is differences in the timing of measurement. Vialou et al. [236] collected fixed brain tissue 24 hours following CSDS, while we collected samples 6-8 days after CSDS in order to focus on more chronic features of stress exposure. Other work using a longer post-defeat delay (20 days) has reported no differences in ΔFOSB protein abundance as measured by Western blotting in the mPFC and vHPC [129], which is less sensitive than IHC detection of individual positive cells. Collectively, these and our findings indicate dynamic stress-related activity changes, and that some differences between controls and stress-exposed mice observed immediately after stress may subside. Changes remaining for substantial periods after stress cessation, such as weeks or months, are likely to be highly relevant for long-term consequences of stress, such as psychopathology.

In addition to being an activity marker, FOSB acts as a TF, altering gene expression. Chromatin immunoprecipitation followed by sequencing (ChIP-seq) has shown that the binding targets of FOSB are enriched in genes contributing to neuronal excitability and neurotransmission [241]. Interestingly, both overexpression and inhibition of FOSB in the dorsal HPC acutely affects neuronal physiology, reducing the frequency of excitatory postsynaptic currents [242]. After stress, local overexpression in the PAG promotes resilience against CSDS in B6 mice [239]. In addition to variance between brain regions, the relationship between ΔFOSB and the response to stress can vary between neuronal subtypes. In the D2-receptor-expressing medium

spiny neurons (MSNs) in the NAc, acetylation of histones influencing the promoter for the *FosB* gene makes mice more susceptible to CSDS. By contrast, the same posttranslational modification in D1-expressing MSNs confers resilience [243]. Based on our findings, it would be of interest to explore the functional role of ΔFOSB specifically in regions where we find it to be more abundant chronically after stress, possibly contributing to its long-term consequences.

To assess putative networks engaged by CSDS, we calculated correlations between numbers of $\Delta FOSB^+$ cells between regions. While *in vivo* neuroimaging is the gold standard for determining functional connectivity between regions [244], activity-related protein abundance has also been reported to correlate between jointly recruited regions in *ex vivo* measurements [245-247]. The correlated numbers of $\Delta FOSB^+$ cells between the vHPC and mPFC subregions (PrL and IL) seen in CSDS-exposed mice is interesting because synchronised activity between these regions has previously been shown in rodents during an anxiogenic task [74]. Local field potential recordings from mice before and after exposure to CSDS also highlighted the mPFC and vHPC as part of vulnerability network, where distinct activity could predict later susceptibility [248]. Pharmacogenetic activation of cells residing in the vHPC and projecting to the mPFC is also anxiogenic [75]. The connectivity between these regions has been mapped across species [249, 250]. The uncinate fasciculus (UF), a major white matter tract connecting these regions in humans, has been implicated by neuroimaging research with MDD and anxiety disorder patients [213, 251]. Childhood maltreatment associates with lower fractional anisotropy (FA) along this tract, and lower FA also predisposes adults to stress-induced negative affective symptoms [252]. However, as reviewed by Ayling et al. and Bracht et al, there are reports for both increased and decreased FA along this tract in relation to anxiety disorders and MDD, possibly due to heterogeneity within and between study samples. A combined staining of an activity marker protein with a cell-type marker would also inform the nature of the activated circuits. Kovacs et al. [253] showed that 14 days of restraint stress induced ΔFOSB in CRF-expressing neurons in the paraventricular nucleus of the hypothalamus, but not in the CEA or BNST. Vialou et al [236] also co-stained samples from the PFC with a marker for GABAergic neurons and report minimal co-localisation, suggesting the signal stems primarily from other neuronal types, such as glutamatergic pyramidal neurons. Animal models could shed light on factors moderating the relationship between stress, structural and functional connectivity, and downstream effects such as psychopathology.

While IHC provides excellent spatial resolution, we are limited by the lack of anatomical landmarks in distinguishing some adjacent brain regions from one another. Recent evidence has also challenged the idea that these landmarks are in every instance the best strategy for defining functionally distinct regions. For example, the molecular atlas provides a gene expression-based signature for hippocampal subregions (e.g. dorsal-ventral domains of pyramidal cell layers CA1 and CA3, [254]), which are difficult to distinguish by any known anatomical borders. This information could be integrated into investigations of regionally specific events, such as neuronal activation, by co-staining with specific domain-defining antibodies. Such methods would bridge the gap between structure and function, helping us truly understand which neuronal network are engaged during chronic stress.

There are limitations in Study I which impact our conclusions. Firstly, using only one inbred strain leaves possible genetic background effects unexplored. Given the differences in behaviour noted in Studies II and III, the possible contribution of differential recruitment of brain regions could be addressed. Acutely after restraint stress there is a difference in the degree to which B6 and Balb/c strain mice show activation of the cingulate cortex [255]. Secondly, in this study it was not possible to address differential activation in resilient and susceptible mice. Only 1/10 of the mice allocated to the CSDS-exposure condition had an SI ratio indicative of susceptibility. Thus, we performed all analyses as CSDS-exposed mice compared to non-stressed controls. Exploring the moderation by genetic background as well as differences between resilient and susceptible mice in the same study system, as was done for Studies II and III, would be highly informative. This would allow addressing the question of whether the differential rate of susceptibility we observed in D2 and B6 strains could relate to recruitment of different neuronal populations. This in turn would greatly enhance our understanding of how individual differences in stress processing contribute to its consequences.

CSDS as a model of psychosocial stress also has some limitations, although generally considered to have good construct validity [256, 257]. Although mostly discussed in the context of MDD, arguing for the validity of any animal model for a complex diagnostic entity such as MDD or anxiety disorders is challenging. It is more straightforward to argue for its validity as a model for the principal environmental risk factor which applied to both of these, namely chronic psychosocial stress. The popularity of CSDS for this purpose is founded in key features, such as being a predominantly social stressor (as opposed to physical environmental stressors like CUMS) and consistently producing some individuals which respond with maladaptive behaviours (i.e. reduced social interest) and some which do not (resilience).

However, it also has some shortcomings. Chiefly, the standard form of the protocol does not consistently work with female mice as the male aggressors typically do not attack females, and even when employing aggressors that do attack only 20 % of the female mice were susceptible [258]. This is in stark contrast with what is known about human females being roughly twice as likely to develop an anxiety disorder or MDD [1, 17, 19], although these epidemiological studies have not accounted for the specific role of stress as a risk factor. With protocol variations it is possible to get male mice to more consistently show dominant behaviours toward the females and induce similar avoidance behaviours as we see in males [258, 259]. However, given that this behaviour requires a high amount of manipulation to occur, it arguably lacks in ethological validity. This makes it difficult to generalise from molecular level findings of CSDS-exposed female mice to naturalistically stressed female humans. Many have worked around this issue by using other rodent species where female-female aggression does naturally occur (such as the mandarin vole, [260]). Others use stress models with social components which do produce consistent results in females, such as social isolation [261], social instability [262] or vicarious exposure to social defeat [263]. Large leaps in our understanding of stress pathophysiology will likely necessitate the inclusion of female subjects in preclinical work, and indeed this is increasingly recognized in the field [264]. Thus, while CSDS can today with confidence only be considered valid for males, future work will reveal whether and how these findings generalise across sexes.

6.3 Genetic background influences the behavioural response to CSDS

In Studies II and III we compared resilient and susceptible mice on measures of social behaviour. Firstly, social interaction was used to phenotype mice as either resilient or susceptible. Because B6 and D2 control mice displayed different SI ratios, this phenotyping was done with respect to a strain-specific cut-off point rather than a universal one. Susceptibility occurred in both strains, but at vastly different rates. In Studies II and III, 33.9 % of B6 mice and 85.0 % of D2 mice were susceptible to CSDS. However, the behavioural profile of susceptibility was very similar between the strains in both Studies II and III. These mice spent less time in the IZ and more time in the corners of the SA test arena when a social target was present, than when the IZ only contained an inanimate object. They also moved less during the test overall, and gained less weight during the 10 days of CSDS than control mice. The resilient mice of both strains were broadly similar to controls in terms of the aforementioned measures. The significant difference in duration of physical interaction between strains likely stems from D2 mice being more susceptible to incur small wounds

during defeat, which was a criterion for ceasing the physical interaction before 10 minutes had elapsed. However, resilient or susceptible status was not a result of different durations spent physically interacting with the aggressor CD1, suggesting that intensity of defeat is not causative of susceptibility.

Replicable differences in anxiety-related behaviours observed between inbred strains have led to propositions to consider certain strains as models of trait anxiety [265], a risk factor for anxiety disorders in humans [117]. Our finding that the strain demonstrating high baseline anxiety-like behaviour (D2) was also more susceptible to stress mirrors work in humans suggesting that trait anxiety mediates the effect of stress exposure on depressive symptoms [266]. The Balb/c strain, also considered high in trait anxiety, is also more susceptible to CSDS than the B6 strain [267]. For animal models of disordered anxiety, capturing trait anxiety is arguably more relevant than state anxiety. Tests of rodent anxiety-like behaviour, such as the approach-avoidance conflict tests detailed in Figure 2, are suitable for assessing state anxiety, but by themselves have limited validity for trait anxiety. Thus, one of the factors potentially slowing the development of new anxiolytics is that they are primarily tested for effects on measures of state anxiety. The future of anxiolytic research hopefully makes better use of diverse genetic backgrounds as trait anxiety models than in the past.

6.4. Resilience – lessons from unboiling an egg

Although differing in frequency between B6 and D2 strains, resilience still occurred in both. Human studies of resilience are frequently limited by cross-sectional design and reliance on retrospective reporting of stress, which may be subject to biases. It is also rare for the same study to include resilient, susceptible and control subjects [268]. However, a deep understanding of what makes some individuals resilient could hold the key to revealing the critical features of susceptibility as well. To illustrate this, consider that one is tasked with finding out how to unboil an egg. Boiling results in alterations in how the proteins in the egg interact, a disordered state caused by the application of heat. The requirements for effectively unboiling an egg have been described [269]. The process requires two steps; the solid mass is first liquified by the addition of urea, after which the dissolved proteins are induced to re-fold by mechanical sheer stress.

Two critical lessons can be learned from this illustration. Firstly, understanding the mechanism by which the disordered state was achieved gave only part of the answer for how to best achieve a re-ordered state. To achieve the state reversal the authors could not simply go back the same

way they got there, by attempting to directly unfold the proteins. Rather, a permissive intermediate step was required, namely the addition of urea. Similarly, when it comes to stress-susceptibility, it may not be sufficient or even possible to simply reverse the disordered molecular-level feature(s) back to the non-stressed state. Rather, we need a thorough understanding of what the allostatic load contributing to the susceptible state is truly composed of, at the levels of molecules, networks, circuits, and finally the whole organism, and indeed new frameworks like RDoC strive to do this [26]. Many of the pieces of this puzzle are collected, but the full picture has not yet emerged. A mechanistic understanding will hopefully enable the identification of what the necessary permissive state for reversing susceptibility is, and how to achieve it.

The second lesson is that while the unboiled state is functionally similar to the pre-boiled state, it is not exactly equivalent. For the purposes of Yuan et al, which was developing a fast and affordable way to re-fold misfolded proteins in pharmaceutical development pipelines, the procedure achieves what was intended. But the unboiled egg has undeniably lost some features, such as palatability by the addition of the urea. Returning the boiled egg fully to the pre-boiled state may turn out to be impossible by the laws of entropy, as may returning a stressed brain to its pre-stress state. Instead, we should focus our efforts on finding a state that satisfies the functional needs. In the case of psychopathology, this state would be an asymptomatic life for the patient. Functionally, this state is likely best captured by resilient subjects; those who went through a stress exposure but experienced adaptive, allostatic consequences rather than maladaptive ones.

This is why studying resilient subjects is absolutely critical, which has also been emphasised in the field in recent years [270]. By truly understanding the states of susceptibility as well as resilience we can hopefully figure out what the functional equivalents of adding urea and mechanical sheering would be when it comes to the stressed brain. Our findings add a layer of complexity to this. Although resilient B6 and D2 mice resemble each other behaviourally, transcriptionally they share very little (Studies II and III). This indicates that genetic background heavily moderates how the resilient state can be achieved after stress. Consequently, ideal therapeutic strategies may also vary by individual difference factors such as genetics. Should, for example, the rescue of myelin-related gene expression in the B6 susceptible mice in future studies turn out to also rescue behavioural effects of stress, it is possible that such a treatment would have no effect in the D2 strain where resilient mice also have lower expression of these genes (see below). Indeed myelin-related genes do respond to

successful recovery of susceptible mice after ketamine treatment in the B6 strain [204], but other strains have yet to be tested. This potential lack of generalisability further underscores the need for a mechanistic understanding of how resilience arises, and how its modulated by individual differences.

6.5. Myelin-related gene expression differs after CSDS, with concurrent differences in myelin structure

Across Studies II and III, we found that myelin component genes are downregulated in the mPFC in susceptible mice of the B6 strain in both bulk tissue and myelin-enriched RNA-seq. The numbers of OPCs and OLGs did not differ between resilient, susceptible and control mice in any of the regions assessed here. Some prior studies report a similar lack of effect of stress [189, 199], while others have found lower numbers of OPCs in adult mice exposed to maternal separation as pups [194]. Cell survival does at least not in our case explain the gene expression differences, but it remains possible that stress could in the long term influence OLG lineage cells. In the bulk mPFC RNA-seq data we did not observe downregulation of myelin-related genes in the D2 susceptible mice, but in the OLG-enriched RNA-seq we did. This suggests that RNA-seq carried out on bulk tissue may not have sufficient resolution to detect gene expression differences occurring in restricted compartments of OLGs, which only make up approximately 20 % of the cells in the cortex and HPC [271]. The power of cell-type enriched sequencing is that it enables the query of such restricted effects, revealing the downregulation of myelin component genes in both of the strains used here. This finding also raises the interesting possibility that stress could alter myelin-related gene expression in different ways in these two strains. Differences seen only in the myelin fraction could be due to, for example, effects of stress targeting the transport machinery, while differences in the soma fraction could reflect effects on transcription. Fraction-selective differences in gene expression can also arise from local mRNA degradation. A wide variety of proteins involved in the regulation of either transcription [147] or vesicular transport and local regulation [233, 272] in OLGs are known. Examining how their function or abundance could be affected by stress would be highly interesting, as a step closer to a mechanistic understanding of how stress could influence myelin.

More generally, we also demonstrated that the gene expression pattern in myelin differs from that of OLGs in the same individuals. Previously, the transcriptome and proteome of myelin has been shown to be unique with respect to bulk tissue [229, 230]. The specificity of gene expression may stem from selective transport of mRNA into the myelin sheath. This process is

well described for key myelin component *Mbp*, which is targeted and packaged into vesicles and transported into the distal parts of the myelin sheath. This enables local effectors, such as Fyn kinase, to rapidly induce translation of MBP to produce more myelin, either to maintain MBP in the face of turnover or to plastically alter myelin properties [272]. Sequences targeting transcripts for transport have been recognized [233, 234]. Our dataset of myelin-enriched transcripts could be used to identify novel targeting sequences and proteins with roles in myelin maintenance or function. Additionally, several miRNAs have been recognized as regulators of OLG differentiation and myelination [273-275], but the subcellular localisation of this regulation is not known. In neurons, miRNAs have been shown to travel to distal dendrites and potentially regulate mRNAs locally [276]. We found a number of miRNAs enriched in the myelin fraction, representing potentially novel regulators of transported mRNAs. Localisation of specific mRNAs and miRNAs to the sheath need to be validated with *in situ* methods before strong conclusions can be drawn, as the MACS-enriched material may also contain contaminating mRNAs from the axons ensheathed by the myelin we collected. Our data will hopefully provide a fruitful starting point for developing our understanding of myelin biology.

To our knowledge, our TEM findings are the first demonstration of myelin thickness differences at the nanometre resolution in two mouse strains after CSDS. In the vHPC, we found that susceptible B6 mice had thinner myelin sheaths than controls, which mirrored their lower myelin gene expression compared to controls. In the D2 strain, despite these genes also being expressed at a lower level than in controls, myelin thickness did not differ in either resilient or susceptible mice compared to controls. By contrast, in the mPFC the B6 susceptible mice had similar myelin thickness to controls, but resilient mice had thicker myelin (restricted to small-diameter axons). D2 resilient mice had thinner myelin sheaths than controls in this region. Young mice exposed to social isolation has previously also been associated with thinner mPFC myelin [191]. Our findings demonstrate that stress occurring in a developmental stage equivalent to late adolescence in humans [277] associates with differences in both myelin gene expression and structure, and that this is controlled by genetic background.

Adding to prior literature associating myelin with stress exposure, we showed structural differences associating specifically in resilience. Intriguingly, resilient mice from B6 and D2 strains showed opposite directions of myelin thickness differences compared to same-strain controls or susceptible mice. While the difference in the D2 strain was seen across all axon diameters, the B6 difference was observed only in axons with small calibres. The identity of neurons projecting these axons cannot be deduced from this data, as for example pyramidal

and inhibitory neurons in the rodent cortex have indistinguishable diameters [278] and both can be myelinated [279]. Some evidence suggests that compared to other areas, prefrontal projection neurons have comparatively thin axons [221], but such patterns have yet to be verified in mice. Neuronal activity is a major regulator of adult myelin plasticity [166], so if the genetic background influences activity patterns it could explain the variance in myelin related to specific axonal tracts as well. As discussed above, it remains unknown whether these two strains differ in stress-induced neuronal activation. This has important implications for our understanding of resilience; it may be achieved via different routes depending on the pre-stress features of an individual.

In humans, myelination patterns in different cortical regions is genetically controlled, implicating individual differences in relevant variants may also influence inter-individual variance in myelin [280]. By extension this means that to promote resilience-related myelin features, different methods may be best suitable for different genetic backgrounds. Most published mouse work uses B6 substrains, although stress-related lower myelinated area has also been reported for Balb/c mice [197]. Research into white matter features of human resilience, such as Tendolkar et al. [281], report a negative correlation between FA in the anterior thalamic radiation, a frontal white matter tract, and the intensity of childhood maltreatment. Although not explicitly phrased as a study of resilience, the study sample was restricted to males reporting any experience of childhood trauma but with no past or current psychiatric disorders. Similar studies [208, 210] have reported lower FA in the cingulate gyrus and UF in stress-exposed but psychiatrically healthy individuals compared to non-stressed controls. By contrast, Fani et al. [282] found higher FA in another frontal tract, the posterior cingulum, in women reporting significant trauma but not PTSD, psychotic or substance abuse symptoms. In both studies resilience was only studied in contrast to susceptibility, and they vary considerably in their definition of resilience and sample characteristics (sex). In light of our findings, it would also be interesting to explore whether genetic signatures, such as those associating with anxiety disorders [4, 5, 44], could group together with different white matter patterns in resilience or susceptibility. While we did not restrict the TEM analysis to functionally equivalent PFC tracts as these studied in humans, our findings comparing the strains suggest that resilience-associated myelin structure may vary based on characteristics such as genetic background.

An alternative explanation for the TEM findings could be that they existed before CSDS and rather predict vulnerability or resilience than occur as a result of stress. There are currently no

available methods for addressing this with longitudinal *in vivo* measurements in our regions of interest (discussed in detail below). Differences even within an isogenic inbred strain do occur, possibly as a result of variation in the early postnatal or even prenatal environment [283, 284]. Variability in myelin thickness within a strain thus remains a possibility. One way to explore the effects of myelin features on behaviour is to use a mouse model with defects in myelin. Such defects, as achieved by KO of relevant genes, also impacts anxiety-like and stress-related behaviour. Cathomas et al. [201] report lower social interaction after exposure to CSDS in *Cnp1*$^{+/-}$ mice but not in wt controls. *Olig2* KO mice display an anxiogenic phenotype on the OFT and high susceptibility to social isolation stress compared to wt mice, and lower ability to distinguish between a novel and a familiar object, indicative of memory deficits [195]. Interestingly, some studies (such as [198]) report lower anxiety-like behaviours in a myelin-related KO model (*Cnp1*$^{-/-}$), along with higher resilience to a chronic mild stress exposure protocol. However, these animal models typically affect myelination in the same direction across the whole brain and lifespan. This makes them less attractive for testing how regionally specific and bidirectional myelin thickness differences would impact the behavioural response to stress in early adulthood. Myelin as a vulnerability for later maladaptive responses to stress are an interesting possibility, and should be assessed with appropriate methods.

6.6. TCF7L2 is a potential upstream regulator of stress-related myelin plasticity

Using a bioinformatic tool based on interactions between specific molecules and gene expression (IPA), we discovered TCF7L2 as a potential upstream regulator of DEGs in myelin and OLGs of B6 susceptible, D2 susceptible, and D2 resilient mice. Myelin component genes were downregulated in these comparisons and were predicted to be targets of TCF7L2. TCF7L2 was also predicted to regulate stress-associated DEGs in the mPFC of male B6 mice in a previous study [203], making it a very interesting target for further research in stress in general, but OLGs in particular.

TCF7L2 is a pleiotropic TF expressed across the body, with well-known functions in the liver and pancreas [285, 286]. Polymorphisms at the *Tcf7l2* locus have been replicably associated with type II diabetes in GWASs [287], but recently also with psychiatric disorders [288]. Haploinsufficiency in mice alters startle responding in a genetic-background dependent way [103]. B6 *Tcf7l2*$^{+/-}$ also show higher anxiety-like behaviour than wt littermates on the OFT and LD tests [289]. As covered in section 2.3.2 of this thesis, it is an important part of the transcriptional machinery across the OLG lineage. It has multiple binding partners, such as β-catenin [290], histone deacetylases (HDAC) 1 and 2 [291], Kaiso, and SOX10 [148]. Knocking

the *Tcf7l2* gene out in rodents with OLG lineage-specific drivers has produced mixed results. Myelin gene expression was reduced if knock-out was done in the whole lineage with an OLIG2 promoter driving the expression of Cre recombinase, but not with a PLP1 promoter which is only active in mature OLGs. However, myelin-related gene expression was reduced in a line using the CNP promoter [292]. *Cnp* is expressed in the mature myelin-producing OLGs and in premyelinating cells [293]. Knocking out specifically the DNA-binding domain of TCF7L2 under an OLIG1 promoter also reduces myelination, OLG differentiation, and remyelination after injury in adult mice, without effects on OPCs [148]. *Cnp-Cre* mediated knock-out of the DNA-binding domain *in vivo* has shown that during early postnatal life it promotes OLG differentiation [290]. TCF7L2 is also highly abundant in early but not chronic sites of MS injury in humans [294] and cuprizone-induced lesions in mice [295]. The role of TCF7L2 in these lesions is disputed, with some arguing that it imposes a blockade on differentiation (as a marker of activated canonical Wnt/β-catenin signalling), and others that it is a marker of attempted (but failing) remyelination [290]. While the jury is still out regarding its exact role in disease progression, it is undeniably involved in the promotion of myelin gene expression at the point when healthy OLGs are maturing.

The IPA prediction of TCF7L2 being a regulator of DEGs would most simply be explained by its direct actions as a DNA-binding transcription factor. Zhao et al. [148] performed ChIP-seq on cultured OLGs at different stages of differentiation. They showed that TCF7L2 has much larger binding peaks in maturing OLGs than immature cells, although there is overlap in the identity of the genes nearest the binding peaks. Curiously, there is only minute overlap between these genes and those identified as TCF7L2 targets in hepatocytes. Myelin component genes like *Mbp* and *Mobp* do not appear to have significant TCF7L2 binding in these experiments. In immature OLGs, TCF7L2 is co-associated with Kaiso, a Wnt signalling inhibitor, which reduces the interaction of TCF7L2 with β-catenin. This event, occurring early in the maturation process, may be necessary for releasing Wnt-induced inhibition of differentiation [296], and promoting TCF7L2 occupancy on the *Myrf* gene, which in turn promotes expression of myelin component genes. *In vitro*, MYRF has been shown to bind at myelin component genes [149, 297]. Mediation of the predicted effects of TCF7L2 inhibition by MYRF remains a possibility as the databases utilised by bioinformatic tools like IPA are continuously updated, with much still to add about a newly discovered TF such as MYRF. *In vitro* studies with perturbations of TCF7L2 and MYRF could be applied to address the question of whether TCF7L2 or MYRF is the closest upstream regulator of stress-related myelin gene expression effects.

Another question of interest is what lies upstream of TCF7L2 in OLGs. In other words, how would stress influence its actions? In Study III *Tcf7l2* was upregulated in the OLGs of B6 susceptible mice, and not differentially expressed in other comparisons. While the role of this in our system would be an interesting avenue of further research, TFs are also frequently regulated on the post-translational level [298]. Regulation can occur also at the level of binding partner, such the competing actions of HDAC1/2 and β-catenin [291]. When bound to the former, TCF7L2 promotes OLG differentiation. Studies on mice with constitutively overactivated β-catenin in the whole OLG lineage throughout development [299] or on remyelination following experimentally-induced injury to myelin [300] suggest that Wnt/β-catenin activity inhibits OLG differentiation, and consequently is inhibitory of myelination. However, others have found that under physiological or intermittently induced Wnt/β-catenin activity myelination is actually promoted [301], and chronic stress exposure may reduce activated β-catenin mediating myelin loss [302]. Interestingly, pharmacologically inhibiting glycogen synthase kinase 3 β (GSK3β, silencer of β-catenin), without altering upstream Wnt signalling, promotes both OPC proliferation and OLG differentiation [296]. Downregulation of GSK3β by small interference (si)-RNA *in vitro* increases the transcription of *Tcf7l2*, which can be mimicked by acute lithium treatment [303]. It is possible that disturbances in different nodes of this molecular network can have interactive effects, and when building a detailed model of how this pathway is involved in stress-induced effects on OLGs it is important to mind this complexity.

A putative network merging our findings regarding TCF7L2, myelin gene expression and myelin thickness in susceptibility and resilience across strains is presented in Figure 10. As the only group without predicted TCF7L2 regulation of DEGs, we propose that B6 resilient mice escape stress-related inhibition of TCF7L2. Due to this, or some additional myelin-promoting effects, these mice show thicker myelin in the mPFC, potentially as a result of activity-related plasticity. By contrast, in the other groups stress inhibits TCF7L2, but the mechanisms of this are not known. In D2 mice, this could relate to the observed lower expression of myelin component genes in the OLGs. In resilient, but not susceptible, D2 mice we observed thinner myelin sheaths, consistent with lower gene expression. If this occurs as an adaptive response, it would suggest that a rapid progression from lower myelin gene expression to thinner myelin on mPFC axons at least in the D2 genetic background promotes resilience. This could occur via adjusting the processing speed of the involved neuronal networks. As for susceptible mice, prior work using longer stress exposures reviewed above, at least in younger mice from the B6

strain, suggest mPFC myelin can become thinner after stress. If this were found to be the case also in adult mice exposed to CSDS, our data would suggest that myelin gene expression downregulation precedes myelin thinning. Lower mRNA availability may over time lead to either reduced capacity for plastic increase in myelin thickness, or gradual loss as a result of failing to compensate for myelin turnover. However, this sequence of events would need to be verified with a longer post-stress delay. The bioinformatic prediction also does not take into account localised regulatory effects of molecules like TCF7L2. It is currently not known whether TCF7L2 has extra-somatic functions, such as regulating mRNA packaging or transport. It may thus be that the upstream regulator of myelin component DEGs in the myelin fraction is rather a factor affecting transport than transcription. Careful and thorough mapping of how stress interacts with this network could provide much-needed insights into the neurobiology of stress susceptibility and myelination.

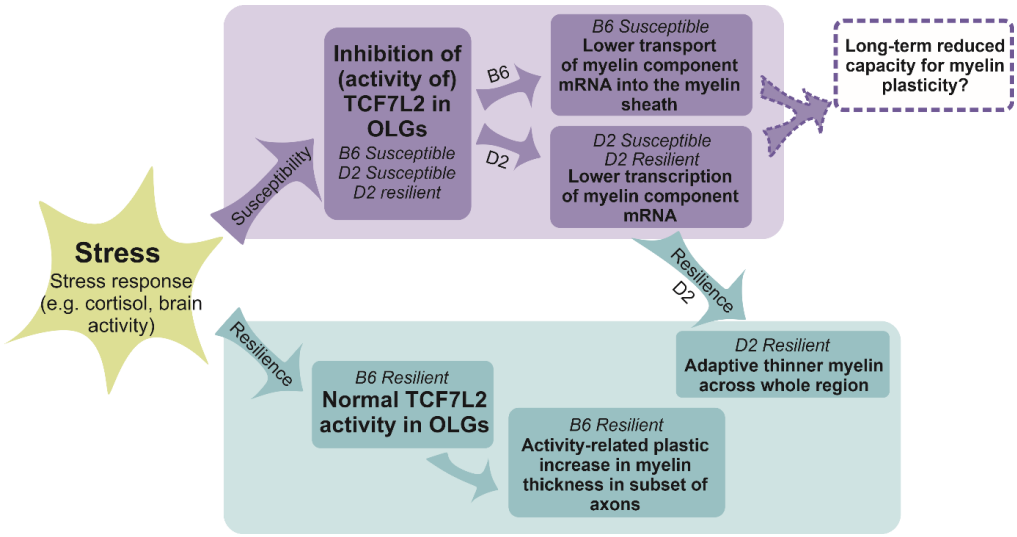

Figure 10. Synthesis of findings regarding TCF7L2, myelin component gene expression, and TEM findings. The network maps out a putative relationship between observed features of susceptibility (top panels) and resilience (bottom panels). The mechanisms underlying the arrows, and the features with dashed outlines, form targets for future research. B6 = C57BL/6NCrl, D2 = DBA/2NCrl.

6.7. Implications for anxiety disorders

Translation of our and other animal model findings linking myelin with stress and its consequences has some challenges. Human neuroimaging has associated several functional features with high or disordered anxiety, including lower activity in the mPFC [77] and higher

reactivity of the amygdala [76] during threat-related tasks. Interestingly, in children with a family history of anxiety disorders regardless of their own current anxiety levels, both the mPFC and HPC are more responsive to viewing emotional faces [304]. White matter tracts within and between these regions also show structural alterations in anxiety disorders, with somewhat conflicting findings across samples and specific diagnoses [212, 213]. Thus both functional and structural neuroimaging features have been associated with both increases and decreases within these regions-of-interest in anxiety. Small samples and variable definitions of anxiety-like traits likely contribute to these inconsistencies, but genuine individual differences may also exist, akin to differences seen between mouse strains even in the same experimental set-up. There is also a lack of published results combining functional and structural image acquisitions, which would help bridge the potential association between myelin plasticity and anxiety. The necessary longitudinal studies following patients through developing and recovering from anxiety disorders, such as those linking adaptations in white matter to learning [176-178], are also sparse. As such, direct parallels between findings from stress-resilient and susceptible mice and those from human patients must be drawn with caution.

The impact myelin plasticity can have on how the brain functions [11] makes it a fascinating candidate for explaining the functional and structural features of anxiety disorders. Perturbing neuronal activity can concurrently influence both myelin thickness and conduction velocity of white matter tracts [173], and a genetic mutation influencing myelin globally also influences spike timing [175]. Thus, plastic adaptations in myelin may be immediately protective against maladaptive behaviours, as seen in our resilient mice, possibly via promoting adaptive functional connectivity. Functional neuroimaging would be required to test the association between this and functional connectivity between regions implicated in Study I, such as the PFC and vHPC. As seen in our susceptible mice, structural changes in myelin are not necessarily seen immediately after stress. Lower expression of myelin component genes could be relevant for later thinning of mPFC myelin, as reported by others and discussed above. The functional consequences of this would then be interested to assess, with respect to the functional alterations seen in humans with an anxiety disorder. A structural analysis of myelin after stress, across several brain regions and time points, would greatly inform this translational effort.

6.8. Future directions

Moving forward, perhaps the most pertinent question is what the role of stress-related myelin plasticity is in psychopathology. As our TEM data suggests, myelin thickness may not be

altered in susceptibility within the time frame applied here (10 days of stress followed by one week of undisturbed housing). Studies using longer exposures, such as several weeks of isolation [189, 191], do report structural differences between stress-exposed and non-stressed animals, but here the relevance of the individual response (resilience of susceptibility) is not addressed. Human *post mortem* work also reports altered myelin structure at a point at which the person has suffered from psychiatric symptoms for many years [207]. At the time point of our measurement, we do still see lower expression of myelin-related genes. Integrating these findings (Figure 10) could suggest a model where stress, by an as-of-yet unknown mechanisms, in the mPFC of susceptible animals impacts the transcriptional and/or transport machinery necessary for myelin maintenance and plasticity. Over time, this would be expected to result in comparatively thinner myelin sheaths.

Currently there are no means by which to longitudinally assess myelin thickness in deeper cortical regions, such as the mPFC, in living mice. Transgenic reporter lines [164] and specialised confocal imaging techniques like spectral reflectometry (SpeRe, [305]) have been used in combination with cranial windows to view dynamics of myelin sheaths in living animals. However, these techniques are limited in terms of depth (approximately 300 µm below the meninges, [164]), and while SpeRe is suggested to achieve a similar resolution to TEM, it may not be able to resolve the source of every type of change the myelin sheath can incur. For example, myelin may appear thicker also if the inner layers swell, an early precursor to myelin pathologies [306]. Thus, at the resolution of TEM and the depth of the mPFC, we are currently not able to address the question of whether the myelin thickness differences we observed were in fact consequences of stress, or pre-existing features which predispose an animal to develop resilience or susceptibility after stress.

An alternative approach to asking whether pre-existing myelin differences contribute to the behavioural response to stress would be to use animals with known defects in myelination. However, transgenic models of hypomyelination (e.g. KO of *Mbp*, *Plp1* or *Cnp* [153, 198, 307]), even if temporally inducible, typically affect the whole brain. Forebrain-specific driver lines (such as *Emx1-Cre*, [308]) exist but still cover a large number of functionally distinct regions, such as the cortex and HPC. Because CSDS appears to have regionally selective impacts, such a system would have undesirable confounders. These, as well as pharmacological models such as cuprizone-induced demyelination or focally injected lysolecithin [309], typically also result in progressive rather than static myelin pathology, making it difficult to parse out the effects of another dynamic exposure such as stress. The wish list of a researcher

interested in dynamic myelin plasticity in stress remains unfulfilled; hopefully one day we will have access to a longitudinal *in vivo* measurement technique, measuring myelin at the nanometre scale across diverse brain regions.

Returning to the big question posed at the beginning of this section, a true understanding of the network consequences of stress-related myelin plasticity also requires knowing which specific connections are affected. Regions such as the mPFC contain a vast variety of neuronal types with both short- and long-range connections, many of which are known to be myelinated [174, 279]. To use our D2 resilient mice as an example, we observed thinner myelin sheaths across varied axonal diameters. TEM data as such cannot distinguish axons belonging to distinct neuronal subtypes, particularly when the diameter range of affected axons is large. Immuno-EM is a possible technique to label subtype-specific proteins with EM-compatible antibodies, and it has been instrumental in determining subcellular localisation of specific proteins [310]. However, the processing steps required for immuno-EM leads to reduced sample quality, critical for accurate measurement of the myelin sheath. An intriguing novel advance is the ascorbate peroxidase 2 (APEX2) system, consisting now of several transgenic mouse lines and viral vectors [311]. Importantly, this system even enables multiplexing, i.e. the simultaneous visualisation of several (up to 4) different tags in the same tissue. Multiplexing in APEX2 relies on specific subcellular targeting of the peroxidase tags, detectable by conventional TEM preparation and imaging methods. It is also compatible with high-pressure freezing [312], a sample preparation protocol that optimally preserves myelin structure [313]. Thus, it would soon be possible to tag specific axon types, such as those belonging to parvalbumin-expressing interneurons and glutamatergic pyramidal neurons, in the same mice, measuring myelin thickness along these axons post-stress. This would be the first step towards finding out which specific circuits are altered in terms of myelin by stress.

Lastly, there are several possible mechanisms for transmitting the effects of stress exposure to OLG function and myelination. Neuronal activity is a well-established regulator of adult myelin plasticity [165-167], and based on the regionally selective differences seen in myelin this is a highly attractive candidate. Pushing the aforementioned imaging system further, it would be incredibly informative to combine the APEX2 tag with an activity-induced effector, such as Fast Light- and Activity-Regulated Expression (FLARE, [314]). FLARE consists of vector-mediated expression of an engineered TF, which requires coincident calcium signalling (driven by endogenous neuronal activity) and light (delivered at a selected time exogenously) to activate detectable fluorescent proteins. Thus, one can mark neurons which were active

during a specific time or task. If this transcription factor could be made to drive the expression of the APEX2 peroxidase, we could tag CSDS-engaged axons enabling their recognition in TEM, assessing whether stress-related myelin thickness differences indeed depend on neuronal activity.

Other possible pathways by which stress exposure could modulate myelin are systemic, such as the exposure of OLGs to stress-induced endocrine components. OLGs in several brain regions, including the cortex and HPC, express GRs [315], but we know very little about how they influence gene expression and other functions in OLGs. Steroid hormones, such as androgens and estrogen, can also influence myelination and are themselves influenced by stress [316-318]. *In vitro* experiments with purified OLGs would be optimal for studying this, as *in vivo* exposures would affect the whole CNS and thus disable the study of cell-specific effects. Several types of OLGs can be relatively easily maintained in culture, including primary cells derived from rodents (usually pups) and immortalised cell lines of either rodent (e.g. Oli-neu, [319]) or human (MO3.13, [320]) origin. These lend themselves well to the study of the basic biology of what exposure to agents like GCs does to OLGs, but they have significant limitations in terms of translation to the *in vivo* situation. Without neurons, OPCs and OLGs lack critical signalling partners, which may impact read-outs of exposure experiments. Even if co-cultured with neurons one may not be able to fully capture the complex, dynamic state in the adult brain. Such studies can, however, generate testable hypotheses taken back to animal models for validation.

These considerations highlight the need for several types of experiments, relying on new and emerging techniques, to thoroughly explore the role of myelin plasticity in susceptibility and resilience to stress. A mere few years ago many of the described experiments would not have been technically possible. Today it is a matter of motivation and resources, although some questions remain dependent on further technical advances. The future for myelin and stress research is bright and will hopefully lead to eventual advancements in our ability to treat stress-related anxiety and other psychiatric disorder much better than we can today.

6.9. Concluding remarks

The motivation behind what we as neuroscientists at the intersection of psychiatry do is rather straight-forward: we wish to help people. In fact, one would be hard-pressed to find an article within this field where the abstract or discussion sections do not conclude with some variation of the idea that the knowledge acquired will hopefully be the basis of novel therapeutic

breakthroughs. These disorders cause immeasurable personal suffering to millions, but our treatment options are limited, and these are the limits we wish to push.

In the studies reported here, we showed the engagement of a putative network of brain regions during chronic psychosocial stress and differences in myelin within some of the nodes of this network. Additionally, we demonstrated that genetic background moderates both the behavioural and myelin-related response to stress. Mice with high baseline anxiety-like behaviour (D2) were also more susceptible to chronic stress than mice from the B6 strain. While myelin plasticity was implicated in both strains, the nature of this association also depended greatly on whether the mice were resilient or susceptible. Collectively, these findings suggest that stress robustly, but via as-of-yet unknown mechanisms, engages the myelin machinery, but the downstream effects are moderated by genetic background. For example, we found that mice with the resilient behavioural phenotype from different strains can show opposite myelin thickness phenotypes in the mPFC. This could arise from different neuronal activation patterns induced by CSDS between strains.

Additional experiments are needed to address crucial questions, such as whether stress is indeed causal of myelin plasticity or lack thereof, and how the observed myelin gene expression differences in susceptibility relate to long-term consequences of stress. Adding this knowledge to what we know about neuronal plasticity and system-level effects of stress will hopefully construct a more complete picture of how resilience and susceptibility emerge. Perhaps myelin plasticity can in the future be harnessed for treating stress-related psychopathology, such as anxiety disorders.

7. References

1. Kessler, R.C., *The global burden of anxiety and mood disorders: putting the European Study of the Epidemiology of Mental Disorders (ESEMeD) findings into perspective.* J Clin Psychiatry, 2007. **68 Suppl 2**: p. 10-9.
2. Calhoon, G.G. and K.M. Tye, *Resolving the neural circuits of anxiety.* Nat Neurosci, 2015. **18**(10): p. 1394-404.
3. Hettema, J.M., M.C. Neale, and K.S. Kendler, *A review and meta-analysis of the genetic epidemiology of anxiety disorders.* Am J Psychiatry, 2001. **158**(10): p. 1568-78.
4. Forstner, A.J., et al., *Genome-wide association study of panic disorder reveals genetic overlap with neuroticism and depression.* Mol Psychiatry, 2019.
5. Purves, K.L., et al., *A major role for common genetic variation in anxiety disorders.* Mol Psychiatry, 2019.
6. Nelson, C.A., 3rd and L.J. Gabard-Durnam, *Early Adversity and Critical Periods: Neurodevelopmental Consequences of Violating the Expectable Environment.* Trends Neurosci, 2020. **43**(3): p. 133-143.
7. Yue, F., et al., *A comparative encyclopedia of DNA elements in the mouse genome.* Nature, 2014. **515**(7527): p. 355-64.
8. Spencer, R.L. and T. Deak, *A users guide to HPA axis research.* Physiol Behav, 2017. **178**: p. 43-65.
9. Cryan, J.F. and F.F. Sweeney, *The age of anxiety: role of animal models of anxiolytic action in drug discovery.* Br J Pharmacol, 2011. **164**(4): p. 1129-61.
10. Kavalali, E.T. and L.M. Monteggia, *Targeting Homeostatic Synaptic Plasticity for Treatment of Mood Disorders.* Neuron, 2020. **106**(5): p. 715-726.
11. O'Rourke, M., R. Gasperini, and K.M. Young, *Adult myelination: wrapping up neuronal plasticity.* Neural Regen Res, 2014. **9**(13): p. 1261-4.
12. Uhlhaas, P.J. and W. Singer, *Neural synchrony in brain disorders: relevance for cognitive dysfunctions and pathophysiology.* Neuron, 2006. **52**(1): p. 155-68.
13. Stefan, K., et al., *Induction of plasticity in the human motor cortex by paired associative stimulation.* Brain, 2000. **123 Pt 3**: p. 572-84.
14. LeDoux, J.E. and D.S. Pine, *Using Neuroscience to Help Understand Fear and Anxiety: A Two-System Framework.* Am J Psychiatry, 2016. **173**(11): p. 1083-1093.
15. Association, A.P., *Diagnostic and statistical manual of mental disorders*. 5th ed. 2013, Washington, DC: Author.
16. World Health Organization, *International classification of diseases for mortality and morbidity statistics*. 11th ed. 2018.
17. McLean, C.P., et al., *Gender differences in anxiety disorders: prevalence, course of illness, comorbidity and burden of illness.* J Psychiatr Res, 2011. **45**(8): p. 1027-35.
18. Remes, O., et al., *A systematic review of reviews on the prevalence of anxiety disorders in adult populations.* Brain Behav, 2016. **6**(7): p. e00497.
19. Pirkola, S.P., et al., *DSM-IV mood-, anxiety- and alcohol use disorders and their comorbidity in the Finnish general population--results from the Health 2000 Study.* Soc Psychiatry Psychiatr Epidemiol, 2005. **40**(1): p. 1-10.
20. Kessler, R.C., et al., *Anxious and non-anxious major depressive disorder in the World Health Organization World Mental Health Surveys.* Epidemiol Psychiatr Sci, 2015. **24**(3): p. 210-26.
21. Hettema, J.M., *What is the genetic relationship between anxiety and depression?* Am J Med Genet C Semin Med Genet, 2008. **148C**(2): p. 140-6.
22. Tambs, K., et al., *The Norwegian Institute of Public Health twin study of mental health: examining recruitment and attrition bias.* Twin Res Hum Genet, 2009. **12**(2): p. 158-68.
23. Pai, A., A.M. Suris, and C.S. North, *Posttraumatic Stress Disorder in the DSM-5: Controversy, Change, and Conceptual Considerations.* Behav Sci (Basel), 2017. **7**(1).
24. Grupe, D.W. and J.B. Nitschke, *Uncertainty and anticipation in anxiety: an integrated neurobiological and psychological perspective.* Nat Rev Neurosci, 2013. **14**(7): p. 488-501.

25. Wakefield, J.C., A.V. Horwitz, and M.F. Schmitz, *Are we overpathologizing the socially anxious? Social phobia from a harmful dysfunction perspective.* Can J Psychiatry, 2005. **50**(6): p. 317-9.
26. Insel, T., et al., *Research domain criteria (RDoC): toward a new classification framework for research on mental disorders.* Am J Psychiatry, 2010. **167**(7): p. 748-51.
27. Smoller, J.W., *The Genetics of Stress-Related Disorders: PTSD, Depression, and Anxiety Disorders.* Neuropsychopharmacology, 2016. **41**(1): p. 297-319.
28. Johnson, E.M. and M.E. Coles, *Failure and delay in treatment-seeking across anxiety disorders.* Community Ment Health J, 2013. **49**(6): p. 668-74.
29. Working group set by the Finnish Medical Society Duodecim and the Finnish Psychiatric Association and the Finnish Youth Psychiatry Association (Suomen Nuorisopsykiatrinen yhdistys ry). *Anxiety Disorders*. 2019 [cited 2020 27.7.2020].
30. Wick, J.Y., *The history of benzodiazepines.* Consult Pharm, 2013. **28**(9): p. 538-48.
31. Taylor, S., J.S. Abramowitz, and D. McKay, *Non-adherence and non-response in the treatment of anxiety disorders.* J Anxiety Disord, 2012. **26**(5): p. 583-9.
32. Sartori, S.B. and N. Singewald, *Novel pharmacological targets in drug development for the treatment of anxiety and anxiety-related disorders.* Pharmacol Ther, 2019. **204**: p. 107402.
33. Crane, G.E., *Iproniazid (marsilid) phosphate, a therapeutic agent for mental disorders and debilitating diseases.* Psychiatr Res Rep Am Psychiatr Assoc, 1957. **8**: p. 142-52.
34. Weizman, A. and R. Weizman, *Serotonin transporter polymorphism and response to SSRIs in major depression and relevance to anxiety disorders and substance abuse.* Pharmacogenomics, 2000. **1**(3): p. 335-41.
35. Trivedi, M.H., et al., *Evaluation of outcomes with citalopram for depression using measurement-based care in STAR*D: implications for clinical practice.* Am J Psychiatry, 2006. **163**(1): p. 28-40.
36. Gollan, J.K., et al., *What are the clinical implications of new onset or worsening anxiety during the first two weeks of SSRI treatment for depression?* Depress Anxiety, 2012. **29**(2): p. 94-101.
37. Umemori, J., et al., *iPlasticity: Induced juvenile-like plasticity in the adult brain as a mechanism of antidepressants.* Psychiatry Clin Neurosci, 2018. **72**(9): p. 633-653.
38. Tolin, D.F., *Is cognitive-behavioral therapy more effective than other therapies? A meta-analytic review.* Clin Psychol Rev, 2010. **30**(6): p. 710-20.
39. Loerinc, A.G., et al., *Response rates for CBT for anxiety disorders: Need for standardized criteria.* Clin Psychol Rev, 2015. **42**: p. 72-82.
40. Ori, R., et al., *Augmentation of cognitive and behavioural therapies (CBT) with d-cycloserine for anxiety and related disorders.* Cochrane Database Syst Rev, 2015(5): p. CD007803.
41. Mataix-Cols, D., et al., *D-Cycloserine Augmentation of Exposure-Based Cognitive Behavior Therapy for Anxiety, Obsessive-Compulsive, and Posttraumatic Stress Disorders: A Systematic Review and Meta-analysis of Individual Participant Data.* JAMA Psychiatry, 2017. **74**(5): p. 501-510.
42. Sanders, J. and C. Nemeroff, *The CRF System as a Therapeutic Target for Neuropsychiatric Disorders.* Trends Pharmacol Sci, 2016. **37**(12): p. 1045-1054.
43. Stein, M.B. and J.W. Smoller, *Precision Psychiatry-Will Genomic Medicine Lead the Way?* JAMA Psychiatry, 2018. **75**(7): p. 663-664.
44. Meier, S.M., et al., *Genetic Variants Associated With Anxiety and Stress-Related Disorders: A Genome-Wide Association Study and Mouse-Model Study.* JAMA Psychiatry, 2019.
45. Berton, O., et al., *Essential role of BDNF in the mesolimbic dopamine pathway in social defeat stress.* Science, 2006. **311**(5762): p. 864-8.
46. Otowa, T., et al., *Meta-analysis of genome-wide association studies of anxiety disorders.* Mol Psychiatry, 2016. **21**(10): p. 1485.
47. Levey, D.F., et al., *Reproducible Genetic Risk Loci for Anxiety: Results From approximately 200,000 Participants in the Million Veteran Program.* Am J Psychiatry, 2020. **177**(3): p. 223-232.
48. Nagel, M., et al., *Meta-analysis of genome-wide association studies for neuroticism in 449,484 individuals identifies novel genetic loci and pathways.* Nat Genet, 2018. **50**(7): p. 920-927.

49. Rutter, M., T.E. Moffitt, and A. Caspi, *Gene-environment interplay and psychopathology: multiple varieties but real effects.* J Child Psychol Psychiatry, 2006. **47**(3-4): p. 226-61.
50. Donner, J., et al., *Support for involvement of glutamate decarboxylase 1 and neuropeptide Y in anxiety susceptibility.* Am J Med Genet B Neuropsychiatr Genet, 2012. **159B**(3): p. 316-27.
51. Hoppen, T.H. and T. Chalder, *Childhood adversity as a transdiagnostic risk factor for affective disorders in adulthood: A systematic review focusing on biopsychosocial moderating and mediating variables.* Clin Psychol Rev, 2018. **65**: p. 81-151.
52. Fergusson, D.M., L.J. Horwood, and M.T. Lynskey, *Childhood sexual abuse and psychiatric disorder in young adulthood: II. Psychiatric outcomes of childhood sexual abuse.* J Am Acad Child Adolesc Psychiatry, 1996. **35**(10): p. 1365-74.
53. Nestor, P.G., et al., *Risk and protective effects of serotonin and BDNF genes on stress-related adult psychiatric symptoms.* Neurobiol Stress, 2019. **11**: p. 100186.
54. Cannon, W.D., *Bodily changes in pain, hunger, fear and rage: An account of recent researches into the function of emotional excitement.* D Appleton & Company., 1915.
55. Selye, H., *The general adaptation syndrome and the diseases of adaptation.* J Clin Endocrinol Metab, 1946. **6**: p. 117-230.
56. Gunnar, M. and K. Quevedo, *The neurobiology of stress and development.* Annu Rev Psychol, 2007. **58**: p. 145-73.
57. Tovote, P., J.P. Fadok, and A. Luthi, *Neuronal circuits for fear and anxiety.* Nat Rev Neurosci, 2015. **16**(6): p. 317-31.
58. Etkin, A., et al., *Individual differences in trait anxiety predict the response of the basolateral amygdala to unconsciously processed fearful faces.* Neuron, 2004. **44**(6): p. 1043-55.
59. Davis, M., D. Rainnie, and M. Cassell, *Neurotransmission in the rat amygdala related to fear and anxiety.* Trends Neurosci, 1994. **17**(5): p. 208-14.
60. Fanselow, M.S. and J.E. LeDoux, *Why we think plasticity underlying Pavlovian fear conditioning occurs in the basolateral amygdala.* Neuron, 1999. **23**(2): p. 229-32.
61. Vyas, A., S. Bernal, and S. Chattarji, *Effects of chronic stress on dendritic arborization in the central and extended amygdala.* Brain Res, 2003. **965**(1-2): p. 290-4.
62. Vyas, A., et al., *Chronic stress induces contrasting patterns of dendritic remodeling in hippocampal and amygdaloid neurons.* J Neurosci, 2002. **22**(15): p. 6810-8.
63. Davis, M., D.L. Walker, and Y. Lee, *Amygdala and bed nucleus of the stria terminalis: differential roles in fear and anxiety measured with the acoustic startle reflex.* Philos Trans R Soc Lond B Biol Sci, 1997. **352**(1362): p. 1675-87.
64. Walker, D.L., L.A. Miles, and M. Davis, *Selective participation of the bed nucleus of the stria terminalis and CRF in sustained anxiety-like versus phasic fear-like responses.* Prog Neuropsychopharmacol Biol Psychiatry, 2009. **33**(8): p. 1291-308.
65. Oka, T., et al., *Neuroanatomical and neurochemical organization of projections from the central amygdaloid nucleus to the nucleus retroambiguus via the periaqueductal gray in the rat.* Neurosci Res, 2008. **62**(4): p. 286-98.
66. Jennings, J.H., et al., *Distinct extended amygdala circuits for divergent motivational states.* Nature, 2013. **496**(7444): p. 224-8.
67. Carlen, M., *What constitutes the prefrontal cortex?* Science, 2017. **358**(6362): p. 478-482.
68. Herman, J.P. and W.E. Cullinan, *Neurocircuitry of stress: central control of the hypothalamo-pituitary-adrenocortical axis.* Trends Neurosci, 1997. **20**(2): p. 78-84.
69. Arnsten, A.F., *Stress signalling pathways that impair prefrontal cortex structure and function.* Nat Rev Neurosci, 2009. **10**(6): p. 410-22.
70. Jacobson, L. and R. Sapolsky, *The role of the hippocampus in feedback regulation of the hypothalamic-pituitary-adrenocortical axis.* Endocr Rev, 1991. **12**(2): p. 118-34.
71. Sheline, Y.I., et al., *Hippocampal atrophy in recurrent major depression.* Proc Natl Acad Sci U S A, 1996. **93**(9): p. 3908-13.
72. McEwen, B.S. and R.M. Sapolsky, *Stress and cognitive function.* Curr Opin Neurobiol, 1995. **5**(2): p. 205-16.
73. Bannerman, D.M., et al., *Regional dissociations within the hippocampus--memory and anxiety.* Neurosci Biobehav Rev, 2004. **28**(3): p. 273-83.

74. Adhikari, A., M.A. Topiwala, and J.A. Gordon, *Synchronized activity between the ventral hippocampus and the medial prefrontal cortex during anxiety.* Neuron, 2010. **65**(2): p. 257-69.
75. Parfitt, G.M., et al., *Bidirectional Control of Anxiety-Related Behaviors in Mice: Role of Inputs Arising from the Ventral Hippocampus to the Lateral Septum and Medial Prefrontal Cortex.* Neuropsychopharmacology, 2017. **42**(8): p. 1715-1728.
76. Shin, L.M. and I. Liberzon, *The neurocircuitry of fear, stress, and anxiety disorders.* Neuropsychopharmacology, 2010. **35**(1): p. 169-91.
77. Bishop, S., et al., *Prefrontal cortical function and anxiety: controlling attention to threat-related stimuli.* Nat Neurosci, 2004. **7**(2): p. 184-8.
78. Vreeburg, S.A., et al., *Parental history of depression or anxiety and the cortisol awakening response.* Br J Psychiatry, 2010. **197**(3): p. 180-5.
79. Dierckx, B., et al., *Persistence of anxiety disorders and concomitant changes in cortisol.* J Anxiety Disord, 2012. **26**(6): p. 635-41.
80. van der Vegt, E.J., et al., *Childhood adversity modifies the relationship between anxiety disorders and cortisol secretion.* Biol Psychiatry, 2010. **68**(11): p. 1048-54.
81. Steudte-Schmiedgen, S., et al., *Hair cortisol concentrations and cortisol stress reactivity in generalized anxiety disorder, major depression and their comorbidity.* J Psychiatr Res, 2017. **84**: p. 184-190.
82. Sterling, P. and J. Eyer, *Allostasis: A new paradigm to explain arousal pathology*, in *Handbook of life stress, cognition and health*, S. Fisher and J. Reason, Editors. 1988, John Wiley & Sons. p. 629-649.
83. McEwen, B.S., *Stress, adaptation, and disease. Allostasis and allostatic load.* Ann N Y Acad Sci, 1998. **840**: p. 33-44.
84. Grissom, N. and S. Bhatnagar, *Habituation to repeated stress: get used to it.* Neurobiol Learn Mem, 2009. **92**(2): p. 215-24.
85. McEwen, B.S., *Physiology and neurobiology of stress and adaptation: central role of the brain.* Physiol Rev, 2007. **87**(3): p. 873-904.
86. Takesian, A.E. and T.K. Hensch, *Balancing plasticity/stability across brain development.* Prog Brain Res, 2013. **207**: p. 3-34.
87. Perrin, J.S., et al., *Growth of white matter in the adolescent brain: role of testosterone and androgen receptor.* J Neurosci, 2008. **28**(38): p. 9519-24.
88. Paus, T., M. Keshavan, and J.N. Giedd, *Why do many psychiatric disorders emerge during adolescence?* Nat Rev Neurosci, 2008. **9**(12): p. 947-57.
89. Kessler, R.C., et al., *Lifetime prevalence and age-of-onset distributions of DSM-IV disorders in the National Comorbidity Survey Replication.* Arch Gen Psychiatry, 2005. **62**(6): p. 593-602.
90. Danese, A. and C.S. Widom, *Objective and subjective experiences of child maltreatment and their relationships with psychopathology.* Nat Hum Behav, 2020.
91. Brody, G.H., et al., *Is resilience only skin deep?: rural African Americans' socioeconomic status-related risk and competence in preadolescence and psychological adjustment and allostatic load at age 19.* Psychol Sci, 2013. **24**(7): p. 1285-93.
92. Weaver, I.C., et al., *Epigenetic programming by maternal behavior.* Nat Neurosci, 2004. **7**(8): p. 847-54.
93. Young, E.A., et al., *Mineralocorticoid receptor function in major depression.* Arch Gen Psychiatry, 2003. **60**(1): p. 24-8.
94. Raison, C.L. and A.H. Miller, *When not enough is too much: the role of insufficient glucocorticoid signaling in the pathophysiology of stress-related disorders.* Am J Psychiatry, 2003. **160**(9): p. 1554-65.
95. Koss, K.J. and M.R. Gunnar, *Annual Research Review: Early adversity, the hypothalamic-pituitary-adrenocortical axis, and child psychopathology.* J Child Psychol Psychiatry, 2018. **59**(4): p. 327-346.
96. Sousa, N., et al., *Reorganization of the morphology of hippocampal neurites and synapses after stress-induced damage correlates with behavioral improvement.* Neuroscience, 2000. **97**(2): p. 253-66.
97. Rocher, C., et al., *Acute stress-induced changes in hippocampal/prefrontal circuits in rats: effects of antidepressants.* Cereb Cortex, 2004. **14**(2): p. 224-9.

98. Maya Vetencourt, J.F., et al., *The antidepressant fluoxetine restores plasticity in the adult visual cortex.* Science, 2008. **320**(5874): p. 385-8.
99. Nosyreva, E., et al., *Age dependence of the rapid antidepressant and synaptic effects of acute NMDA receptor blockade.* Front Mol Neurosci, 2014. **7**: p. 94.
100. Anderzhanova, E., T. Kirmeier, and C.T. Wotjak, *Animal models in psychiatric research: The RDoC system as a new framework for endophenotype-oriented translational neuroscience.* Neurobiol Stress, 2017. **7**: p. 47-56.
101. Cryan, J.F. and A. Holmes, *The ascent of mouse: advances in modelling human depression and anxiety.* Nat Rev Drug Discov, 2005. **4**(9): p. 775-90.
102. Prescott, M.J. and K. Lidster, *Improving quality of science through better animal welfare: the NC3Rs strategy.* Lab Anim (NY), 2017. **46**(4): p. 152-156.
103. Sittig, L.J., et al., *Genetic Background Limits Generalizability of Genotype-Phenotype Relationships.* Neuron, 2016. **91**(6): p. 1253-1259.
104. Hovatta, I., et al., *Glyoxalase 1 and glutathione reductase 1 regulate anxiety in mice.* Nature, 2005. **438**(7068): p. 662-6.
105. Walz, N., A. Muhlberger, and P. Pauli, *A Human Open Field Test Reveals Thigmotaxis Related to Agoraphobic Fear.* Biol Psychiatry, 2016. **80**(5): p. 390-7.
106. Sousa, N., O.F. Almeida, and C.T. Wotjak, *A hitchhiker's guide to behavioral analysis in laboratory rodents.* Genes Brain Behav, 2006. **5 Suppl 2**: p. 5-24.
107. Gouveia, K. and J.L. Hurst, *Optimising reliability of mouse performance in behavioural testing: the major role of non-aversive handling.* Sci Rep, 2017. **7**: p. 44999.
108. File, S.E., P.S. Mabbutt, and P.K. Hitchcott, *Characterisation of the phenomenon of "one-trial tolerance" to the anxiolytic effect of chlordiazepoxide in the elevated plus-maze.* Psychopharmacology (Berl), 1990. **102**(1): p. 98-101.
109. Schneider, P., et al., *A novel elevated plus-maze procedure to avoid the one-trial tolerance problem.* Front Behav Neurosci, 2011. **5**: p. 43.
110. Vogel, J.R., B. Beer, and D.E. Clody, *A simple and reliable conflict procedure for testing anti-anxiety agents.* Psychopharmacologia, 1971. **21**(1): p. 1-7.
111. Bodnoff, S.R., et al., *The effects of chronic antidepressant treatment in an animal model of anxiety.* Psychopharmacology (Berl), 1988. **95**(3): p. 298-302.
112. Merali, Z., C. Levac, and H. Anisman, *Validation of a simple, ethologically relevant paradigm for assessing anxiety in mice.* Biol Psychiatry, 2003. **54**(5): p. 552-65.
113. Crawley, J.N., *Neuropharmacologic specificity of a simple animal model for the behavioral actions of benzodiazepines.* Pharmacol Biochem Behav, 1981. **15**(5): p. 695-9.
114. Crawley, J. and F.K. Goodwin, *Preliminary report of a simple animal behavior model for the anxiolytic effects of benzodiazepines.* Pharmacol Biochem Behav, 1980. **13**(2): p. 167-70.
115. Lister, R.G., *The use of a plus-maze to measure anxiety in the mouse.* Psychopharmacology (Berl), 1987. **92**(2): p. 180-5.
116. Shepherd, J.K., et al., *Behavioural and pharmacological characterisation of the elevated "zero-maze" as an animal model of anxiety.* Psychopharmacology (Berl), 1994. **116**(1): p. 56-64.
117. Weger, M. and C. Sandi, *High anxiety trait: A vulnerable phenotype for stress-induced depression.* Neurosci Biobehav Rev, 2018. **87**: p. 27-37.
118. Marin, M.F., et al., *Multimodal Categorical and Dimensional Approaches to Understanding Threat Conditioning and Its Extinction in Individuals With Anxiety Disorders.* JAMA Psychiatry, 2020.
119. Meaney, M.J., et al., *Postnatal handling attenuates certain neuroendocrine, anatomical, and cognitive dysfunctions associated with aging in female rats.* Neurobiol Aging, 1991. **12**(1): p. 31-8.
120. Caldji, C., et al., *Maternal care during infancy regulates the development of neural systems mediating the expression of fearfulness in the rat.* Proc Natl Acad Sci U S A, 1998. **95**(9): p. 5335-40.
121. Plaznik, A., R. Stefanski, and W. Kostowski, *Restraint stress-induced changes in saccharin preference: the effect of antidepressive treatment and diazepam.* Pharmacol Biochem Behav, 1989. **33**(4): p. 755-9.

122. Guth, P.H. and R. Mendick, *The Effect of Chronic Restraint Stress on Gastric Ulceration in the Rat.* Gastroenterology, 1964. **46**: p. 285-6.
123. Katz, R.J. and G. Baldrighi, *A further parametric study of imipramine in an animal model of depression.* Pharmacol Biochem Behav, 1982. **16**(6): p. 969-72.
124. Molina, V.A., et al., *Effect of chronic variable stress on monoamine receptors: influence of imipramine administration.* Pharmacol Biochem Behav, 1990. **35**(2): p. 335-40.
125. Golden, S.A., et al., *A standardized protocol for repeated social defeat stress in mice.* Nat Protoc, 2011. **6**(8): p. 1183-91.
126. Krishnan, V., et al., *Molecular adaptations underlying susceptibility and resistance to social defeat in brain reward regions.* Cell, 2007. **131**(2): p. 391-404.
127. Kessler, R.C., et al., *Prevalence, severity, and comorbidity of 12-month DSM-IV disorders in the National Comorbidity Survey Replication.* Arch Gen Psychiatry, 2005. **62**(6): p. 617-27.
128. Russo, S.J., et al., *Neurobiology of resilience.* Nat Neurosci, 2012. **15**(11): p. 1475-84.
129. Vialou, V., et al., *Prefrontal cortical circuit for depression- and anxiety-related behaviors mediated by cholecystokinin: role of DeltaFosB.* J Neurosci, 2014. **34**(11): p. 3878-87.
130. Malenka, R.C. and M.F. Bear, *LTP and LTD: an embarrassment of riches.* Neuron, 2004. **44**(1): p. 5-21.
131. Buwalda, B., et al., *Long-term effects of social stress on brain and behavior: a focus on hippocampal functioning.* Neurosci Biobehav Rev, 2005. **29**(1): p. 83-97.
132. Von Frijtag, J.C., et al., *Chronic imipramine treatment partially reverses the long-term changes of hippocampal synaptic plasticity in socially stressed rats.* Neurosci Lett, 2001. **309**(3): p. 153-6.
133. Xu, H., et al., *Effects of Duloxetine Treatment on Cognitive Flexibility and BDNF Expression in the mPFC of Adult Male Mice Exposed to Social Stress during Adolescence.* Front Mol Neurosci, 2016. **9**: p. 95.
134. Colangelo, A.M., et al., *Neural plasticity and adult neurogenesis: the deep biology perspective.* Neural Regen Res, 2019. **14**(2): p. 201-205.
135. Font, M.A., A. Arboix, and J. Krupinski, *Angiogenesis, neurogenesis and neuroplasticity in ischemic stroke.* Curr Cardiol Rev, 2010. **6**(3): p. 238-44.
136. Krystal, J.H. and M.W. State, *Psychiatric disorders: diagnosis to therapy.* Cell, 2014. **157**(1): p. 201-14.
137. Hare, B.D. and R.S. Duman, *Prefrontal cortex circuits in depression and anxiety: contribution of discrete neuronal populations and target regions.* Mol Psychiatry, 2020.
138. Seidl, A.H., E.W. Rubel, and A. Barria, *Differential conduction velocity regulation in ipsilateral and contralateral collaterals innervating brainstem coincidence detector neurons.* J Neurosci, 2014. **34**(14): p. 4914-9.
139. Ford, M.C., et al., *Tuning of Ranvier node and internode properties in myelinated axons to adjust action potential timing.* Nat Commun, 2015. **6**: p. 8073.
140. Chomiak, T. and B. Hu, *What is the optimal value of the g-ratio for myelinated fibers in the rat CNS? A theoretical approach.* PLoS One, 2009. **4**(11): p. e7754.
141. Czopka, T., C. Ffrench-Constant, and D.A. Lyons, *Individual oligodendrocytes have only a few hours in which to generate new myelin sheaths in vivo.* Dev Cell, 2013. **25**(6): p. 599-609.
142. Baraban, M., S. Koudelka, and D.A. Lyons, *Ca (2+) activity signatures of myelin sheath formation and growth in vivo.* Nat Neurosci, 2018. **21**(1): p. 19-23.
143. Krasnow, A.M., et al., *Regulation of developing myelin sheath elongation by oligodendrocyte calcium transients in vivo.* Nat Neurosci, 2018. **21**(1): p. 24-28.
144. Lee, S., et al., *A culture system to study oligodendrocyte myelination processes using engineered nanofibers.* Nat Methods, 2012. **9**(9): p. 917-22.
145. Koudelka, S., et al., *Individual Neuronal Subtypes Exhibit Diversity in CNS Myelination Mediated by Synaptic Vesicle Release.* Curr Biol, 2016. **26**(11): p. 1447-55.
146. Hughes, A.N. and B. Appel, *Oligodendrocytes express synaptic proteins that modulate myelin sheath formation.* Nat Commun, 2019. **10**(1): p. 4125.
147. Sock, E. and M. Wegner, *Transcriptional control of myelination and remyelination.* Glia, 2019. **67**(11): p. 2153-2165.

148. Zhao, C., et al., *Dual regulatory switch through interactions of Tcf7l2/Tcf4 with stage-specific partners propels oligodendroglial maturation.* Nat Commun, 2016. **7**: p. 10883.
149. Bujalka, H., et al., *MYRF is a membrane-associated transcription factor that autoproteolytically cleaves to directly activate myelin genes.* PLoS Biol, 2013. **11**(8): p. e1001625.
150. Li, Z., Y. Park, and E.M. Marcotte, *A Bacteriophage tailspike domain promotes self-cleavage of a human membrane-bound transcription factor, the myelin regulatory factor MYRF.* PLoS Biol, 2013. **11**(8): p. e1001624.
151. Hornig, J., et al., *The transcription factors Sox10 and Myrf define an essential regulatory network module in differentiating oligodendrocytes.* PLoS Genet, 2013. **9**(10): p. e1003907.
152. Chang, K.J., S.A. Redmond, and J.R. Chan, *Remodeling myelination: implications for mechanisms of neural plasticity.* Nat Neurosci, 2016. **19**(2): p. 190-7.
153. Kimura, M., et al., *Molecular genetic analysis of myelin-deficient mice: shiverer mutant mice show deletion in gene(s) coding for myelin basic protein.* J Neurochem, 1985. **44**(3): p. 692-6.
154. Snaidero, N., et al., *Antagonistic Functions of MBP and CNP Establish Cytosolic Channels in CNS Myelin.* Cell Rep, 2017. **18**(2): p. 314-323.
155. Wake, H., P.R. Lee, and R.D. Fields, *Control of local protein synthesis and initial events in myelination by action potentials.* Science, 2011. **333**(6049): p. 1647-51.
156. Schmitt, S., L.C. Castelvetri, and M. Simons, *Metabolism and functions of lipids in myelin.* Biochim Biophys Acta, 2015. **1851**(8): p. 999-1005.
157. Arshad, M., J.A. Stanley, and N. Raz, *Adult age differences in subcortical myelin content are consistent with protracted myelination and unrelated to diffusion tensor imaging indices.* Neuroimage, 2016. **143**: p. 26-39.
158. Pajevic, S., P.J. Basser, and R.D. Fields, *Role of myelin plasticity in oscillations and synchrony of neuronal activity.* Neuroscience, 2014. **276**: p. 135-47.
159. Noori, R., et al., *Activity-dependent myelination: A glial mechanism of oscillatory self-organization in large-scale brain networks.* Proc Natl Acad Sci U S A, 2020. **117**(24): p. 13227-13237.
160. Auer, F., S. Vagionitis, and T. Czopka, *Evidence for Myelin Sheath Remodeling in the CNS Revealed by In Vivo Imaging.* Curr Biol, 2018. **28**(4): p. 549-559 e3.
161. Suminaite, D., D.A. Lyons, and M.R. Livesey, *Myelinated axon physiology and regulation of neural circuit function.* Glia, 2019. **67**(11): p. 2050-2062.
162. Chapman, T.W. and R.A. Hill, *Myelin plasticity in adulthood and aging.* Neurosci Lett, 2020. **715**: p. 134645.
163. Thornton, M.A. and E.G. Hughes, *Neuron-oligodendroglia interactions: Activity-dependent regulation of cellular signaling.* Neurosci Lett, 2020. **727**: p. 134916.
164. Bacmeister, C.M., et al., *Motor learning promotes remyelination via new and surviving oligodendrocytes.* Nat Neurosci, 2020. **23**(7): p. 819-831.
165. Hughes, E.G., et al., *Myelin remodeling through experience-dependent oligodendrogenesis in the adult somatosensory cortex.* Nat Neurosci, 2018. **21**(5): p. 696-706.
166. Gibson, E.M., et al., *Neuronal activity promotes oligodendrogenesis and adaptive myelination in the mammalian brain.* Science, 2014. **344**(6183): p. 1252304.
167. Mitew, S., et al., *Pharmacogenetic stimulation of neuronal activity increases myelination in an axon-specific manner.* Nat Commun, 2018. **9**(1): p. 306.
168. Geraghty, A.C., et al., *Loss of Adaptive Myelination Contributes to Methotrexate Chemotherapy-Related Cognitive Impairment.* Neuron, 2019. **103**(2): p. 250-265 e8.
169. McKenzie, I.A., et al., *Motor skill learning requires active central myelination.* Science, 2014. **346**(6207): p. 318-22.
170. Pan, S., et al., *Preservation of a remote fear memory requires new myelin formation.* Nat Neurosci, 2020. **23**(4): p. 487-499.
171. Micu, I., et al., *The molecular physiology of the axo-myelinic synapse.* Exp Neurol, 2016. **276**: p. 41-50.
172. Jeffries, M.A., et al., *ERK1/2 Activation in Preexisting Oligodendrocytes of Adult Mice Drives New Myelin Synthesis and Enhanced CNS Function.* J Neurosci, 2016. **36**(35): p. 9186-200.

173. Etxeberria, A., et al., *Dynamic Modulation of Myelination in Response to Visual Stimuli Alters Optic Nerve Conduction Velocity.* J Neurosci, 2016. **36**(26): p. 6937-48.
174. Tomassy, G.S., et al., *Distinct profiles of myelin distribution along single axons of pyramidal neurons in the neocortex.* Science, 2014. **344**(6181): p. 319-24.
175. Kato, D., et al., *Motor learning requires myelination to reduce asynchrony and spontaneity in neural activity.* Glia, 2020. **68**(1): p. 193-210.
176. Scholz, J., et al., *Training induces changes in white-matter architecture.* Nat Neurosci, 2009. **12**(11): p. 1370-1.
177. Bengtsson, S.L., et al., *Extensive piano practicing has regionally specific effects on white matter development.* Nat Neurosci, 2005. **8**(9): p. 1148-50.
178. Mackey, A.P., K.J. Whitaker, and S.A. Bunge, *Experience-dependent plasticity in white matter microstructure: reasoning training alters structural connectivity.* Front Neuroanat, 2012. **6**: p. 32.
179. Filippi, M., et al., *Diffusion tensor magnetic resonance imaging in multiple sclerosis.* Neurology, 2001. **56**(3): p. 304-11.
180. Sampaio-Baptista, C., et al., *White matter structure and myelin-related gene expression alterations with experience in adult rats.* Prog Neurobiol, 2020. **187**: p. 101770.
181. Jones, D.K., T.R. Knosche, and R. Turner, *White matter integrity, fiber count, and other fallacies: the do's and don'ts of diffusion MRI.* Neuroimage, 2013. **73**: p. 239-54.
182. Harnisch, K., et al., *Myelination in Multiple Sclerosis Lesions Is Associated with Regulation of Bone Morphogenetic Protein 4 and Its Antagonist Noggin.* Int J Mol Sci, 2019. **20**(1).
183. Chang, A., et al., *Premyelinating oligodendrocytes in chronic lesions of multiple sclerosis.* N Engl J Med, 2002. **346**(3): p. 165-73.
184. Patani, R., et al., *Remyelination can be extensive in multiple sclerosis despite a long disease course.* Neuropathol Appl Neurobiol, 2007. **33**(3): p. 277-87.
185. Yeung, M.S., et al., *Dynamics of oligodendrocyte generation and myelination in the human brain.* Cell, 2014. **159**(4): p. 766-74.
186. Buscham, T.J., et al., *Turning to myelin turnover.* Neural Regen Res, 2019. **14**(12): p. 2063-2066.
187. Luders, K.A., et al., *Maintenance of high proteolipid protein level in adult central nervous system myelin is required to preserve the integrity of myelin and axons.* Glia, 2019. **67**(4): p. 634-649.
188. Boda, E., *Myelin and oligodendrocyte lineage cell dysfunctions: New players in the etiology and treatment of depression and stress-related disorders.* Eur J Neurosci, 2019.
189. Liu, J., et al., *Impaired adult myelination in the prefrontal cortex of socially isolated mice.* Nat Neurosci, 2012. **15**(12): p. 1621-3.
190. Liu, J., et al., *Widespread transcriptional alternations in oligodendrocytes in the adult mouse brain following chronic stress.* Dev Neurobiol, 2018. **78**(2): p. 152-162.
191. Makinodan, M., et al., *A critical period for social experience-dependent oligodendrocyte maturation and myelination.* Science, 2012. **337**(6100): p. 1357-60.
192. Liu, J., et al., *Clemastine Enhances Myelination in the Prefrontal Cortex and Rescues Behavioral Changes in Socially Isolated Mice.* J Neurosci, 2016. **36**(3): p. 957-62.
193. Alttoa, A., et al., *Differential gene expression in a rat model of depression based on persistent differences in exploratory activity.* Eur Neuropsychopharmacol, 2010. **20**(5): p. 288-300.
194. Teissier, A., et al., *Early-life stress impairs postnatal oligodendrogenesis and adult emotional behaviour through activity-dependent mechanisms.* Mol Psychiatry, 2020. **25**(6): p. 1159-1174.
195. Chen, X., et al., *Myelin Deficits Caused by Olig2 Deficiency Lead to Cognitive Dysfunction and Increase Vulnerability to Social Withdrawal in Adult Mice.* Neurosci Bull, 2020. **36**(4): p. 419-426.
196. Swire, M., et al., *Endothelin signalling mediates experience-dependent myelination in the CNS.* Elife, 2019. **8**.
197. Zhang, H., et al., *The recovery trajectory of adolescent social defeat stress-induced behavioral, (1)H-MRS metabolites and myelin changes in Balb/c mice.* Sci Rep, 2016. **6**: p. 27906.
198. Edgar, N.M., et al., *Resilient emotionality and molecular compensation in mice lacking the oligodendrocyte-specific gene Cnp1.* Transl Psychiatry, 2011. **1**: p. e42.

199. Lehmann, M.L., et al., *Chronic social defeat reduces myelination in the mouse medial prefrontal cortex.* Sci Rep, 2017. **7**: p. 46548.
200. Bonnefil, V., et al., *Region-specific myelin differences define behavioral consequences of chronic social defeat stress in mice.* Elife, 2019. **8**.
201. Cathomas, F., et al., *Oligodendrocyte gene expression is reduced by and influences effects of chronic social stress in mice.* Genes Brain Behav, 2019. **18**(1): p. e12475.
202. Luo, Y., et al., *Running exercise protects oligodendrocytes in the medial prefrontal cortex in chronic unpredictable stress rat model.* Transl Psychiatry, 2019. **9**(1): p. 322.
203. Pena, C.J., et al., *Early life stress alters transcriptomic patterning across reward circuitry in male and female mice.* Nat Commun, 2019. **10**(1): p. 5098.
204. Bagot, R.C., et al., *Ketamine and Imipramine Reverse Transcriptional Signatures of Susceptibility and Induce Resilience-Specific Gene Expression Profiles.* Biol Psychiatry, 2017. **81**(4): p. 285-295.
205. Aston, C., L. Jiang, and B.P. Sokolov, *Transcriptional profiling reveals evidence for signaling and oligodendroglial abnormalities in the temporal cortex from patients with major depressive disorder.* Mol Psychiatry, 2005. **10**(3): p. 309-22.
206. Nagy, C., et al., *Single-nucleus transcriptomics of the prefrontal cortex in major depressive disorder implicates oligodendrocyte precursor cells and excitatory neurons.* Nat Neurosci, 2020. **23**(6): p. 771-781.
207. Lutz, P.E., et al., *Association of a History of Child Abuse With Impaired Myelination in the Anterior Cingulate Cortex: Convergent Epigenetic, Transcriptional, and Morphological Evidence.* Am J Psychiatry, 2017. **174**(12): p. 1185-1194.
208. Poletti, S., et al., *Gender-specific differences in white matter microstructure in healthy adults exposed to mild stress.* Stress, 2020. **23**(1): p. 116-124.
209. Jensen, S.K.G., et al., *Associations between prenatal, childhood, and adolescent stress and variations in white-matter properties in young men.* Neuroimage, 2017.
210. McCarthy-Jones, S., et al., *Childhood adversity associated with white matter alteration in the corpus callosum, corona radiata, and uncinate fasciculus of psychiatrically healthy adults.* Brain Imaging Behav, 2018. **12**(2): p. 449-458.
211. Westlye, L.T., et al., *Linking an anxiety-related personality trait to brain white matter microstructure: diffusion tensor imaging and harm avoidance.* Arch Gen Psychiatry, 2011. **68**(4): p. 369-77.
212. Lee, K.S. and S.H. Lee, *White Matter-Based Structural Brain Network of Anxiety.* Adv Exp Med Biol, 2020. **1191**: p. 61-70.
213. Ayling, E., et al., *Diffusion tensor imaging in anxiety disorders.* Curr Psychiatry Rep, 2012. **14**(3): p. 197-202.
214. Carballedo, A., et al., *Reduced fractional anisotropy in the uncinate fasciculus in patients with major depression carrying the met-allele of the Val66Met brain-derived neurotrophic factor genotype.* Am J Med Genet B Neuropsychiatr Genet, 2012. **159B**(5): p. 537-48.
215. Koch, S.B.J., et al., *Decreased uncinate fasciculus tract integrity in male and female patients with PTSD: a diffusion tensor imaging study.* J Psychiatry Neurosci, 2017. **42**(5): p. 331-342.
216. Eschenko, O., et al., *Mapping of functional brain activity in freely behaving rats during voluntary running using manganese-enhanced MRI: implication for longitudinal studies.* Neuroimage, 2010. **49**(3): p. 2544-55.
217. Silva, A.C. and N.A. Bock, *Manganese-enhanced MRI: an exceptional tool in translational neuroimaging.* Schizophr Bull, 2008. **34**(4): p. 595-604.
218. Dudek, M., et al., *Brain activation induced by voluntary alcohol and saccharin drinking in rats assessed with manganese-enhanced magnetic resonance imaging.* Addict Biol, 2015. **20**(6): p. 1012-21.
219. Kramer, A., et al., *Causal analysis approaches in Ingenuity Pathway Analysis.* Bioinformatics, 2014. **30**(4): p. 523-30.
220. Franklin, K.B.J. and G. Paxinos, *The Mouse Brain in Stereotaxic Coordinates*. 3rd ed. 2008, USA:New York, NY: Academic Press.
221. Tomasi, S., R. Caminiti, and G.M. Innocenti, *Areal differences in diameter and length of corticofugal projections.* Cereb Cortex, 2012. **22**(6): p. 1463-72.

222. Benjamini, Y. and Y. Hochberg, *Controlling the False Discovery Rate: A Practical and Powerful Approach to Multiple Testing.* J R Stat Soc Series B Stat Methodol, 1995. **57**(1): p. 289-300.
223. Hanley, J.A., et al., *Statistical analysis of correlated data using generalized estimating equations: an orientation.* Am J Epidemiol, 2003. **157**(4): p. 364-75.
224. Smith, B.M., et al., *Human airway branch variation and chronic obstructive pulmonary disease.* Proc Natl Acad Sci U S A, 2018. **115**(5): p. E974-E981.
225. Li, B., et al., *Fluoxetine-mediated 5-HT2B receptor stimulation in astrocytes causes EGF receptor transactivation and ERK phosphorylation.* Psychopharmacology (Berl), 2008. **201**(3): p. 443-58.
226. Nomaru, H., et al., *Fosb gene products contribute to excitotoxic microglial activation by regulating the expression of complement C5a receptors in microglia.* Glia, 2014. **62**(8): p. 1284-98.
227. Perrotti, L.I., et al., *Induction of deltaFosB in reward-related brain structures after chronic stress.* J Neurosci, 2004. **24**(47): p. 10594-602.
228. Carle, T.L., et al., *Proteasome-dependent and -independent mechanisms for FosB destabilization: identification of FosB degron domains and implications for DeltaFosB stability.* Eur J Neurosci, 2007. **25**(10): p. 3009-19.
229. Ishii, A., et al., *Human myelin proteome and comparative analysis with mouse myelin.* Proc Natl Acad Sci U S A, 2009. **106**(34): p. 14605-10.
230. Thakurela, S., et al., *The transcriptome of mouse central nervous system myelin.* Sci Rep, 2016. **6**: p. 25828.
231. Marx, M., R.A. Perlmutter, and J.A. Madri, *Modulation of platelet-derived growth factor receptor expression in microvascular endothelial cells during in vitro angiogenesis.* J Clin Invest, 1994. **93**(1): p. 131-9.
232. Bhat, R.V., et al., *Expression of the APC tumor suppressor protein in oligodendroglia.* Glia, 1996. **17**(2): p. 169-74.
233. Ainger, K., et al., *Transport and localization elements in myelin basic protein mRNA.* J Cell Biol, 1997. **138**(5): p. 1077-87.
234. Torvund-Jensen, J., et al., *The 3'UTRs of Myelin Basic Protein mRNAs Regulate Transport, Local Translation and Sensitivity to Neuronal Activity in Zebrafish.* Front Mol Neurosci, 2018. **11**: p. 185.
235. Zhong, X., W. Pu, and S. Yao, *Functional alterations of fronto-limbic circuit and default mode network systems in first-episode, drug-naive patients with major depressive disorder: A meta-analysis of resting-state fMRI data.* J Affect Disord, 2016. **206**: p. 280-286.
236. Vialou, V., et al., *Differential induction of FosB isoforms throughout the brain by fluoxetine and chronic stress.* Neuropharmacology, 2015. **99**: p. 28-37.
237. Vialou, V., et al., *Serum response factor promotes resilience to chronic social stress through the induction of DeltaFosB.* J Neurosci, 2010. **30**(43): p. 14585-92.
238. Vialou, V., et al., *DeltaFosB in brain reward circuits mediates resilience to stress and antidepressant responses.* Nat Neurosci, 2010. **13**(6): p. 745-52.
239. Berton, O., et al., *Induction of deltaFosB in the periaqueductal gray by stress promotes active coping responses.* Neuron, 2007. **55**(2): p. 289-300.
240. Scalize Hirata, R.Y., et al., *Chronic corticosterone increases DeltaFOSB and CRFR1 immunoreactivity in brain regions that modulate aversive conditioning.* Behav Brain Res, 2019. **356**: p. 107-119.
241. Stephens, G.S., et al., *Genes Bound by DeltaFosB in Different Conditions With Recurrent Seizures Regulate Similar Neuronal Functions.* Front Neurosci, 2020. **14**: p. 472.
242. Eagle, A.L., et al., *DeltaFosB Decreases Excitability of Dorsal Hippocampal CA1 Neurons.* eNeuro, 2018. **5**(4).
243. Hamilton, P.J., et al., *Cell-Type-Specific Epigenetic Editing at the Fosb Gene Controls Susceptibility to Social Defeat Stress.* Neuropsychopharmacology, 2018. **43**(2): p. 272-284.
244. van den Heuvel, M.P. and H.E. Hulshoff Pol, *Exploring the brain network: a review on resting-state fMRI functional connectivity.* Eur Neuropsychopharmacol, 2010. **20**(8): p. 519-34.

245. Johnson, Z.V., et al., *Central oxytocin receptors mediate mating-induced partner preferences and enhance correlated activation across forebrain nuclei in male prairie voles.* Horm Behav, 2016. **79**: p. 8-17.
246. Wheeler, A.L., et al., *Identification of a functional connectome for long-term fear memory in mice.* PLoS Comput Biol, 2013. **9**(1): p. e1002853.
247. Plaisier, F., C. Hume, and J. Menzies, *Neural connectivity between the hypothalamic supramammillary nucleus and appetite- and motivation-related regions of the rat brain.* J Neuroendocrinol, 2020. **32**(2): p. e12829.
248. Hultman, R., et al., *Brain-wide Electrical Spatiotemporal Dynamics Encode Depression Vulnerability.* Cell, 2018. **173**(1): p. 166-180 e14.
249. Tripathi, A., et al., *The hippocampal to prefrontal cortex circuit in mice: a promising electrophysiological signature in models for psychiatric disorders.* Brain Struct Funct, 2016. **221**(4): p. 2385-91.
250. Li, M., C. Long, and L. Yang, *Hippocampal-prefrontal circuit and disrupted functional connectivity in psychiatric and neurodegenerative disorders.* Biomed Res Int, 2015. **2015**: p. 810548.
251. Bracht, T., D. Linden, and P. Keedwell, *A review of white matter microstructure alterations of pathways of the reward circuit in depression.* J Affect Disord, 2015. **187**: p. 45-53.
252. Hanson, J.L., et al., *Lower structural integrity of the uncinate fasciculus is associated with a history of child maltreatment and future psychological vulnerability to stress.* Dev Psychopathol, 2015. **27**(4 Pt 2): p. 1611-9.
253. Kovacs, L.A., et al., *Corticotropin-Releasing Factor-Producing Cells in the Paraventricular Nucleus of the Hypothalamus and Extended Amygdala Show Age-Dependent FOS and FOSB/DeltaFOSB Immunoreactivity in Acute and Chronic Stress Models in the Rat.* Front Aging Neurosci, 2019. **11**: p. 274.
254. Ortiz, C., et al., *Molecular atlas of the adult mouse brain.* Sci Adv, 2020. **6**(26): p. eabb3446.
255. O'Mahony, C.M., et al., *Restraint stress-induced brain activation patterns in two strains of mice differing in their anxiety behaviour.* Behav Brain Res, 2010. **213**(2): p. 148-54.
256. Krishnan, V. and E.J. Nestler, *Animal models of depression: molecular perspectives.* Curr Top Behav Neurosci, 2011. **7**: p. 121-47.
257. Gururajan, A., et al., *The future of rodent models in depression research.* Nat Rev Neurosci, 2019. **20**(11): p. 686-701.
258. Takahashi, A., et al., *Establishment of a repeated social defeat stress model in female mice.* Sci Rep, 2017. **7**(1): p. 12838.
259. Harris, A.Z., et al., *A Novel Method for Chronic Social Defeat Stress in Female Mice.* Neuropsychopharmacology, 2018. **43**(6): p. 1276-1283.
260. Wang, L., et al., *Effects of chronic social defeat on social behaviors in adult female mandarin voles (Microtus mandarinus): Involvement of the oxytocin system in the nucleus accumbens.* Prog Neuropsychopharmacol Biol Psychiatry, 2018. **82**: p. 278-288.
261. Kumari, A., et al., *Social isolation mediated anxiety like behavior is associated with enhanced expression and regulation of BDNF in the female mouse brain.* Physiol Behav, 2016. **158**: p. 34-42.
262. Haller, J., et al., *Defeat is a major stressor in males while social instability is stressful mainly in females: towards the development of a social stress model in female rats.* Brain Res Bull, 1999. **50**(1): p. 33-9.
263. Warren, B.L., et al., *Can I Get a Witness? Using Vicarious Defeat Stress to Study Mood-Related Illnesses in Traditionally Understudied Populations.* Biol Psychiatry, 2020. **88**(5): p. 381-391.
264. Shansky, R.M., *Are hormones a "female problem" for animal research?* Science, 2019. **364**(6443): p. 825-826.
265. Belzung, C. and G. Griebel, *Measuring normal and pathological anxiety-like behaviour in mice: a review.* Behav Brain Res, 2001. **125**(1-2): p. 141-9.
266. Kok, L., et al., *Trait anxiety mediates the effect of stress exposure on post-traumatic stress disorder and depression risk in cardiac surgery patients.* J Affect Disord, 2016. **206**: p. 216-223.

267. Razzoli, M., et al., *Different susceptibility to social defeat stress of BalbC and C57BL6/J mice.* Behav Brain Res, 2011. **216**(1): p. 100-8.
268. Moreno-Lopez, L., et al., *The Resilient Emotional Brain: A Scoping Review of the Medial Prefrontal Cortex and Limbic Structure and Function in Resilient Adults With a History of Childhood Maltreatment.* Biol Psychiatry Cogn Neurosci Neuroimaging, 2020. **5**(4): p. 392-402.
269. Yuan, T.Z., et al., *Shear-stress-mediated refolding of proteins from aggregates and inclusion bodies.* Chembiochem, 2015. **16**(3): p. 393-6.
270. Murrough, J.W. and S.J. Russo, *The Neurobiology of Resilience: Complexity and Hope.* Biol Psychiatry, 2019. **86**(6): p. 406-409.
271. Valerio-Gomes, B., et al., *The Absolute Number of Oligodendrocytes in the Adult Mouse Brain.* Front Neuroanat, 2018. **12**: p. 90.
272. White, R., et al., *Activation of oligodendroglial Fyn kinase enhances translation of mRNAs transported in hnRNP A2-dependent RNA granules.* J Cell Biol, 2008. **181**(4): p. 579-86.
273. Kornfeld, S.F., et al., *MiRNA-145-5p prevents differentiation of oligodendrocyte progenitor cells by regulating expression of myelin gene regulatory factor.* J Cell Physiol, 2020.
274. Wang, H., et al., *miR-219 Cooperates with miR-338 in Myelination and Promotes Myelin Repair in the CNS.* Dev Cell, 2017. **40**(6): p. 566-582 e5.
275. Shin, D., et al., *miR-32 and its target SLC45A3 regulate the lipid metabolism of oligodendrocytes and myelin.* Neuroscience, 2012. **213**: p. 29-37.
276. Rajgor, D., et al., *Local miRNA-Dependent Translational Control of GABAAR Synthesis during Inhibitory Long-Term Potentiation.* Cell Rep, 2020. **31**(12): p. 107785.
277. Semple, B.D., et al., *Brain development in rodents and humans: Identifying benchmarks of maturation and vulnerability to injury across species.* Prog Neurobiol, 2013. **106-107**: p. 1-16.
278. Hofflin, F., et al., *Heterogeneity of the Axon Initial Segment in Interneurons and Pyramidal Cells of Rodent Visual Cortex.* Front Cell Neurosci, 2017. **11**: p. 332.
279. Stedehouder, J., et al., *Activity-Dependent Myelination of Parvalbumin Interneurons Mediated by Axonal Morphological Plasticity.* J Neurosci, 2018. **38**(15): p. 3631-3642.
280. Liu, S., et al., *Genetic influences on cortical myelination in the human brain.* Genes Brain Behav, 2019. **18**(4): p. e12537.
281. Tendolkar, I., et al., *Physical neglect during childhood alters white matter connectivity in healthy young males.* Hum Brain Mapp, 2018. **39**(3): p. 1283-1290.
282. Fani, N., et al., *White matter integrity in highly traumatized adults with and without post-traumatic stress disorder.* Neuropsychopharmacology, 2012. **37**(12): p. 2740-6.
283. Loos, M., et al., *Within-strain variation in behavior differs consistently between common inbred strains of mice.* Mamm Genome, 2015. **26**(7-8): p. 348-54.
284. Lathe, R., *The individuality of mice.* Genes Brain Behav, 2004. **3**(6): p. 317-27.
285. Boj, S.F., et al., *Diabetes risk gene and Wnt effector Tcf7l2/TCF4 controls hepatic response to perinatal and adult metabolic demand.* Cell, 2012. **151**(7): p. 1595-607.
286. Facchinello, N., et al., *Tcf7l2 plays pleiotropic roles in the control of glucose homeostasis, pancreas morphology, vascularization and regeneration.* Sci Rep, 2017. **7**(1): p. 9605.
287. Peng, S., et al., *TCF7L2 gene polymorphisms and type 2 diabetes risk: a comprehensive and updated meta-analysis involving 121,174 subjects.* Mutagenesis, 2013. **28**(1): p. 25-37.
288. Bem, J., et al., *Wnt/beta-catenin signaling in brain development and mental disorders: keeping TCF7L2 in mind.* FEBS Lett, 2019. **593**(13): p. 1654-1674.
289. Savic, D., et al., *Modulation ofTcf7l2 expression alters behavior in mice.* PLoS One, 2011. **6**(10): p. e26897.
290. Weng, C., et al., *Transcription factor 7 like 2 promotes oligodendrocyte differentiation and remyelination.* Mol Med Rep, 2017. **16**(2): p. 1864-1870.
291. Ye, F., et al., *HDAC1 and HDAC2 regulate oligodendrocyte differentiation by disrupting the beta-catenin-TCF interaction.* Nat Neurosci, 2009. **12**(7): p. 829-38.
292. Hammond, E., et al., *The Wnt effector transcription factor 7-like 2 positively regulates oligodendrocyte differentiation in a manner independent of Wnt/beta-catenin signaling.* J Neurosci, 2015. **35**(12): p. 5007-22.

293. Zhang, Y., et al., *An RNA-sequencing transcriptome and splicing database of glia, neurons, and vascular cells of the cerebral cortex.* J Neurosci, 2014. **34**(36): p. 11929-47.
294. Lurbke, A., et al., *Limited TCF7L2 expression in MS lesions.* PLoS One, 2013. **8**(8): p. e72822.
295. Fu, H., S. Kesari, and J. Cai, *Tcf7l2 is tightly controlled during myelin formation.* Cell Mol Neurobiol, 2012. **32**(3): p. 345-52.
296. Azim, K. and A.M. Butt, *GSK3beta negatively regulates oligodendrocyte differentiation and myelination in vivo.* Glia, 2011. **59**(4): p. 540-53.
297. Emery, B., et al., *Myelin gene regulatory factor is a critical transcriptional regulator required for CNS myelination.* Cell, 2009. **138**(1): p. 172-85.
298. Filtz, T.M., W.K. Vogel, and M. Leid, *Regulation of transcription factor activity by interconnected post-translational modifications.* Trends Pharmacol Sci, 2014. **35**(2): p. 76-85.
299. Feigenson, K., et al., *Wnt signaling is sufficient to perturb oligodendrocyte maturation.* Mol Cell Neurosci, 2009. **42**(3): p. 255-65.
300. Lee, H.K., et al., *Apcdd1 stimulates oligodendrocyte differentiation after white matter injury.* Glia, 2015. **63**(10): p. 1840-9.
301. Ortega, F., et al., *Oligodendrogliogenic and neurogenic adult subependymal zone neural stem cells constitute distinct lineages and exhibit differential responsiveness to Wnt signalling.* Nat Cell Biol, 2013. **15**(6): p. 602-13.
302. Choi, M.H., et al., *Role of Dopamine D2 Receptor in Stress-Induced Myelin Loss.* Sci Rep, 2017. **7**(1): p. 11654.
303. Struewing, I., et al., *The balance of TCF7L2 variants with differential activities in Wnt-signaling is regulated by lithium in a GSK3beta-independent manner.* Biochem Biophys Res Commun, 2010. **399**(2): p. 245-50.
304. Christensen, R., M. Van Ameringen, and G. Hall, *Increased activity of frontal and limbic regions to emotional stimuli in children at-risk for anxiety disorders.* Psychiatry Res, 2015. **233**(1): p. 9-17.
305. Kwon, J., et al., *Label-free nanoscale optical metrology on myelinated axons in vivo.* Nat Commun, 2017. **8**(1): p. 1832.
306. Weil, M.T., et al., *Loss of Myelin Basic Protein Function Triggers Myelin Breakdown in Models of Demyelinating Diseases.* Cell Rep, 2016. **16**(2): p. 314-322.
307. Griffiths, I., et al., *Axonal swellings and degeneration in mice lacking the major proteolipid of myelin.* Science, 1998. **280**(5369): p. 1610-3.
308. Iwasato, T., et al., *Dorsal telencephalon-specific expression of Cre recombinase in PAC transgenic mice.* Genesis, 2004. **38**(3): p. 130-8.
309. Kipp, M., et al., *Experimental in vivo and in vitro models of multiple sclerosis: EAE and beyond.* Mult Scler Relat Disord, 2012. **1**(1): p. 15-28.
310. McLaurin, J., C.A. Ackerley, and M.A. Moscarello, *Localization of basic proteins in human myelin.* J Neurosci Res, 1993. **35**(6): p. 618-28.
311. Zhang, Q., et al., *Multiplexed peroxidase-based electron microscopy labeling enables simultaneous visualization of multiple cell types.* Nat Neurosci, 2019. **22**(5): p. 828-839.
312. Mihelc, E.M., et al., *The CryoAPEX Method for Electron Microscopy Analysis of Membrane Protein Localization Within Ultrastructurally-Preserved Cells.* J Vis Exp, 2020(156).
313. Mobius, W., K.A. Nave, and H.B. Werner, *Electron microscopy of myelin: Structure preservation by high-pressure freezing.* Brain Res, 2016. **1641**(Pt A): p. 92-100.
314. Wang, W., et al., *A light- and calcium-gated transcription factor for imaging and manipulating activated neurons.* Nat Biotechnol, 2017. **35**(9): p. 864-871.
315. Matsusue, Y., et al., *Distribution of corticosteroid receptors in mature oligodendrocytes and oligodendrocyte progenitors of the adult mouse brain.* J Histochem Cytochem, 2014. **62**(3): p. 211-26.
316. He, Q., et al., *Effects of estrogen replacement therapy on the myelin sheath ultrastructure of myelinated fibers in the white matter of middle-aged ovariectomized rats.* J Comp Neurol, 2018. **526**(5): p. 790-802.
317. Humphreys, G.I., Y.S. Ziegler, and A.M. Nardulli, *17beta-estradiol modulates gene expression in the female mouse cerebral cortex.* PLoS One, 2014. **9**(11): p. e111975.

318. Rivier, C. and S. Rivest, *Effect of stress on the activity of the hypothalamic-pituitary-gonadal axis: peripheral and central mechanisms.* Biol Reprod, 1991. **45**(4): p. 523-32.
319. Jung, M., et al., *Lines of murine oligodendroglial precursor cells immortalized by an activated neu tyrosine kinase show distinct degrees of interaction with axons in vitro and in vivo.* Eur J Neurosci, 1995. **7**(6): p. 1245-65.
320. McLaurin, J., et al., *A human glial hybrid cell line differentially expressing genes subserving oligodendrocyte and astrocyte phenotype.* J Neurobiol, 1995. **26**(2): p. 283-93.

8. Acknowledgements

It takes a village to raise a child, and a whole lab to raise a scientist. This work is a perfect example of that. Each experiment required the specialist expertise of several people, without whom I could not have effectively conducted the parts for which I was responsible. My BSc thesis supervisor (Prof Lawrence Wilkinson) told me that "in science, there is no ego". What I took his words to mean was that science is a collaborative effort, where it makes no difference who makes the discoveries and in what position, but only that the discoveries are made. This has thankfully also been the philosophy of the Hovatta lab, resulting in a supportive atmosphere which is actively maintained by Iiris and the other lab members.

The village supporting this thesis also extended beyond the walls of our lab. I'm grateful to the Doctoral Programme Brain & Mind for enabling me to pay my rent while working a job I loved, and to the Faculty of Biological and Environmental Sciences and the SleepWell Research Program for providing the facilities and inspiring research environments across two campuses. To my thesis committee members, Professors Eero Castrén and Pentti Tienari, thank you for always taking the time to immerse yourself in my little corner of science and helping me keep the work steered in the most interesting directions. Your inputs sparked fascinating discussions about science and careers within it. To the pre-examiners Professor Laura Airas and Adjunct Professor Jukka Jolkkonen, I'm grateful for your thoughtful comments on the final written work. Completing and defending a PhD thesis during the global COVID-19 pandemic put us all in unfamiliar waters, cautiously hoping for normalcy but always prepared for something rather else. I thank Professor Jaanus Harro for so quickly accepting our invitation to serve as the opponent of this thesis, despite the state of the world not encouraging us to make long-term plans. As the nation barricaded itself into home offices, getting through the final stages of paperwork was all but a done deal. I thank Professor Juha Partanen, who also serves as the custos for this thesis, for his time and effort in getting us over the finish line on schedule.

To Professor Iiris Hovatta, my supervisor from when I was merely a fresh-faced MSc student in the Summer of 2015. Firstly, thank you for taking me onboard despite my somewhat limited lab experience. When the time came to decide if I wished to stay for a PhD (and I feel incredibly lucky for having been able to make a choice phrased roughly in these terms), it was probably the easiest career decision I have been and will be faced with. Thank you for believing in me when I did not, and for questioning me when I did not. I have learned both confidence and accountability from working with you, and these are skills I will treasure.

To each of my co-authors, and especially Zuzanna Misiewicz and Kalle Trontti: thank you for your immense efforts in making the publications included in this thesis what they are. Without your tireless search to understand, apply and develop novel methods for analysing the eye-wateringly large amounts of data generated by the experiments, they would not have been understandable to the rest of us. To Zuzanna and Marie Mennesson I am also grateful for their patience in teaching me most of the mouse work skills I regularly rely on. I also owe a special gratitude to Ewa Sokolowska, who set up the behavioural protocols and laid the foundations for the project which my thesis builds upon.

Iiris also gave me the chance to supervise students very early on, much earlier than I would have had the confidence to say I wanted to. It is said that we don't really know how to do something until we have taught somebody else to do it, and this certainly holds true for much of science. I have been blessed with supervisory duties of some incredibly talented and hard-working people, most closely Aino Heikkinen, Sarah Journée, and Giulia Mazzini for their MSc theses. I thoroughly enjoyed the whole process of helping you and other students develop their skills and grow as scientists.

Finally, to the person who probably had to deal with me on the most regular basis, my fellow glia-nerd Sarah Steffens: thank you for being the most supportive colleague another PhD student could ever dream of[1]. Thank you for smiling understandingly at my sometimes alien efforts to explain myself, and for bringing literal and figurative light into the office and animal facility especially at times when it was lacking. Thank you for insisting that I stand up for myself when I was being "fluffy", and for reminding me to go home at the end of a long day.

[1] Get it? Because you're a sleep researcher. And explaining jokes invariably improves them.

SCIENTIFIC REPORTS

OPEN

Brain activation induced by chronic psychosocial stress in mice

Mikaela A. Laine[1], Ewa Sokolowska[1], Mateusz Dudek[2], Saija-Anita Callan[1], Petri Hyytiä[2] & Iiris Hovatta[1]

Received: 14 July 2017
Accepted: 27 October 2017
Published online: 08 November 2017

Chronic psychosocial stress is a well-established risk factor for neuropsychiatric diseases. Abnormalities in brain activity have been demonstrated in patients with stress-related disorders. Global brain activation patterns during chronic stress exposure are less well understood but may have strong modifying effects on specific brain circuits and thereby influence development of stress-related pathologies. We determined neural activation induced by chronic social defeat stress, a mouse model of psychosocial stress. To assess chronic activation with an unbiased brain-wide focus we used manganese-enhanced magnetic resonance imaging (MEMRI) and immunohistochemical staining of ΔFOSB, a transcription factor induced by repeated neural activity. One week after 10-day social defeat we observed significantly more activation in several brain regions known to regulate depressive and anxiety-like behaviour, including the prefrontal cortex, bed nucleus of stria terminalis, ventral hippocampus and periaqueductal grey in stressed compared to control mice. We further established that the correlation of ΔFOSB positive cells between specific brain regions was altered following chronic social defeat. Chronic activation of these neural circuits may relate to persistent brain activity changes occurring during chronic psychosocial stress exposure, with potential relevance for the development of anxiety and depression in humans.

Psychosocial stress increases the risk for both somatic and psychiatric diseases and worsens their prognosis[1–4]. This term refers to a broad range of experiences, including lack of normative care, abuse, and problems in peer relationships such as bullying[5]. Stress-related mental disorders like major depressive disorder (MDD) and anxiety disorders are associated with altered activation of specific brain regions. For example, neuroimaging has revealed that resting-state activity is reduced in the prefrontal cortex (PFC)[6] and increased in the hippocampus[7] while task-related reactivity is decreased in the hippocampus[8] and nucleus accumbens[9] of MDD patients. Interpretation of the human imaging findings is difficult as activation patterns in tasks carried out during brain imaging may differ from those occurring during naturalistic chronic stress exposure. Because patients enrolled in these studies also tend to have an extensive history of symptoms and medication use, it is challenging to reveal direct consequences of chronic psychosocial stress itself. In contrast, animal models allow investigation of specific stressors in a controlled manner to establish the mechanisms connecting chronic psychosocial stress exposure, brain activation, and subsequent emotional and social behaviour.

Chronic social defeat stress (CSDS) is a rodent model of psychosocial stress, which produces many behavioural features similar to the symptoms of human anxiety and mood disorders, such as social aversion, anhedonia (decreased sucrose-preference) and increased self-administration of drugs of abuse[10,11]. These behavioural phenotypes last for several weeks post-stress[10], and can be reversed by chronic treatment with selective serotonin re-uptake inhibitors or tricyclic antidepressants[12], or a single dose of ketamine[13]. Thus, CSDS is an excellent mouse model to determine psychosocial stress-induced chronically occurring neural activation patterns, which may underlie the behavioural outcomes of stress exposure.

We hypothesized that CSDS induces neural activation in an extensive network of brain regions, including those previously implicated in acute stress and stress-related psychiatric disorders. We employed a combination of two methods for assessing neural activation in mice: manganese-enhanced magnetic resonance imaging (MEMRI) and ΔFOSB immunohistochemistry. MEMRI is based on the influx of paramagnetic Mn^{2+} ions into excitable cells through voltage-gated Ca^{2+} channels during depolarization, which increases T1-weighted signal intensity and thereby provides a marker of activated neurons[14,15]. Due to the slow efflux of Mn^{2+} from the brain, MEMRI allows functional brain imaging in anesthetized animals that have previously undergone

[1]Department of Biosciences, University of Helsinki, Helsinki, Finland. [2]Department of Pharmacology, University of Helsinki, Helsinki, Finland. Correspondence and requests for materials should be addressed to P.H. (email: petri.hyytia@helsinki.fi) or I.H. (email: iiris.hovatta@helsinki.fi)

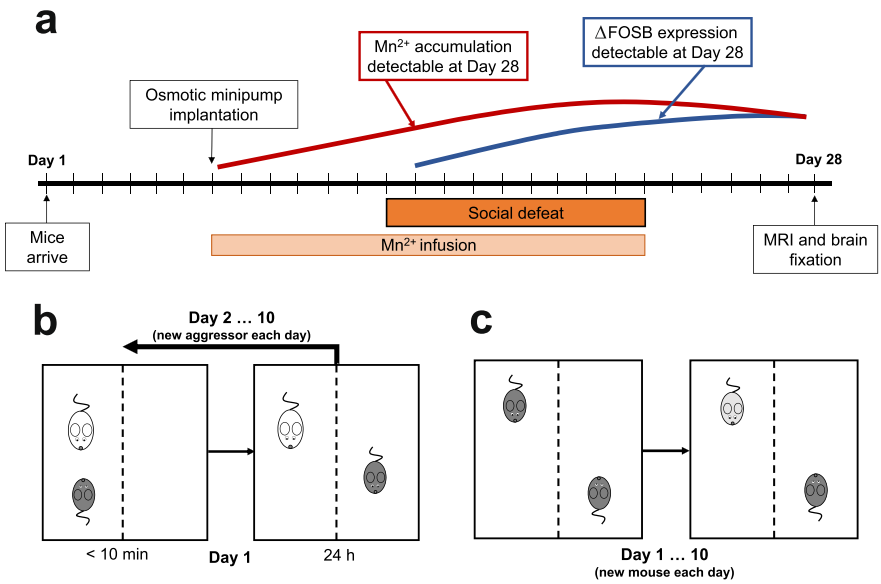

Figure 1. Timeline of the experiment and illustration of the chronic social defeat stress (CSDS) protocol. (**a**) Timeline of CSDS, manganese-enhanced magnetic resonance imaging and tissue collection. Each perpendicular line indicates one day. Estimated timeline for detection of Mn^{2+} by MEMRI and ΔFOSB by immunohistochemical staining is indicated by red and blue lines, respectively. (**b**) The experimental mouse in the defeated group (dark grey) was placed into the cage of a resident aggressor mouse (white) for a maximum of 10 minutes. It was then placed into the adjacent compartment of the same cage for 24 hours, retaining sensory contact without physical contact. The procedure was repeated for 10 days, each day in a novel resident aggressor mouse's cage. (**c**) The control mouse was placed in a compartment adjacent to another control mouse, allowing sensory but not physical contact, for 24 hours. Each day the control mouse was placed into another cage with a novel control mouse, and the procedure was repeated for 10 days. MRI = magnetic resonance imaging.

pharmacological or behavioural testing[16,17]. In addition, Mn^{2+} ions are transported along axons, released from the terminals into the synaptic cleft, and taken up by the postsynaptic neuron[18,19], providing a global measure of network activation.

ΔFOSB is a truncated hyperstable splice variant of the transcription factor FOSB. While the parent isoform FOSB is rapidly induced and degraded, the ΔFOSB form accumulates through repeated stimuli during a course of a chronic treatment, with each acute stimulus inducing a low level of ΔFOSB, and the repeated stress exposure causing the gradual increase in its total levels[20]. Since the estimated half-life of ΔFOSB is 8 days it is a useful marker for repeatedly activated neurons[20–22].

In contrast to MEMRI that enables brain-wide mapping of neural activation and activity-dependent connectivity, ΔFOSB immunohistochemistry detects nuclear activation with high cellular resolution. By combining these methods, we compared CSDS-exposed and control mice one week after cessation of stress to determine brain regions activated due to chronic psychosocial stress exposure.

Results

Functional MEMRI mapping shows widespread brain activation by CSDS. We exposed mice to the 10-day CSDS protocol, during which $MnCl_2$ was infused from an implanted osmotic minipump (Fig. 1). Socially defeated mice showed significant enhancement of T1 signal intensity in MEMRI compared to control mice as shown by statistical parametric maps in Fig. 2. Enhanced T1 intensity reflects accumulation of Mn^{2+} into repeatedly activated brain regions, suggesting increased brain activity in mice exposed to CSDS. We did not detect signal decreases in stressed mice compared to the controls. It is possible that this is due to the principle of MEMRI, i.e., Mn^{2+} influx into active neurons by voltage-gated Ca^{2+} channels, which renders the method less sensitive to deactivation than activity-induced signal increase. We observed increased activation throughout the brain, mostly confined to specific anatomical regions. In the PFC, increased signal was found in the orbital cortex (O) and forceps minor (fmi), a white matter tract. More caudally, the nucleus accumbens (Acb), caudate putamen (CPu), and lateral septum (LS) exhibited increased activation. Both the striatal and septal clusters were also activated by chronic stress in more caudal sections. In the basal forebrain, ventral parts of the bed nucleus of the stria terminalis (BNST) and preoptic area (LPO) were more activated in stressed compared to the control mice. The preoptic activation continued caudally as a distinct activation cluster encompassing the lateral hypothalamus (LH) with ventrolateral thalamic (VL) connections. We detected stronger MEMRI signal in the midbrain,

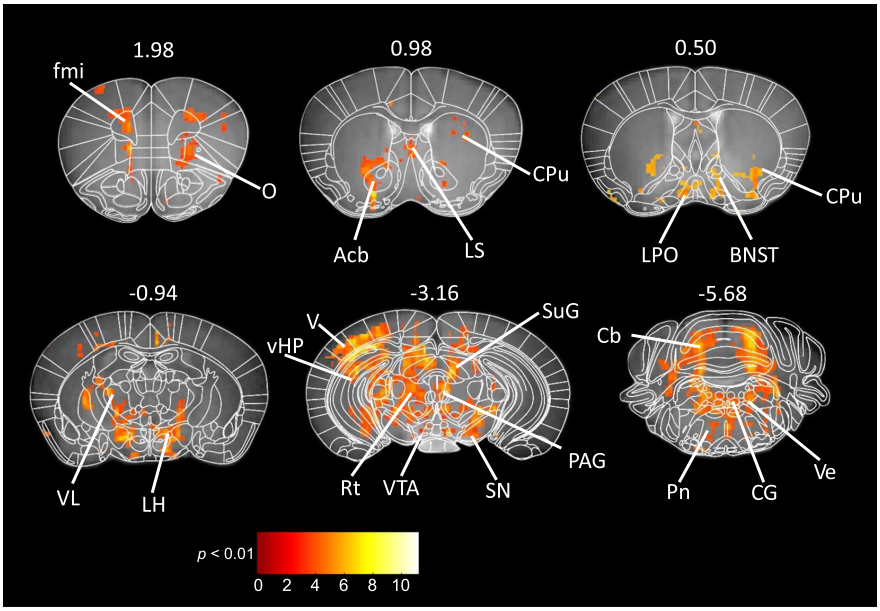

Figure 2. Differences in brain activity between socially defeated and control mice revealed by MEMRI. Statistical t-maps (thresholded at $p < 0.01$, corrected for multiple comparisons) are superimposed on a custom-made mouse brain template, with corresponding atlas sections[58] manually overlaid using anatomical landmarks. Numbers indicate the positions of the sections from bregma in millimetres. Brain region abbreviations: BNST (bed nucleus of the stria terminalis), CPu (caudate putamen), Cb (cerebellum), CG (central grey), fmi (forceps minor), LH (lateral hypothalamus), LPO (lateral preoptic area), LS (lateral septum), Acb (nucleus accumbens), O (orbital cortex), PAG (periaqueductal grey), Pn (pontine nuclei), Rt (reticular formation), SN (substantia nigra), SuG (superior colliculus), V (visual cortex), VL (ventrolateral thalamic nucleus), vHP (ventral hippocampus), Ve (vestibular nuclei), VTA (ventral tegmental area).

including the ventral tegmental area (VTA), substantia nigra (SN), periaqueductal grey (PAG), superior colliculus (SuG), ventral hippocampus (vHP), dentate gyrus (DG), and reticular formation (Rt) in stressed compared to the control mice. Cortical activation was found in the visual cortex (V). In the hindbrain, social defeat was associated with increased signal intensity in the pontine (Pn) and vestibular nuclei (Ve), with connectivity with the cerebellum (Cb).

ΔFOSB staining reveals localised cell populations with repeated activation in stressed mice. We counted the number of ΔFOSB-expressing cells in 18 pre-selected brain regions and compared the control and defeated groups with either *t*- or *U*-tests depending on normality of distributions (Table 1). We selected the regions based on our results from MEMRI and on prior findings on brain activation in stress and emotional processing[23,24]. As shown in Fig. 3, we observed significantly larger numbers of ΔFOSB positive cells in the BNST (anterodorsal), CPu, lateral septum (ventral, LSV), lateral thalamus (VL), LH, vHP and the DG (ventral) in stressed compared to control mice. While no comparisons survived correction for a false discovery rate (FDR) of 5%, given the large number of regions examined, the aforementioned regions remained significant when correcting for FDR < 20%. The number of ΔFOSB positive cells in midbrain regions such as the VTA and PAG (dorsolateral) was overall very low, and we did not detect differences in their number between stressed and control animals in either region (Fig. 2A). Expression of ΔFOSB in the infralimbic (IL) and prelimbic (PrL) regions of the prefrontal cortex did not differ significantly between groups (Table 1). No differences between groups were observed for the negative control region piriform cortex (Pir), as expected, as it does not have a known role in the regulation of stress. There were very few ΔFOSB-positive cells in the CPu, VL and LH, especially in the VL, prohibiting calculation of the percentage change between groups.

CSDS alters the correlation of ΔFOSB expression between brain regions. To identify putative network-level consequences of CSDS, we took advantage of the nuclear specificity and excellent spatial resolution of immunohistochemistry and calculated correlation coefficients (Pearson's *r*) of the number of ΔFOSB positive cells between each brain region, separately for defeated and control mice (see Supplementary Table S1 for full correlation matrix). We observed notable differences in the correlation profiles of defeated and control mice for specific brain regions (Fig. 4). The correlation profiles of prefrontal regions IL and PrL were similar within the control group and the stressed group, but the two groups differed considerably from each other. The number of

Brain region	Full name	*N* control	*N* defeated	*% change*$^{+}$	*t/U*	*P*
MO	*Medial orbital cortex*	7	7	+39.7	1.072 (*t*)	0.315
IL	*Infralimbic cortex*	7	8	+109.1	1.801 (*t*)	0.095
PrL	*Prelimbic cortex*	7	8	+66.9	1.536 (*t*)	0.148
BNST	*Bed nucleus of stria terminalis (anterodorsal)*	6	7	+306.4	2.644 (*t*)	**0.034**
AcbC	*Nucleus accumbens (core)*	7	8	+139.4	1.389 (*U*)	0.189
AcbSh	*Nucleus accumbens (shell)*	6	8	+82.3	0.645 (*U*)	0.573
CPu	*Caudate putamen*	7	8	+753.7	2.083 (*U*)	**0.006**
LSV	*Lateral septum (ventral)*	7	8	+89.0	2.142 (*t*)	**0.035**
VL	*Thalamus (ventrolateral)*	6	7	n/a	2.448 (*U*)	**0.035**
LH	*Lateral hypothalamus*	6	7	+153.1	2.436 (*t*)	**0.033**
BLA	*Basolateral amygdala*	6	7	+54.2	0.886 (*t*)	0.394
BMA	*Basomedial amygdala*	6	7	+73.5	1.206 (*t*)	0.253
CeA	*Central amygdala*	6	7	+83.7	1.410 (*t*)	0.186
vHP	*Ventral hippocampus (CA1 & CA3)*	7	8	+261.5	2.083 (*U*)	**0.040**
DG	*Dentate gyrus (ventral)*	6	6	+153.4	2.695 (*t*)	**0.032**
PAG	*Periaqueductal grey (dorsolateral)*	7	8	+112.8	1.582 (*t*)	0.138
VTA	*Ventral tegmental area*	6	6	−22.7	0.601 (*t*)	0.561
Pir	*Piriform cortex*	7	8	+16.1	0.401 (*t*)	0.695

Table 1. Differences in the number of ΔFOSB-positive cells between defeated and control mice in each brain region of interest. The number of positive cells between control and defeated mice was compared with either an independent Student's *t*-test (normally distributed data, indicated with *t*) or a Mann-Whitney U-test (non-normally distributed data, indicated with *U*). *N* = number of animals, *P* = nominal *p*-value, +change in mean number of stained cells in defeated mice compared to controls in percentage points. Significant *p*-values (<0.05) which also survive correction for multiple comparisons (false discovery rate < 20%) are marked in bold.

ΔFOSB positive cells correlated significantly ($r > 0.8$, $p < 0.05$) in both groups with expression in the DG and AcbC, while in defeated mice we also observed correlation of both regions with the CPu and VL (Fig. 4a and b). Activation of the BNST was also significantly correlated with the activation of subcortical structures, PrL and DG following CSDS but not in control mice (Fig. 4c). The basomedial amygdala (BMA, Fig. 4d) shared correlated activation with the VTA both in control and defeated mice. For the defeated mice, the only notable change in BMA co-activation occurred with other amygdalar nuclei, namely the central nucleus (CeA), with no significant correlations with frontal and other subcortical regions. Lastly, both the vHP (Fig. 4e) and PAG (Fig. 4f) cell counts were significantly correlated with frontal regions in defeated mice but not in controls, despite the very low number of ΔFOSB positive cells observed in the PAG. To control for potential biases in correlation coefficients caused by an overall increase in ΔFOSB expressing cells in stressed mice, we tested for a correlation of mean ΔFOSB cell number and mean value of *r* for each brain region, separately for the two groups. In defeated mice there was no correlation between ΔFOSB and *r*, suggesting that the emerging correlation profiles cannot be explained by a rise in absolute ΔFOSB expression (see Supplementary Fig. S1).

Discussion

To determine mouse brain regions repeatedly activated due to chronic stress exposure, we carried out neuroimaging by MEMRI and immunohistochemical detection of ΔFOSB one week after the cessation of 10-day CSDS in mice. Our approach allowed unbiased covering of the whole brain, enabling the discovery of previously unreported associations between repeated neuronal activity and chronic stress experience. Regions in which both methods revealed significantly more activation in stressed compared to control mice included subcortical structures (BNST, CPu, LSV, VL, LH), and the vHP and DG. MEMRI revealed stress-induced activation at the orbital cortex and fmi, an anterior portion of the corpus callosum, possibly reflecting the spread of Mn^{2+} along white matter tracts[25]. A stronger MEMRI signal was also observed in the midbrain regions of stressed compared to control mice, but without any differences in the number of ΔFOSB positive cells between the groups. To assess putative stress effects at the network level, we also surveyed correlations of ΔFOSB expression between brain regions, separately within the defeated and control groups. The correlation profiles of the IL, PrL, BNST, vHP and PAG were considerably altered following CSDS.

Although both ΔFOSB expression and MEMRI mapping are expected to reveal differences in brain activation induced by chronic psychosocial stress, the observed regional pattern of activation was not completely overlapping. These findings are not contradictory, but rather reflect methodological differences, and represent complementary measures of repeated brain activation. While ΔFOSB immunohistochemistry allows measurement of high resolution neuronal activation, MEMRI can also reveal long-range connectivity in activated pathways due to anterograde axonal Mn^{2+} transport in addition to local activity[18,19]. Therefore, strong MEMRI signal can also be found in regions with low ΔFOSB expression levels but dense axonal tracts passing through them, as seen in VL, LH and midbrain regions. For example, the LH receives strong inputs from the extended amygdala, striatum, septum, and hippocampal formation, which had higher numbers of ΔFOSB positive cells in stressed compared to control mice. These regions also send reciprocal projections to the hypothalamus. In addition, the LH

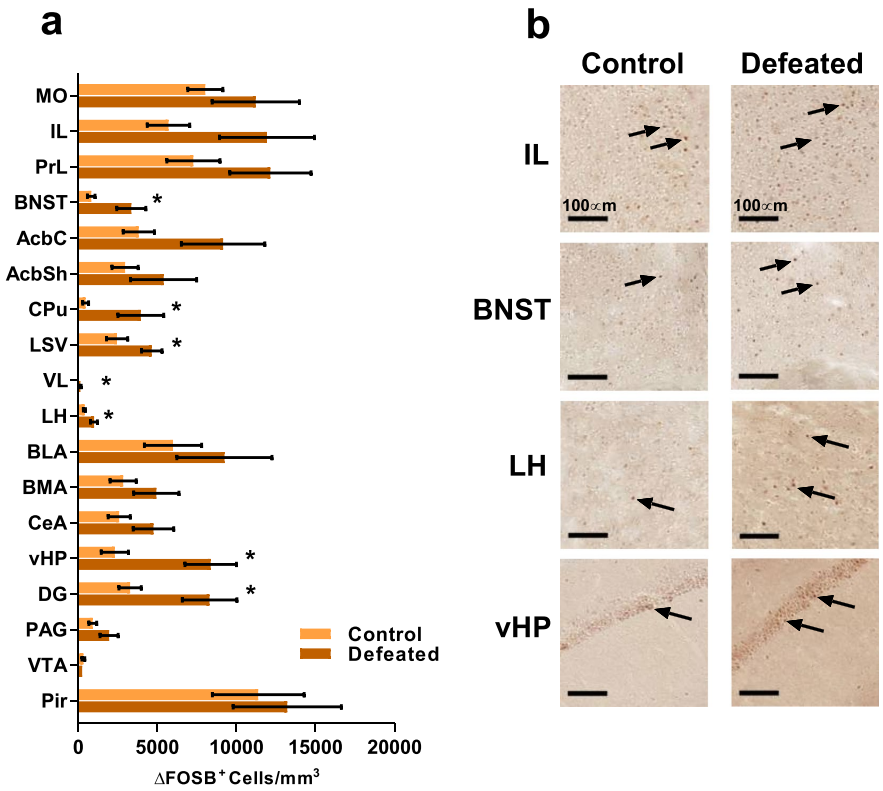

Figure 3. Chronic social defeat induces changes in brain activation as measured by expression of ΔFOSB. (**a**) The mean number of cells staining positive for ΔFOSB in defeated and control mice. Error bars ± 1 SEM, $^{*}p < 0.05$, see Table 1 for exact statistical values. (**b**) Representative images of immunohistochemical staining for ΔFOSB, positive cells indicated by black arrows, in the infralimbic cortex (IL), bed nucleus of stria terminals (BNST), lateral hypothalamus (LH) and ventral hippocampus (vHP). Scale bar = 100 µm. See Supplementary Fig. S2 for representative images from each of the brain regions analysed.

is connected with the midbrain and brainstem[26] which had widespread MEMRI signal enhancement in stressed mice. These regions play an important role in somatomotor, sensory, and autonomic control mechanisms that have been implicated in stress and anxiety[27].

Neither MEMRI nor ΔFOSB mapping allows us to determine the exact time of neuronal activation giving rise to the observed differences between stressed and control animals. However, with the 8-day half-life of ΔFOSB[21], the number of ΔFOSB positive cells we observe one week after 10-day CSDS likely reflects repeated activation that occurred during defeat and/or the time between CSDS and dissection. The half-life of Mn^{2+} in the brain is longer than that of ΔFOSB, and therefore brain activation measured by MEMRI one week after social defeat may partly reflect acute stress effects that occurred during the first days of social defeat. However, we have previously shown that activation induced by a week of alcohol exposure either largely subsided or exhibited an altered pattern following a week-long abstinence from alcohol, suggesting that the changes seen during abstinence could not be ascribed to acute alcohol exposure alone[17]. Similarly, the MEMRI signal measured one week after CSDS could reflect neuronal activation related to long-term physiological and behavioral changes observed in defeated animals[10].

The regions we selected for immunohistochemical analysis have been implicated in the processing of social and emotional behaviour in mice and humans[6,23,24,28]. However, we only observed repeated activation of a subset of these regions during chronic psychosocial stress in mice. These differences to previous publications are most likely due to varying nature of stress and the interval between the stress exposure and measurement of brain activation. Similarly to our findings, the dorsal BNST, CPu, LSV and DG were previously found to be activated already 24 h following CSDS in mice[29], and the PFC, LH and DG were activated less than 24 h after chronic variable stress in rats[30]. No differences were observed in ΔFOSB expression 20 days post-defeat between the control and defeated mice using Western blot detection of FOSB isoforms in bulk tissue samples including the whole PFC and whole hippocampus[31]. Also the Acb, basolateral amygdala (BLA) and dorsal raphe nuclei were found

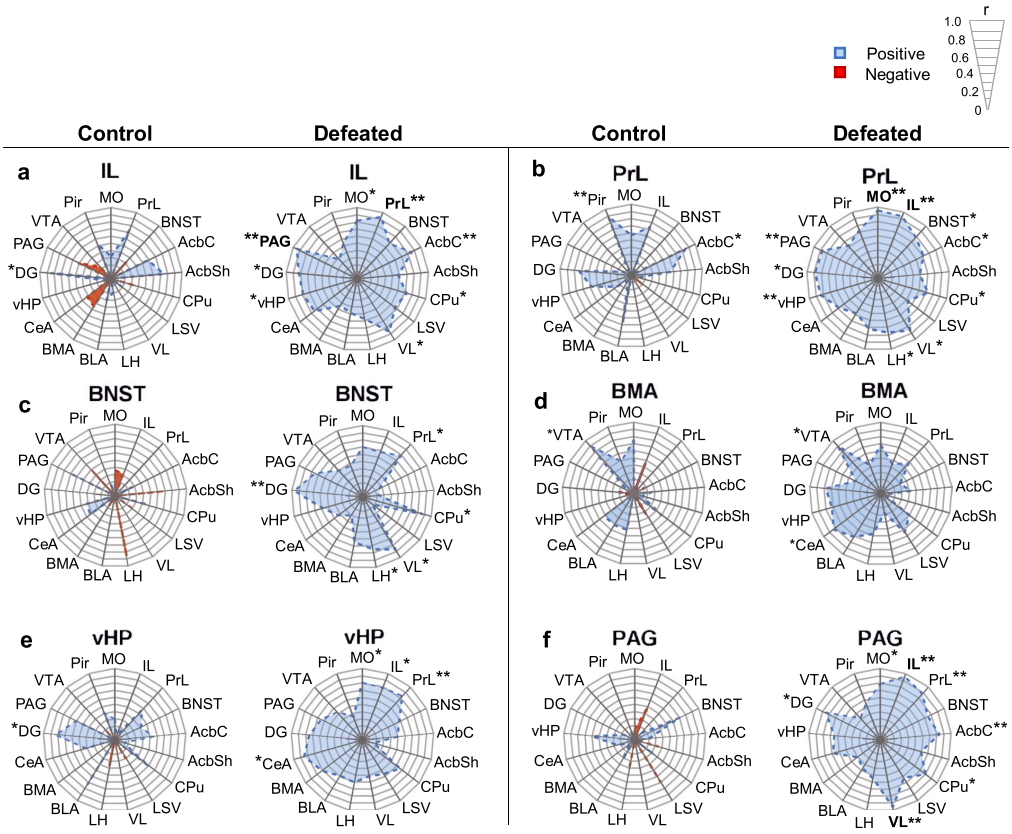

Figure 4. Chronic social defeat stress associates with alterations in ΔFOSB positive cell number correlation profiles of specific brain regions. Radar graphs depict the absolute value of *r* for the infralimbic cortex (IL, a), prelimbic cortex (PrL, b), bed nucleus of stria terminalis (BNST, c), basomedial amygdala (BMA, d), ventral hippocampus (vHP, e), and periaqueductal grey (PAG, f) comparison of the number of ΔFOSB-positive cells per mm^3 with the other brain regions. Figure key indicates the sign and magnitude of *r*. Regions that correlate significantly with the title region are indicated by an asterisk (*$p < 0.05$, **$p < 0.01$), and correlations remaining significant after correction for false discovery rate (<5%) are marked with bold text. See Table 1 for brain region abbreviations.

to be activated 24 h following stress[29], but not in our study with a longer post-defeat delay. These regions could therefore be involved more significantly during early stress exposure, as ΔFOSB produced in the early days but not later days of stress exposure may have decayed by the time we measured its expression. The regions displaying activation in our study may mediate the effects of chronic psychosocial stress in the long term and are potential sites of alterations that may also contribute to the development of behavioural outcomes of stress.

When two brain regions jointly participate in a task, their activity becomes correlated as measured by functional neuroimaging in humans[32,33], electrical recordings in monkeys[34] and staining for activity-induced proteins in rodents[35,36]. Although immunohistochemical data analysis reveals such functional connections, directionality of the connections remains elusive. Some regions are even known to be connected by parallel tracts with functionally opposed consequences on activation[37]. Furthermore, regions that engage in correlated activation are not necessarily physically connected, but rather part of the same functional network. Despite these limitations, we aimed at addressing functional connectivity for establishing how chronic psychosocial stress is processed by specific brain networks.

The BNST is implicated in risk assessment and anxiety-like behaviour in mice[38], but its activation in CSDS has not been extensively studied. BNST neurons mediate anxiety-like behaviour and regulate endocrine functions following acute stress exposure[39]. Some of its subregions have opposing roles in anxiety-like behaviour: the anterodorsal nuclei produce anxiogenic responses, while the ventral nuclei mediate anxiolysis[23,37]. The dorsal segment shows increased activation 24 h following 10-day CSDS[29]. We found that the anterodorsal BNST is repeatedly activated in stress-exposed mice, and that in the stressed mice the BNST ΔFOSB expression correlation with

other brain regions, including the DG, LH, VL, CPu and PrL, was altered. The BNST has afferent and efferent connections with several regions, including the amygdala, LH, PAG and the PFC[40–42], and neural activity of BNST could partly contribute to increased MEMRI signal in these areas through axonal transport. However, out of these established connections we only observed significant correlation of BNST activation with the LH and the PrL following CSDS. The observed correlation between the BNST and DG is interesting because no direct structural connections are reported for these regions in mice[43], suggesting that their functional connectivity may be mediated by one or more other regions. Therefore, while structural and functional connections of the BNST are wide-reaching, only some of these connections may be involved in the response to chronic psychosocial stress. In particular, our data suggest that networks connecting the BNST, PFC, LH and DG are activated during chronic stress, and may mediate previously unprobed long-term adaptive changes after stress.

The vHP and PFC both regulate emotionality and depressive states in humans. In patients with MDD the vHP is less active during a memory task[8], but more active at rest[7] compared to healthy controls, while the PFC exhibits decreased activity at rest[6]. Both regions are activated in humans during an acutely stressful task[44,45]. We observed repeated activation of both regions and a significant correlation of ΔFOSB expression between them in mice exposed to CSDS. In mice these regions are connected by a monosynaptic tract[46], in addition to several indirect connective loops[47]. Temporally synchronized firing between these regions occurs during anxiety-provoking tasks[48], and inhibiting activity along this pathway optogenetically reduces anxiety-like behaviour[49]. Interestingly, in humans the tract connecting the hippocampal region to the PFC, the uncinate fasciculus, shows decreased white matter integrity by diffusion tensor imaging in adults with a history of childhood maltreatment[50]. We observed that the fmi, another major white matter tract of the PFC, was more active in defeated than control mice as measured by MEMRI, suggesting that this connection also becomes recruited during chronic stress. White matter alterations have also been found in this tract in mice exposed to social isolation[51] and in MDD patients[52]. Thus, chronic psychosocial stress in mice, and acute social stress in humans, both increase activity in the circuit involving the PFC and vHP.

We did not detect altered ΔFOSB expression in the PAG after stress, but observed marked changes in its correlation profile. This region contains connections to and from the cortex, basal ganglia, VL and LH[53], and it is an important mediator of defensive behavioural responses via inputs from the amygdala[54]. Similarly to the BNST, only a subset of the regions with direct synaptic connectivity with the PAG showed significantly correlated activation in the stressed mice, including the PFC, AcbC, and VL. Anatomical connectivity of these regions with PAG may also lead to the increased Mn^{2+} accumulation we observed. The emergence of correlation between low PAG ΔFOSB expression and other regions suggests that the observed correlations were not artefacts arising from an increased number of ΔFOSB expressing cells (see Supplementary Fig. S1). Our finding of low ΔFOSB expression in the PAG parallel with significant functional connections may point to a small specific neuronal ensemble participating in chronic stress processing. Intriguingly, fewer than 10% of PAG neurons receive input from the cortex, and these cells mediate social behaviour following chronic stress exposure[53].

In conclusion, our data suggest that a functional network of specific frontal, subcortical and midbrain regions is repeatedly activated by CSDS, and that chronic stress alters inter-region co-activation. These brain regions, including the PFC, BNST and other subcortical structures, vHP and PAG, provide targets for future studies seeking to determine long-lasting effects of chronic psychosocial stress on the mouse brain.

Methods

Animals. Animal procedures were approved by the project authorization board of the Regional State Administration Agency for Southern Finland and carried out in accordance to directive 2010/63/EU of the European Parliament and of the Council, and the Finnish Act on the Protection of Animals Used for Science or Educational Purposes (497/2013).

We used 21 male mice (C57BL/6NCrl, Charles River, Sulzfeld, Germany), aged 5 weeks on arrival. During a 7-day acclimatization period they were group-housed in Makrolon type III cages. The housing facility was temperature- and humidity-controlled with a 12 h light/dark cycle (light phase: 6:00–18:00). Mice had *ad libitum* access to standard pellet food and water.

Aggressor mice used for the chronic social defeat stress (CSDS) procedure (see below) were male Clr:CD1 (Charles River) mice aged between 13 and 26 weeks. Following a 7-day acclimatization period in single-housed individually ventilated cages we screened them for appropriate levels of aggression by assessing their propensity for attacking an intruder mouse (no sooner than 10 seconds or later than 90 seconds after introduction to a C57BL/6NCrl test mouse). Twenty-four hours before the start of CSDS each selected aggressor mouse was placed alone into a cage to be used for CSDS.

Experimental design. The experimental procedures are illustrated in Fig. 1. At the end of the habituation period, mice were surgically implanted with osmotic minipumps for delivery of $MnCl_2$. The mice were allowed to recover from the surgery for one week, after which they underwent the 10-day CSDS procedure or the control housing procedure. Manganese was infused constitutively during CSDS. After the end of CSDS, all mice were placed in single-housed cages until the MRI scan and dissections. We wanted to mainly assess chronic brain activation without bias from acute activation occurring at the beginning of the social defeat and therefore set the post-defeat delay to six days.

Osmotic minipump implantation. Subcutaneous osmotic minipumps (Alzet, model 2002) delivering 200 µl of $MnCl_2$ (0.5 µl/h) were implanted as described previously[55]. $MnCl_2$ was dissolved into Tris-buffered saline (pH 7.4) and administered with osmotic minipumps during the 16-day infusion, corresponding to a total $MnCl_2$ dose of 160 mg/kg/week. The concentration of $MnCl_2$ in the pumps was adjusted to the body weight of the animals. Before the surgery, the pumps were primed overnight in a 37 °C saline solution. Animals were anesthetized

with 5% isoflurane and the pumps were implanted subcutaneously on the dorsum, slightly caudal to the scapulae. For post-surgical analgesia, animals received one subcutaneous injection of carprofen (5 mg/kg) immediately after implantation.

Chronic social defeat stress (CSDS). Following recovery from implantation mice allocated to the defeated group ($N = 11$) were exposed to CSDS[56]. In short, the mouse was placed into a cage containing an aggressor mouse. The mice were observed for a maximum of 10 min, after which they were separated by a perforated plexiglass wall, exposing the experimental mouse to sensory cues from the aggressor mouse without risk of physical contact. If during the initial observation phase the aggressor mouse exhibited excessive physical aggression (caused a significant wound, particularly in the vicinity of the minipump) the mice were separated before the 10-minute time had elapsed. The average contact time throughout the experiment was 6.43 min. The sensory contact phase lasted for 24 h, after which the experimental mouse was placed into the cage of a novel aggressor mouse and the 10-min physical contact + 24 h sensory contact cycle was repeated. This procedure was repeated for 10 consecutive days. Control mice ($N = 10$) were housed in similar cages but with another control mouse as a neighbour and no physical contact, switching cage-mates daily. The social aversion test was performed 24 h after the last session of social defeat for both defeated and control mice[56]. Briefly, mice were placed in an arena containing a perforated cylinder for 150 s. The mice were placed back in the home cage, and the cylinder replaced with one containing a novel CD-1 mouse. The mouse was then returned to the arena for 150 s. The social preference score (ratio of time spent near the cylinder when it contained another mouse compared to the trial with the empty cylinder) did not differ ($p = 0.256$) between the groups due to small sample size and large variation between animals.

MRI acquisition and data analysis. Magnetic resonance imaging was performed with a 4.7 T scanner (Bruker, PharmaScan 47/16 US, Ettlingen, Germany) using a 38 mm linear volume coil for transmit and receive. Mice were transferred from the vivarium to the scanner room, immediately anaesthetized with 5% isoflurane in oxygen (0.8–1 L/min) and positioned on a custom-made holder with a stabilizing tooth bar and a nose cone. Accurate positioning was confirmed with the help of scout images and all inaccuracies were corrected by adjusting the position and angles of the field. During scanning anaesthesia was maintained with 2–3% isoflurane and the body temperature was kept constant at 37 °C with a heating pad. The scanning order was counterbalanced according to the experimental groups. T1-weighted images were acquired using a three-dimensional rapid acquisition-relaxation enhanced (RARE) pulse sequence (repetition time = 300 ms, effective echo time = 10.7 ms, echo train length = 8, flip angle = 180°, number of averages = 8, field of view FOV = 12.8 × 12.8 × 12.8 mm, acquired matrix size = 200/200/200, reconstructed matrix size = 100/100/100, resulting in 0.128 × 0.128 × 0.128 mm^3 voxel resolution). Values for the automatically adjusted receiver gain were collected to verify that the observed group differences were not caused by changes in receiver gain. Total scanning time, including acquisition of scout images, was approximately 60 min per animal.

All MRI images were converted to Analyze format, scaled by a factor of 10 and spatially preprocessed with SPM8 software running under MATLAB (version R2015). All T1-weighted images were spatially normalized to a custom-made mouse brain template. Bias correction was performed to eliminate field inhomogeneity of the magnetic field. For creating statistical parametric maps of differential brain activation between experimental groups, the groups were compared by voxel-wise independent two-tailed *t*-test using SPM8. Despite careful adjustment of $MnCl_2$ concentration in individual animals, systemic infusion can lead to differences in brain Mn^{2+} accumulation, causing activation-independent differences in the mean global signal intensity between subjects. To eliminate global effects, the mean intensity was included as a nuisance factor in the statistical model, on a voxel-by-voxel basis[57]. For the defeated < control contrast, the resulting statistical parametric maps were thresholded voxelwise at the arbitrary significance of $p < 0.001$. Then the cluster size was thresholded with a threshold of k = 71 voxels, resulting in an overall significance level of $p < 0.01$ corrected for multiple comparisons across the whole brain. k was computed based on Monte Carlo simulations. Brain regions were identified by superimposing brain atlas sections[58] on the MRI scans using prominent landmarks, including white matter tracts (e.g. corpus callosum, anterior and posterior commissures), the overall shape of the brain and ventricle location, and defined grey matter structures (e.g. caudate putamen). The observed increased MEMRI signal in stressed animals is likely not attributable to alterations in Ca^{2+} channel function as we did not observe any gene coding for Ca^{2+} channel components (GO:0005891) to be differentially expressed between stressed and control animals in RNA sequencing data from the medial PFC or vHP (data not shown).

Tissue processing and immunohistochemistry. Following the MRI scan mice were injected with a lethal dose of pentobarbital (Mebunat Vet, Orion Pharma) without breaks in anaesthesia. Mice were transcardially perfused with 4% paraformaldehyde (PFA) in PBS. We postfixed the brains in 4% PFA for 2–24 h, cryoprotected them in 20% sucrose for 24 h, froze them in 2-methyl butane, and stored them in −80 °C. We then cryosectioned the brains with a Leica CM3050 cryostat (Leica Biosystems, Nussloch, Germany). Sections were stored in −20 °C submerged in cryoprotectant. One defeated animal died during MRI acquisition and was not further analysed.

All immunohistochemical, microscopy and quantification procedures were carried out blind to the condition of each animal. Five animals (3 controls, 2 defeated) were not stained due to issues with fixation. Tissue sections were stained in batches with balanced numbers of mice belonging to each experimental group. The sections were rinsed in TBS and endogenous peroxidase activity was quenched with hydrogen peroxide. We blocked non-specific binding with 10% normal goat serum (NGS) with 0.5% Tween-20 detergent (Sigma Aldrich) in TBS. Primary antibody incubation with a polyclonal rabbit anti-FOSB antibody [1:500 (0.4 µg/mL), sc-7203, Santa Cruz Biotechnology, Dallas, TX, U.S.A.] in TBS with 10% NGS + 0.5% Tween-20 was carried out for 18 h in ambient room temperature. Biotinylated affinity-purified goat anti-rabbit [1:200 (7.5 µg/mL), ABC detection

kit (PK-6101), Vector laboratories, Burlingame, CA, U.S.A] diluted in TBS with 1.5% NGS was used as the secondary antibody and incubated for 2 h in room temperature. The sections were incubated in an avidin-biotin solution prepared in PBS (ABC detection kit, Vector Laboratories), rinsed in 0.1 M PB and staining detected with 3,3′-diaminobenzidine (DAB, Vector Laboratories). Sections were dehydrated and stored at +4 °C.

The primary antibody detects also the full-length FOSB protein, but it is induced only by acute stimulation with a half-life of 1.6 hours[20,21] and is thus not expected to contribute to our findings. As the mice were kept anaesthetized throughout the scanning, which lasted approximately 60 min, and the perfusion was done immediately after the scan, acute stress effects incurred during transport from the vivarium to the scanning room are expected to be minimal. Due to the counterbalanced order of scanning, any minor acutely induced full-length FOSB did not impact our results. The primary antibody was tested on male C57BL/6NCrl mice receiving injections of saline or cocaine for 6 consecutive days (15 mg/kg daily), and naïve controls ($N = 2$/group). Cocaine is known to induce both full-length and ΔFOSB in the caudoputamen after acute exposure, but only ΔFOSB following chronic exposure[59]. Mice receiving cocaine had significantly more ΔFOSB positive cells than both saline and naïve control mice ($p < 0.001$ in both contrasts, see Supplementary Fig. S1). Validity of staining was also ensured with test staining omitting the primary antibody.

Stained sections were imaged with a Pannoramic FLASH II digital scanner using a 0.8 NA objective at a resolution of 0.24 µm/pixel (3DHistech, Budapest, Hungary) at the Institute of Biotechnology (University of Helsinki). We captured regions of interest images from the digital scans at 20x magnification using the Pannoramic Viewer software version 1.15.3 (3DHistech) based on anatomical landmarks indexed in the Mouse Brain Atlas[58]. The numbers of stained cells were quantified using ImageJ version 1.47 v (National Institutes of Health), using a colour deconvolution plugin with a vector for DAB-staining built in to this version of the software. Thresholded images were analysed for particles larger than 15 μm^2 in size and quantified with automated measurement.

Cell count statistical analysis. ΔFOSB cell counts were acquired from 18 relevant brain regions (see Table 1) from 3–6 sections from each animal. The piriform cortex (Pir), an olfactory processing region[60], was included due to its expected lack of involvement in CSDS. Exclusion criteria for single cell count data points was a deviation of ≥ 3 times the interquartile range below or above the median of the group. If half or more data points collected from one animal within one brain region were outliers based on this criterion, the whole animal was excluded from analyses concerning that region. Another criterion for excluding an animal from any specific test was insufficient fixation (total number of animals included per brain region is indicated in Table 1). Distribution normality was assessed with the Shapiro-Wilk test. For regions where the data were normally distributed the groups were compared using independent *t*-tests, and for non-normally distributed regions using the Mann-Whitney *U*-test.

Correlations were assessed using Pearson's *r*. To assess correlated activity between regions, for each brain region pair we included all animals with cell count data available for both regions. Correlation coefficients were calculated separately for control and defeated groups, pairing each brain region with each of the other brain regions.

All *p*-values were assessed against a two-tailed α-level of 0.05 to determine significance. SPSS Statistics version 24 (IBM) was used for all analyses. The Benjamini Hochberg procedure was used for correcting multiple comparisons for false discoveries[61].

Data availability Statement. All data are available from the corresponding authors upon request.

References

1. Kemeny, M. E. & Schedlowski, M. Understanding the interaction between psychosocial stress and immune-related diseases: A stepwise progression. *Brain Behav Immun* **21**, 1009–18 (2007).
2. O'Donnell, M. J. *et al.* Risk factors for ischaemic and intracerebral haemorrhagic stroke in 22 countries (the INTERSTROKE study): A case-control study. *The Lancet* **376**, 112–23 (2010).
3. Donner, J. *et al.* Support for involvement of glutamate decarboxylase 1 and neuropeptide y in anxiety susceptibility. *Am J Med Genet B Neuropsychiatr Genet* **159B**, 316–327 (2012).
4. Moffitt, T. E. *et al.* Generalized anxiety disorder and depression: Childhood risk factors in a birth cohort followed to age 32. *Psychol Med* **37**, 441–52 (2007).
5. Bick, J. & Nelson, C. A. Early adverse experiences and the developing brain. *Neuropsychopharmacology.* **41**, 177–196 (2016).
6. Zhong, X., Pu, W. & Yao, S. Functional alterations of fronto-limbic circuit and default mode network systems in first-episode, drug-naïve patients with major depressive disorder: A meta-analysis of resting-state fMRI data. *J Affect Disord* **206**, 280–286 (2016).
7. Fitzgerald, P. B., Laird, A. R., Maller, J. & Daskalakis, Z. J. A meta-analytic study of changes in brain activation in depression. *Hum Brain Mapp* **29**, 683–695 (2008).
8. Milne, A. M. B., MacQueen, G. M. & Hall, G. B. C. Abnormal hippocampal activation in patients with extensive history of major depression: An fMRI study. *J Psychiatry Neurosci* **37**, 28–36 (2012).
9. Pizzagalli, D. A. *et al.* Reduced caudate and nucleus accumbens response to rewards in unmedicated individuals with major depressive disorder. *Am J Psychiatry* **166**, 702–710 (2009).
10. Krishnan, V. *et al.* Molecular Adaptations Underlying Susceptibility and Resistance to Social Defeat in Brain Reward Regions. *Cell* **131**, 391–404 (2007).
11. Norman, K. J. *et al.* Social stress and escalated drug self-administration in mice I. Alcohol and corticosterone. *Psychopharmacology (Berl)* **232**, 991–1001 (2015).
12. Tsankova, N. M. *et al.* Sustained hippocampal chromatin regulation in a mouse model of depression and antidepressant action. *Nat Neurosci* **9**, 519–525 (2006).
13. Zanos, P. *et al.* NMDAR inhibition-independent antidepressant actions of ketamine metabolites. *Nature* **533**, 481–486 (2016).
14. Lin, Y.-J. & Koretsky, A. P. Manganese ion enhances T1-weighted MRI during brain activation: An approach to direct imaging of brain function. *Mag Reson Med* **38**, 378–388 (1997).
15. Silva, A. C. & Bock, N. A. Manganese-enhanced MRI: An exceptional tool in translational neuroimaging. *Schizophr Bull* **34**, 595–604 (2008).

16. Eschenko, O. *et al*. Mapping of functional brain activity in freely behaving rats during voluntary running using manganese-enhanced MRI: Implication for longitudinal studies. *Neuroimage*. **49**, 2544–2555 (2010).
17. Dudek, M. *et al*. Brain activation induced by voluntary alcohol and saccharin drinking in rats assessed with manganese-enhanced magnetic resonance imaging. *Addict Biol* **20**, 1012–1021 (2015).
18. Dudek, M., Canals, S., Sommer, W. H. & Hyytiä, P. Modulation of nucleus accumbens connectivity by alcohol drinking and naltrexone in alcohol-preferring rats: A manganese-enhanced magnetic resonance imaging study. *Eur Neuropsychopharmacol* **26**, 445–455 (2016).
19. Inoue, T., Majid, T. & Pautler, R. G. Manganese enhanced MRI (MEMRI): Neurophysiological applications. *Rev Neurosci* **22**, 675–694 (2011).
20. Nestler, E. J. δfosB: A transcriptional regulator of stress and antidepressant responses. *Eur J Pharmacol* **753**, 66–72 (2015).
21. Carle, T. L. *et al*. Proteasome-dependent and -independent mechanisms for FosB destabilization: Identification of FosB degron domains and implications for ΔFosB stability. *Eur J Neurosci* **25**, 3009–3019 (2007).
22. Perrotti, L. I. *et al*. Induction of ΔFosB in reward-related brain structures after chronic stress. *J Neuroscience* **24**, 10594–602 (2004).
23. Tovote, P., Fadok, J. P. & Lüthi, A. Neuronal circuits for fear and anxiety. *Nature Rev Neurosci* **16**, 317–331 (2015).
24. Calhoon, G. G. & Tye, K. M. Resolving the neural circuits of anxiety. *Nat Neurosci* **18**, 1394–1404 (2015).
25. Massaad, C. A. & Pautler, R. G. Manganese-enhanced magnetic resonance imaging (MEMRI). *Methods Mol Biol* **711**, 145–174 (2010).
26. Berthoud, H.-R. & Münzberg, H. The lateral hypothalamus as integrator of metabolic and environmental needs: From electrical self-stimulation to opto-genetics. *Physiol Behav* **104**, 29–39 (2011).
27. Myers, B., Scheimann, J. R., Franco-Villanueva, A. & Herman, J. P. Ascending mechanisms of stress integration: Implications for brainstem regulation of neuroendocrine and behavioral stress responses. *Neurosci Biobehav Rev* **74**, 366–375 (2017).
28. Kim, Y. *et al*. Mapping social behavior-induced brain activation at cellular resolution in the mouse. *Cell Reports* **10**, 292–305 (2015).
29. Vialou, V. *et al*. Prefrontal cortical circuit for depression- and anxiety-related behaviors mediated by cholecystokinin: Role of ΔFosB. *J Neurosci* **34**, 3878–3887 (2014).
30. Flak, J. N., Solomon, M. B., Jankord, R., Krause, E. G. & Herman, J. P. Identification of chronic stress-activated regions reveals a potential recruited circuit in rat brain. *Eur J Neurosci* **36**, 2547–2555 (2012).
31. Vialou, V. *et al*. Differential induction of FosB isoforms throughout the brain by fluoxetine and chronic stress. *Neuropharmacol* **99**, 28–37 (2015).
32. Homae, F., Yahata, N. & Sakai, K. L. Selective enhancement of functional connectivity in the left prefrontal cortex during sentence processing. *Neuroimage* **20**, 578–586 (2003).
33. Johnstone, T., Van Reekum, C. M., Urry, H. L., Kalin, N. H. & Davidson, R. J. Failure to regulate: Counterproductive recruitment of top-down prefrontal-subcortical circuitry in major depression. *J Neurosci* **27**, 8877–8884 (2007).
34. Livneh, U. & Paz, R. Amygdala-prefrontal synchronization underlies resistance to extinction of aversive memories. *Neuron* **75**, 133–142 (2012).
35. Johnson, Z. V. *et al*. Central oxytocin receptors mediate mating-induced partner preferences and enhance correlated activation across forebrain nuclei in male prairie voles. *Horm Behav* **79**, 8–17 (2016).
36. Wheeler, A. L. *et al*. Identification of a Functional Connectome for Long-Term Fear Memory in Mice. *PLoS Comput Biol* **9**, e1002853 (2013).
37. Jennings, J. H. *et al*. Distinct extended amygdala circuits for divergent motivational states. *Nature* **496**, 224–228 (2013).
38. Davis, M., Walker, D. L., Miles, L. & Grillon, C. Phasic vs sustained fear in rats and humans: Role of the extended amygdala in fear vs anxiety. *Neuropsychopharmacology* **35**, 105–135 (2010).
39. Henckens, M. J. A. G. *et al*. CRF receptor type 2 neurons in the posterior bed nucleus of the stria terminalis critically contribute to stress recovery. *Mol Psychiatry* [ePub ahead of print (AOP)], https://doi.org/10.1038/mp.2016.133 (2016).
40. Vertes, R. P. Differential Projections of the Infralimbic and Prelimbic Cortex in the Rat. *Synapse* **51**, 32–58 (2004).
41. Dong, H.-W., Petrovich, G. D., Watts, A. G. & Swanson, L. W. Basic organization of projections from the oval and fusiform nuclei of the bed nuclei of the stria terminalis in adult rat brain. *J Comp Neurol* **436**, 430–455 (2001).
42. Krüger, O., Shiozawa, T., Kreifelts, B., Scheffler, K. & Ethofer, T. Three distinct fiber pathways of the bed nucleus of the stria terminalis to the amygdala and prefrontal cortex. *Cortex* **66**, 60–68 (2015).
43. Oh, S. W. *et al*. A mesoscale connectome of the mouse brain. *Nature* **508**, 207–214 (2014).
44. Grimm, S. *et al*. Early life stress modulates oxytocin effects on limbic system during acute psychosocial stress. *Soc Cog Affect Neurosci* **9**, 1828–1835 (2014).
45. Lederbogen, F. *et al*. City living and urban upbringing affect neural social stress processing in humans. *Nature* **474**, 498–501 (2011).
46. Tripathi, A., Schenker, E., Spedding, M. & Jay, T. M. The hippocampal to prefrontal cortex circuit in mice: a promising electrophysiological signature in models for psychiatric disorders. *Brain Struct Func* **221**, 2385–2391 (2015).
47. Li, M., Long, C. & Yang, L. Hippocampal-prefrontal circuit and disrupted functional connectivity in psychiatric and neurodegenerative disorders. *BioMed Res Int* **2015**, ArticleID:810548 (2015).
48. Adhikari, A., Topiwala, M. A. & Gordon, J. A. Synchronized Activity between the Ventral Hippocampus and the Medial Prefrontal Cortex during Anxiety. *Neuron* **65**, 257–269 (2010).
49. Padilla-Coreano, N. *et al*. Direct Ventral Hippocampal-Prefrontal Input Is Required for Anxiety-Related Neural Activity and Behavior. *Neuron*. **89**, 857–66 (2016).
50. Hanson, J. L., Knodt, A. R., Brigidi, B. D. & Hariri, A. R. Lower structural integrity of the uncinate fasciculus is associated with a history of child maltreatment and future psychological vulnerability to stress. *Dev Psychopathol* **27**, 1611–1619 (2015).
51. Liu, C. *et al*. Altered structural connectome in adolescent socially isolated mice. *Neuroimage* **139**, 259–270 (2016).
52. Lyden, H. *et al*. Electroconvulsive therapy mediates neuroplasticity of white matter microstructure in major depression. *Transl Psychiatry* **4**, e380 (2014).
53. Franklin, T. B. *et al*. Prefrontal cortical control of a brainstem social behavior circuit. *Nat Neurosci* **20**, 260–270 (2017).
54. Tovote, P. *et al*. Midbrain circuits for defensive behaviour. *Nature* **534**, 206–212 (2016).
55. Dudek, M. & Hyytiä, P. Alcohol preference and consumption are controlled by the caudal linear nucleus in alcohol-preferring rats. *Eur J Neurosci* **43**, 1440–1448 (2016).
56. Golden, S. A., Covington, H. E., Berton, O. & Russo, S. J. A standardized protocol for repeated social defeat stress in mice. *Nat Protoc* **6**, 1183–1191 (2011).
57. Friston, K. J. *et al*. The relationship between global and local changes in PET scans. *J Cereb Blood Flow Metab* **10**, 458–466 (1990).
58. Franklin, K. B. J. & Paxinos, G. The Mouse Brain in Stereotaxic Coordinates (3rd ed). (Academic Press, 2008).
59. Larson, E. B. *et al*. Striatal regulation of ΔfosB, FosB, and cFos during cocaine self-administration and withdrawal. *J Neurochem* **115**, 112–122 (2010).
60. Mukherjee, B. & Yuan, Q. NMDA receptors in mouse anterior piriform cortex initialize early odor preference learning and L-type calcium channels engage for long-term memory. *Sci Rep* **6**, 35256 (2016).
61. Benjamini, Y. & Yekutieli, D. The control of the false discovery rate in multiple testing under dependency. *Ann Stat* **29**, 1165–88 (2001).

Acknowledgements

This research was supported by the Academy of Finland (grant TRANSALC 01EW1112, M.D. and P.H.), the Sigrid Jusélius Foundation (I.H.), The European Research Council Starting Grant (GenAnx, I.H.), the University of Helsinki (I.H.), and the University of Helsinki Doctoral Program Brain & Mind (M.L.). We thank Sanna Kängsep for help during pilot tests of behavioural protocols, Lana Dokleja for help with the FOSB immunohistochemistry protocol, Sari Latvala for help in testing the FOSB antibody, and Paula Collin-Olkkonen from the Institute of Biotechnology, University of Helsinki, for technical assistance with the digital scanning of microscopy glasses.

Author Contributions

P.H. and I.H. conceived and designed the overall study, supervised experiments and helped with data interpretations. E.S., M.D. and S.-A.C. designed, carried out and analysed the social defeat procedures and MEMRI experiments. M.A.L. and E.S. carried out and analysed the immunohistochemistry experiments. M.A.L., M.D., P.H. and I.H. wrote the manuscript. All authors discussed results and commented on the manuscript.

Additional Information

Supplementary information accompanies this paper at https://doi.org/10.1038/s41598-017-15422-5.

Competing Interests: The authors declare that they have no competing interests.

Publisher's note: Springer Nature remains neutral with regard to jurisdictional claims in published maps and institutional affiliations.

eNeuro

New Research

Disorders of the Nervous System

Genetic Control of Myelin Plasticity after Chronic Psychosocial Stress

Mikaela A. Laine,[1*] Kalevi Trontti,[1*] Zuzanna Misiewicz,[1*] Ewa Sokolowska,[1*] Natalia Kulesskaya,[1] Aino Heikkinen,[1] Suvi Saarnio,[1] Ingrid Balcells,[1] Pierre Ameslon,[1] Dario Greco,[2] Pirkko Mattila,[3] Pekka Ellonen,[3] Lars Paulin,[2] Petri Auvinen,[2] Eija Jokitalo,[2] and Iiris Hovatta[1]

https://doi.org/10.1523/ENEURO.0166-18.2018

[1]Molecular and Integrative Biosciences Research Program, University of Helsinki, Helsinki FI-00014, Finland, [2]Institute of Biotechnology, University of Helsinki, Helsinki FI-00014, Finland, and [3]Finnish Institute of Molecular Medicine, University of Helsinki, Helsinki FI-00014, Finland

Visual Abstract

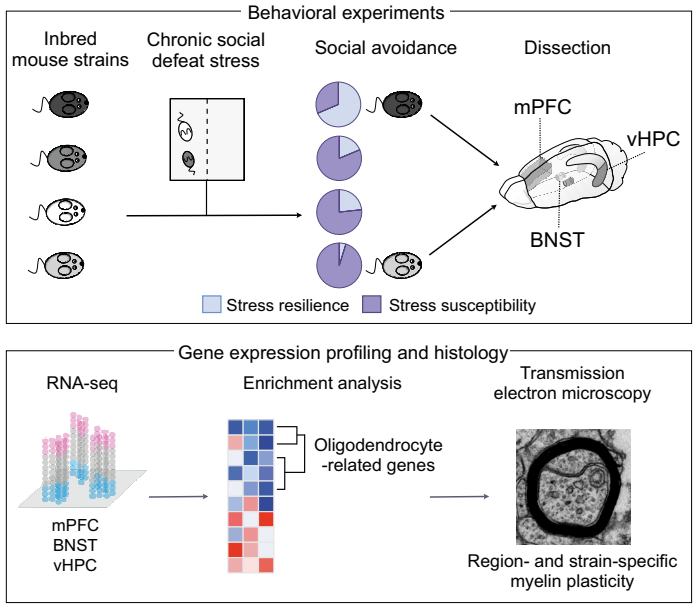

Significance Statement

Chronic psychosocial stress is a well-established risk factor for anxiety disorders, but the development of targets for therapeutic intervention is limited by ignorance of the underlying molecular and cellular mechanisms. We used inbred genetically defined mice to identify neurobiological pathways that underlie stress-induced social avoidance (SA), a type of anxiety. We found genetically controlled differences in myelin-related gene expression in stress-exposed mice, with concurrent differences in myelin thickness, suggesting that myelin plasticity is a major stress response of the brain. The adaptive response to stress may increase or decrease myelin thickness, depending on the demands of the specific circuit. Our findings provide a foundation for the identification of specific genetic regulators of chronic stress-induced myelin plasticity.

Anxiety disorders often manifest in genetically susceptible individuals after psychosocial stress, but the mechanisms underlying these gene-environment interactions are largely unknown. We used the chronic social defeat stress (CSDS) mouse model to study resilience and susceptibility to chronic psychosocial stress. We identified a strong genetic background effect in CSDS-induced social avoidance (SA) using four inbred mouse strains: 69% of C57BL/6NCrl (B6), 23% of BALB/cAnNCrl, 19% of 129S2/SvPasCrl, and 5% of DBA/2NCrl (D2) mice were stress resilient. Furthermore, different inbred mouse strains responded differently to stress, suggesting they use distinct coping strategies. To identify biological pathways affected by CSDS, we used RNA-sequencing (RNA-seq) of three brain regions of two strains, B6 and D2: medial prefrontal cortex (mPFC), ventral hippocampus (vHPC), and bed nucleus of the stria terminalis (BNST). We discovered overrepresentation of oligodendrocyte (OLG)-related genes in the differentially expressed gene population. Because OLGs myelinate axons, we measured myelin thickness and found significant region and strain-specific differences. For example, in resilient D2 mice, mPFC axons had thinner myelin than controls, whereas susceptible B6 mice had thinner myelin than controls in the vHPC. Neither myelin-related gene expression in several other regions nor corpus callosum thickness differed between stressed and control animals. Our unbiased gene expression experiment suggests that myelin plasticity is a substantial response to chronic psychosocial stress, varies across brain regions, and is genetically controlled. Identification of genetic regulators of the myelin response will provide mechanistic insight into the molecular basis of stress-related diseases, such as anxiety disorders, a critical step in developing targeted therapy.

Key words: anxiety; chronic social defeat stress; inbred mouse strain; myelin; RNA-sequencing; transmission electron microscopy

Introduction

Anxiety disorders, including panic disorder, social anxiety disorder, specific phobias, and generalized anxiety disorder, are the most common mental disorders with a prevalence of 14% (Wittchen et al., 2011). Human genetic studies of anxiety disorders have confirmed a modest heritability and considerable environmental component (Hettema et al., 2001). However, identification of replicated risk variants is challenging due to genetic heterogeneity, environmental factors that cannot be well-controlled in human settings, and poor availability of large patient cohorts with accurate phenotypes (Hovatta and Barlow, 2008; Smoller, 2016). Consequently, many investigators have resorted to animal models, which allow controlled experiments on both genetic and environmental risk factors, to reveal the biological mechanisms underlying these diseases.

Chronic psychosocial stress is a well-established risk factor for anxiety disorders (Kemeny and Schedlowski, 2007; Moffitt et al., 2007; Donner et al., 2012). It can be modeled in mice by the chronic social defeat stress (CSDS) paradigm, that has etiological, predictive, and face validity for affective and anxiety disorders (Hammels et al., 2015). It leads to social avoidance (SA) and long-term plastic changes in the brain (Avgustinovich et al., 2005; Krishnan et al., 2007). However, only a portion of mice exhibit SA after CSDS, and thus the defeated animals can be divided into stress-susceptible and resilient. Comparison of these groups allows investigation of the mechanistic basis of stress-induced SA and anxiety-like behavior and resilience to it. Understanding the underlying risk factors and promotion of the resilience factors in susceptible individuals should facilitate development of secondary prevention methods of anxiety disorders after traumatic events, and selective pharmacological treatment of anxiety (Howlett and Stein, 2016).

Most insight into the molecular mechanisms of CSDS comes from the C57BL/6 mouse strain, in which specific genetic, epigenetic, and neurophysiological mechanisms underlie stress susceptibility and resilience (Han and Nes-

Received April 30, 2018; accepted June 25, 2018; First published July 02, 2018.

The authors declare no competing financial interests.

Author contributions: M.A.L., K.T., Z.M., E.S., and I.H. designed research; M.A.L., K.T., Z.M., E.S., N.K., A.H., S.S., I.B., P.Am., P.M., P.E., L.P., P.Au., E.J., and I.H. performed research; D.G. contributed unpublished reagents/analytic tools; M.A.L., K.T., Z.M., E.S., N.K., A.H., S.S., and I.H. analyzed data; M.A.L., K.T., Z.M., N.K., and I.H. wrote the paper.

This work was supported by the European Research Council Starting Grant GenAnx 281559 (to I.H.), ERA-NET NEURON (AnxBio; I.H.), University of Helsinki (I.H.), Sigrid Jusélius Foundation (I.H.), Doctoral Program Brain and Mind, University of Helsinki (M.L. and Z.M.), and the A*MIDEX Grant ANR-11-IDEX-0001-02 funded by the French Government "Investissements d'Avenir" Program (to P.A.). The EM-unit is supported by the Institute of Biotechnology (University of Helsinki), Helsinki Institute of Life Science and Biocenter Finland (E.J.).

*M.A.L., K.T., Z.M., and E.S. contributed equally to this work.

Acknowledgments: We thank Saija-Anita Callan, Sanna Kängsepp, and Laura Salminen for help with mouse work; Maria Razzoli for help with setting up the CSDS protocol; Vootele Voikar from the Mouse Behavioral Phenotyping Facility [supported by University of Helsinki (HiLIFE) and Biocenter Finland] for support with behavioral testing; Jenni Lahtinen for RNA-seq library preparation; Juho Väänänen and Birgitta Paranko for help with bioinformatic analyses; Mervi Lindman, Arja Strandell and Helena Vihinen for help with electron microscopy; Päivi Laamanen, Harri Kangas and Matias Rantanen from the Institute of Biotechnology (University of Helsinki) for RNA-seq; the IT Center for Science (CSC) for computing facilities; and Petri Hyytiä, Anders Paetau, Eva Rikandi, Outi Mantere, Tuula Kieseppä, Jaana Suvisaari, Tuukka Raij, and Hovatta lab members for helpful discussions. We also thank the Sequencing Unit at FIMM Technology Center supported by University of Helsinki and Biocenter Finland.

Correspondence should be addressed to Dr. Iiris Hovatta, Molecular and Integrative Biosciences Research Program, P.O. Box 56, University of Helsinki, Helsinki FI-00014, Finland, E-mail iiris.hovatta@helsinki.fi.

https://doi.org/10.1523/ENEURO.0166-18.2018

tler, 2017). Because genetic background strongly modulates mouse behavior (Threadgill et al., 1995; Hovatta et al., 2005; Sittig et al., 2016), hypotheses of any mechanisms should be tested across different mouse strains. Such studies are also critical for translating the results to genetically heterogeneous humans. CSDS has different behavioral and physiologic consequences in C57BL/6J and BALB/c strains (Razzoli et al., 2011a,b; Savignac et al., 2011), reflecting underlying genetic, and by extension, gene expression differences between the strains. Therefore, comprehensive unbiased transcriptomic approaches applied to mouse strains with different responses to CSDS should reveal gene-environment interactions that explain why some individuals are more susceptible to stress-induced maladaptive behaviors than others.

To examine how genetic background affects the behavioral response to chronic stress, we performed behavioral testing in four inbred mouse strains after CSDS. We selected C57BL/6NCrl (B6) and BALB/cAnNCrl (BALB) strains, which differ in behavioral and metabolic responses to CSDS (Razzoli et al., 2011a,b; Savignac et al., 2011), and DBA/2NCrl (D2) and 129S2/SvPasCrl (129) as they are sensitive to stress-induced anxiety- and depression-like behavior in general (Ducottet and Belzung, 2005; Millstein and Holmes, 2007). To identify the major underlying biological pathways, we performed unbiased transcriptomic analysis in the B6 and D2 strains that showed the largest differences in susceptibility to stress. We studied three brain regions, the medial prefrontal cortex (mPFC), ventral hippocampus (vHPC), and bed nucleus of the stria terminalis (BNST), which critically regulate anxiety and the stress response (Garakani et al., 2009; Calhoon and Tye, 2015; Tovote et al., 2015), and are activated by CSDS (Vialou et al., 2014; Laine et al., 2017). In the follow-up gene expression and histologic analyses, we found that myelination was significantly altered after stress in a strain and brain region-dependent manner. Our results illustrate that genetic background has a large effect on both the behavioral and brain transcriptomic response to chronic psychosocial stress. Moreover, we demonstrate that the pattern of stress-induced myelination changes is dependent on the genetic background and varies across brain regions.

Materials and Methods

Animals

We ordered five-week-old male mice from four inbred strains [DBA/2NCrl (D2), 129S2/SvPasCrl (129), BALB/cAnNCrl (BALB), and C57BL/6NCrl (B6); Charles River Laboratories] for all CSDS experiments and let them acclimatize for 10 d before CSDS, housed in groups in a temperature (22 $\pm$ 2°C) and humidity (50 $\pm$ 15%) controlled facility on a 12/12 h light/dark cycle (lights on 6 A.M. to 6 P.M.). From the end of CSDS to the time of dissection, all mice were single-housed. As aggressors for CSDS, we used male Clr-CD1 mice (CD1, Charles River Laboratories), aged 13–26 weeks. All mice had ad libitum access to food and water throughout the experiment, except for the durations of behavioral tests. Aspen chip bedding (Tapvei Oy) in the cages was changed weekly (except for the duration of the CSDS) and standard environmental enrichment [aspen strips as nesting material (Tapvei Oy) and an aspen brick (Tapvei Oy)] was provided throughout the experiment. Animal procedures were approved by the Regional State Administration Agency for Southern Finland (ESAVI-3801-041003-2011 and ESAVI/2766/04.10.07/2014) and conducted in accordance to directive 2010/63/EU of the European Parliament and of the Council, and the Finnish Act on the Protection of Animals Used for Science or Educational Purposes (497/2013).

Behavioral experiments

CSDS

We conducted CSDS as previously described (Golden et al., 2011; Laine et al., 2017). Briefly, aggressor CD1 mice were first checked for appropriate aggression levels during a 3-d screening before all social defeat experiments. The selected aggressors had to meet the following criteria: attack in at least two consecutive sessions, had latency to attack of $<$90 s and do not attack within 1–5 s in any of the sessions. For CSDS, each defeated mouse was placed into the cage of an aggressor mouse for max. 10 min. The mouse was then transferred to another compartment of the cage, separated from the aggressor by a perforated Plexiglas wall, for 24 h. This procedure was repeated for 10 d, and each day the experimental mouse encountered a novel aggressor. Physical contact time was shortened in the case of severe physical aggression. Control mice were housed in similar cages but with another control mouse as a cage-mate, and without physical contact, switching cage-mates daily. The day after the last defeat session, all mice were separated into single-housed cages and maintained like this until dissection. The order of testing for all consecutive behavioural tests was randomized.

SA test

Twenty-four hours after the last social defeat session, at the start of the dark phase of the light cycle, we tested both defeated and control mice in the SA test. All animals were brought to the experiment room at least 30 min before the start of the test, and animals performing the test were separated from experimenters and the remaining animals by a screen. For the first trial (no-target), the mouse was placed in the center of an open arena (42 $\times$ 42 cm) with an empty perforated Plexiglas cylinder located next to one of the walls. The movements of the mouse were tracked using a camera and EthoVision XT10 software (Noldus Information Technology) for 150 s, after which the mouse was placed back into the home cage. The arena was cleaned and the Plexiglas cylinder was replaced with another one containing an unfamiliar CD1 social target mouse. The test mouse was then placed back in the middle of the arena and tracked for 150 s (target trial). The amount of time the mice spent in the interaction zone (IZ), defined as a semicircle (370 cm^2) around the perforated Plexiglas cylinder, was measured and a social interaction (SI) ratio calculated by dividing the IZ time of the social target trial with the IZ time of the

no-target trial, multiplied by 100. Thus, a low SI ratio indicates high SA.

To account for strain differences in baseline social behavior, we assessed the response of defeated mice in relation to same-strain controls, following the statistical approach previously implemented by Nasca et al. (2015). We calculated mean SI ratios of control mice from each strain based on several cohorts (*n*: 129 = 8, BALB = 40, B6 = 126, D2 = 114). We used log-transformation to normalize the distribution, removed outliers (>3 IQRs from the median), and divided the defeated mice to stress-resilient (resembling controls) and susceptible (showing SA) based on SI ratios, with the border determined as the controls' mean score minus 1 SD. SI ratio border values for each strain were: 129 = 62.68, BALB = 81.76, B6 = 76.49, D2 = 105.99.

Body weight

Body weight was recorded at the beginning of CSDS (day 1) and on every second day throughout the CSDS (days 2, 4, 6, 8, and 10). The amount of body weight gain was calculated as the difference between the first and the last measurement.

Open field (OF) test

We assessed spontaneous locomotor activity and anxiety-like behavior with an automatic MedAssociates system at the start of the light phase of the light cycle. Individual mouse cages were brought to the experimental room in two groups. After 30 min adaptation to the experimental room (lit at 100 lux), the mouse was released to the corner of the experimental chamber (27 × 27 × 20 cm, transparent walls and white floor virtually divided into a 19 × 19 squares grid) and allowed to explore freely for 5 min.

Elevated zero maze (EZM)

EZM was performed at the start of the light phase of the light cycle. All animals were brought to the experiment room at least 30 min before the test, and animals performing the test were separated from experimenters and the remaining animals by a screen. The apparatus consisted of plastic annular runway (diameter = 50 cm, width = 5 cm) elevated 40 cm above the floor. The runway was divided into four sectors: two open sectors opposing each other and two opposing closed sectors protected by inner and outer non-transparent walls (height = 15 cm). After 30 min of adaptation to the experimental room (dimly lit at 15–20 lux), the mouse was placed in the middle of one of the closed sectors and allowed to explore the maze freely for 5 min. The mouse was video-tracked with EthoVision XT10.

Forced swim test (FST)

All animals were brought to the experiment room at least 30 min before the test, and animals performing the test were separated from experimenters and the remaining animals by a screen. After adaptation to the experimental room (150 lux), the mouse was placed in a glass cylinder (diameter = 18 cm, height = 25 cm) filled with water (room temperature) to the height of 15 cm. The immobility time (passive floating) was detected with EthoVision XT10 system for 6 min with 2-min time bins. Data from the last 4 min were used.

Gene expression profiling

Dissections

We dissected the mPFC (B6: Con *n* = 6, Res *n* = 6, Sus *n* = 6; D2: Con *n* = 6, Sus *n* = 8), BNST (B6: Con *n* = 5, Res *n* = 5, Sus *n* = 5; D2: Con *n* = 5, Res *n* = 3, Sus *n* = 5), and vHPC (B6: Con *n* = 6, Res *n* = 8, Sus *n* = 3; D2: Con *n* = 6, Sus *n* = 5) 6–8 d after the last CSDS (mice aged eight weeks). Mice were killed by cervical dislocation between 8 and 11 A.M. to avoid circadian differences in gene expression, and the order was counterbalanced across groups (resilient, susceptible, and control mice). Dissections were performed on a sterile chilled Petri dish within 7 min, and tissue was flash frozen in liquid N_2.

RNA-sequencing (RNA-seq)

Total RNA was extracted with TriReagent (Molecular Research Center Inc.) and RNA quality was assessed with a 2100 Bioanalyzer (Agilent Technologies) using Agilent RNA 600 Nano Chip kit (Agilent Technologies). rRNA was depleted with Ribo-Zero Gold rRNA Removal kit (Illumina Inc; mPFC and vHPC) or custom Insert Dependent Adaptor Cleavage (InDA-C) primers (BNST). RNA was fragmented using the S2 ultrasonicator (Covaris Inc.) and sequencing libraries were prepared with Nextera (Illumina; vHPC), ScriptSeq v2 (Epicentre; mPFC), or Ovation Universal RNA-Seq System (NuGEN; BNST) RNA-seq library preparation kits. Libraries were size-selected with Pippin Prep (Sage Science) and sequencing was conducted on HighSeq 2000 (vHPC, paired-end 91 bp, Illumina) or NextSeq 500 platforms (mPFC and BNST, single-end 96 bp; Illumina).

The RNA-seq reads were trimmed for adapters with Cutadapt v1.8.3 (vHPC) and FastX toolkit (mPFC, BNST) and PCR duplicates were removed with PRINSEQ v0.20.4. Reads were aligned using STARv 2.5.0c (Dobin et al., 2013) with default settings to mouse genome GRCm38, and annotated to gene exons with HTSeq v0.6.1 (Anders et al., 2015) using GTF release 86 (update 2016-10).

Differential expression (DE) analysis

DE analysis was conducted using limma eBayes (Ritchie et al., 2015; Phipson et al., 2016) comparing resilient and susceptible mice to same-strain controls within brain regions. RNA-seq data were filtered to remove low-abundance genes, keeping genes with at least 1 count per million (CPM) in at least six samples (Anders et al., 2015). Subsequently, the data were normalized with voom (Law et al., 2014), and adjusted for sequencing (vHPC) and library preparation batches (vHPC, mPFC, and BNST) with ComBat (Johnson et al., 2007). To identify top DE genes, we calculated -log10(*p*)∗logFC for each gene and ranked them accordingly (Xiao et al., 2014).

Gene expression data are available in Gene Expression Omnibus (GEO; GSE109315).

Rank-rank hypergeometric overlap (RRHO) test (Plaisier et al., 2010)

RRHO infers pair-wise similarity between two DE result lists, where genes are ranked by DE (-log10(*p*)∗logFC) between resilient and control, or between susceptible and control mice, by calculating significance of overlapping

genes at different rank bins (Plaisier et al., 2010). We used step size of 100 genes to bin the genes and applied the same -log(*p*) scale to comparisons within brain regions. Significant overlap of genes in rank groups containing up- and downregulated genes in both lists (lower left corner and upper right corner of square matrix, respectively, see Fig. 2*C*,*D*) shows a shared transcriptome-wide gene expression pattern in response to CSDS.

Gene set enrichment analysis (GSEA)

We conducted GSEA using the GSEA Preranked module implemented in GSEA Desktop v3.0 (Mootha et al., 2003; Subramanian et al., 2005) and the curated gene sets (C2) of the Molecular Signature Database (MSigDB) v6.0 (http://www.broad.mit.edu/gsea/). The pre-ranked GSEA was performed with 1000 permutations. The top five gene sets with the highest positive and negative normalized enrichment scores (NESs; $p_{FDR} < 0.05$) within each comparison were selected for further analysis. From the selected top up- and downregulated gene sets, all present in at least two comparisons and two brain regions were visualized using Circos software (Krzywinski et al., 2009). The overlap between the top enriched gene sets, presented on the Circos plot, was further investigated with the hypergeometric test implemented in the MSigDB v6.0.

Gene ontology (GO) term enrichment

We analyzed GO term enrichment separately for top 300 upregulated and 300 downregulated differentially expressed genes from each comparison with topGO (Alexa et al., 2006), using the weight01 model to account for GO term dependencies. In RNA-seq, long transcripts yield more read counts and are more easily passed through low-abundance filtering than short genes with the same expression level, and genes with high number of counts have greater statistical power being detected as DE than genes with low number of counts. To minimize these selection biases (Young et al., 2010), we matched the background genes, i.e., the gene universe used to compare the top DE genes with, with the top DE genes using R package genefilter (Gentleman et al., 2017), resulting in 6882 (±290 SEM) background genes.

Visualizing oligodendrocyte (OLG) progenitor cell (OPC) and OLG marker genes

We manually curated a list of OPC and OLG-specific marker genes, based on prior publications (Zhang et al., 2014; Marques et al., 2016). Figures were constructed based on previously published scripts (Haarman et al., 2014).

q-RT-PCR

q-RT-PCR was applied to validate five myelin-related genes from RNA-seq. We used published primers to amplify *Mobp* and *Plp1* (Liu et al., 2012) and designed primer pairs (5'-3' forward, reverse) using NCBI primer designing tool (https://www.ncbi.nlm.nih.gov/tools/primer-blast/) for *Opalin* (ACTGCCATCGAATACGACATC, CCTCTACGGG CTCATCATCG), *Ermn* (AACCAGGCAGGAGACAACTG, GATGGCCTGGTGAACAACGA), and *Mbp* (ACACAC-GAGAACTACCCATTATGG, AGAAATGGACTACTGGG TTTTCATCT). RNA samples of mPFC and BNST were the same as used in RNA-seq, and for vHPC samples overlapped by 37.5% (12/32 samples); 250 ng of DNase I (Thermo Scientific)-treated total RNA was converted to cDNA with iScript select cDNA synthesis kit (Bio-Rad Laboratories) and amplified with 250 nM primers in CFX384 Real-Time PCR cycler using IQ SYBR Green supermix (Bio-Rad Laboratories). Expression levels were normalized to *Ppib* (GGAGATGGCACAGGAGGAAA, CCCGTAGTGCTTCAGCTTGAA). Each reaction was run in triplicate and relative expression level was calculated using a standard curve (7.15, 10.0, 5.0, 2.0, 1.0, 0.5, and 0.25 ng of cDNA) present on each assay plate with CFX Manager (Bio-Rad Laboratories). Statistical analysis (Pearson's *r*) was conducted with GraphPad Prism v7.02 (GraphPad Software Inc.).

Immunohistochemistry

Mice were anaesthetized 6–8 d after CSDS with a lethal dose of pentobarbital (Mebunat Vet 60 mg/ml, Orion Pharma) and transcardially perfused with 4% paraformaldehyde (PFA) in PBS. After postfixation in 4% PFA overnight (+4°C), the brains were cut into 20-μm coronal sections using a Leica VT-1200S vibratome (Leica Biosystems) and stored at –20°C free-floating in cryoprotectant. Sections were washed 3× in PBS and mounted on Superfrost Ultra Plus (ThermoFisher Scientific) slides. We performed antigen retrieval by submerging the slides in 0.01 M citrate buffer, heated to a boil for 20 min. Slides were blocked in 2.5% BSA in 0.5% PBST + 7.5% normal goat serum, followed by primary antibody incubation with mouse anti-CNPase (1:250, Merck Life Science, #MAB326R) overnight at +4°C. Slides were washed in PBS before goat anti-mouse Alexa Fluor 488 secondary antibody incubation (1:400, ThermoFisher Scientific, #A-11029) for 2 h at room temerture. After washing in PBS, we coverslipped the slides with Vectashield + DAPI mounting medium (Vector Laboratories, #H-1200). We acquired images with ZEISS Apotome.2 system (Zeiss) and analyzed them with ImageJ software (National Institutes of Health). We measured corpus callosum thickness on both sides of the midline from each section (two to six sections per animal, distance from bregma between 0.22 and -0.10) using ImageJ, and calculated their mean.

Transmission electron microscopy (TEM)

Mice were anaesthetized 6–8 d after CSDS with a lethal dose of pentobarbital (Mebunat Vet). We transcardially perfused the mice with PBS followed by fixation with 100 ml 2% glutaraldehyde (GA)/2% PFA in 0.1 M sodium cacodylate (NaCac) buffer (GA, PFA, and NaCac: Sigma Aldrich), heated to +37°C. The brains were postfixed in the same fixative for 2–4 h and immersed in 0.1 M NaCac buffer for 2–24 h, both at +4°C. We cut them into 200-μm sagittal slices with a Leica VT-1200S vibratome (Leica Biosystems) in 0.1 M phosphate buffer. Regions of the mPFC, BNST, and vHPC were cut manually by using anatomic landmarks (Extended Data Fig. 5-1).

We postfixed the sections in osmium tetroxide [1%, +1.5% K4[Fe(CN)6] in 0.1 M NaCac] for 2 h at +4°C, stained en bloc with uranyl acetate for 1 h at +4°C, dehydrated with EtOH and acetone, and embedded them

Table 1. Statistical table

Figure	Data structure	Statistical test	Statistical significance (α)
1*B*	Categorical data	χ^2	0.05
1*C*	Normal distribution	Mixed ANOVA	0.0167
1*D*	Normal distribution	Mixed ANOVA	0.0167
1*E*	Normal distribution	One-way ANOVA	0.0167
1*F*	Normal distribution	One-way ANOVA (129, BALB and B6 strains), independent *t* test (D2 strain)	0.0167
1*G*	Normal distribution	One-way ANOVA	0.0167
1*H*	Normal distribution	One-way ANOVA	0.0167
1*I*	Normal distribution	One-way ANOVA (group comparisons), mixed ANOVA (within-group comparison of weight before and after CSDS)	0.0167
4*A–F*	Normal distribution	Mixed ANOVA	0.003 (B6) 0.01 (D2)
4*H,I*	Normal distribution	One-way ANOVA	0.0167
5*A–L*	Normal distribution	Generalized estimating equations (GEEs)	0.0167

Outline of statistical tests and significance levels applied for each experiment.

into hard Epon; 60- to 70-nm sections were cut with an ultramicrotome and placed on copper grids for microscopy and stained with lead citrate. We imaged the ultrathin sections using a Jem-1400 transmission electron microscope (Jeol) and randomly selected and imaged myelinated axons at 5000× magnification.

We measured myelin thickness, axon diameter, and g ratio using ImageJ. We calculated the diameter by measuring the area of the whole fiber and the area of the axon (inside the compacted myelin sheath). The diameters of geometric circles with the same areas were calculated for both parameters. We calculated the g ratio by dividing the diameter of the axon with the diameter of the whole fiber. Myelin thickness was measured at three fully compacted positions and their average calculated.

Statistical analysis

Statistical analyses were conducted with SPSS Statistics 24 (IBM) or GraphPad Prism 7.02 (GraphPad Software Inc.). Planned *post hoc* comparisons (control vs resilient, control vs susceptible, and resilient vs susceptible) were conducted by Fisher's LSD. For these tests we report nominal *p* values, evaluated for significance against an α-level adjusted for multiple corrections with test-wise Bonferroni correction (Table 1). Only *p* values which survive this correction are shown.

Group differences in TEM data were assessed using generalized estimating equations (GEEs) to control for within-subject dependencies of individual axons measured from the same animal (ranges for each region: mPFC = 93–104, BNST = 31–69, and vHPC = 54–62 axons per animal). We selected this approach due to the low number of animals per group, which could not be reliably analyzed by ANOVA. GEE has been proposed as a suitable approach for analyzing data with non-independent features (Hanley et al., 2003), such as axons measured from the same individual. Pair-wise contrasts were computed for comparing groups with Fisher's LSD and significance determined against the Bonferroni corrected α-level as above.

Data analysis of RNA-seq data were performed as described above. Multiple testing correction was done by the Benjamini–Hochberg method (Benjamini and Hochberg, 1995).

Results

Genetic background influences behavioral response to CSDS

To determine whether genetic background affects the behavioral response to psychosocial stress, we conducted 10-d CSDS in mice from four inbred strains, D2, 129, BALB, and B6 (Fig. 1*A*). Twenty-four hours after the last defeat session, we conducted the SA test to assess their SA phenotype. To account for the strain differences in baseline social behavior during SA test, we evaluated the response of defeated mice in relation to same-strain controls. We divided the defeated mice into stress-susceptible and resilient groups, considering mice with SI ratios within 1 SD, or above, of the same-strain control mean as resilient (i.e., resembling the control mice), and those with the SI ratio below 1 SD from the mean as susceptible. We observed a significant difference in the distribution of susceptible and resilient mice between the strains ($\chi^2 = 63.401$, $p = 1.102 \times 10^{-13}$), with the B6 defeated mice being mostly resilient and the 129, BALB, and D2 mice mostly susceptible to stress (Fig. 1*B*). During the social target trial of the SA test, susceptible mice from all strains spent significantly less time in the IZ (Fig. 1*C*) and more time in the corners of the arena (Fig. 1*D*) than during the no-target trial.

We next determined how CSDS influences other behaviors. To assess locomotor behavior, we measured the distance moved during the no-target trial of the SA test (Fig. 1*E*) and the OF test (Fig. 1*F*). B6 and D2 defeated mice moved significantly less than control mice during both tests. We did not observe differences in distance traveled between defeated and control 129 or BALB mice. For the B6 strain, we also performed the EZM and FST to assess anxiety-like and despair behavior, respectively. Susceptible mice showed increased anxiety-like, but not despair behavior, compared to controls (Fig. 1*G*,*H*). To study metabolic effects of CSDS, we measured body weight before and after CSDS (Fig. 1*I*). All B6 mice gained weight (mixed ANOVA *post hoc* comparison before versus

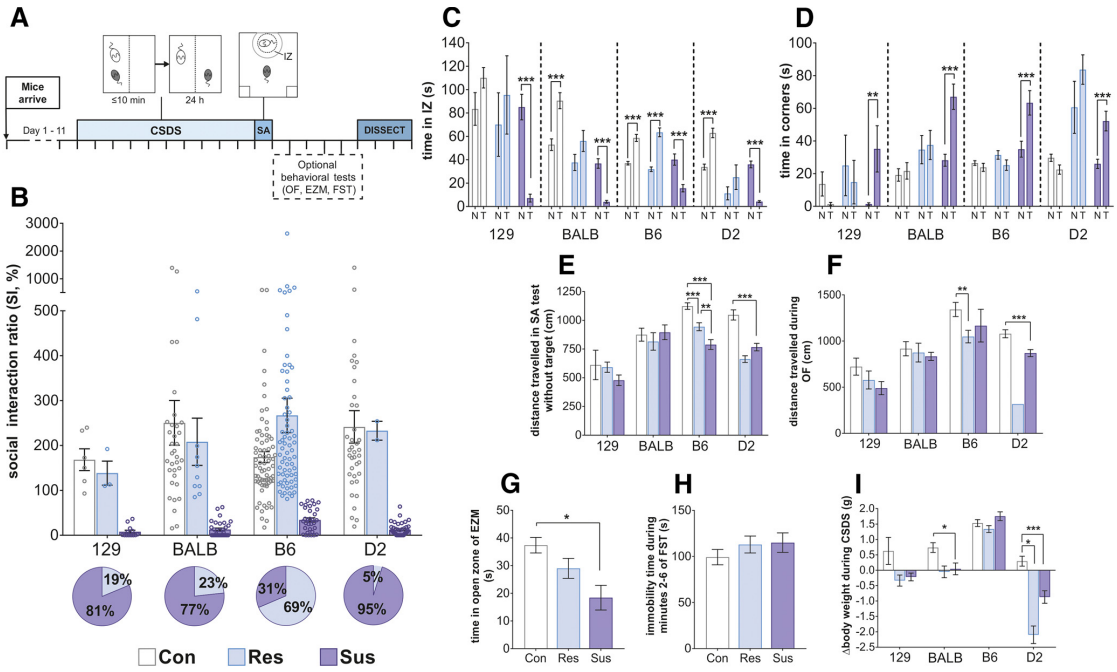

Figure 1. Strong genetic background effect on the behavioral response to CSDS. ***A***, Timeline of experiments. Each perpendicular line represents 1 d. ***B***, SI ratios of the four strains in the SA test. Pie charts represent the proportion of resilient and susceptible mice in each mouse strain. 129, BALB, and D2 strains were highly susceptible to CSDS, while B6 strain was the most resilient to CSDS. Time spent in the IZ (***C***) and the corner zones (***D***) of the SA test during sessions with no social target (N) and a CD1 mouse as a social target (T). Susceptible mice of all strains spent less time in the IZ when the target was present compared to when it was not. ***E***, Distance traveled during the no-target trial of the SA test. In the B6 strain, both susceptible and resilient mice had lower locomotor activity, while in the D2 strain only susceptible mice moved significantly less than controls; n (***B–E***, ***I***) = 129: Con = 7, Res = 3, Sus = 13; C: Con = 34, Res = 10, Sus = 33; B6: Con = 72, Res = 70, Sus = 32; D2: Con = 39, Res = 2, Sus = 40. ***F***, Distance traveled during the 5-min OF test. B6 resilient and D2 susceptible mice traveled significantly shorter distances than their same-strain control mice; n = 129: Con = 7, Res = 3, Sus = 13; C: Con = 18, Res = 6, Sus = 19; B6: Con = 20, Res = 19, Sus = 4; D2: Con = 19, Res = 1 (not analyzed), Sus = 22. ***G***, Time B6 mice spent in the open area of the EZM. Susceptible mice spent significantly less time in the open zones compared to controls; n: Con = 20, Res = 29, Sus = 11. ***H***, Immobility time of B6 mice during minutes 2–6 of the FST did not differ between groups; n = Con = 28, Res = 32, Sus = 21. ***I***, Difference in body weight before and after CSDS. B6 defeated mice gained weight during CSDS similarly to their same-strain controls, BALB susceptible mice gained significantly less weight than controls, and both resilient and susceptible D2 mice lost weight. All figures depict mean ± 1 SEM; $*p < 0.05$, $**p < 0.01$, $***p < 0.001$, see Extended Data Figure 1-1 for exact p values. D2: DBA/2NCrl strain; BALB: Balb/cAnNCrl; 129: 129S2/SvPasCrl; B6: C57BL/6NCrl; Con: control; Res: resilient; Sus: susceptible; mPFC: medial prefrontal cortex; BNST: bed nucleus of the stria terminalis; vHPC: ventral hippocampus.

after CSDS: controls $p = 9.98 \times 10^{-28}$, resilient $p = 2.21 \times 10^{-26}$ and susceptible $p = 6.23 \times 10^{-20}$). BALB and 129 controls gained weight ($p = 4.90 \times 10^{-5}$ and $p = 0.012$, respectively), while the weight of the defeated mice of these strains did not change during CSDS. Both D2 resilient and susceptible mice lost weight ($p = 0.004$ and $p = 2.53 \times 10^{-6}$, respectively).

Oligodendrocyte (OLG)-related genes are differentially expressed in response to stress

To establish which biological pathways were affected by chronic stress, we conducted RNA-seq one week after CSDS in mPFC, vHPC, and BNST (Fig. 2*A* Extended Data Fig. 2-1). We selected the B6 and D2 strains for this analysis as they represented the phenotypic extremes in the proportions of susceptible and resilient mice. We were not able to analyze gene expression levels of resilient D2 mice for mPFC and vHPC due to low number of animals in this group. We always compared the stress-susceptible or resilient mice to the same-strain controls. We first determined the overlap of the top 300 up- and downregulated genes between the strains in each brain region (Fig. 2*B*; Extended Data Fig. 2-2), followed up by the RRHO analysis, which shows the overall similarity and direction of DE of all genes (Fig. 2*C*,*D*; Extended Data Fig. 2-3). In the mPFC, only 26 (2.2%) of the top differentially expressed genes between the susceptible versus control mice were shared between the B6 and D2 strains, and the RRHO analysis confirmed the highly divergent stress response of the two strains. In the BNST, the transcriptomic response of the two strains was marginally more similar as resilient B6 and D2 mice shared 67 (5.9%), and suscep-

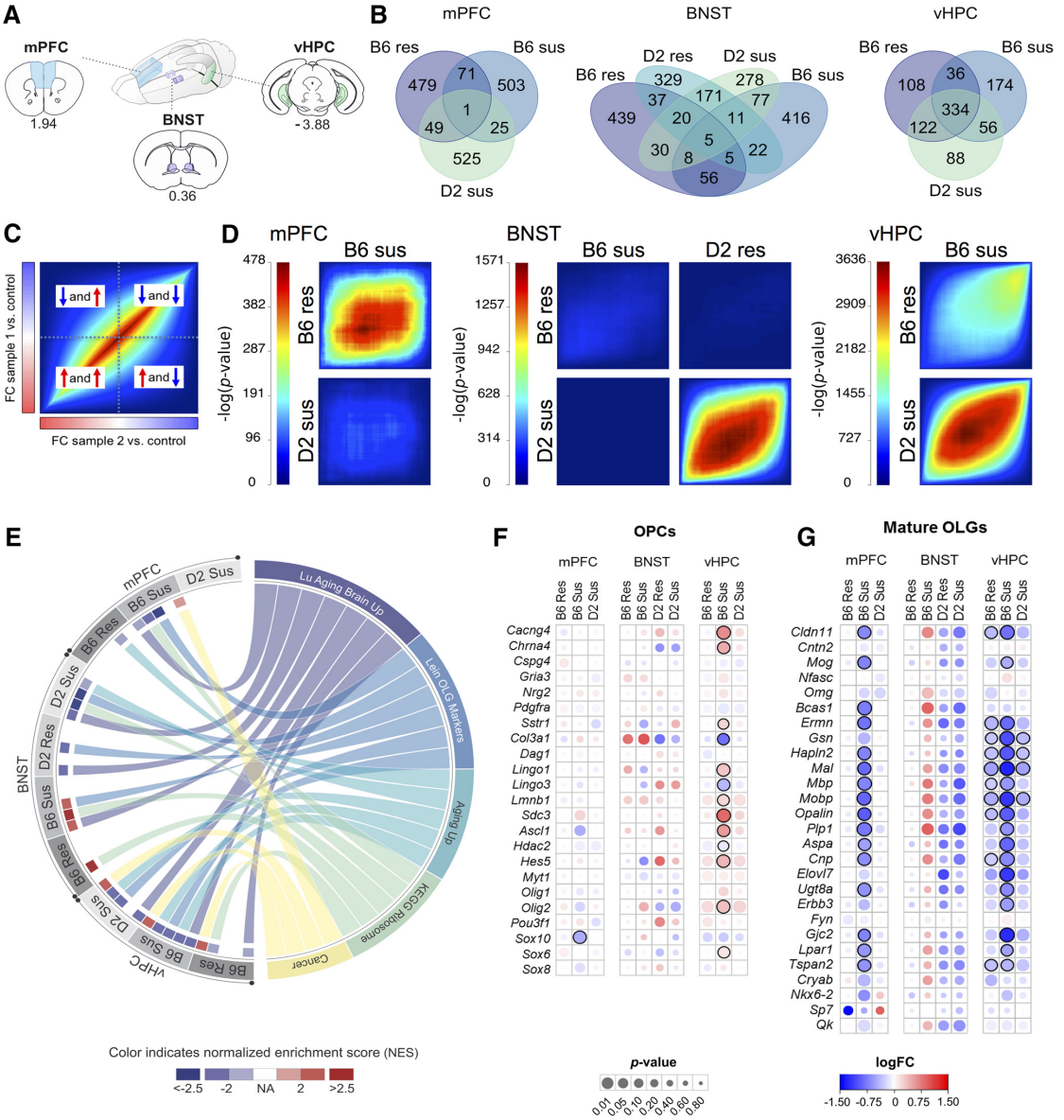

Figure 2. RNA-seq implicates OLG-related gene expression changes after CSDS. ***A***, Regions dissected for RNA-seq from D2 and B6 mice (for sample and RNA-seq details, see Extended Data Fig. 2-1). ***B***, Overlap of 300 top downregulated and 300 top upregulated genes between stressed and control mice, separately for each brain region (see Extended Data Fig. 2-2 for top 300 differentially expressed genes and Extended Data Fig. 2-3*A*,*B* for overlap separately for upregulated and downregulated genes). ***C***, Key to RRHO showing a hypothetical heatmap of two identical datasets ("FC sample 1 versus control" and "FC sample 2 versus control"). Following differential gene expression analysis, genes were ranked by their fold change (FC) and assigned to bins of 100 genes. Overlap of genes was then compared between each ranking matched bin of "sample 1 versus control" and "sample 2 versus control." Heatmap color represents the significance of the overlap [-log10(*p*)] of genes between bins. Thus significant *p* values in the bottom-left corner indicate that the two datasets have shared upregulated genes, significant *p* values in the top-right corner indicate shared downregulated genes, and significant *p* values in the middle indicate genes not differentially expressed or with small FC. Significant *p* values in the top-left or bottom-right corner represent genes regulated in opposite directions between the two datasets. ***D***, RRHO shows significant similarity in the gene expression response to CSDS between resilient and susceptible mice within strains (B6 mPFC and vHPC, D2 BNST) and between susceptible mice of B6 and D2 strains (vHPC). Scale bar = –log(*p*) of rank classes ($n = 100$), for

continued
each brain region separately. ***E***, Circos plot showing the top five enriched gene sets overlapping between the brain regions in stress-resilient and susceptible mice compared to controls. Only normalized enrichment scores (NESs) achieving significance ($p_{FDR} < 0.05$) are shown. A positive (or negative) NES for a given gene set indicates its overrepresentation at the top (or bottom, respectively) of the ranked list of upregulated (or downregulated, respectively) genes. See Extended Data Figures 2-4, 2-5 for GSEA and GO analyses, respectively; see Extended Data Figure 2-3*C* for expression FC for genes in the Lein OLG Markers gene set. ***F***, ***G***, Merged heat map showing the expression FC (logFC) and significance (*p*) of OPC-specific (***F***) and OLG-specific (***G***) genes. B6: C57BL/6NCrl strain; D2: DBA/2NCrl strain; Res: resilient; Sus: susceptible; mPFC: medial prefrontal cortex; BNST: bed nucleus of the stria terminalis; vHPC: ventral hippocampus; Lu Aging Brain Up: LU_AGING_BRAIN_UP; Lein OLG Markers: LEIN_OLIGODENDROCYTE-_MARKERS; Aging Up: DEMAGALHAES_AGING_UP; KEGG Ribosome: KEGG_RIBOSOME; Cancer: GINESTIER_BREAST_CANCER_ZNF217_AMPLIFIED_DN.

tible B6 and D2 mice shared 101 (9.2%) of the top genes. We detected the greatest overlap of the gene expression response between the strains in the vHPC, where B6- and D2 susceptible mice shared 390 (48.1%) of the top genes. Unlike in the mPFC or BNST, the stress effect was stronger than the strain effect in the vHPC. However, in the vHPC, several genes were downregulated both in the B6 susceptible and resilient mice.

To ask which biological pathways were affected by CSDS, we conducted GSEA and GO term enrichment analysis. GSEA showed significant enrichment of several gene sets (Extended Data Fig. 2-4), of which aging- and OLG-related sets were enriched in nearly all comparisons in all brain regions and both strains (Fig. 2*E*; Extended Data Fig. 2-3*C*). Although functionally diverse, the genes included in the aging-related gene sets were significantly overrepresented in the "Lein OLG Markers" gene set ($p_{FDR} = 1.2 \times 10^{-16}$). In accordance with GSEA, the most enriched GO terms were related to myelination and OLG development, in particular among the downregulated genes of B6 susceptible mice in the mPFC (Extended Data Fig. 2-5). These combined results from both enrichment analyses prompted us to further investigate OLG-related genes.

Mature OLGs develop from OPCs, which persist even in the adult brain as committed precursors. We asked whether either OPC or OLG cell populations dominantly contributed to the observed DE. The transcriptomic signature associated with CSDS was stronger in the mature OLG markers (Fig. 2*G*) than in the OPC markers (Fig. 2*F*). To validate the RNA-seq findings, we analyzed *Opalin*, *Ermn*, *Mobp*, *Plp1*, and *Mbp* gene expression levels with q-RT-PCR in mPFC, BNST, and vHPC and found high correlation with RNA-seq and q-RT-PCR measurements of these myelination-related genes (mean $r = 0.82$; Fig. 3).

Myelin-related variation after stress is not observed globally in the brain

To test whether differences in myelin-related gene expression were observed across the brain, we measured expression levels of *Opalin, Ermn, Mobp, Plp1*, and *Mbp* in the whole cortex (lacking the mPFC), hypothalamus, and dorsal hippocampus (dHPC) by q-RT-PCR. Using mixed ANOVA we determined that there was no significant main effect by the group (control, resilient or susceptible) on myelin-related gene expression in any of the brain regions of either strain. While *Opalin* expression was lower in D2 susceptible mice compared to controls in the hypothalamus as determined by *post hoc* comparison ($p = 0.006$), the expression levels of the other genes did not differ between the stressed and control mice in any region (Fig. 4*A–F*). We also measured the thickness of the corpus callosum in brain sections stained with a myelin-binding antibody (anti-CNPase) (Fig. 4*G*). We observed no differences in stress-susceptible or resilient mice compared to controls (Fig. 4*H*,*I*).

Myelin thickness and g ratio differ in brain region and genetic background-dependent manner

To determine whether CSDS affects myelination, we conducted TEM of myelinated axons in mPFC, BNST, and vHPC. In addition to analyzing axons of different diameters within each brain region and stress group together (Extended Data Fig. 5-2), we divided the axons to three size groups given that different types of neuronal projections may differ in axon diameter (Fig. 5; Extended Data Fig. 5-3). We discovered several brain region- and strain-specific differences between stress groups in g ratio, i.e., the ratio of the inner axonal diameter to the total outer diameter, myelin thickness, and axon diameter. Overall, D2 resilient mice had higher g ratio and thinner myelin in the mPFC compared to susceptible mice. B6 susceptible mice had thinner myelin in the vHPC compared to controls and thicker myelin in the BNST compared to resilient mice (Extended Data Fig. 5-2). In addition to these general findings, we found significant differences between stress susceptible or resilient mice compared to controls in axons of certain diameter (Fig. 5). We also observed modestly but significantly smaller axon diameter (without the myelin sheath) in the mPFC of D2 susceptible mice compared to controls (Extended Data Fig. 5-2).

Discussion

We established that the behavioral and brain transcriptomic responses to chronic psychosocial stress are genetically controlled. We discovered that BALB, 129, and D2 mice were more susceptible to chronic stress than B6 mice. We demonstrated, by unbiased RNA-seq, that after CSDS the most significantly affected gene sets and biological pathways in the mPFC, vHPC, and BNST were related to myelination. Consistently, we observed significant brain region and strain-dependent differences in myelin thickness after stress. Neither myelin gene expression in other cortical regions or the dHPC, nor corpus callosum thickness, differed between stressed and control mice, suggesting no overall white matter changes due to CSDS.

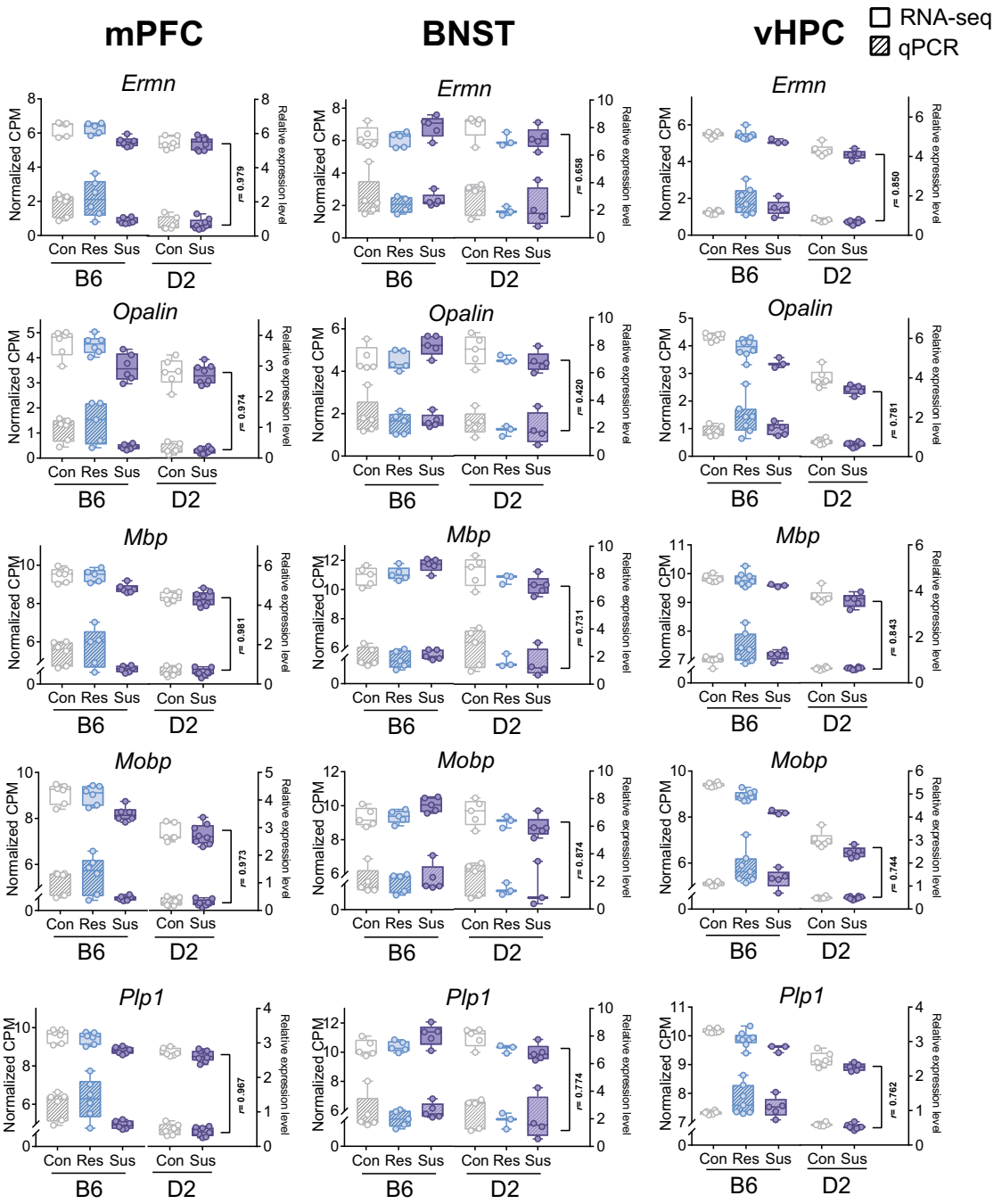

Figure 3. Strong correlation of gene expression levels of selected myelin-related genes determined by RNA-seq and q-RT-PCR. Box plots show the gene expression levels of five myelin-related genes (*Ermn*, *Opalin*, *Mbp*, *Mobp*, and *Plp1*) measured by RNA-seq (voom normalized number of reads, left *y*-axis, solid fill) and q-RT-PCR (right *y*-axis, striped fill). Pearson correlation coefficient (*r*) was calculated across the five (mPFC, vHPC) or six (BNST) group means. Box plots show distribution of values from min to max. mPFC: medial prefrontal cortex; vHPC: ventral hippocampus; BNST: bed nucleus of the stria terminalis; B6: C57BL/6NCrl: D2: DBA/2NCrl; Con: control; Res: resilient; Sus: susceptible.

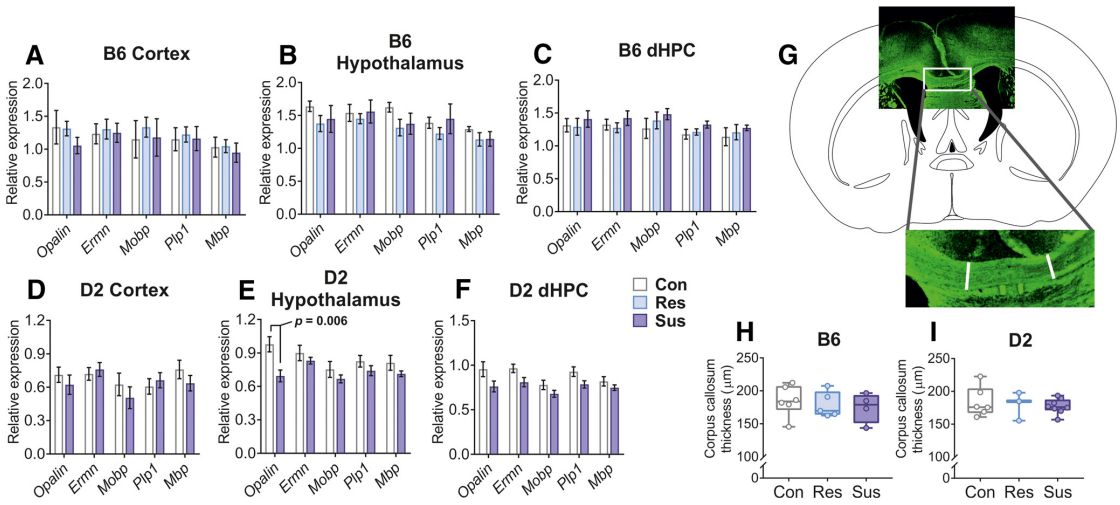

Figure 4. No generalized effects on OLG-related gene expression or corpus callosum thickness after CSDS. ***A–F***, Bar graphs showing the normalized expression levels of myelin-related genes in the hypothalamus and two brain regions not critically influenced by CSDS [cortex (without mPFC) and dHPC]. B6 and D2 mice were analyzed 6–8 d following CSDS. Myelin-related gene expression did not differ between phenotype groups in any of the brain regions of either strain. Only *Opalin* was expressed at a lower level in the hypothalamus of D2 susceptible mice compared to controls as shown by *post hoc* analysis. Mean ± 1 SEM is shown. ***G***, ***H***, CSDS does not affect corpus callosum thickness in B6 or D2 mice. Myelin visualized by anti-CNPase staining. Atlas outline modified from Franklin and Paxinos (2008); n = B6: Con = 6, Res = 5, Sus = 4; D2: Con = 6, Res = 3, Sus = 8. Error bars = min – max; D2: DBA/2NCrl strain; B6: C57BL/6NCrl strain; Con: control; Res: resilient; Sus: susceptible; dHPC: dorsal hippocampus.

We first established the CSDS paradigm in four inbred mouse strains and demonstrated that genetic factors control their adaptive behavior to stress. Consistently with prior findings (Razzoli et al., 2011a; Savignac et al., 2011), BALB mice were more sensitive to CSDS-induced SA than B6 mice. Additionally, innately anxious D2 and 129 mice were also highly susceptible to CSDS, suggesting that anxious strains may in general be stress-sensitive. CSDS did not affect locomotor activity of 129 or BALB mice, but both resilient and susceptible mice failed to gain weight during the defeat period. By contrast, the defeated D2 mice had lower locomotor activity than controls, and they lost weight during defeat. Differently to the other strains, the defeated B6 mice had lower locomotor activity compared to controls but they gained weight during defeat, similarly to controls. We also investigated other behaviors in this strain, and found that the stress-susceptible mice had increased anxiety-like behavior, but no difference in despair behavior, as in previous studies (Krishnan et al., 2007; Razzoli et al., 2011a). We acknowledge that due to limitations of our animal facility, all mice were brought into the experimental room together before behavioral testing, where they stayed behind a screen during the testing of other animals, possibly introducing confounding factors. Overall, our results suggest that the studied strains use different coping strategies to stress, and that such behavior has a strong genetic basis.

In addition to different behavioral responses to CSDS, we observed large differences in the brain transcriptomic response to stress between B6 and D2 strains. mPFC and BNST expression patterns were more similar within strains, between the resilient and susceptible mice, than between susceptible or resilient mice of different strains. However, in vHPC, the transcriptomic response of B6 and D2 susceptible mice was highly similar. This result may reflect the different organization and roles of these three brain regions in processing stress-related signals. It may be that the vHPC relays primary information regarding stress, while the BNST and mPFC may have more interpreting and processing roles, and therefore little genetic variation is tolerated within the hippocampal stress response. vHPC gene expression is influenced by glucocorticoids through glucocorticoid receptors, which are strongly expressed in the hippocampus (Ahima and Harlan, 1990; Ahima et al., 1991; Gray et al., 2017). BNST receives projections from several amygdalar nuclei and mediates anxiety-related information to hypothalamic and brainstem targets (Davis et al., 2010). The mPFC influences stress-associated social behavior by evaluation of perceived threats, top-down control of goal-directed behavior (Carlén, 2017), and emotion regulation (Etkin et al., 2015). These differences reflected on the transcriptomic response to stress may contribute to the distinct coping strategies of the strains.

We found significant enrichment of OLG- and aging-related genes within the differentially expressed genes in both strains and all brain regions. The highly significant overlap between both of these gene sets suggests similar changes in OLG-related gene expression may be associated with both aging and chronic psychosocial stress. This OLG-related signal was derived mostly from genes expressed in mature OLGs, which are the myelin-

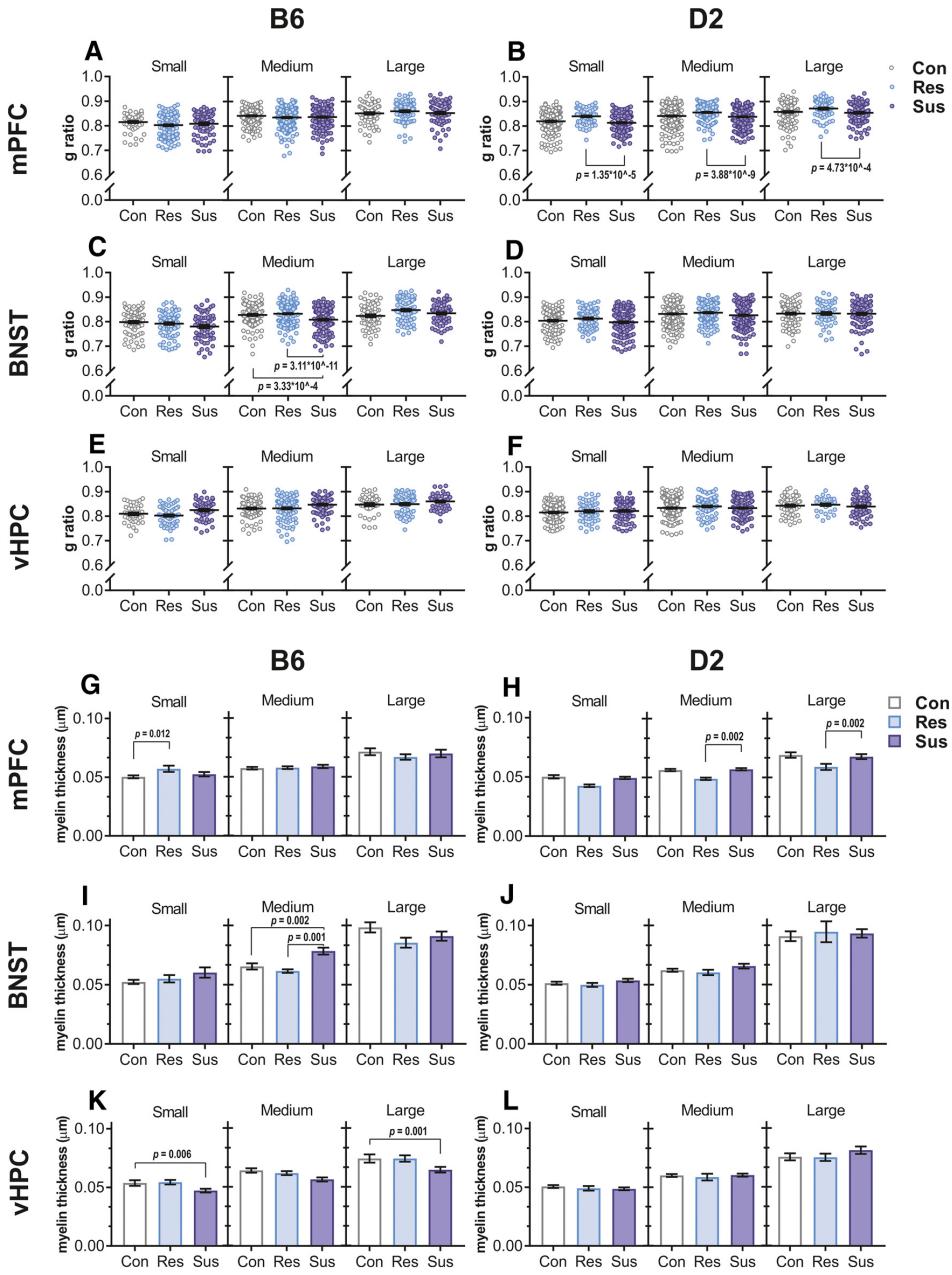

Figure 5. CSDS influences g ratio, myelin thickness, and axon diameter as measured by TEM. ***A–F***, Scatter plots of g ratio with mean indexed by a horizontal line. G ratio was lower in medium sized BNST axons of B6 susceptible mice compared to both control and resilient mice, and higher in all axon size categories in the mPFC of D2 resilient mice compared to susceptible mice. ***G–L***, Bar graphs of mean myelin thickness. Concurrently to g ratio measurements, B6 susceptible mice had thicker myelin on medium sized axons in the BNST compared to resilient or control mice, and D2 resilient mice had thinner myelin on medium and large axons in the mPFC compared to susceptible mice. Additionally, myelin was thicker in the small axons of the mPFC in B6 resilient mice compared to controls and thinner in the small and large axons of the vHPC in B6 susceptible mice compared to controls; n = B6: Con = 3, Res = 4, Sus = 3; D2: Con = 6, Res = 3, Sus = 5. Error bars ± 1 SEM. See Extended Data Figure 5-1 for schematics of dissected regions, Extended Data Figure 5-2 for analyses without division of axons into size categories, and Extended Data Figure 5-3 for size category division

continued

criteria. All nominal *p* values surviving Bonferroni correction are shown. D2: DBA/2NCrl; B6: C57BL/6NCrl; mPFC: medial prefrontal cortex; BNST: bed nucleus of the stria terminalis; vHPC: ventral hippocampus; Con: control; Res: resilient; Sus: susceptible.

producing cells in the central nervous system. Myelin plasticity, a response of OLGs to neuronal activity (Gautier et al., 2015; Koudelka et al., 2016; Purger et al., 2016; Mitew et al., 2018), is retained in adulthood (Bengtsson et al., 2005; McKenzie et al., 2014). Downregulation of OLG-related genes was especially pronounced in the vHPC, and also in the mPFC of B6 susceptible mice. On the structural level, vHPC myelin sheaths of B6 susceptible mice were thinner than in control mice, concurring with the downregulation of myelin-related genes. Interestingly, in the BNST, B6 susceptible mice had thicker myelin sheaths and smaller g ratio compared to both resilient and control mice, also concurring with the gene expression patterns. D2 susceptible mice had an opposite gene expression pattern in the BNST, which, however, was not supported by changes in myelin sheath thickness or g ratio. Opposite gene expression changes in different inbred mouse strains in response to stress have previously been observed in other models, but the underlying mechanisms are not fully understood (Mozhui et al., 2010; Malki et al., 2015). In mice, various stressors have diverse effects on myelination, likely reflecting involvement of distinct neural processes, developmental stage at the time of stress exposure, and duration of stress. Early life stress affects myelin-related gene expression in the mPFC (Bordner et al., 2011; Makinodan et al., 2012), and myelination of the amygdala (Ono et al., 2008). In adult mice, social isolation (Liu et al., 2012) and 14-d CSDS in susceptible mice (Lehmann et al., 2017) reduce myelin-related gene expression and myelination within the frontal cortex. Intermittent social defeat stress leads to reduced MBP-stained myelin area in the mPFC (Zhang et al., 2016). Corpus callosum myelination is decreased after chronic restraint stress (Choi et al., 2017). Also chronic variable stress induces temporally variable myelin-related gene expression changes, and these changes were regionally selective in the mPFC, nucleus accumbens, and corpus callosum (Liu et al., 2018). Therefore, it is likely that alterations in gene expression and physical parameters of the myelin sheaths occur dynamically over days and weeks (Montesinos et al., 2015; Almeida and Lyons, 2017), possibly explaining thicker myelin in B6 resilient mice in the mPFC, without differences in myelin-related gene expression compared to controls. Overall, our results concur with earlier studies and suggest that stress does not simply cause widespread downregulation of myelin-related genes or myelin loss, but that stress-influenced myelin-plasticity involves specific stress-associated brain circuits.

Our strategy to divide the stressed animals to susceptible and resilient groups allowed identification of specific patterns of myelination-related differences between these groups. We observed that chronic stress associates with thicker myelin in the susceptible (in the BNST of B6 mice) and thinner myelin in resilient mice (D2 mPFC). No prior studies exist, to our knowledge, on resilience-related myelin thinning. Although DTI measures are only considered proxies for myelination, in humans, baseline fractional anisotropy has been demonstrated to correlate positively with state anxiety, but following exposure to a traumatic event, correlation is negative (Sekiguchi et al., 2014). Furthermore, increased fractional anisotropy, suggestive of enhanced integrity, has been reported in the cingulate gray matter of panic disorder patients (Han et al., 2008). Also, the number of mature OLGs in the ventromedial PFC of depressed subjects with childhood abuse is increased (Tanti et al., 2017). Our results suggest that these complex patterns are strongly modulated by genetic factors.

Although myelination studies on human anxiety disorders and chronic stress are scarce, major depression has been consistently associated with white matter disruptions (Wang et al., 2014). Depressed suicide completers with childhood abuse have impaired myelin-related gene expression and reduced myelin thickness in the anterior cingulate cortex (Lutz et al., 2017). Interestingly, this effect was only seen in small caliber axons, similarly to our finding of mPFC myelin thickness being larger in B6 resilient mice compared to controls. Axons of different diameter may represent specific types of neurons (Perge et al., 2012) and therefore be differentially vulnerable to the effects of stress. For example, in the macaque cortex, axons which project longer distance from the point of origin have larger diameters than those projecting to proximal targets (Innocenti et al., 2014). Based on the axon diameters measured by TEM, it is not possible to infer the type of neurons affected in our experiment but this question could be addressed with immuno-electron microscopy.

How may structural changes in myelin affect behavior? Myelin thickness is a key component in determining axonal conduction speed, thereby influencing circuit function. Myelin deficient rats have altered conduction time and lower average synchrony levels in the cerebellum (Lang and Rosenbluth, 2003). Mice have increased synchronous activity between the vHPC and mPFC in an anxiogenic environment (Adhikari et al., 2010). Furthermore, in primates, increased power and phase synchrony in the theta range has been detected in the amygdala-prefrontal circuit during aversive conditioning (Taub et al., 2018). Altered synchrony has also been recorded in human psychiatric disorders (Schulman et al., 2011; Leuchter et al., 2015). Genetic factors affect synchronous oscillations during sleep in the inbred mouse strains (Franken et al., 1998; Tafti et al., 2003). The role of brain oscillations in myelination and psychiatric phenotypes are still poorly understood, but myelin plasticity may be a mechanism that allows regulation of axonal conduction and spatial connectivity.

Overall, our unbiased brain gene expression analysis suggests that myelin plasticity is among the most significant responses to chronic psychosocial stress. Our strategy to divide the mice into stress-susceptible and resilient

groups allowed us to demonstrate significant differences in myelination-related gene expression and myelin thickness between these groups. Furthermore, variable myelin plasticity across brain regions suggests that chronic stress has localized effects on myelination. Importantly, by using two different inbred mouse strains we demonstrated that stress-induced myelin plasticity is genetically controlled. Identification of the genetic regulators of the myelin response will provide mechanistic insight into the molecular basis of stress-induced anxiety, a critical step in developing targeted therapy for anxiety disorders.

References

Adhikari A, Topiwala MA, Gordon JA (2010) Synchronized activity between the ventral hippocampus and the medial prefrontal cortex during anxiety. Neuron 65:257–269. CrossRef Medline

Ahima RS, Harlan RE (1990) Charting of type II glucocorticoid receptor-like immunoreactivity in the rat central nervous system. Neuroscience 39:579–604. Medline

Ahima RS, Krozowski Z, Harlan R (1991) Type I corticosteroid receptor-like immunoreactivity in the rat CNS: distribution and regulation by corticosteroids. J Comp Neur 313:522–538. CrossRef Medline

Alexa A, Rahnenführer J, Lengauer T (2006) Improved scoring of functional groups from gene expression data by decorrelating GO graph structure. Bioinformatics 22:1600–1607. CrossRef Medline

Almeida RG, Lyons DA (2017) On myelinated axon plasticity and neuronal circuit formation and function. J Neurosci 37:10023–10034. CrossRef Medline

Anders S, Pyl PT, Huber W (2015) HTSeq–a Python framework to work with high-throughput sequencing data. Bioinformatics 31:166–169. CrossRef Medline

Avgustinovich DF, Kovalenko IL, Kudryavtseva NN (2005) A model of anxious depression: persistence of behavioral pathology. Neurosci Behav Physiol 35:917–924. CrossRef Medline

Bengtsson SL, Nagy Z, Skare S, Forsman L, Forssberg H, Ullén F (2005) Extensive piano practicing has regionally specific effects on white matter development. Nat Neurosci 8:1148–1150. CrossRef Medline

Benjamini Y, Hochberg Y (1995) Controlling the false discovery rate: a practical and powerful approach to multiple testing. J R Stat Soc Series B Stat Methodol 57:289–300.

Bordner KA, George ED, Carlyle BC, Duque A, Kitchen RR, Lam TT, Colangelo CM, Stone KL, Abbott TB, Mane SM, Nairn AC, Simen AA (2011) Functional genomic and proteomic analysis reveals disruption of myelin-related genes and translation in a mouse model of early life neglect. Front Psychiatry 2:18. CrossRef

Calhoon GG, Tye KM (2015) Resolving the neural circuits of anxiety. Nat Neurosci 18:1394–1404. CrossRef Medline

Carlén M (2017) What constitutes the prefrontal cortex? Science 358:478–482. CrossRef

Choi MH, Na JE, Yoon YR, Lee HJ, Yoon S, Rhyu IJ, Baik JH (2017) Role of dopamine D2 receptor in stress-induced myelin loss. Sci Rep 7:11654. CrossRef Medline

Davis M, Walker DL, Miles L, Grillon C (2010) Phasic vs sustained fear in rats and humans: role of the extended amygdala in fear vs anxiety. Neuropsychopharmacology 35:105–135. CrossRef Medline

Dobin A, Davis CA, Schlesinger F, Drenkow J, Zaleski C, Jha S, Batut P, Chaisson M, Gingeras TR (2013) STAR: ultrafast universal RNA-seq aligner. Bioinformatics 29:15–21. CrossRef Medline

Donner J, Sipilä T, Ripatti S, Kananen L, Chen X, Kendler KS, Lönnqvist J, Pirkola S, Hettema JM, Hovatta I (2012) Support for involvement of glutamate decarboxylase 1 and neuropeptide Y in anxiety susceptibility. Am J Med Genet B Neuropsychiatr Genet 159B:316–327. CrossRef Medline

Ducottet C, Belzung C (2005) Correlations between behaviours in the elevated plus-maze and sensitivity to unpredictable subchronic mild stress: evidence from inbred strains of mice. Behav Brain Res 156:153–162. CrossRef Medline

Etkin A, Büchel C, Gross JJ (2015) The neural bases of emotion regulation. Nat Rev Neurosci 16:693–700. CrossRef Medline

Franken P, Malafosse A, Tafti M (1998) Genetic variation in EEG activity during sleep in inbred mice. Am J Physiol 275:R1127–R1137. Medline

Franklin KBJ, Paxinos G (2008) The mouse brain in stereotaxic coordinates, Ed 3. New York, NY: Academic Press.

Garakani A, Murrough JW, Charney JD, Bremner JD (2009) The neurobiology of anxiety disorders. In: Neurobiology of mental illness, Ed 4 (Charney DS, Sklar P, Buxbaum J, Nestler EJ, eds), pp 655–690. Oxford; New York: Oxford University Press.

Gautier HO, Evans KA, Volbracht K, James R, Sitnikov S, Lundgaard I, James F, Lao-Peregrin C, Reynolds R, Franklin RJ, Káradóttir RT (2015) Neuronal activity regulates remyelination via glutamate signalling to oligodendrocyte progenitors. Nat Commun 6:8518. CrossRef Medline

Gentleman R, Carey V, Huber W, Hahne F (2017) Genefilter: methods for filtering genes from high-throughput experiments. R package version 1.60.0.

Golden SA, Covington HE 3rd, Berton O, Russo SJ (2011) A standardized protocol for repeated social defeat stress in mice. Nat Protoc 6:1183–1191. CrossRef

Gray JD, Kogan JF, Marrocco J, McEwen BS (2017) Genomic and epigenomic mechanisms of glucocorticoids in the brain. Nat Rev Endocrinol 13:661–673. CrossRef Medline

Haarman BC, Riemersma-Van der Lek RF, Burger H, Netkova M, Drexhage RC, Bootsman F, Mesman E, Hillegers MH, Spijker AT, Hoencamp E, Drexhage HA, Nolen WA (2014) Relationship between clinical features and inflammation-related monocyte gene expression in bipolar disorder - towards a better understanding of psychoimmunological interactions. Bipolar Disord 16:137–150. CrossRef Medline

Hammels C, Pishva E, De Vry J, van den Hove DL, Prickaerts J, van Winkel R, Selten JP, Lesch KP, Daskalakis NP, Steinbusch HW, van Os J, Kenis G, Rutten BP (2015) Defeat stress in rodents: from behavior to molecules. Neurosci Biobehav Rev 59:111–140. CrossRef Medline

Han DH, Renshaw PF, Dager SR, Chung A, Hwang J, Daniels MA, Lee YS, Lyoo IK (2008) Altered cingulate white matter connectivity in panic disorder patients. J Psychiatr Res 42:399–407. CrossRef Medline

Han MH, Nestler EJ (2017) Neural substrates of depression and resilience. Neurotherapeutics 14:677–686. CrossRef Medline

Hanley JA, Negassa A, Edwardes MD, Forrester JE (2003) Statistical analysis of correlated data using generalized estimating equations: an orientation. Am J Epidemiol 157:364–375. Medline

Hettema JM, Neale MC, Kendler KS (2001) A review and meta-analysis of the genetic epidemiology of anxiety disorders. Am J Psychiatry 158:1568–1578. CrossRef Medline

Hovatta I, Barlow C (2008) Molecular genetics of anxiety in mice and men. Ann Med 40:92–109. CrossRef Medline

Hovatta I, Tennant RS, Helton R, Marr RA, Singer O, Redwine JM, Ellison JA, Schadt EE, Verma IM, Lockhart DJ, Barlow C (2005) Glyoxalase 1 and glutathione reductase 1 regulate anxiety in mice. Nature 438:662–666. CrossRef Medline

Howlett JR, Stein MB (2016) Prevention of trauma and stressor-related disorders: a review. Neuropsychopharmacology 41:357–369. CrossRef Medline

Innocenti GM, Vercelli A, Caminiti R (2014) The diameter of cortical axons depends both on the area of origin and target. Cereb Cortex 24:2178–2188. CrossRef Medline

Johnson WE, Li C, Rabinovic A (2007) Adjusting batch effects in microarray expression data using empirical Bayes methods. Biostatistics 8:118–127. CrossRef Medline

Kemeny ME, Schedlowski M (2007) Understanding the interaction between psychosocial stress and immune-related diseases: a

stepwise progression. Brain Behav Immun 21:1009–1018. CrossRef Medline
Koudelka S, Voas MG, Almeida RG, Baraban M, Soetaert J, Meyer MP, Talbot WS, Lyons DA (2016) Individual neuronal subtypes exhibit diversity in CNS myelination mediated by synaptic vesicle release. Curr Biol 26:1447–1455. CrossRef Medline
Krishnan V, Han MH, Graham DL, Berton O, Renthal W, Russo SJ, Laplant Q, Graham A, Lutter M, Lagace DC, Ghose S, Reister R, Tannous P, Green TA, Neve RL, Chakravarty S, Kumar A, Eisch AJ, Self DW, Lee FS, et al. (2007) Molecular adaptations underlying susceptibility and resistance to social defeat in brain reward regions. Cell 131:391–404. CrossRef Medline
Krzywinski M, Schein J, Birol I, Connors J, Gascoyne R, Horsman D, Jones SJ, Marra MA (2009) Circos: an information aesthetic for comparative genomics. Genome Res 19:1639–1645. CrossRef
Laine MA, Sokolowska E, Dudek M, Callan SA, Hyytiä P, Hovatta I (2017) Brain activation induced by chronic psychosocial stress in mice. Sci Rep 7:15061. CrossRef Medline
Lang EJ, Rosenbluth J (2003) Role of myelination in the development of a uniform olivocerebellar conduction time. J Neurophysiol 89: 2259–2270. CrossRef Medline
Law CW, Chen Y, Shi W, Smyth GK (2014) voom: precision weights unlock linear model analysis tools for RNA-seq read counts. Genome Biol 15:R29. CrossRef Medline
Lehmann ML, Weigel TK, Elkahloun AG, Herkenham M (2017) Chronic social defeat reduces myelination in the mouse medial prefrontal cortex. Sci Rep 7:46548. CrossRef Medline
Leuchter AF, Hunter AM, Krantz DE, Cook IA (2015) Rhythms and blues: modulation of oscillatory synchrony and the mechanism of action of antidepressant treatments. Ann NY Acad Sci 1344:78–91. CrossRef Medline
Liu J, Dietz K, DeLoyht JM, Pedre X, Kelkar D, Kaur J, Vialou V, Lobo MK, Dietz DM, Nestler EJ, Dupree J, Casaccia P (2012) Impaired adult myelination in the prefrontal cortex of socially isolated mice. Nat Neurosci 15:1621–1623. CrossRef Medline
Liu J, Dietz K, Hodes GE, Russo SJ, Casaccia P (2018) Widespread transcriptional alternations in oligodendrocytes in the adult mouse brain following chronic stress. Dev Neurobiol 78:152–162. CrossRef Medline
Lutz PE, Tanti A, Gasecka A, Barnett-Burns S, Kim JJ, Zhou Y, Chen GG, Wakid M, Shaw M, Almeida D, Chay MA, Yang J, Larivière V, M'Boutchou MN, van Kempen LC, Yerko V, Prud'homme J, Davoli MA, Vaillancourt K, Théroux JF, et al. (2017) Association of a history of child abuse with impaired myelination in the anterior cingulate cortex: convergent epigenetic, transcriptional, and morphological evidence. Am J Psychiatry 174:1185–1194. CrossRef Medline
Makinodan M, Rosen KM, Ito S, Corfas G (2012) A critical period for social experience-dependent oligodendrocyte maturation and myelination. Science 337:1357–1360. CrossRef Medline
Malki K, Mineur YS, Tosto MG, Campbell J, Karia P, Jumabhoy I, Sluyter F, Crusio WE, Schalkwyk LC (2015) Pervasive and opposing effects of unpredictable chronic mild stress (UCMS) on hippocampal gene expression in BALB/cJ and C57BL/6J mouse strains. BMC Genomics 16:262. CrossRef Medline
Marques S, Zeisel A, Codeluppi S, van Bruggen D, Mendanha Falcão A, Xiao L, Li H, Häring M, Hochgerner H, Romanov RA, Gyllborg D, Muñoz Manchado A, La Manno G, Lönnerberg P, Floriddia EM, Rezayee F, Ernfors P, Arenas E, Hjerling-Leffler J, et al. (2016) Oligodendrocyte heterogeneity in the mouse juvenile and adult central nervous system. Science 352:1326–1329. CrossRef Medline
McKenzie IA, Ohayon D, Li H, de Faria JP, Emery B, Tohyama K, Richardson WD (2014) Motor skill learning requires active central myelination. Science 346:318–322. CrossRef Medline
Millstein RA, Holmes A (2007) Effects of repeated maternal separation on anxiety- and depression-related phenotypes in different mouse strains. Neurosci Biobehav Rev 31:3–17. CrossRef Medline
Mitew S, Gobius I, Fenlon LR, McDougall SJ, Hawkes D, Xing YL, Bujalka H, Gundlach AL, Richards LJ, Kilpatrick TJ, Merson TD, Emery B (2018) Pharmacogenetic stimulation of neuronal activity increases myelination in an axon-specific manner. Nat Commun 9:306. CrossRef
Moffitt TE, Caspi A, Harrington H, Milne BJ, Melchior M, Goldberg D, Poulton R (2007) Generalized anxiety disorder and depression: childhood risk factors in a birth cohort followed to age 32. Psychol Med 37:441–452. CrossRef
Montesinos J, Pascual M, Pla A, Maldonado C, Rodríguez-Arias M, Miñarro J, Guerri C (2015) TLR4 elimination prevents synaptic and myelin alterations and long-term cognitive dysfunctions in adolescent mice with intermittent ethanol treatment. Brain Behav Immun 45:233–244. CrossRef Medline
Mootha VK, Lindgren CM, Eriksson KF, Subramanian A, Sihag S, Lehar J, Puigserver P, Carlsson E, Ridderstråle M, Laurila E, Houstis N, Daly MJ, Patterson N, Mesirov JP, Golub TR, Tamayo P, Spiegelman B, Lander ES, Hirschhorn JN, Altshuler D, et al. (2003) PGC-1alpha-responsive genes involved in oxidative phosphorylation are coordinately downregulated in human diabetes. Nat Genet 34:267–273. CrossRef Medline
Mozhui K, Karlsson RM, Kash TL, Ihne J, Norcross M, Patel S, Farrell MR, Hill EE, Graybeal C, Martin KP, Camp M, Fitzgerald PJ, Ciobanu DC, Sprengel R, Mishina M, Wellman CL, Winder DG, Williams RW, Holmes A (2010) Strain differences in stress responsivity are associated with divergent amygdala gene expression and glutamate-mediated neuronal excitability. J Neurosci 30: 5357–5367. CrossRef Medline
Nasca C, Bigio B, Zelli D, Nicoletti F, McEwen BS (2015) Mind the gap: glucocorticoids modulate hippocampal glutamate tone underlying individual differences in stress susceptibility. Mol Psychiatry 20:755–763. CrossRef Medline
Ono M, Kikusui T, Sasaki N, Ichikawa M, Mori Y, Murakami-Murofushi K (2008) Early weaning induces anxiety and precocious myelination in the anterior part of the basolateral amygdala of male Balb/c mice. Neuroscience 156:1103–1110. CrossRef Medline
Perge JA, Niven JE, Mugnaini E, Balasubramanian V, Sterling P (2012) Why do axons differ in caliber? J Neurosci 32:626–638. CrossRef Medline
Phipson B, Lee S, Majewski IJ, Alexander WS, Smyth GK (2016) Robust hyperparameter estimation protects against hypervariable genes and improves power to detect differential expression. Ann Appl Stat 10:946–963. CrossRef Medline
Plaisier SB, Taschereau R, Wong JA, Graeber TG (2010) Rank-rank hypergeometric overlap: identification of statistically significant overlap between gene-expression signatures. Nucleic Acids Res 38:e169. CrossRef Medline
Purger D, Gibson EM, Monje M (2016) Myelin plasticity in the central nervous system. Neuropharmacology 110:563–573. CrossRef Medline
Razzoli M, Carboni L, Andreoli M, Ballottari A, Arban R (2011a) Different susceptibility to social defeat stress of BalbC and C57BL6/J mice. Behav Brain Res 216:100–108. CrossRef
Razzoli M, Carboni L, Andreoli M, Michielin F, Ballottari A, Arban R (2011b) Strain-specific outcomes of repeated social defeat and chronic fluoxetine treatment in the mouse. Pharmacol Biochem Behav 97:566–576. CrossRef
Ritchie ME, Phipson B, Wu D, Hu Y, Law CW, Shi W, Smyth GK (2015) limma powers differential expression analyses for RNA-sequencing and microarray studies. Nucleic Acids Res 43:e47. CrossRef Medline
Savignac HM, Finger BC, Pizzo RC, O'Leary OF, Dinan TG, Cryan JF (2011) Increased sensitivity to the effects of chronic social defeat stress in an innately anxious mouse strain. Neuroscience 192:524–536. CrossRef
Schulman JJ, Cancro R, Lowe S, Lu F, Walton KD, Llinás RR (2011) Imaging of thalamocortical dysrhythmia in neuropsychiatry. Front Hum Neurosci 5:69. CrossRef Medline
Sekiguchi A, Sugiura M, Taki Y, Kotozaki Y, Nouchi R, Takeuchi H, Araki T, Hanawa S, Nakagawa S, Miyauchi CM, Sakuma A, Kawashima R (2014) White matter microstructural changes as vul-

nerability factors and acquired signs of post-earthquake distress. PLoS One 9:e83967. CrossRef Medline

Sittig LJ, Carbonetto P, Engel KA, Krauss KS, Barrios-Camacho CM, Palmer AA (2016) Genetic background limits generalizability of genotype-phenotype relationships. Neuron 91:1253–1259. CrossRef Medline

Smoller JW (2016) The genetics of stress-related disorders: PTSD, depression, and anxiety disorders. Neuropsychopharmacology 41:297–319. CrossRef Medline

Subramanian A, Tamayo P, Mootha VK, Mukherjee S, Ebert BL, Gillette MA, Paulovich A, Pomeroy SL, Golub TR, Lander ES, Mesirov JP (2005) Gene set enrichment analysis: a knowledge-based approach for interpreting genome-wide expression profiles. Proc Natl Acad Sci USA 102:15545–15550. CrossRef Medline

Tafti M, Petit B, Chollet D, Neidhart E, de Bilbao F, Kiss JZ, Wood PA, Franken P (2003) Deficiency in short-chain fatty acid beta-oxidation affects theta oscillations during sleep. Nat Genet 34: 320–325. CrossRef Medline

Tanti A, Kim JJ, Wakid M, Davoli MA, Turecki G, Mechawar N (2017) Child abuse associates with an imbalance of oligodendrocyte-lineage cells in ventromedial prefrontal white matter. Mol Psychiatry Advance online publication. Retrieved November 21, 2017. doi:10.1038/mp.2017.231.

Taub AH, Perets R, Kahana E, Paz R (2018) Oscillations synchronize amygdala-to-prefrontal primate circuits during aversive learning. Neuron 97:291–298.e3. CrossRef

Threadgill DW, Dlugosz AA, Hansen LA, Tennenbaum T, Lichti U, Yee D, LaMantia C, Mourton T, Herrup K, Harris RC, et al. (1995) Targeted disruption of mouse EGF receptor: effect of genetic background on mutant phenotype. Science 269:230–234. Medline

Tovote P, Fadok JP, Lüthi A (2015) Neuronal circuits for fear and anxiety. Nat Rev Neurosci 16:317–331. CrossRef Medline

Wang L, Leonards CO, Sterzer P, Ebinger M (2014) White matter lesions and depression: a systematic review and meta-analysis. J Psychiatr Res 56:56–64. CrossRef Medline

Vialou V, Bagot RC, Cahill ME, Ferguson D, Robison AJ, Dietz DM, Fallon B, Mazei-Robison M, Ku SM, Harrigan E, Winstanley CA, Joshi T, Feng J, Berton O, Nestler EJ (2014) Prefrontal cortical circuit for depression- and anxiety-related behaviors mediated by cholecystokinin: role of ΔFosB. J Neurosci 34:3878–3887. CrossRef Medline

Wittchen HU, Jacobi F, Rehm J, Gustavsson A, Svensson M, Jönsson B, Olesen J, Allgulander C, Alonso J, Faravelli C, Fratiglioni L, Jennum P, Lieb R, Maercker A, van Os J, Preisig M, Salvador-Carulla L, Simon R, Steinhausen HC (2011) The size and burden of mental disorders and other disorders of the brain in Europe 2010. Eur Neuropsychopharmacol 21:655–679. CrossRef Medline

Xiao Y, Hsiao TH, Suresh U, Chen HI, Wu X, Wolf SE, Chen Y (2014) A novel significance score for gene selection and ranking. Bioinformatics 30:801–807. CrossRef Medline

Young MD, Wakefield MJ, Smyth GK, Oshlack A (2010) Gene ontology analysis for RNA-seq: accounting for selection bias. Genome Biol 11:R14. CrossRef Medline

Zhang H, Yan G, Xu H, Fang Z, Zhang J, Zhang J, Wu R, Kong J, Huang Q (2016) The recovery trajectory of adolescent social defeat stress-induced behavioral (1)H-MRS metabolites and myelin changes in Balb/c mice. Sci Rep 6:27906. CrossRef Medline

Zhang Y, Chen K, Sloan SA, Bennett ML, Scholze AR, O'Keeffe S, Phatnani HP, Guarnieri P, Caneda C, Ruderisch N, Deng S, Liddelow SA, Zhang C, Daneman R, Maniatis T, Barres BA, Wu JQ (2014) An RNA-sequencing transcriptome and splicing database of glia, neurons, and vascular cells of the cerebral cortex. J Neurosci 34:11929–11947. CrossRef

Differential gene expression response of oligodendrocytes and myelin to chronic psychosocial stress in C57BL/6NCrl and DBA/2NCrl mice

Laine MA[1,2,3,4], Trontti K[1,2,3,4], Gigliotta A[1,2,3,4], Saarnio S[3], Paranko B[3], Kulesskaya N[3], & Hovatta I[1,2,3,4].

1 SleepWell Research Program, Faculty of Medicine, University of Helsinki, Finland
2 Department of Psychology and Logopedics, Faculty of Medicine, University of Helsinki, Finland
3 Molecular and Integrative Biosciences Research Program, University of Helsinki, Finland
4 Neuroscience Center, Helsinki Institute of Life Sciences (HiLIFE), University of Helsinki, Finland

Abstract

Chronic stress is a common life experience that predisposes to many health problems, such as anxiety disorders. Myelin plasticity has recently been associated with the mammalian response to chronic stress. However, it remains unknown which biological pathways stress influences in the myelin-producing cells (oligodendrocytes, OLGs). Here we used the chronic social defeat stress (CSDS) paradigm as a murine model of chronic psychosocial stress. We used mice from two inbred strains (C57BL/6NCrl and DBA/2NCrl) to investigate the effects of genetic background on stress responses. Following CSDS-exposure mice can be classified as stress-susceptible (lower social interest than non-stressed controls) or -resilient (similar social behavior to controls). We used magnetic-activated cell sorting (MACS) to enrich OLGs and myelin from the medial prefrontal cortex (mPFC) of resilient, susceptible and control mice. The OLG and myelin transcriptomes differed significantly; 20 % of detected genes were enriched in OLGs while 25 % were enriched in myelin. These patterns were largely similar between the two strains; 64 % of the OLG-enriched and 71 % of the myelin-enriched genes were shared between strains. To investigate the stress effect, we compared resilient and susceptible mice to their same-strain controls and each other. We found unique patterns of CSDS-associated differential expression in OLGs and myelin. For example, genes encoding myelin components (*Mbp, Mobp*) were downregulated in the myelin fraction of B6 susceptible mice, and in the OLG fraction of D2 resilient and susceptible mice compared to controls. Using the Ingenuity Pathway Analysis we discovered TCF7L2 to be a predicted inhibited upstream regulator in susceptible mice from B6 and D2 strains, and in D2 resilient mice. Among its predicted targets were several myelin component genes, such as *Mbp* and *Mobp*, which were downregulated in the aforementioned comparisons. To conclude, in addition to OLGs and myelin having non-identical gene expression patterns, they responded differently to stress, possibly converging on effects on the myelin sheath via expression of its target components. Furthermore, our data suggest TCF7L2 as an upstream regulator of the differentially expressed genes.

Introduction

Myelin plasticity refers to adjustments to the properties of myelin sheaths, such as their thickness, length or quantity, occurring in response to changing environmental demands (Almeida & Lyons, 2017; Etxeberria et al., 2016; Gibson et al., 2014). It has been suggested to play a critical role in learning in mammals (Bengtsson et al., 2005; McKenzie et al., 2014), but also in maladaptive processes such as social isolation stress (Liu et al., 2012; Makinodan, Rosen, Ito, & Corfas, 2012). We showed recently that myelin-related genes are strongly differentially expressed in mice after chronic social defeat stress (CSDS), an extensively validated model of chronic psychosocial stress in mice. This effect was also dependent on the genetic background of the mice, and on whether they were stress-susceptible (i.e. showed lower social interest than same-strain controls) or –resilient (showed similar social interest as controls). Susceptible mice of the C57BL/6NCrl (B6) strain had lower expression levels than controls of genes encoding myelin components, such as *Mbp*, *Mobp* and *Plp1*, in the medial prefrontal cortex (mPFC) and ventral hippocampus (vHPC), while susceptible mice from DBA/2NCrl (D2) did not. Additionally, myelin gene expression levels were higher in B6 susceptible compared to controls in the bed nucleus of stria terminalis (BNST), a region critically involved in anxiety-like and risk assessment behavior. Corpus callosum thickness or myelin gene expression in the rest of the cortex and dorsal hippocampus did not differ after CSDS. These findings suggest that stress susceptibility is not associated with global de- or hypomyelination, but rather with specific adaptations within key stress-related neural circuits, consistent with the notion of myelin plasticity (Laine et al., 2018).

Also other studies using CSDS have shown differences in myelin-related features in stressed rodents compared to controls. For example, stress-exposed Balb/c and B6 mice have smaller myelin basic protein (MBP) stained area in the mPFC compared to controls (Lehmann, Weigel, Elkahloun, & Herkenham, 2017; H. Zhang et al., 2016). MBP is a highly abundant myelin protein localising to the myelin sheath, and it is used as a proxy for the amount of myelin influenced by both the number of sheaths and their thickness. Cathomas et al. (Cathomas et al., 2019) reported that CSDS reduced myelin gene expression in the mPFC and amygdala, but the numbers of oligodendrocytes (OLGs), the myelin-producing cells in the CNS, remained unchanged by stress. Social isolation in both juvenile and adult mice associates with thinner myelin sheaths and lower expression of myelin-related genes in the mPFC (Liu et al., 2012; Liu, Dietz, Hodes, Russo, & Casaccia, 2018; Makinodan et al., 2012). Another chronic stressor, chronic unpredictable stress, results in lower abundance of MBP and OLIG2 proteins in the rat hippocampus, and this feature was at least partially restored by physical exercise (Tang et al., 2019). Thus, several converging lines of evidence associate myelin, particularly on the level of gene expression, with maladaptive consequences of stress.

Understanding how stress interacts with adult myelin is relevant for several chronic stress-related psychiatric disorders, such as anxiety disorders. Anxiety disorders are a heterogeneous diagnostic class characterized by pervasive and disproportionate worry and agitation, which may occur either generally

(generalized anxiety disorder), in response to specific stimuli (specific phobias) or in specific circumstances (social anxiety disorder). Both genetic factors and chronic psychosocial stress play a role in disorder etiology, but their interaction is particularly important (Hoppen & Chalder, 2018). They often manifest in adolescents and young adults (Kessler, Ruscio, Shear, & Wittchen, 2010), an age at which the myelination of cortical grey matter is still ongoing (Kwon, Pfefferbaum, Sullivan, & Pohl, 2020).

A key open question is whether and how stress impacts the functions of OLGs and myelin. Oligodendrocytes make use of both cell-type specific transcriptional programmes (such as maturation and myelin production) and non-specific programmes (such as Wnt/beta-catenin pathways, (Feigenson, Reid, See, Crenshaw, & Grinspan, 2009). Furthermore, the myelin compartment, while being an extension of the OLG, has a distinct proteome (Ishii et al., 2009) and transcriptome (Thakurela et al., 2016) produced at least in part by selective transport of mRNAs to the distal parts of the membrane for local translation (Torvund-Jensen, Steengaard, Askebjerg, Kjaer-Sorensen, & Laursen, 2018). Resolving if and how these fractions are impacted by stress is optimally done in a system that allows their separation, such as magnetic activated cell sorting (MACS).

We hypothesized that chronic psychosocial stress influences gene expression of OLG lineage cells and transport of transcripts to the myelin compartment of the OLGs. We set to test this hypothesis in the mPFC, a brain region that regulates anxiety and where we previously identified myelin-related changes after CSDS (Laine et al., 2018). To assess the effect of the genetic background on gene expression, we used mice from two inbred strains; B6 and D2. These strains differ in both innate anxiety-like behavior and response to stress (Hovatta et al., 2005; Laine et al., 2018). Additionally, to understand the differences between OLG and myelin fraction gene expression patterns, we compared them in non-stressed control mice. To this end, we carried out RNA-seq of enriched OLG lineage cells and myelin. Using bioinformatic analyses, we also identified potential upstream regulators of genes differentially expressed in susceptible and resilient mice compared to controls.

Materials and Methods

Chronic social defeat stress

Animal procedures were approved by the Regional State Administration Agency for Southern Finland (ESAVI/3119/04.10.07/2017) and carried out in accordance to directive 2010/63/EU of the European Parliament and Council, and the Finnish Act on the Protection of Animals Used for Science or Educational Purposes (497/2013). Throughout the experiment mice had ad libitum access to standard rodent chow and filtered tap water [except during the physical interaction phase of chronic social defeat stress (CSDS)]. Cages were outfitted with aspen chip bedding (Tapvei Oy, Harjumaa, Estonia) and standard environmental enrichment items (one aspen brick and a nest of aspen strips, both from Tapvei Oy). Bedding and enrichment items were changed weekly, except for during 10 day CSDS/control

housing. The animal housing facility was temperature (22 ±2 °C) and humidity (50 ±15 %) controlled, with a 12 h light/dark cycle (lights on 0600 – 1800).

Male mice [6 weeks old, C57BL/6NCrl (B6) and DBA/2NCrl (D2) strains, Charles River, Sulzfeld, Germany] were subjected to CSDS according to standard procedures (Golden, Covington, Berton, & Russo, 2011; Laine et al., 2018) for 10 consecutive days following a 10-day acclimatization period at the laboratory animal facility (group housed 4-6 mice/cage). Briefly, at the end of the light phase, mice were introduced into a cage containing a resident CD1 male mouse [Clr-CD1 (Charles River), aged 13-26 weeks, screened for appropriate levels of aggressive behaviour] for a maximum of 10 min physical contact, and housed in an adjacent compartment of the same cage for 24 h (separated by a perforated Plexiglass wall). The physical contact phase was terminated before 10 min had elapsed if the mice incurred visible wounds, and all wounds were treated with antiseptic cooling spray (Dermacool, Virbac, Carros, France). Each day for 10 days the mice were introduced to a novel resident aggressor mouse. The mean durations of physical contact were 464 s for B6 mice and 266.3 s for D2 (no differences between resilient and susceptible mice within either strain, Student's *t*-test, Supplementary Figure 1). Control mice were handled daily and housed in similar divided cages, but always with another control mouse on the other side, switching cage-mates daily but with no physical contact phases.

Twenty-four hours after the last day of CSDS, and the start of the dark phase, we performed the social avoidance test to determine the phenotype (resilient/susceptible to stress) of each defeated mouse. The mice were first allowed to explore an arena (42 x 42 cm) containing an empty perforated Plexiglass cylinder for 150 s (no-target trial). We placed the mice back into their home cages while the cylinder in the arena was replaced with one containing an unfamiliar CD-1 male mouse as a social target. The mice were then placed back into the arena for 150 s (target trial). The time spent in an interaction zone (IZ) around the circumference of the cylinder when there was a social target was divided by the time spent in the IZ when the cylinder was empty. Multiplying this score by 100 produces the social interaction (SI) ratio.

Based on previous experiments (Laine et al., 2018), we define as susceptible those mice which, after exposure to CSDS, had SI ratios below a boundary defined as the strain-specific control mean score minus 1 standard deviation. The boundary score for B6 mice is 76.49, and the boundary score for D2 mice is 105.99. All other mice were defined as resilient. Two defeated mice from the D2 strain and one from the B6 strain did not have SI ratios due to making no entries into the interaction zone (IZ) during the trial without a social target. However, these mice spent considerable time in the IZ during the social target trial, comparably to their strain-specific resilient mice, and were thus phenotyped as resilient (Supplementary Figure 1).

Following the SA test all mice were housed in single cages until dissection.

The weights of the mice were monitored throughout the experiment. Firstly, allocation to control or CSDS condition was counterbalanced for weight, with each group-housed cage contributing at least 1 mouse to each condition and overall weight distributions between conditions maintained equal. Mice were also weighed on the 2nd, 4th, 6th, 8th and 10th day of CSDS/control housing, 1 day after the SA test, and on the day of dissection (Supplementary Figure 1). One mouse (D2) was euthanized and excluded from analyses due to loss of weight > 15 % from the first measurement.

For all experiments, mice were dissected 6-8 days following the last session of defeat. Mice were counterbalanced across phenotypes and strains on the dissection days, and on each day all dissections were done in the morning (8 am – 12 pm) to reduce circadian effects on gene expression differences.

Dissociation and magnetic sorting (MACS) of oligodendrocytes and myelin

Mice were anaesthetized with a lethal dose of pentobarbital and perfused with +4 °C sterile 0.9 % NaCl. We removed the brain and dissected the medial prefrontal cortex (mPFC) on ice using anatomical coordinates defined previously (Laine et al., 2018). Cells were dissociated using the Papain Dissociation System (Worthington Biochemical Corporation, cat.no. LK003150) according to the manufacturer's instructions. Briefly, tissue pieces were incubated in 37 °C under constant agitation in a mixture containing papain for 45-90 minutes. Cells were suspended and washed after an inhibitor containing DNase was added to stop the papain reaction, after which the cells were maintained at 4 °C in Dulbecco's PBS (ThermoFisher Scientific, cat. no. 14287080).

We then performed phase separation of cells and myelin using a debris removal solution (Miltenyi Biotec, cat.no. 130-109-398). The debris phase (containing myelin) was separated from the cell phase (containing OLGs), and incubated with anti-myelin (Miltenyi Biotec, cat. no. 130-104-257) or anti-O4 (Miltenyi Biotec, cat. no. 130-094-543) microbeads respectively, according to the manufacturer's instructions. We used the octoMACS (Miltenyi Biotec) system to positively select the labelled myelin or OLGs, which were immediately lysed by vortexing in RLT lysis buffer (RNeasy Plus Micro kit, Qiagen) and stored in -20 °C until RNA extraction.

RNA extraction

We extracted total RNA from the OLG and myelin samples using the RNeasy Plus Micro kit (Qiagen), protocol for Purification of total RNA Containing Small RNAs from Cells (Appendix D). Genomic DNA was removed using a spin column containing DNase. Extracted samples were run with the 2100 Bioanalyzer Instrument with RNA 6000 Pico kit (Agilent) to estimate yield. RNA yields varied between 13-18 ng (OLG) and 4.5-11 ng (myelin). The whole amount of RNA was used for either digital droplet PCR (ddPCR) or RNA sequencing library preparation (see below).

Digital droplet PCR

To validate the enrichment of the isolated OLGs and myelin fractions, we performed digital droplet PCR (ddPCR,) using isolated OLGs, isolated myelin, bulk mPFC tissue and bulk mouse heart tissue. We synthesised cDNA using the iScript™ cDNA Synthesis Kit (BioRad). 20 µl cDNA was diluted in 30 µl water and 5.5 µl of the dilution was used for each ddPCR reaction. We used the QX200™ ddPCR™ EvaGreen® Supermix combined with QX200 AutoDG Droplet Digital PCR System (both BioRad) to perform ddPCR. Primer concentrations were 250 nM and annealing temperature 60 °C. The following primer sequences were used (5'-3'): *Sst* (forward: CCACCGGGAAACAGGAACTG, reverse: TTGCTGGGTTCGAGTTGGC, PrimerBank ID: 6678034c1 (Spandidos, Wang, Wang, & Seed, 2010)), *Gfap* (forward: CGGAGACGCATCACCTCTG, reverse: AGGGAGTGGAGGAGTCATTCG, PrimerBank ID: 30692526a1), *Ugt8a* (forward: AGAGGCGCTCTCCAACT, reverse: TTCCAACAGCACTCCACAGG), and *Mbp* (forward: ACACACGAGAACTACCCATTATGG, reverse: AGAAATGGACTACTGGGTTTTCATCT). *Ppib* was used for normalization (forward: GGAGATGGCACAGGAGGAAA, reverse: CCCGTAGTGCTTCAGCTTGAA).

Library preparation and RNA-Sequencing

RNA-seq libraries for mRNA were prepared with Ovation SoLo RNA-Seq Systems kit (NuGEN, CA, USA) and with TruSeq Small RNA Library Preparation kit (Illumina) for miRNA from 35 myelin samples and 35 OLG samples, collected from the same mice (B6: control n = 6, resilient n = 6, susceptible n = 6; D2: control n = 6, resilient n = 5, susceptible n = 6). Samples were selected based on RNA quality and balancing the number from each group. mRNA libraries were sequenced with NextSeq 500 (Illumina, USA), in five runs containing both strains and cell fractions and all three phenotypes mixed, and one NextSeq 500 round for the miRNAs. Sequence quality was controlled by FastQC (www.bioinformatics.babraham.ac.uk/projects/fastqc/). For mRNA-seq, we removed PCR duplicates based on combination of the read and the unique molecule identifier (UMI) sequences using PRINSEQ (Schmieder & Edwards, 2011). Unique Molecular Identifiers (UMIs) and 3'-adapter contamination were trimmed using FASTX-Toolkit (http://hannonlab.cshl.edu/fastx_toolkit), and low-complexity reads were removed (dust value < 25 using PRINSEQ). For miRNA-sequencing, we trimmed 3'-adapters from reads and kept reads matching with known miRNA sizes (17-32 bp; miRBase v21 (Kozomara & Griffiths-Jones, 2014). Two samples (mRNA D2 control, OLG fraction; miRNA B6 resilient, myelin fraction) were excluded due to failed library preparation, as revealed by QC.

Differential expression analysis

We aligned the RNA-seq reads to the mmu10 genome with STAR version 2.5.3a (Dobin et al., 2013) and annotated alignments to exons (GTF version 85) using HTSeq version 0.7.2 (Anders, Pyl, & Huber, 2014). For miRNA-seq, we aligned the 17-32 bp reads to the mmu10 genome using miRDeep2 mapper.pl script (Friedlander et al., 2008).

We used the limma R package (Law, Chen, Shi, & Smyth, 2014; Phipson, Lee, Majewski, Alexander, & Smyth, 2016; Ritchie et al., 2015) to determine differential gene expression between groups within the OLG or myelin cell fraction. We first filtered expression count matrices for low abundance genes, requiring 1 CPM in at least 6 samples, normalized gene counts with the voom package included in limma, and adjusted data for library sets with ComBat (Leek, Johnson, Parker, Jaffe, & Storey, 2012). Pairwise gene expression differences were analyzed using eBayes (Johnson, Li, & Rabinovic, 2007) between same-strain resilient, susceptible, and control mice.

In addition, we used Rank Rank Hypergeometric Overlap (RRHO; (Plaisier, Taschereau, Wong, & Graeber, 2010) to compare transcriptome level similarities of OLG and myelin fractions in controls, and between resilient, susceptible and control mice within strains. RRHO identifies significantly overlapping genes across two DE result lists after genes are ranked into bins by DE (-log10(p)*logFC) between comparisons. Gene bin sizes of 50 or 5 genes were used to bin RNAs or miRNAs respectively. The same -log(p) scale was applied to comparisons within OLG and myelin fractions.

Pathway analysis

We used the Ingenuity Pathway Analysis software (IPA v. 01-12, July 2019 release; Qiagen, Hilden, Germany (Kramer, Green, Pollard, & Tugendreich, 2014) to determine functional pathways of gene expression differences in OLG and myelin fractions. Focus was placed on predicted upstream regulators, as these molecules are positioned to mediate the effects of CSDS on gene expression and the behavioural response. Input DEGs were filtered by average expression level to restrict the analyses to robustly expressed genes (limma-normalized log2 counts > 0). Because of the exploratory nature of this analysis, nominal $p < 0.05$ was used as the significance criterion for selecting genes for pathway analysis, in addition to logFC > |0.25|. Analyses were limited to interactions reported for "Nervous System" under "Tissues".

Supplementary material

The supplementary materials referred to in this manuscript can be accessed online (https://tinyurl.com/StudyIIISupplements, password: myeliniscool) until the publication of this data in a peer-reviewed journal, at which point all relevant supplements will be accessible through the journal's website.

Results

Enrichment of OLGs and myelin from CSDS-exposed and control mice

To identify biological pathways from mPFC OLGs and myelin affected by chronic stress we exposed mice from B6 and D2 strains to CSDS (Figure 1 A). After the 10-day stress period, we measured the social avoidance behavior of non-stressed controls and the stressed mice to distribute the stress-exposed mice into stress-resilient or susceptible groups (Figure 1 B).

To enrich OLG and myelin from the mPFC we performed magnetic-activated cell sorting (MACS), and extracted total RNA from these samples. On a test cohort (n = 4 mice) we first used ddPCR to quantify the expression level of neuronal (*Sst*), astrocytic (*Gfap*) and OLG-specific (*Mbp* and *Ugt8a*) genes. Neuronal and astrocytic marker genes were significantly depleted while OLG markers were enriched in OLG and myelin fractions compared to bulk mPFC and mouse heart tissue as a non-CNS control (Supplementary Figure 2). We then conducted RNA-seq and miRNA-seq of enriched myelin and OLG total RNA from CSDS-exposed and control mice. By comparing the expression levels of marker genes of different brain cell types in our previously published bulk mPFC tissue RNA-seq dataset, we observed enrichment of OLG- (*Cnp*, *Mag*, *Mbp*, *Mobp* and *Olig2*) and OPC-specific genes (*Cspg4*, *Pdgfra*, *Cacng4* and *Sdc3*) in the MACS enriched fractions (Figure 1 D). In contrast, markers for microglia (*Aif1*, *Cd68*, *Cd11b* and *Trem2*), astrocytes (*Gfap*, *Aqp4*, *Slc4a4* and *Aldh1l1*) and neurons (*Syp*, *Map2*, *Nefl*, *Gad2*) had lower expression levels in the MACS fractions than in bulk tissue.

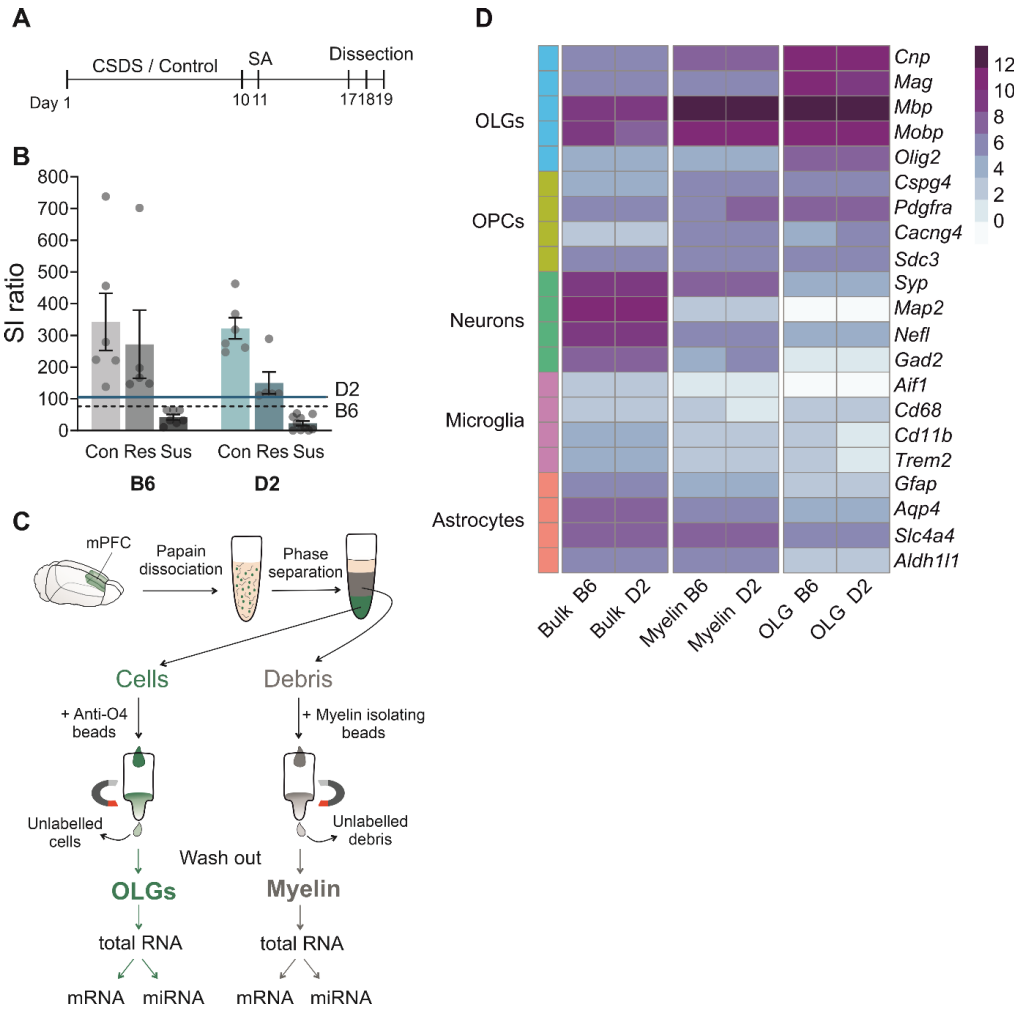

Figure 1. Demonstration of behavioral and MACS procedures. A) Timeline of experimental procedure. Each vertical line represents one day. **B)** Social interaction (SI) ratios of B6 and D2 mice. Cut-off lines for susceptibility illustrated by a dashed black line for B6 and a solid blue line for D2 strains. Data points represent individual animals. **C)** Illustration of the enrichment of OLGs and myelin using the MACS procedure. **D)** Heatmap showing the expression levels of marker genes for myelin, OPCs, newly formed and myelinating OLGs, neurons, microglia and astrocytes (Bennett et al., 2016; Cahoy et al., 2008; Y. Zhang et al., 2014) in the mPFC (bulk tissue) of the B6 and D2 strains compared with OLG and myelin fractions enriched by MACS. Legend = (normalized) logCPM. CSDS = chronic social defeat stress, SA = social avoidance test, SI = social interaction, B6 = C57BL/6NCrl, D2 = DBA/2NCrl, mPFC = medial prefrontal cortex, OLGs = oligodendrocytes, MACS = magnetic activated cell sorting. LogCPM = Log counts per million.

OLG and myelin gene expression patterns differ from each other but are highly similar between the two strains

To investigate how genetic background influences the OLG and myelin transcriptomes in the mPFC, we compared their RNA and miRNA expression profiles from non-stressed control mice from the two strains (B6 and D2). We first quantified the similarity of RNA and miRNA expression patterns of the OLG and myelin fractions within the strains. We found that, averaged between the two strains, 20.2 % of all detected RNAs (18205) and 14.3 % of all detected miRNAs (856) were expressed at a significantly higher levels in OLGs than in myelin ($p_{adj} \leq 0.05$, referred to as OLG-enriched genes). In myelin, 24.8 % and 18.8 % of all detected RNAs and of miRNAs, respectively, were expressed at a significantly higher level than in OLGs (referred to as myelin-enriched genes). A correlation matrix showing the Euclidean distance of the top 50 % most abundant RNAs and miRNAs between fractions revealed a clear clustering of the OLG and myelin fractions that was independent from the strain (Figure 2 A-B).

To further investigate the similarities of the OLG and myelin gene expression patterns between strains, we conducted Rank Rank Hypergeometric Overlap (RRHO) analysis based on B6 OLG vs myelin and D2 OLG vs myelin comparisons. This analysis enables the direct comparison of two lists of differentially expressed genes (DEGs) to visualize their similarities (Figure 2 C). RRHO analysis of DEGs in B6 OLG vs myelin and D2 OLG vs myelin comparisons revealed a high correlation of ranked genes with the highest *p*-values following the diagonal of the plot. We observed more significant *p*-values in the upper right corner of the RRHO plot, suggesting that the myelin transcriptomes were more similar between strains than the OLG transcriptomes (Figure 2 C). Identical analysis of miRNAs revealed a substantial transcriptomic resemblance between fractions, and that the myelin fraction had more overlap between strains than the OLG fraction (Figure 2 D).

To analyse how the similarities of the OLG and myelin transcriptomes are influenced by genetic background, we calculated the number of OLG- and myelin-enriched genes shared between the strains (Figure 2 E, Supplementary Table 1). 70.6 % of the myelin-enriched (3637) and 63.5 % of the OLG-enriched (2734) genes were shared between strains. The non-shared proportion in the enriched genes are still present in OLGs and myelin but do not show a significant enrichment in one or the other. We also found enriched miRNAs to be shared to a greater extent in myelin compared to OLGs, with 88.5 % (145) and 65.0 % (76) of them shared in myelin and OLG, respectively (Figure 2 F, Supplementary Table 1). We also performed RNA and miRNA DE analysis in B6 myelin vs D2 myelin and B6 OLG vs D2 OLG comparisons in non-stressed animals. We found a small number of genes DE in myelin and OLG between strains (115 in myelin, 372 in OLGs). Similarly, only 15 miRNAs were DE between strains in myelin and 19 were DE in OLGs (Supplementary Table 2).

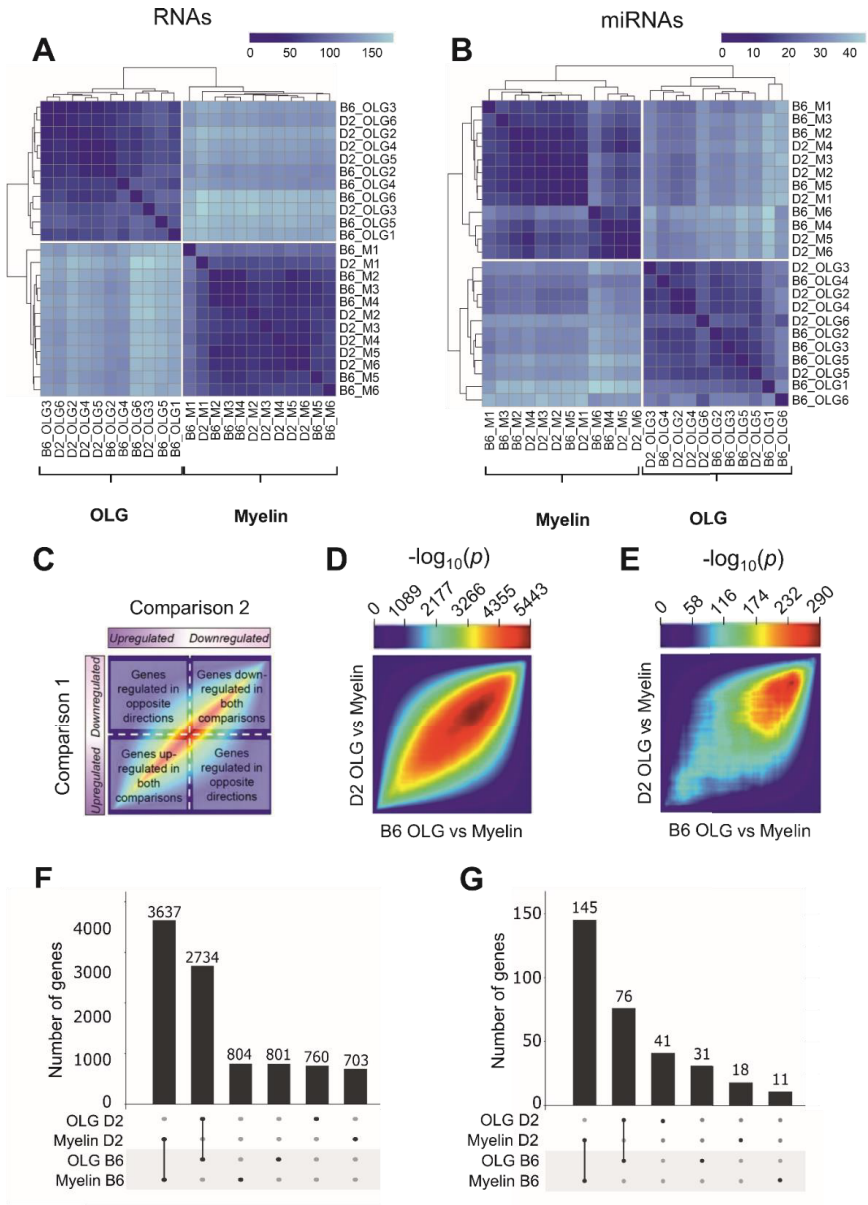

Figure 2. OLGs and myelin have distinct gene expression patterns that are largely shared between the two inbred strains. A-B) Correlation matrix and dendrogram showing the Euclidean distance between the top 50 % of expressed OLG and myelin RNAs (A) and miRNAs (B) in non-stressed D2 and B6 mice. Darker color indicates stronger correlation. **C)** Key to RRHO showing a theoretical heatmap of two identical datasets ("Comparison 1 and Comparison 2"). Genes are ranked into bins by differential expression (-log10(p)*logFC) after differential gene expression analysis. The significance of the overlap -$\log_{10}(p)$ between gene bins is showed by the heatmap color. P values in the top right corner and bottom left corner refer to genes that are differentially expressed (DE) in the same direction in both comparisons (down- or upregulated, respectively). P values located in the top left and bottom right corner represent genes that are DE in opposite directions. **D-E)** RRHO following differential gene expression analysis between OLG and myelin fractions in non-stressed D2 and B6 mice for RNAs (D)

and miRNAs (E). Genes were ranked by their fold change and assigned to bins of 50 (RNAs) or 5 (miRNAs). Overlap of genes was then compared between each ranking matched bin. Color represents the significance of the overlap [-log10(p)] of genes between rank-matched bins. High -log10(p) values in the bottom-left quadrant indicate that the two datasets have shared OLG-enriched genes, high -log10(p)-values in the top-right quadrant indicate shared myelin-enriched genes, and high -log10(p)-values in the center indicate genes not DE or with small FC. The top-left and bottom-right quadrants represent genes regulated in opposite directions between the two datasets. **F-G)** Upset plots of the DE ($p_{adj} \leq 0.05$) RNAs (F) and miRNAs (G). The number of DE genes in each comparison is shown on the right. The number of overlapping DE genes between two comparisons (connected by a black line) is represented by the histogram above. B6 = C57BL/6NCrl, D2 = DBA/2NCrl, OLGs = oligodendrocytes, RRHO = rank-rank hypergeometric overlap, DE = differentially expressed.

CSDS associates with different DEGs in OLGs and myelin

To investigate CSDS-associated gene expression differences we identified DEGs between susceptible and control, resilient and control, and susceptible and resilient mice in the OLG and myelin fractions. No gene expression difference reached statistical significance after correction for multiple comparisons (Benjamini-Hochberg). To conduct exploratory analyses of DEGs we used a threshold for nominal significance ($p \leq 0.05$) and fold change (logFC $\geq |0.25|$). Using these criteria, we observed the largest number of DEGs in the OLG fraction of B6 susceptible vs resilient mice (1406, 8.1 % of expressed genes, Figure 3 A, Supplementary Table 3). The comparison with the fewest DEGs was the myelin fraction of B6 resilient vs control mice (111, 0.7 % of expressed genes, Figure 3 A). To analyse the similarities between the transcriptomic response of susceptible and resilient mice between strains, we compared their DEG (susceptible/resilient vs control) overlap within myelin and OLG fractions using RRHO analysis (Figure 3 B-C). We also calculated the number of shared up- and down-regulated genes, as well as genes DE in opposite directions between resilient vs control and susceptible vs control comparisons between strains (Figure 3 D). Resilient vs control and susceptible vs control comparisons within B6 and D2 strains shared several up- and down-regulated genes in both OLG and myelin fractions, with more shared genes present in the OLG fraction (Figure 3 D left). The RRHO also revealed overlap between resilient and susceptible mice compared to the controls in both fractions. These findings suggest that a large number of the OLG and myelin DEGs responded generally to the stress exposure, irrespective of susceptibility or resilience. We observed a larger overlap of DEGs in the OLGs after stress in D2 resilient and susceptible mice compared to B6 resilient and susceptible mice Figure 3 B). The overlap patterns in the myelin fraction were more similar between the strains than the overlap in the OLG fraction (Figure 3 C), suggesting that genetic background may have less influence on the gene expression response to stress in myelin than in OLGs. Although the B6 OLG fraction showed the greatest number of shared DEGs between susceptible and resilient comparisons (Figure 3 D), the overlap between the whole transcriptomes in these comparisons was less significant (Figure 3 B) than in the myelin fraction (Figure 3 C). This indicates that outside the DEGs, B6 susceptible and resilient gene expression patterns are less similar in OLGs than myelin.

We also compared the B6 and D2 gene expression patterns within the same stress-response (for example B6 OLG resilient vs D2 OLG resilient, Figure 1 D middle). While there was some overlap between strains within a stress group (resilient or susceptible) and fraction, approximately half (31.5 – 87.1 %) of the shared DEGs were DE in opposite directions between the two strains. Similarly to the overlap within resilient or susceptible mice, most of the strain overlap was observed in the OLG fraction. In the RRHO plot there was very little detectable overlap between the ranks of all expressed genes between strains, indicating strain-specific gene expression patterns for resilience and susceptibility. Lastly, we compared the DEGs across fractions (e.g. B6 OLG resilient vs B6 myelin resilient) and found lower rates of overlap than in the other two comparison groups (Figure 1 D right). This suggests that the OLG and myelin genes respond rather differently to stress even within the same individual.

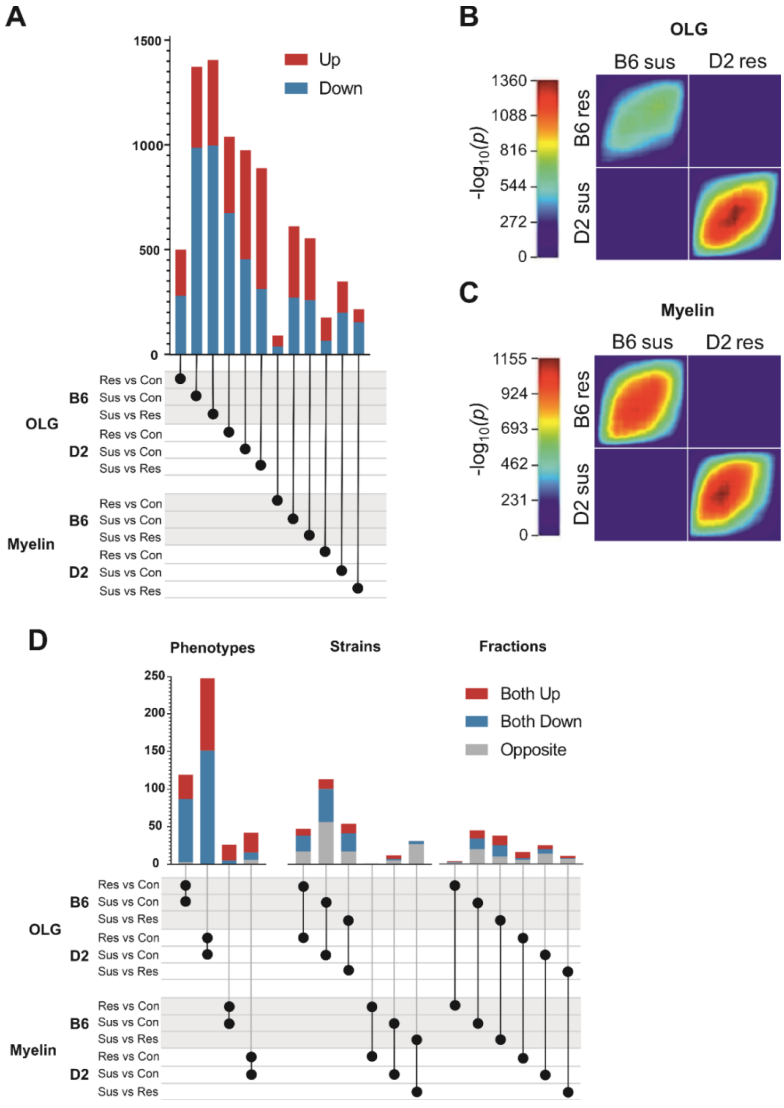

Figure 3. Distinct gene expression patterns in OLGs and myelin after CSDS. A) Bar graph depicting the number of DEGs ($p < 0.05$, logFC $\geq |0.25|$) within each comparison, showing the numbers of up- (red) and downregulated (blue) genes separately. **B-C)** RRHO analysis of OLG (B) and myelin (C) fractions within and across strains. Colour represents the significance of the overlap [-log10(p)] of genes between rank-matched bins. Bin size = 50. **D)** Upset plot depicting the overlap in DEGs between comparisons (indicated by dots connected by a black line). Red portions of the bars indicate genes which are upregulated in both comparisons, and blue portions indicate shared downregulated genes. Grey portions include genes which are DE in both comparisons but in opposite directions. CSDS = chronic social defeat stress, DEG = differentially expressed gene, B6 = C57BL/6NCrl, D2 = DBA/2NCrl, OLGs = oligodendrocytes, Con = control, Res = resilient, Sus = susceptible, DE = differentially expressed.

TCF7L2 predicted to regulate DEGs in B6 susceptible, D2 susceptible and D2 resilient mice

To explore whether CSDS-associated DEGs are over-represented in predicted targets of upstream regulators, we used Ingenuity Pathway Analysis (IPA). The five predicted regulators with the greatest absolute value of activation Z-score for each comparison are presented in Figure 4 A. TCF7L2 was predicted to be a significant upstream regulator in 4 out of 2 comparisons. Among the predicted targets of TCF7L2 are genes encoding myelin components (Supplementary Table 5). To examine the expression levels of other genes known to be involved in the differentiation, proliferation or maturation of OLGs, and in the production of the myelin sheath, we manually curated a list of genes and examined their expression levels (Figure 4 B). In the OLG fraction myelin component genes (*Mbp*, *Mobp*) were expressed on a lower level in both D2 resilient and susceptible mice, but not in the B6 mice compared to controls. On the contrary, these genes were expressed at a lower level in B6 susceptible mice compared to B6 resilient mice in the myelin fraction.

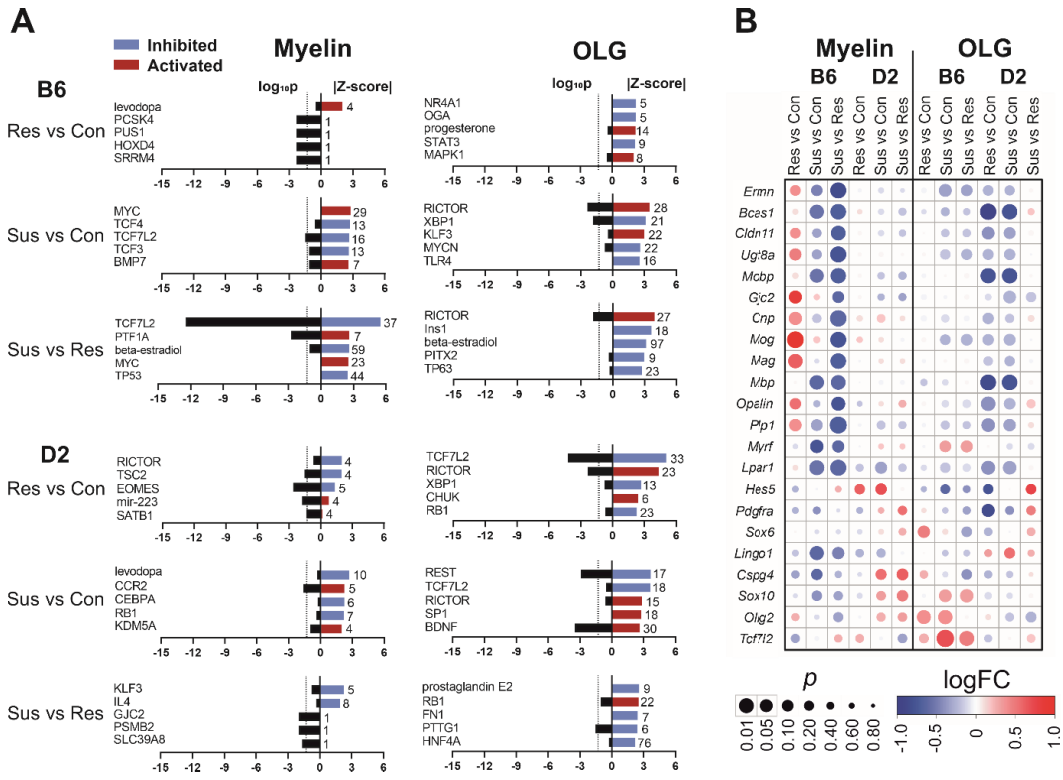

Figure 4. Ingenuity Pathway Analysis predicts TCF7L2 as a major upstream regulator of differentially expressed genes (DEGs) in several comparisons. A) Bar graphs showing $\log_{10}(p)$ and activation Z-score of the top 5 predicted upstream regulators (ranked by Z-score) of observed DEGs in each comparison. Comparisons within the myelin and the OLG fractions are shown separately. Z-scores are plotted as absolute values, with color indicating predicted up- (red) or downregulation (blue). The number of predicted target DEGs within the comparison is given for each regulator on the right of the bar plot. Dotted line indicates threshold for nominal significance ($p = 0.05$). **B)** Bubble plot showing differential expression of manually selected genes encoding myelin components, OPC proliferation, and OLG differentiation/maturation. The size of each bubble indicates significance of differential expression, and color denotes logFC. DEG = differentially expressed gene, OLG = oligodendrocyte, OPC = oligodendrocyte progenitor cell, B6 = C57BL/6NCrl, D2 = DBA/2NCrl, Con = control, Res = resilient, Sus = susceptible

Discussion

How chronic stress influences OLGs specifically has become a major question since the influx of studies associating myelin-related gene expression changes in bulk tissue RNA-sequencing with stress in mice (Cathomas et al., 2019; Laine et al., 2018; Liu et al., 2018). Here, we extended our previous work by enriching the OLG and myelin fractions from the mPFC after CSDS in two inbred mouse strains to study specifically OLG-related stress response. We first investigated the extent to which the OLG and myelin transcriptomes differ from each other. We found that both the OLG and myelin fractions had genes which were expressed on a significantly higher level compared to the other fraction. The two mouse strains were more similar to each other than the two cellular fractions were to one another. Regarding the stress effect, we observed a larger number of DEGs in resilient and susceptible mice compared to same-strain controls in the OLGs than in myelin, and largely unique DEGs in the two fractions of the same comparisons. Among the DEGs in four comparisons (B6 susceptible vs control and vs resilient in the myelin fraction, D2 susceptible vs control and resilient vs control in the OLG fraction) we found lower expression levels of several myelin component genes. IPA predicted TCF7L2 as an upstream regulator of these genes.

Overall the vast majority of the detected genes were expressed in both OLG and myelin fractions. The 20 - 25 % of expressed genes which were significantly more abundant in one fraction over the other are of interest because they may be related to biological mechanisms with local regulation. Prior work has described the myelin transcriptome in comparison to bulk tissue (Thakurela et al., 2016), but a comparison to the transcripts in OLGs is needed to infer selective localisation. Genes enriched in the myelin fraction may be ones selected by the transport machinery, known to depend on recognition of the 3' untranslated region (UTR) and an RNA transport signal sequence (Ainger et al., 1997; Torvund-Jensen et al., 2018). Analysis of the genomic elements of the myelin-enriched genes we identified here may further elucidate how this machinery selects transcripts for transport, and functional *in situ* analyses of specific mRNAs and miRNAs could reveal new biological processes important for the myelin sheath. For example, *Adcyap1* was enriched in the myelin fraction of both B6 and D2 mice. In humans, a polymorphism within an estrogen response element sequence in this gene (encoding the protein PACAP) associates with PTSD symptoms in females (Ressler et al., 2011). This gene is also highly expressed in neurons (Y. Zhang et al., 2014). *In situ* hybridization and *in vitro* experiments would be required to validate its expression and function in myelin, as axonal contamination in MACS-enriched myelin is possible. The two strains compared here also showed highly similar profiles of myelin and OLG gene enrichment. This suggests that the transport machinery targets the same transcripts largely independent of genetic background.

We found that myelin component genes (such as *Mbp* and *Mobp*) were downregulated in the myelin fraction of B6 stress susceptible mice compared to resilient and control mice, but in the OLG fraction of D2 resilient and susceptible mice compared to controls. In our previous bulk RNA-seq experiment

we showed lower expression level of myelin component genes in B6 susceptible compared to control mice, but no differences within the D2 strain (Laine et al., 2018). This could suggest that bulk tissue RNA-seq lacks resolution to detect differences occurring only within the cell bodies of relatively low-abundance cell types such as OLGs (Valerio-Gomes, Guimaraes, Szczupak, & Lent, 2018), but captures effects taking place in the larger area of the myelin sheath. Observing the same genes DE in different fractions in the two strains suggests the existence of alternate ways of stress influencing myelin component transcripts; one occurring at the cell body (mediated, for example, by transcription factors) and another affecting the transport of transcripts or their local regulation. Exploring these possibilities could be done using selective perturbation of transcription- and transport-related cellular mechanisms, such as DNA-binding of key transcription factors or RNA-binding of key ribonucleoproteins (Hoek, Kidd, Carson, & Smith, 1998) respectively. This finding also highlights the importance of considering different genetic backgrounds in preclinical studies. A greater understanding of how genetic factors influence processes by which stress alters myelin gene expression will be needed for development of personalised treatments for stress-related diseases.

Furthermore, particularly in the D2 strain OLG fraction, many of the DEGs in susceptible vs control and resilient vs control comparisons were shared. This shared proportion of the response represents a general effect by stress, rather than effects differentiating resilient and susceptible mice from each other. To best utilize preclinical data for development of treatments for stress-related disorders, it is critical to understand which components are related to the maladaptive response, which ones to the adaptive resilience response, and which ones relate to both (Russo, Murrough, Han, Charney, & Nestler, 2012). Optimal treatment strategies are likely those which either rescue susceptible-specific changes or promote resilience-related changes. Targeting a shared pathway, such as myelin-related genes in the D2 strain, may not produce a therapeutic response, because resilience is evidently achievable without changes in this pathway. Much of our knowledge about resilience comes from rodent work (Murrough & Russo, 2019; Russo et al., 2012), although human psychobiological (Feder, Fred-Torres, Southwick, & Charney, 2019) and genetic (Elbau, Cruceanu, & Binder, 2019) factors have also been described. However, our findings suggest that resilience, in addition to being an individual difference factor, is influenced by individual differences such as genetic background. While behaviorally similar, the neurobiological path to resilience is different in our two strains, suggesting a genetic influence on which factors provide the adaptive response to stress.

Our bioinformatic analysis predicted that inhibited activity of transcription factor TCF7L2 could be responsible for downregulation of several genes, including myelin component genes, in B6 susceptible, D2 susceptible and D2 resilient mice compared to their respective controls. TCF7L2 is expressed across many CNS cell types (Y. Zhang et al., 2014) and is a binding partner of β-catenin, an effector protein in the Wnt signalling pathway (Bem et al., 2019; Ye et al., 2009). Genetic variants in the *TCF7L2* gene have been associated with several psychiatric conditions, including schizophrenia and bipolar disorder

(Bem et al., 2019). Heterozygous knock-out of the mouse homolog *Tcf7l2* is anxiogenic. *Tcf7l2*$^{+/-}$ mice had lower locomotor activity, spent less time in the center zone of the open field test (OFT) and the light area of the light-dark test (LD), and had higher rates of freezing in measurements of both contextual and cued fear conditioning compared to wildtype mice. Overexpression of *Tcf7l2* did not alter the behavior of the mice on the OFT or LD (Savic et al., 2011). However, haploinsufficiency of *Tcf7l2* in different inbred strains and sexes produces highly variable effects on the forced swim test, suggesting that genetic background critically influences its function (Sittig et al., 2016). These studies perturbed *Tcf7l2* expression across all CNS cell types, so linking the findings to its function in OLGs is not directly possible. OLG lineage-specific knock-out of *Tcf7l2* or its DNA-binding domain has produced variable results, with reports of both reduced expression of myelin component genes in some (Hammond et al., 2015; Zhao et al., 2016) and promotion of OLG differentiation in other publications (Weng, Ding, Fan, Cao, & Lu, 2017). To our knowledge no OLG-specific KO studies have assessed behavioral effects. The mixed findings concerning myelination may stem in part from the developmental stage-specific actions of TCF7L2. In vitro, it has been shown to preferentially bind with co-activator Kaiso in immature and with SOX10 in maturing OLGs (Zhao et al., 2016). While it remains unknown whether TCF7L2 directly binds to and thus affects the transcription of myelin component genes, chromatin-immunoprecipitation (ChIP) sequencing has suggested that it strongly occupies the promoter region of myelin regulatory factor (MYRF). MYRF is an OLG-specific transcription factor, which is known to promote transcription of these genes and is critical for adult myelin maintenance (Bujalka et al., 2013; Emery et al., 2009; McKenzie et al., 2014). Lastly, while TCF7L2 was a predicted regulator in both strains, the myelin component genes were only DE in the myelin fraction of the B6 susceptible mice. Little is known about its possible actions outside the nucleus. Some transcription factors, such as MYRF, have extranuclear functions as well. MYRF resides on the endoplasmic reticulum (ER), and an autocleavage event releases the homotrimerized N-terminal for translocation into the nucleus and DNA-binding. Although not confirmed, it is hypothesised that the C-terminal may perform some additional functions, such as protein processing at the ER (Bujalka et al., 2013; Li, Park, & Marcotte, 2013). Functional studies, such as OLG-specific knock-out or overexpression, are needed to resolve the function of TCF7L2 in stress-related myelin gene expression.

In summary, we showed that mRNAs and miRNAs in OLGs and their myelin sheaths are not present in equal proportions, despite the latter being a membrane extension of the former. This could be due to selective transport of certain transcripts to the myelin sheath or their local regulation. We also replicated prior findings (Laine et al., 2018) that myelin component genes are downregulated in the mPFC of CSDS-susceptible mice from the B6 background, pinpointing this difference to the myelin fraction. Additionally, we showed lower expression levels of these genes in the OLG fraction of both stress-susceptible and resilient D2 mice compared to controls. Bioinformatic predictions provided potential candidates upstream of these DE genes. Follow-up studies are required to validate the role of TCF7L2

is stress-related myelin plasticity, stress-resilience and -susceptibility. Identifying the components of this pathway may contribute to the development of improved treatments for stress-related disorders.

Acknowledgements

Funded by the European Research Council Starting Grant (GenAnx, to IH), Academy of Finland (to IH), Sigrid Jusélius Foundation (to IH), and University of Helsinki Doctoral Programme Brain & Mind (to ML and AG). We thank Laura Salminen and the Mouse Behavioral Phenotyping Facility [supported by University of Helsinki (HiLIFE) and Biocenter Finland] for help with with behavioral testing, and the DNA Sequencing and Genomics unit (Institute of Biotechnology, HiLIFE, University of Helsinki) for conducting RNA-sequencing.

References

Ainger, K., Avossa, D., Diana, A. S., Barry, C., Barbarese, E., & Carson, J. H. (1997). Transport and localization elements in myelin basic protein mRNA. *J Cell Biol, 138*(5), 1077-1087. doi:10.1083/jcb.138.5.1077

Almeida, R. G., & Lyons, D. A. (2017). On Myelinated Axon Plasticity and Neuronal Circuit Formation and Function. *J Neurosci, 37*(42), 10023-10034. doi:10.1523/JNEUROSCI.3185-16.2017

Anders, S., Pyl, P. T., & Huber, W. (2014). HTSeq--a Python framework to work with high-throughput sequencing data. *Bioinformatics, 31*(2), 166-169. doi:10.1093/bioinformatics/btu638

Bem, J., Brozko, N., Chakraborty, C., Lipiec, M. A., Kozinski, K., Nagalski, A., . . . Wisniewska, M. B. (2019). Wnt/beta-catenin signaling in brain development and mental disorders: keeping TCF7L2 in mind. *FEBS Lett, 593*(13), 1654-1674. doi:10.1002/1873-3468.13502

Bengtsson, S. L., Nagy, Z., Skare, S., Forsman, L., Forssberg, H., & Ullen, F. (2005). Extensive piano practicing has regionally specific effects on white matter development. *Nat Neurosci, 8*(9), 1148-1150. doi:10.1038/nn1516

Bennett, M. L., Bennett, F. C., Liddelow, S. A., Ajami, B., Zamanian, J. L., Fernhoff, N. B., . . . Barres, B. A. (2016). New tools for studying microglia in the mouse and human CNS. *Proc Natl Acad Sci U S A, 113*(12), E1738-1746. doi:10.1073/pnas.1525528113

Bujalka, H., Koenning, M., Jackson, S., Perreau, V. M., Pope, B., Hay, C. M., . . . Emery, B. (2013). MYRF is a membrane-associated transcription factor that autoproteolytically cleaves to directly activate myelin genes. *PLoS Biol, 11*(8), e1001625. doi:10.1371/journal.pbio.1001625

Cahoy, J. D., Emery, B., Kaushal, A., Foo, L. C., Zamanian, J. L., Christopherson, K. S., . . . Barres, B. A. (2008). A transcriptome database for astrocytes, neurons, and oligodendrocytes: a new resource for understanding brain development and function. *J Neurosci, 28*(1), 264-278. doi:10.1523/JNEUROSCI.4178-07.2008

Cathomas, F., Azzinnari, D., Bergamini, G., Sigrist, H., Buerge, M., Hoop, V., . . . Pryce, C. R. (2019). Oligodendrocyte gene expression is reduced by and influences effects of chronic social stress in mice. *Genes Brain Behav, 18*(1), e12475. doi:10.1111/gbb.12475

Dobin, A., Davis, C. A., Schlesinger, F., Drenkow, J., Zaleski, C., Jha, S., . . . Gingeras, T. R. (2013). STAR: ultrafast universal RNA-seq aligner. *Bioinformatics, 29*(1), 15-21. doi:10.1093/bioinformatics/bts635

Elbau, I. G., Cruceanu, C., & Binder, E. B. (2019). Genetics of Resilience: Gene-by-Environment Interaction Studies as a Tool to Dissect Mechanisms of Resilience. *Biol Psychiatry, 86*(6), 433-442. doi:10.1016/j.biopsych.2019.04.025

Emery, B., Agalliu, D., Cahoy, J. D., Watkins, T. A., Dugas, J. C., Mulinyawe, S. B., . . . Barres, B. A. (2009). Myelin gene regulatory factor is a critical transcriptional regulator required for CNS myelination. *Cell, 138*(1), 172-185. doi:10.1016/j.cell.2009.04.031

Etxeberria, A., Hokanson, K. C., Dao, D. Q., Mayoral, S. R., Mei, F., Redmond, S. A., . . . Chan, J. R. (2016). Dynamic Modulation of Myelination in Response to Visual Stimuli Alters Optic Nerve Conduction Velocity. *J Neurosci, 36*(26), 6937-6948. doi:10.1523/JNEUROSCI.0908-16.2016

Feder, A., Fred-Torres, S., Southwick, S. M., & Charney, D. S. (2019). The Biology of Human Resilience: Opportunities for Enhancing Resilience Across the Life Span. *Biol Psychiatry, 86*(6), 443-453. doi:10.1016/j.biopsych.2019.07.012

Feigenson, K., Reid, M., See, J., Crenshaw, E. B., 3rd, & Grinspan, J. B. (2009). Wnt signaling is sufficient to perturb oligodendrocyte maturation. *Mol Cell Neurosci, 42*(3), 255-265. doi:10.1016/j.mcn.2009.07.010

Friedlander, M. R., Chen, W., Adamidi, C., Maaskola, J., Einspanier, R., Knespel, S., & Rajewsky, N. (2008). Discovering microRNAs from deep sequencing data using miRDeep. *Nat Biotechnol, 26*(4), 407-415. doi:10.1038/nbt1394

Gibson, E. M., Purger, D., Mount, C. W., Goldstein, A. K., Lin, G. L., Wood, L. S., . . . Monje, M. (2014). Neuronal activity promotes oligodendrogenesis and adaptive myelination in the mammalian brain. *Science, 344*(6183), 1252304. doi:10.1126/science.1252304

Golden, S. A., Covington, H. E., 3rd, Berton, O., & Russo, S. J. (2011). A standardized protocol for repeated social defeat stress in mice. *Nat Protoc, 6*(8), 1183-1191. doi:10.1038/nprot.2011.361

Hammond, E., Lang, J., Maeda, Y., Pleasure, D., Angus-Hill, M., Xu, J., . . . Guo, F. (2015). The Wnt effector transcription factor 7-like 2 positively regulates oligodendrocyte differentiation in a manner independent of Wnt/beta-catenin signaling. *J Neurosci, 35*(12), 5007-5022. doi:10.1523/JNEUROSCI.4787-14.2015

Hoek, K. S., Kidd, G. J., Carson, J. H., & Smith, R. (1998). hnRNP A2 selectively binds the cytoplasmic transport sequence of myelin basic protein mRNA. *Biochemistry, 37*(19), 7021-7029. doi:10.1021/bi9800247

Hoppen, T. H., & Chalder, T. (2018). Childhood adversity as a transdiagnostic risk factor for affective disorders in adulthood: A systematic review focusing on biopsychosocial moderating and mediating variables. *Clin Psychol Rev, 65*, 81-151. doi:10.1016/j.cpr.2018.08.002

Hovatta, I., Tennant, R. S., Helton, R., Marr, R. A., Singer, O., Redwine, J. M., . . . Barlow, C. (2005). Glyoxalase 1 and glutathione reductase 1 regulate anxiety in mice. *Nature, 438*(7068), 662-666. doi:10.1038/nature04250

Ishii, A., Dutta, R., Wark, G. M., Hwang, S. I., Han, D. K., Trapp, B. D., . . . Bansal, R. (2009). Human myelin proteome and comparative analysis with mouse myelin. *Proc Natl Acad Sci U S A, 106*(34), 14605-14610. doi:10.1073/pnas.0905936106

Johnson, W. E., Li, C., & Rabinovic, A. (2007). Adjusting batch effects in microarray expression data using empirical Bayes methods. *Biostatistics, 8*(1), 118-127. doi:10.1093/biostatistics/kxj037

Kessler, R. C., Ruscio, A. M., Shear, K., & Wittchen, H. U. (2010). Epidemiology of anxiety disorders. *Curr Top Behav Neurosci, 2*, 21-35.

Kozomara, A., & Griffiths-Jones, S. (2014). miRBase: annotating high confidence microRNAs using deep sequencing data. *Nucleic Acids Res, 42*(Database issue), D68-73. doi:10.1093/nar/gkt1181

Kramer, A., Green, J., Pollard, J., Jr., & Tugendreich, S. (2014). Causal analysis approaches in Ingenuity Pathway Analysis. *Bioinformatics, 30*(4), 523-530. doi:10.1093/bioinformatics/btt703

Kwon, D., Pfefferbaum, A., Sullivan, E. V., & Pohl, K. M. (2020). Regional growth trajectories of cortical myelination in adolescents and young adults: longitudinal validation and functional correlates. *Brain Imaging Behav, 14*(1), 242-266. doi:10.1007/s11682-018-9980-3

Laine, M. A., Trontti, K., Misiewicz, Z., Sokolowska, E., Kulesskaya, N., Heikkinen, A., . . . Hovatta, I. (2018). Genetic Control of Myelin Plasticity after Chronic Psychosocial Stress. *eNeuro, 5*(4). doi:10.1523/ENEURO.0166-18.2018

Law, C. W., Chen, Y., Shi, W., & Smyth, G. K. (2014). voom: Precision weights unlock linear model analysis tools for RNA-seq read counts. *Genome Biol, 15*(2), R29. doi:10.1186/gb-2014-15-2-r29

Leek, J. T., Johnson, W. E., Parker, H. S., Jaffe, A. E., & Storey, J. D. (2012). The sva package for removing batch effects and other unwanted variation in high-throughput experiments. *Bioinformatics, 28*(6), 882-883. doi:10.1093/bioinformatics/bts034

Lehmann, M. L., Weigel, T. K., Elkahloun, A. G., & Herkenham, M. (2017). Chronic social defeat reduces myelination in the mouse medial prefrontal cortex. *Sci Rep, 7*, 46548. doi:10.1038/srep46548

Li, Z., Park, Y., & Marcotte, E. M. (2013). A Bacteriophage tailspike domain promotes self-cleavage of a human membrane-bound transcription factor, the myelin regulatory factor MYRF. *PLoS Biol, 11*(8), e1001624. doi:10.1371/journal.pbio.1001624

Liu, J., Dietz, K., DeLoyht, J. M., Pedre, X., Kelkar, D., Kaur, J., . . . Casaccia, P. (2012). Impaired adult myelination in the prefrontal cortex of socially isolated mice. *Nat Neurosci, 15*(12), 1621-1623. doi:10.1038/nn.3263

Liu, J., Dietz, K., Hodes, G. E., Russo, S. J., & Casaccia, P. (2018). Widespread transcriptional alternations in oligodendrocytes in the adult mouse brain following chronic stress. *Dev Neurobiol, 78*(2), 152-162. doi:10.1002/dneu.22533

Makinodan, M., Rosen, K. M., Ito, S., & Corfas, G. (2012). A critical period for social experience-dependent oligodendrocyte maturation and myelination. *Science, 337*(6100), 1357-1360. doi:10.1126/science.1220845

McKenzie, I. A., Ohayon, D., Li, H., de Faria, J. P., Emery, B., Tohyama, K., & Richardson, W. D. (2014). Motor skill learning requires active central myelination. *Science, 346*(6207), 318-322. doi:10.1126/science.1254960

Murrough, J. W., & Russo, S. J. (2019). The Neurobiology of Resilience: Complexity and Hope. *Biol Psychiatry, 86*(6), 406-409. doi:10.1016/j.biopsych.2019.07.016

Phipson, B., Lee, S., Majewski, I. J., Alexander, W. S., & Smyth, G. K. (2016). Robust Hyperparameter Estimation Protects against Hypervariable Genes and Improves Power to Detect Differential Expression. *Ann Appl Stat, 10*(2), 946-963. doi:10.1214/16-AOAS920

Plaisier, S. B., Taschereau, R., Wong, J. A., & Graeber, T. G. (2010). Rank-rank hypergeometric overlap: identification of statistically significant overlap between gene-expression signatures. *Nucleic Acids Res, 38*(17), e169. doi:10.1093/nar/gkq636

Ressler, K. J., Mercer, K. B., Bradley, B., Jovanovic, T., Mahan, A., Kerley, K., . . . May, V. (2011). Post-traumatic stress disorder is associated with PACAP and the PAC1 receptor. *Nature, 470*(7335), 492-497. doi:10.1038/nature09856

Ritchie, M. E., Phipson, B., Wu, D., Hu, Y., Law, C. W., Shi, W., & Smyth, G. K. (2015). limma powers differential expression analyses for RNA-sequencing and microarray studies. *Nucleic Acids Res, 43*(7), e47. doi:10.1093/nar/gkv007

Russo, S. J., Murrough, J. W., Han, M. H., Charney, D. S., & Nestler, E. J. (2012). Neurobiology of resilience. *Nat Neurosci, 15*(11), 1475-1484. doi:10.1038/nn.3234

Savic, D., Distler, M. G., Sokoloff, G., Shanahan, N. A., Dulawa, S. C., Palmer, A. A., & Nobrega, M. A. (2011). Modulation ofTcf7l2 expression alters behavior in mice. *PLoS One, 6*(10), e26897. doi:10.1371/journal.pone.0026897

Schmieder, R., & Edwards, R. (2011). Quality control and preprocessing of metagenomic datasets. *Bioinformatics, 27*(6), 863-864. doi:10.1093/bioinformatics/btr026

Sittig, L. J., Carbonetto, P., Engel, K. A., Krauss, K. S., Barrios-Camacho, C. M., & Palmer, A. A. (2016). Genetic Background Limits Generalizability of Genotype-Phenotype Relationships. *Neuron, 91*(6), 1253-1259. doi:10.1016/j.neuron.2016.08.013

Spandidos, A., Wang, X., Wang, H., & Seed, B. (2010). PrimerBank: a resource of human and mouse PCR primer pairs for gene expression detection and quantification. *Nucleic Acids Res, 38*(Database issue), D792-799. doi:10.1093/nar/gkp1005

Tang, J., Liang, X., Zhang, Y., Chen, L., Wang, F., Tan, C., . . . Tang, Y. (2019). The effects of running exercise on oligodendrocytes in the hippocampus of rats with depression induced by chronic unpredictable stress. *Brain Res Bull, 149*, 1-10. doi:10.1016/j.brainresbull.2019.04.001

Thakurela, S., Garding, A., Jung, R. B., Muller, C., Goebbels, S., White, R., . . . Tiwari, V. K. (2016). The transcriptome of mouse central nervous system myelin. *Sci Rep, 6*, 25828. doi:10.1038/srep25828

Torvund-Jensen, J., Steengaard, J., Askebjerg, L. B., Kjaer-Sorensen, K., & Laursen, L. S. (2018). The 3'UTRs of Myelin Basic Protein mRNAs Regulate Transport, Local Translation and Sensitivity to Neuronal Activity in Zebrafish. *Front Mol Neurosci, 11*, 185. doi:10.3389/fnmol.2018.00185

Valerio-Gomes, B., Guimaraes, D. M., Szczupak, D., & Lent, R. (2018). The Absolute Number of Oligodendrocytes in the Adult Mouse Brain. *Front Neuroanat, 12*, 90. doi:10.3389/fnana.2018.00090

Weng, C., Ding, M., Fan, S., Cao, Q., & Lu, Z. (2017). Transcription factor 7 like 2 promotes oligodendrocyte differentiation and remyelination. *Mol Med Rep, 16*(2), 1864-1870. doi:10.3892/mmr.2017.6843

Ye, F., Chen, Y., Hoang, T., Montgomery, R. L., Zhao, X. H., Bu, H., . . . Lu, Q. R. (2009). HDAC1 and HDAC2 regulate oligodendrocyte differentiation by disrupting the beta-catenin-TCF interaction. *Nat Neurosci, 12*(7), 829-838. doi:10.1038/nn.2333

Zhang, H., Yan, G., Xu, H., Fang, Z., Zhang, J., Zhang, J., . . . Huang, Q. (2016). The recovery trajectory of adolescent social defeat stress-induced behavioral, (1)H-MRS metabolites and myelin changes in Balb/c mice. *Sci Rep, 6*, 27906. doi:10.1038/srep27906

Zhang, Y., Chen, K., Sloan, S. A., Bennett, M. L., Scholze, A. R., O'Keeffe, S., . . . Wu, J. Q. (2014). An RNA-sequencing transcriptome and splicing database of glia, neurons, and vascular cells of the cerebral cortex. *J Neurosci, 34*(36), 11929-11947. doi:10.1523/JNEUROSCI.1860-14.2014

Zhao, C., Deng, Y., Liu, L., Yu, K., Zhang, L., Wang, H., . . . Lu, Q. R. (2016). Dual regulatory switch through interactions of Tcf7l2/Tcf4 with stage-specific partners propels oligodendroglial maturation. *Nat Commun, 7*, 10883. doi:10.1038/ncomms10883